

**CHARACTERIZATION OF GLASS FIBRE REINFORCED
POLYAMIDE/ACRYLONITRILE BUTADIENE STYRENE COMPOSITE
FOR AUTOMOTIVE APPLICATION**

**(PENCIRIAN KOMPOSIT POLIAMIDA/AKRILONITRIL BUTADIENA STIRENA
BERTETULANG GENTIAN KACA BAGI PENGGUNAAN AUTOMOTIF)**

ABDUL RAZAK RAHMAT

AZMAN HASSAN

MAT UZIR WAHIT

AGUS ARSAD

**FAKULTI KEJURUTERAAN KIMIA DAN KEJURUTERAAN SUMBER ASLI
UNIVERSITI TEKNOLOGI MALAYSIA**

2009

ACKNOWLEDGEMENTS

We wish to express our appreciation to the technician of Polymer Engineering, especially Miss Zainab, Mr. Suhee Tan and Mr. Nordin Ahmad, the Quality Control staff in Poly-Star Compounds Sdn. Bhd. and MINT for their help and support in this research. We wish to thank Mr. Shaiful Nizam Iskandar for helpful discussions and exchange of ideas regarding rheology of the polymer blends. Also, all the staff of Technical Service Laboratory, Polyethylene (M) Sdn Bhd, Kertih, for giving the opportunity to use their capillary and oscillatory rheology, without them, the rheological study could not be materialised.

Last but not least we would like to acknowledge Ministry of Higher Education, Malaysia (MOHE) for generous financial funding.

ABSTRACT

Polyamide-6 (PA6), acrylonitrile-butadiene-styrene (ABS) and their blends are an important class of engineering thermoplastics that are widely used especially for automotive industries. Many efforts have been taken to improve the properties of both pure components and the blends. It was for this reason that the dynamic mechanical and rheological properties of PA6/ABS blend systems compatibilised by acrylonitrile-butadiene-styrene-maleic anhydride (ABS-g-MAH) was studied. The compatibiliser level was kept up to 5wt. % in the blends. Short glass fibre (SGF) was used to improve the stiffness of the compatibilised blends and the concentration was varied from 10 to 30 wt. %. Therefore, the reason behind of blending the PA6/ABS blends with short glass fibre was to balance the toughness and stiffness. The blends and corresponding composites were compounded using a co-counter twin screw extruder. Tensile, flexural and impact properties were determined using the injection moulded test samples according to ASTM standards. Dynamic mechanical analyses (DMA) were carried out to investigate the dynamic mechanical behaviour of the blends and composites. Rheological properties were carried out using dynamic and capillary rheometer. In general, the mechanical strength either dynamic (refer to DMA) or static conditions were improved by incorporation of compatibiliser to the PA6/ABS blends. The incorporation of SGF into the PA6/ABS blends enhanced the mechanical strength however, reduced the toughness of the composites. The rheological measurements confirmed the increased interaction between the blend components with the incorporation of compatibiliser. The compatibiliser has no favourable effect on the mechanical properties of the composites although it has significant effect on the blends of PA6/ABS. ABS-g-MAH increases the melt viscosity of the blends. The SGF increased the rheological properties especially viscosity and flowability of the composites. The optimum ratio compatibiliser and SGF concentration were successfully determined using power law and consistency index analysis. From the analysis the optimum ratio obtained was 1.5 wt. % for 50/50 and 60/40 PA6/ABS blends and 3 wt. % for 70/30 PA6/ABS blends. When the SGF introduced at 20 wt. % concentration, the values of n drastically decreased indicating more pseudoplastic nature for the composites and concluded that, the optimum concentration of SGF was about 20 wt. %.

ABSTRAK

Poliamida-6 (PA6), akrilonitril-butadiena-sterina dan adunan keduanya merupakan satu bahan kejuruteraan termoplastik yang penting dan sangat luas penggunaannya terutama dalam industri automotif. Pelbagai usaha telah diambil untuk memperbaiki sifat-sifat kedua-dua komponen dan adunannya, Ini menjadikan alasan kajian terhadap sifat-sifat dinamik mekanikal dan reologi sistem adunan PA6/ABS yang telah diserasikan oleh akrilonitril-butadiena-sterina-melaik anhadrida (ABS-g-MAH). Aras penserasi dalam adunan PA6/ABS telah ditetapkan sehingga 5 wt. %. Gentian kaca pendek (SGF) telah digunakan untuk mempebaiki kekakuan adunan yang telah diserasikan dan kandungan SGF dalam adunan diubah dari 10 hingga 30 wt. %. Oleh yang demikian, ini adalah alasan disebalik campuran adunan PA6/ABS dengan gentian kaca pendek mengimbangkan kekakuan dan kekukuhan adunan. Adunan dan komposit telah diadun dengan menggunakan penyemperit skru berkembar arah berlawanan. Sifat-sifat ketegangan, kelenturan dan hentaman telah ditentukan dengan sampel yang dibentuk dengan menggunakan acuan penyuntikan berdasarkan piawaiian ASTM. Analisis dinamik mekanikal (DMA) telah dilakukan untuk menyiasat kelakuan dinamik mekanikal adunan dan komposit. Sifat-sifat reologi telah dikaji menggunakan alatan reologi rerambut dan pengayun. Secara umumnya, kekuatan mekanikal sama ada dinamik (rujuk kepada DMA) atau kekautan mekanik statik telah diperbaiki dengan penambahan penserasi ke dalam adunan PA6/ABS. Penambahan SGF pula ke dalam adunan telah mempebaiki kekuatan mekanikal bahan, walau bagaimanapun menurunkan kekukuhan komposit. Kajian reologi telah menentukan peningkatan interaksi antara komponen adunan dengan penambahan SGF. Penserasi tidak mempunyai kesan terhadap sifat-sifat mekanik komposit, walaupun ada kesan yang ketara terhadap adunan PA6/ABS. Di mana juga, ABS-g-MAH meningkatkan kelikatan leburan adunan. SGF pula meningkatkan sifat-sifat reologi komposit terutamanya kelikatan dan kebolehalirannya. Pecahan penserasi dan kepekatan SGF yang optimum telah berjaya ditentukan dengan menggunakan analisis indek hukum kuasa dan ketetapan. Dari analisis pecahan kandungan optimum yang telah didapati adalah 1.5 wt. % untuk adunan PA6/ABS 50/50 dan 60/40 PA6 dan 3 wt. % pulak untuk adunan PA6/ABS 70/30. Apabila SGF telah ditambahkan pada kepekatan 20 wt. %, nilai indek hokum kuasa menurun secara mendadak menunjukkan komposit mempunyai sifata-sifat pseudoplastik yang jelas dan disimpulkan bahawa 20 wt. % adalah kepekatan optimum bagi komposit PA6/ABS 60/40.

TABLE OF CONTENTS

CHAPTER	TITLE	PAGE
	DECLARATION	ii
	DEDICATION	iii
	ACKNOWLEDGEMENT	iv
	ABSTRACT	v
	ABSTRAK	vi
	TABLE OF CONTENT	vii
	LIST OF TABLES	xii
	LIST OF FIGURES	xv
	LIST OF ABBREVIATIONS	xix
	LIST OF SYMBOLS	xxii
	LIST OF APPENDICES	xxiii
1	INTRODUCTION	1
	1.1 Introduction	1
	1.2 Problem Statements	4
	1.3 Objectives	5
	1.4 Scope of Study	6
2	LITERATURE REVIEW	9
	2.1 Polymer Blends	9
	2.2 Overview of Polymer Composite	11
	2.3 Compatibilisation of Polymer Blends and Composites	13
	2.4 Overview of Polymer Rheology	15
	2.5 Significant of Rheological Properties Studies	17

2.6	Application of Rheology to Polymer Processing	19
2.7	Rheometers	22
2.7.1	Introduction	22
2.7.2	Measuring of Rheological Parameters	27
2.7.2.1	Capillary Rheometer	27
2.7.2.2	Rotational Rheometer	30
2.8	Dynamic Mechanical Analysis	32
2.9	Polyamide 6 (PA6) Polymer	35
2.10	Acrylonitrile Butadiene Styrene (ABS) Polymer	38
2.11	Role of Compatibilizer	40
2.12	Glass Fibre (GF) Reinforcement	42
2.13	Glass Fibre Reinforced Polymer Composite	43
2.14	Uncompatibilised PA6/ABS Blends	45
2.15	Compatibilised PA6/ABS Blends.	47
2.16	Ternary Blends of PA6/ABS	52
2.17	Glass Fibre Reinforced PA6/Polymer Composites	53
2.17.1	Introduction	53
2.17.2	Glass fibre Polyamide Composites	54
2.17.3	Glass Fibre Reinforced PA6/ABS Composites	55
3	METHODOLOGY	58
3.1	Introduction	58
3.2	Raw Materials	60
3.2.1	PA6 and ABS	60
3.2.2	Compatibilizer	61
3.2.3	Short Glass Fibre (SGF) Reinforcement	62
3.3	Sample Preparation	62
3.3.1	Blend Formulation	62
3.3.2	Preparation of Blends	63
3.3.3	Melt Extrusion Blending	64
3.3.4	Injection Moulding	64

3.4	Mechanical Testing and Analysis Procedure	65
3.4.1	Tensile Test	65
3.4.2	Flexural Test	66
3.4.3	Izod Impact Test	67
3.4.4	Dynamic Mechanical Analysis (DMA)	67
3.5	Differential Scanning Calorimetry (DSC)	68
3.6	Rheological Testing and Analysis	69
3.6.1	Capillary Rheometer	69
3.6.2	Rotational Rheometer	71
3.7	Fourier Transform Infrared (FTIR)	73
3.8	Scanning Electron Microscope (SEM)	73
4	RESULTS AND DISCUSSION	75
4.1	Mechanical Properties	75
4.1.1	Tensile Properties of PA6/ABS Blends	75
4.1.2	Flexural Properties of PA6/ABS Blends	80
4.1.3	Impact Properties of PA6/ABS Blends	82
4.1.4	Tensile Properties of 60/40 PA6/ABS Composites	84
4.1.5	Flexural Properties of 60/40 PA6/ABS Composites	91
4.1.6	Impact Properties of 60/40 PA6/ABS Composites	93
4.2	Thermal Properties Analysis	90
4.2.1	Thermal Properties of PA6/ABS Blends	90
4.2.2	Thermal Properties of 60/40 PA6/ABS Composites	95
4.3	Dynamic Mechanical Analysis (DMA)	98
4.3.1	PA6/ABS Blends	98
4.3.1.1	Storage Modulus of PA6/ABS Blends	98
4.3.1.2	Loss Modulus of PA6/ABS Blends	102
4.3.1.3	Tangent delta ($\tan \delta$) of PA6/ABS Blends	106
4.3.2	PA6/ABS Composites	111
4.3.2.1	Storage and Loss Modulus of 60/40 PA6/ABS Composites	111

4.3.2.2	Tangent delta ($\tan \delta$) of 60/40 PA6/ABS Blends	114
4.4	Rheological Properties	117
4.4.1	Rheological Properties of Virgin PA6 and ABS	117
4.4.2	Dynamic Rheological Properties of PA6/ABS Blends	119
4.4.2.1	Complex Viscosity Analysis	119
4.4.2.2	Storage Modulus Analysis	122
4.4.2.3	Loss Modulus Analysis	125
4.4.2.4	Tan δ Analysis	128
4.4.2.5	The Cole-cole Plot Analysis	131
4.4.2.6	Activation Energy of Flow	138
4.4.3	Capillary Rheological Properties of PA6/ABS Blends	139
4.4.3.1	Shear Stress Analysis	139
4.4.3.2	Shear Viscosity Analysis	142
4.4.3.3	Power Law Index Analysis	145
4.4.4	Dynamic Rheological Properties of 60/40 PA6/ABS Composites	149
4.4.4.1	Loss and Storage Modulus Analysis	149
4.4.4.2	Complex Viscosity Analysis	151
4.4.4.3	Tan δ Analysis	152
4.4.4.4	The Cole-cole plot analysis	153
4.4.4.5	Activation Energy of Flow	154
4.4.5	Capillary Rheological Properties of 60/40 PA6/ABS Composites	156
4.4.5.1	Shear Stress Analysis	156
4.4.5.2	Shear Viscosity Analysis	157
4.4.5.3	Power Law Index Analysis	159
4.5	Fourier Transform Infrared (FTIR) Analysis	161
4.6	SEM Micrograph Analysis	164

5	CONCLUSION AND RECOMMENDATION	168
5.1	Conclusion	173
5.2	Recommendation for Future Work	173
	REFERENCES	174

LIST OF TABLES

TABLE NO.	TITLE	PAGE
3.1	Material Properties of Super High Impact ABS (100-X01) (Toray Industries, 2006)	63
3.2	Material Properties of PA6 (Amilan CM1017) (Toray Industries, 2006)	64
3.3 (a)	Blend formulations for polyamide 6 and ABS blending process without compatibiliser	66
3.3 (b)	Blend formulations for polyamide 6 and ABS blending process with ABS-g-MAH as compatibiliser	67
3.3 (c)	Blend formulations for compatibiliser PA6/ABS blends and short glass fibre blending process	67
4.1	DSC data for 50/50 PA6/ABS Blends	93
4.2	DSC data for 60/40 PA6/ABS Blends	93
4.3	DSC data for 70/30 PA6/ABS Blends	93
4.4	DSC data for 60/40 PA6/ABS Composites	97
4.5	The T_g , compositional dependence of maximum $\tan \delta$ and peak width at half height for PA6/ABS blends with various ABS-g-MAH contents. The maximum $\tan \delta$ was collected by measuring the height of peaks in $\tan \delta$ curve versus temperature	111
4.6	Area under the curve at $\tan \delta$ maximum, $\tan \delta$ maximum, T_g for SAN rich phase and peak width of 60/40 PA6/ABS composites at different fibre loading	116

LIST OF FIGURES

FIGURE NO	TITLE	PAGE
2.1	Factors influencing the mechanical performance of reinforced polymer blends (Karger-Kocsis, 2000)	13
2.2	Rheological parameters acting as a link between molecular structure and final properties a polymer (Markus Gahleitner, 2001)	20
2.3	Shear flow results when plates move past one another	23
2.4	Sketch of capillary rheometer geometry	28
2.5	Sketch of parallel disk rheometer geometry	31
2.6	Sketch of cone and plate geometry.	31
2.7	Plot of dynamic stress-strain	37
2.8	Dynamic mechanical analysis relationship	39
2.9	Typical molecular structure of polyamide series	40
2.10	Molecular structure of acrylonitrile-butadiene-styrene (ABS)	42
3.1	Research flow chart	59
3.2	Picture of Rosand Capillary Rheometer, Technical Service Laboratory, Polyethyelene (M) Sdn. Bhd. Kertih, Terengganu	70
3.3	Picture of Rheostresss TC501 at Technical Service Laboratory, Polyethylene (M) Sdn. Bhd. Kertih, Terengganu	72
3.4	Picture of compression moulding, for preparation of dynamic rheological specimens	73
4.1	Potential chemical reactions between PA6 and maleic anhydride	77

4.2	Effect of compatibiliser composition on tensile modulus of PA6/ABS blends	88
4.3	Effect of compatibiliser composition on tensile strength of PA6/ABS blends	79
4.4	Effect of compatibiliser composition on elongation at break of PA6/ABS blends.	79
4.5	Effect of compatibiliser composition on flexural modulus of PA6/ABS blends.	81
4.6	Effect of compatibiliser composition on flexural strength of PA6/ABS blends.	81
4.7	Effect of compatibiliser composition on impact strength of PA6/ABS blends.	84
4.8	Effect of glass fibre composition on tensile modulus of 60/40 PA6/ABS composites	86
4.9	Effect of glass fibre composition on tensile strength of 60/40 PA6/ABS composites.	86
4.10	Effect of glass fibre composition on elongation at break of 60/40 PA6/ABS composites.	87
4.11	Effect of glass fibre composition on flexural modulus of PA6/ABS composites.	87
4.12	Effect of glass fibre composition on flexural strength of PA6/ABS composites.	87
4.13	Effect of glass fibre composition on notched Izod impact strength of 60/40 PA6/ABS composites	87
4.14	DSC second heating run thermogram of 50/50 PA6/ABS blends at different composition of compatibiliser.	94
4.15	DSC second heating run thermogram of 60/40 PA6/ABS blends at different composition of compatibiliser.	94
4.16	DSC second heating run thermogram of 70/30 PA6/ABS blends at different composition of compatibiliser.	95
4.17	Degree of crystallinity of PA6/ABS blends as a function of ABS-g-MAH concentration, for various PA6 compositions	95

4.18	Degree of crystallinity of 60/40 PA6/ABS composites as a function of different amount of short glass fibre	97
4.19	Storage modulus vs. temperature plot for different composition of compatibiliser in 50/50 of PA6/ABS blends	100
4.20	Storage modulus vs. temperature plot at different composition of compatibiliser in 60/40 PA6/ABS blends	101
4.21	Storage modulus vs. temperature plots at different composition of compatibiliser in 70/30 PA6/ABS blends	102
4.22	Loss modulus vs. temperature plot for different compositions of compatibiliser in 50/50 of PA6/ABS blends	104
4.23	Loss modulus vs. temperature plot at different composition of compatibiliser in 60/40 PA6/ABS blends	105
4.24	Loss modulus vs. temperature plot for different composition of compatibiliser in 70/30 of PA6/ABS blends	105
4.25	Tan δ vs. temperature plots at different composition of compatibiliser in 50/50 PA6/ABS blends	109
4.26	Tan δ vs. temperature plot for different composition of compatibiliser in 60/40 of PA6/ABS blends	110
4.27	Tan δ vs. temperature plots at different composition of compatibiliser in 70/30 PA6/ABS blends	110
4.28	Effect of SGF loading with temperature on the storage modulus values of 60/40 PA6/ABS composites	113
4.29	Effect of SGF loading with temperature on the loss modulus values of 60/40 PA6/ABS composites	114
4.30	Effect of SGF loading with temperature on the tan δ values of the 60 40 PA6/ABS composites	116
4. 31	Complex viscosities of blend components (PA6 and ABS) measured at 230 °C	118
4.32	Dynamic moduli of blend components (PA6 and ABS) measured at 230 °C	119

4.33	Plot of complex viscosity versus frequency at different amount of compatibiliser for 50/50 PA6/ABS blends, at 230°C	121
4.34	Plot of complex viscosity versus frequency at different amount of compatibiliser for 60/40 PA6/ABS blends, at 230°C	121
4.35	Plot of complex viscosity versus frequency at different amount of compatibiliser for 70/30 PA6/ABS blends, at 230°C	122
4.36	Plot of storage modulus versus frequency at different amount of compatibiliser for 50/50 PA6/ABS blends, at 230°C	123
4.37	Plot of storage modulus versus frequency at different amount of compatibiliser for 60/40 PA6/ABS blends, at 230°C	124
4.38	Plot of storage modulus versus frequency at different amount of compatibiliser for 70/30 PA6/ABS blends, at 230°C	125
4.39	Plot of loss modulus versus frequency at different amount of compatibiliser for 50/50 PA6/ABS blends, at 230°C	126
4.40	Plot of loss modulus versus frequency at different amount of compatibiliser for 60/40 PA6/ABS blends, at 230°C	127
4.41	Plot of loss modulus versus frequency at different amount of compatibiliser for 70/30 PA6/ABS blends, at 230°C	127
4.42	Plot of $\tan \delta$ versus frequency at different amount of compatibiliser for 50/50 PA6/ABS blends, at 230°C	129
4.43	Plot of $\tan \delta$ versus frequency at different amount of compatibiliser for 60/40 PA6/ABS blends, at 230°C	130
4.44	Plot of $\tan \delta$ versus frequency at different amount of compatibiliser for 70/30 PA6/ABS blends, at 230°C	130
4.45	Plot of $\log G'$ versus $\log G''$ for 50/50 PA6/ABS blends at different amount of compatibiliser, at 230°C	132
4.46	Plot of $\log G'$ versus $\log G''$ for 60/40 PA6/ABS blends at different amount of compatibiliser, at 230°C	133
4.47	Plot of $\log G'$ versus $\log G''$ for 70/30 PA6/ABS blends at different amount of compatibiliser, at 230°C	133
4.48	Effect of temperature on shift factor, a_T of 50/50 PA6/ABS	135

	blends at different compatibiliser concentration	
4.49	Effect of temperature on shift factor, a_T of 60/40 PA6/ABS blends at different compatibiliser concentration	136
4.50	Effect of temperature on shift factor, a_T of 70/30 PA6/ABS blends at different compatibiliser concentration	137
4.51	Plot of activation energy of flow versus amount of compatibiliser at different concentration of PA6	139
4.52	Plots of shear stress as a function of shear rate for 50/50 PA6/ABS blend at different compositions of ABS-g-MAH	140
4.53	Plots of shear stress as a function of shear rate for 60/40 PA6/ABS blend at different compositions of ABS-g-MAH	141
4.54	Plots of shear stress as a function of shear rate for 70/30 PA6/ABS blend at different compositions of ABS-g-MAH	141
4.55	Plots of shear viscosity as a function of shear rate for 50/50 PA6/ABS blend at different compositions of ABS-g-MAH	143
4.56	Plots of shear viscosity as a function of shear rate for 60/40 PA6/ABS blend at different compositions of ABS-g-MAH	144
4.57	Plots of shear viscosity as a function of shear rate for 70/30 PA6/ABS blend at different compositions of ABS-g-MAH	145
4.58	Power law index, n and consistency index, K for 50/50 PA6/ABS blends with various amount of compatibiliser at 230 °C	147
4.59	Power law index, n and consistency index, K for 60/40 PA6/ABS Blends with various amount of compatibiliser at 230 °C	148
4.60	Power law index, n and consistency index, K for 70/30 PA6/ABS Blends with various amount of compatibiliser at 230 °C	149
4.61	Effects of loss modulus of 60/40 PA6/ABS composite versus frequency at different amount of SGF	150
4.62	Effects of storage modulus of 60/40 PA6/ABS composite versus frequency at different amount of SGF	150
4.63	Effects of complex modulus of 60/40 PA6/ABS composite versus frequency at different amount of SGF	151

4.64	Effects of short glass fibre on the composite $\tan \delta$ of the PA6/ABS blends	153
4.65	Plot of storage modulus, G' versus loss modulus, G'' of 60/40 PA6/ABS composites at different amount of SGF, at 230°	154
4.66	Effect of temperature on shift factor, a_T for 60/40 PA6/ABS Composites	155
4.67	Effect of activation energy for 60/40 PA6/ABS composites with different composition of SGF	156
4.68	Effects of short glass fibre on the composite shear stress of the PA6/ABS blends	157
4.69	Effects of short glass fibre on the composite shear viscosity of the PA6/ABS blends	159
4.70	Power law index, n and consistency index, K for 60/40 PA6/ABS composites with various amount of short glass fibre at 230 °C	160
4.71	FTIR spectra of (a) virgin of PA6, (b) 60/40 PA6/ABS blend compatibilised by 3 wt. % of ABS-g-MAH and (c) virgin of ABS-g-MAH	162
4.72	FTIR spectra of (a) 1 wt. % (b) 3 wt. % and (c) 5 wt. % of ABS-g-MAH in PA6/ABS blends	163
4.73	SEM photographs of fractured of 50/50 PA6/ABS blends at various amount of ABS-g-MAH (a) 0 wt. %, (b) 1 wt. %, (c) 3 wt. % and (d) 5 wt. %	165
4.74	SEM photographs of fractured of 60/40 PA6/ABS blends at various amount of ABS-g-MAH (a) 0 wt. %, (b) 1 wt. %, (c) 3 wt. % and (d) 5 wt. %	166
4.75	SEM photographs of fractured of 70/30 PA6/ABS blends at various amount of ABS-g-MAH (a) 0 wt. %, (b) 1 wt. %, (c) 3 wt. % and (d) 5 wt. %	167

LIST OF ABBREVIATIONS

ABS	Acrylonitrile Butadiene Styrene polymer
ABS-g-MAH	Acrylonitrile Butadiene Styrene-grafted-Maleic Anhydride
CPE	Crosslinked Polyethylene
CaCO ₃	Calcium Carbonate
DMA	Dynamic Mechanical Analyser
DSC	Differential Scanning Calorimetry
EPR-g-MA	Ethylene Propylene Rubber-grafted-Maleic Anhydride
FRP	Fibre reinforced polymer
FTIR	Fourier Transform Infrared
GF	Glass Fibre
GMA-MMA	Glycidyl Methacrylate/Methyl Methacrylate
IA	Imidized Acrylic
LCP	Liquid Crystalline Polymer
MA	Maleic Anhydride
MAP	Maleic Anhydride-grafted-Polypropylene
MFI	Melt Flow Index
MMA-GMA	Poly(Methyl Methacrylate-co-Glycidyl Methacrylate)
MMA-MA	Poly(Methyl Methacrylate-co-Maleic Anhydride)
PA	Polyamide or Nylon
PA/ABS	Polyamide/Acrylonitrile Butadiene Styrene
PA6	Polyamide 6
PA6,6	Polyamide 6,6
PA6/ABS	Polyamide 6/Acrylonitrile Butadiene Styrene
Par	Polyarylate
PB	Polybutadiene
PB-g-MA	Polybutadiene-grafted-Maleic Anhydride
PBT	Poly Butylene Terephthalate
PC	Polycarbonate
PE	Polyethylene
PEEK	Poly(Ether Ether Ketone)
PEI	Poly(Ether Imide)
POE-g-MA	Metallocene Polyethylene-grafted-Maleic Anhydride
PP	Polypropylene
PPO	Polyphenylene Oxide
PPS	Poly(phenylene sulphide)
PVC	Polyvinyl Chloride
SAN	Styrene Acrylonitrile
SANMA	Styrene/Acrylonitrile/Maleic Anhydride
SEBS	Styrene Ethylene Butylene Styrene

SEBS-g-MA	Styrene Ethylene Butylene Styrene-grafted-Maleic Anhydride
SGF	Short Glass Fibre
SMA	Styrene Maleic Anydride
UV	Ultraviolet

LIST OF SYMBOLS

τ_a	Apparent shear stress
η^*	Complex viscosity
ρ	Density
D_f	Desirability factor
X_i	Percentage of component, i , in blend
P_i	Price of component i
$\dot{\gamma}$	Shear rate
$\phi_{polymer}$	Mass fraction of polymer
$\dot{\gamma}_w$	Wall shear rate/actual shear rate
τ_w	Wall shear stress/actual shear stress
τ	Stress
ω	Frequency
γ	Strain
ΔH_c	Heat of crystallisation
ΔH_f	Heat of fusion
ΔH_{mix}	Heat of mixing
ΔH_m	Heat of melting
$\bar{\omega}, \Omega$	Rotational velocity, angular velocity
ΔG_{mix}	Gibbs energy of mixing
η_w	Wall shear viscosity/actual shear viscosity
η_a	Apparent viscosity
$\dot{\gamma}_a$	Apparent shear rate
A	Pre-exponential factor
a_T	Temperature shift factor
c_p	Specific heat
E'	Dynamic mechanical storage modulus
E''	Dynamic mechanical loss modulus
E_a	Energy of activation for viscous flow
F	Force
F_d	Dynamic or Oscillatory force
F_s	Static or Clamping force
G'	Rheological Elastic or storage modulus
G^*	Complex modulus
G''	Rheological Viscous or loss modulus

G_z	Graetz number
HLMI	High load melt index
Hz	Hertz
K	consistency index
L_f	Flow Length
M	Torque
$m, wt.$	weight
MFI	Melt flow index
n	Power law index
P_d	Driving Pressure
Q	Volumetric flow rate
R	Universal gas constant
T	Temperature
Tan δ	Loss tangent delta
T_c	Crytallisation Temperature
T_g	Glass transition temperature
T_m	Melting temperature
V_e	Mean velocity
X_c	Degree of crystallisation
λ	Thermal conductivity
η_o	Zero-shear viscosity

CHAPTER 1

INTRODUCTION

1.1 Introduction

Polyamides (PA)s are a particularly attractive class of polymers due to their good strength and stiffness, low friction and excellent chemical and wear resistance. The beneficial properties have led to the wide range of usage especially in automotive, electrical and mechanical application. However, PAs has some disadvantages associated with their processing instability – high mould shrinkage and dimensional stability – due to inherent properties of rapid crystallisation (Jang and Kim, 2000) and high moisture sensitive because their hygroscopic nature (Acierno and Puyvelde, 2004). These characteristics significantly limit to their utility. Fortunately, the inherent chemical functionality of PA makes them an attractive for modification. Therefore, several efforts have been put forth to minimise the drawbacks by blending with appropriate polymer or material.

Polyamide 6 (PA6) is often blended with suitable elastomers with chemical functionality that can react with PA chain ends. PA6 also can be blended with other

copolymers and reduce water absorption ability. Many authors discussed the approaches of improving the toughness by reacting polymers which contain appropriate chemical functionalities with acid or amine end groups of the PA during melt processing and also blended with elastomers such as Acrylonitrile Butadiene Styrene (ABS) (Kudva *et al.*, 2000; Araujo *et al.*, 2002; Araujo *et al.*, 2003), Ethylene-Propylene-Diene (EPDM), Poly(phenylene oxide), polyolefin elastomer (Wahit *et al.*, 2005; Wahit *et al.*, 2006), ethylene copolymer (Triacca *et al.*, 1991) and natural rubber (NR) (Carone *et al.*, 2000).

The strong reasons behind the blending of ABS with PA6 is that the relatively lower price of ABS compared to PA6, good processibility, low water absorption and high impact strength (Howe and Wolkowicz, 1987). ABS is also stronger than PA6 and low mould shrinkage, even if other mechanical and thermal properties are not as good as PA6. However, blends of PA6 and ABS are immiscible throughout the whole range of compositions and exhibit low impact toughness because large butadiene particles formed during the melt blending process reduce the interfacial adhesion (Tjong *et al.*, 2002). In absence of compatibiliser, such blends lack the interfacial adhesion and generally exhibit poor mechanical properties. Therefore, reactive compatibilisation is the most promising way to enhance the interfacial adhesion and improve the compatibility of PA6 and ABS blends. Few types of compatibiliser have been used in the previous studies of PA6/ABS blends, however, very little literature reported on using ABS-grafted-maleic anhydride as compatibiliser of PA6/ABS blends. Therefore, in this research, a desirable combination of toughness of ABS and rigidity of PA6 will be realised by adding ABS-g-MAH as compatibiliser to enhance the phase adhesion of the blends.

Compatibilised PA6/ABS blends still have a few weaknesses, even though other properties could be improved. It has been shown that the strength of PA6/ABS blend especially tensile strength is lower than the virgin PA6 (Meincke *et al.*, 2004; Kudva *et al.*, 2000) and depending on the ratio of PA6 added into the blends (Cho and Paul, 2001), impact property became poorer when the proportion of PA6 in the system was decreased (Chiu and Hsiao, 2004). The PA6 blends can be 'supertough' that is, having Izod impact strength higher than 800 J/m (Cho and Paul, 2001)

however; it is believe that, the incorporation of a rubber phase in PA6 reduces the strength and stiffness relative to virgin PA6. Consequently, the blends of PA6 with ABS are still not a right answer to become an alternative material and will not contribute synergistic effects for the both properties. Reinforcement by inorganic (Tjong and Xu, 2001) or short glass fibre (Nair *et al.*, 1997) can restore the required strength and stiffness of rubber toughened PA6s, leading to the formation of ternary or hybrid composites.

The additions of rubber or elastomeric materials such as ABS into PA6 lead to a reduction of strength and stiffness. In contrast, reinforcing thermoplastics by short glass fibre (SGF) will improve both strength and high mechanical stiffness (Tjong *et al.*, 2000; Fu *et al.*, 2000) but a high content of glass fibres are necessary to achieve high strength and high stiffness (Fu and Lauke, 1998; Fu *et al.*, 2000; Bader and Collins, 1983; Biolzi *et al.*, 1994). Unfortunately, there was considerable loss in toughness and ductility when these short glass fibres were incorporated to the composite (Ahn and Paul, 2006). As a result, the combination of reinforcement and ABS will balance the impact and stiffness of the materials.

Some questions would arise; will this composite be easily processed through injection moulding process or any other thermoplastics processing conditions? Will this composite material be easily moulded to form small and critical part especially in automotive? Most of the composite materials containing fibres are difficult to produce by injection moulding due to its high viscosity. The composite materials are then processed either by using compression moulding or extrusion. Thus, in order to investigate the processibility, the rheological properties of the composite have to be thoroughly investigated by using rheological apparatus such as dynamic and capillary rheometer.

1.2 Problem statements

The important reason in polymer blend either reinforced or non-reinforced development is to achieve a good combination set of properties and processibility. Since, only a few literature reviews have been reported on short glass fibre reinforced PA6/ABS composites, it is the objective of the present research to investigate specifically the dynamic mechanical and rheological properties of the composites. Until the present time, the rheological properties of non-reinforced PA6/ABS blends have only been studied for a narrow range of compositions (Jafari *et al.*, 2002).

Followings are the current problem to be investigated, discussed and explained in the present study.

- i. How the composition of SGF affects the thermal properties of the composites?
- ii. Does the dynamic mechanical and mechanical properties of the composites improved by incorporation of SGF?
- iii. What is the rheological behaviour of the composites when the amounts of SGF vary from 0 up to 30%?
- iv. What is the optimum composition of short glass fibre, referring to the dynamic mechanical and rheological properties?

1.3 Objectives

This present study has three stages of sub-study. First is to study the effect of ABS in PA6 blends without compatibiliser. This study focuses on mechanical properties and thermal properties. The study on the effect of compatibiliser in the blends will be conducted in the second stage.

The study on the dynamic mechanical and rheological properties of polymer blends is of great theoretical and practical importance that will help to understand the dynamic mechanical behaviour of the blends and the rheological properties of polymer blends and composites.

While prior research has been performed on the rheology and dynamic mechanical properties of PA6/ABS blends, more extensive analysis on the glass fibre reinforced PA6/ABS composites is still quite necessary due to many questions still unanswered. This study dealt on the dynamic mechanical, processing, thermal, and morphology of the PA6/ABS blends and compositions. Direct outcomes of this research may lead to factors that may or enhance desired properties in automotive parts. Overall, the objectives of this study are:

- i. To study the effects of incorporating various composition of SGF on PA6/ABS composites on thermal properties.
- ii. To investigate the improvement with introduction of glass fibre into PA6/ABS composites on dynamic mechanical and mechanical properties of automotive parts.
- iii. To explore the rheological behaviour of the composites by increasing the amount of SGF from 0 to 30 wt. %.
- iv. To determine the optimum composition of SGF, referring to the dynamic mechanical and rheological properties.

1.4 Scopes of Study

In order to achieve the objectives, the scopes covered are as follows:

1. Sample preparation of PA6/ABS blends

- In this work, sample was prepared using melt intercalation method which was carried out using a twin-screw extruder over the set range of compositions between ABS, PA6 and ABS-g-MAH. This was followed by the injection moulding process to prepare test specimen according to the ASTM testing standard.
- There were two set of samples with the set of range composition prepared for testing and analysing: uncompatibilised PA6/ABS blends and compatibilised PA6/ABS blends.
- The PA6 contents in PA6/ABS blends range from 70% - 50% weight ratio. While, the ABS-g-MAH percentage as compatibiliser was varied from 1, 3 and 5 wt. %.

2. Sample preparation of PA6/ABS composites

- The composite samples were prepared using melt intercalation method.
- The PA6, ABS and ABS-g-MAH composition were selected based on the optimum ratio which was obtained from the study of polymer blends.
- The amounts of glass fibre were added into PA6/ABS blends gradually from 0 to 30 wt. %.

3. The entire samples specimens were tested in order to study the mechanical and dynamic mechanical properties: - tensile, flexural and impact for automotive parts according to ASTM standard as well as dynamic mechanical analysis (DMA).
4. Differential Scanning Calorimetry (DSC) was used to investigate the compatibility of the sample by obtaining thermal properties; the glass transition temperature, melting temperature and degree of crystallinity.
5. Rheological studies – capillary and rotational rheometer were used to investigate the rheological parameters of polymer composites and blends.
6. Scanning electron microscopy analysis was carried out to evaluate the morphology of the blends and composites.
7. Fourier transforms infrared analysis was carried out to confirm the reaction during melt intercalation process.
8. Scanning electron microscopy was carried out to investigate the morphological structure of the samples.

CHAPTER 2

LITERATURE REVIEW AND THEORY

2.1 Polymer Blends

Polymers blends play an important role in widen the plastics application because of their ability to produce new products with a wide range of properties interest with minimal investment (Paul, 1978) and became one of the fastest growing segments of polymer technology in commercial applications and developments (Utracki *et al.*, 1989). The term polymer blend can be used to describe a mixture of at least two macromolecular substances, polymers or copolymers (Utracki, 2002). Another word is a polymer alloy; it can be described as an immiscible polymer blend with a distinct phase-morphology (Utracki, 1990) or with stabilised morphologies (Utracki *et al.*, 1989). An interpenetrating polymer network is also a polymer blend in which one or more components undergo polymerization or crosslinked in the presence of the other (Utracki *et al.*, 1989). Another term being adopted in this study is compatible polymer blends, which indicate commercially useful materials, a mixture of polymer without strong repulsive forces that is homogenous to the eye (Utracki *et al.*, 1989). Other terms can be

used to describe polymer blends for example compatibilised polymer blends and these primarily relate to state of miscibility of the blend.

The polymer blends are classified as either miscible and immiscible; the former defined as homogenous down to the molecular level, having the negative free energy of mixing: $\Delta G_{mix} \approx \Delta H_{mix} \leq 0$ and a positive value of the second derivative: $\partial^2 \Delta G_{mix} / \partial \phi^2 > 0$, where ϕ , G_{mix} and H_{mix} are the volume fraction of the dispersed phase, Gibbs energy of mixing and heat of mixing, respectively. Most polymer pairs are immiscible (Kumar and Gupta, 1998; Utracki, 1990) and need to be compatibilised to achieve a stable morphology and set of performance characteristics. The blending process of two polymers can be melted-blending in an extruder or dissolved in a common solvent and then removing the solvent, however, the procedure does not ensure that the two polymers will mix on a microscopic level. It is well known that the production of miscible, immiscible binary and ternary blends of polymers can lead to composite materials with special chemical, thermal, mechanical and rheological properties. These materials normally have more favourable properties than those of their pure constituents. These properties include reduced viscosities; improved moduli and tensile strength (Sridan *et al.*, 1998; Shonaik *et al.*, 1995; Fayt *et al.*, 1982) induced by processing (Pellerin *et al.*, 2000; Doi and Ohta, 1991) and enhanced crystallinity (Guschl *et al.*, 2002; Chen and Porter, 1993). Typical polymer blends consists of two or more dissimilar materials such that the resultant blend will have combined properties of each constituent. The blending of a semicrystalline polymer (ductile) with an amorphous polymer (brittle) also will end up with a material with both elastic and rigid characteristics, depending on the amount/composition/proportions of the blending constituents.

2.2 Overview of polymer composite

Introduced over 50 years ago, composites are fibre-reinforced plastics used in a variety of products, applications and industries. The term "composite" can apply to any combination of individual materials consisting two or more distinct phases with an interface between them (Karger-Kocsis, 2000). Composites focus on fibres, primarily glasses that have been impregnated with a plastic resin matrix. Combining glass fibres with resin matrix is resulted in composites that are strong, lightweight, corrosion-resistant and dimensionally stable. They also provide good design flexibility and high dielectric strength, and usually require lower tooling costs. Because of these advantages, composites are being used in a wide variety of applications, such as sport and leisure and as replacement of automotive part. Their tremendous strength-to-weight and design flexibility make them ideal in structural components for the transportation industry. High-strength lightweight premium composite materials such as carbon fibre and epoxies are being used for aerospace applications and high performance sporting goods. Their superior electrical insulating properties also make them ideal for appliances, tools and machinery. Tanks and pipes constructed with corrosion-resistant composites offer extended service life over those made from metals.

The roles of matrix in the composite are as follows:-

- for transferring the load from the matrix to the reinforcement
- for distributing the stress among the reinforcement's elements
- for protecting the reinforcement from environmental attack
- for positioning the reinforcing material

Meanwhile, the reinforcement functions is to carry the load and interface (2 dimensions) or interphase (3 dimensions) is a negligible or finite thin layer with its own

properties, and to transfer the stress from the matrix to the reinforcement (Karger-Kocsis, 1996).

One of composite main advantages is how their components for example glass fiber and resin matrix complements each other. While thin glass fibres are quite strong, they are also susceptible to damage. Certain plastics are relatively weak, yet extremely versatile and tough. Combining these two components together, however, results in a material that is more useful than either is separately. With the right fibre, resin and manufacturing process, designers can tailor composites to meet final product requirements that could not be met by using other materials. The purpose of reinforcement in the polymeric material is aimed to improve the toughness of the composites, and achieving the desired balance between stiffness and toughness, also to reduce the brittleness of matrix and inhibits notch sensitivity. The goals of the polymer composite also are to improve the heat distortion temperature and reduce some environmental effects such as water susceptibility and reduce the cost of materials and processing. The mechanical performance of the related composites also can be tailored by adding a coupling agent, compatibiliser and impact modifier. As a result, these added materials improve the interfacial adhesion between the reinforcement and matrix.

Factors affecting the mechanical performance of reinforced thermoplastics blends are summarised in Figure 2.1: -

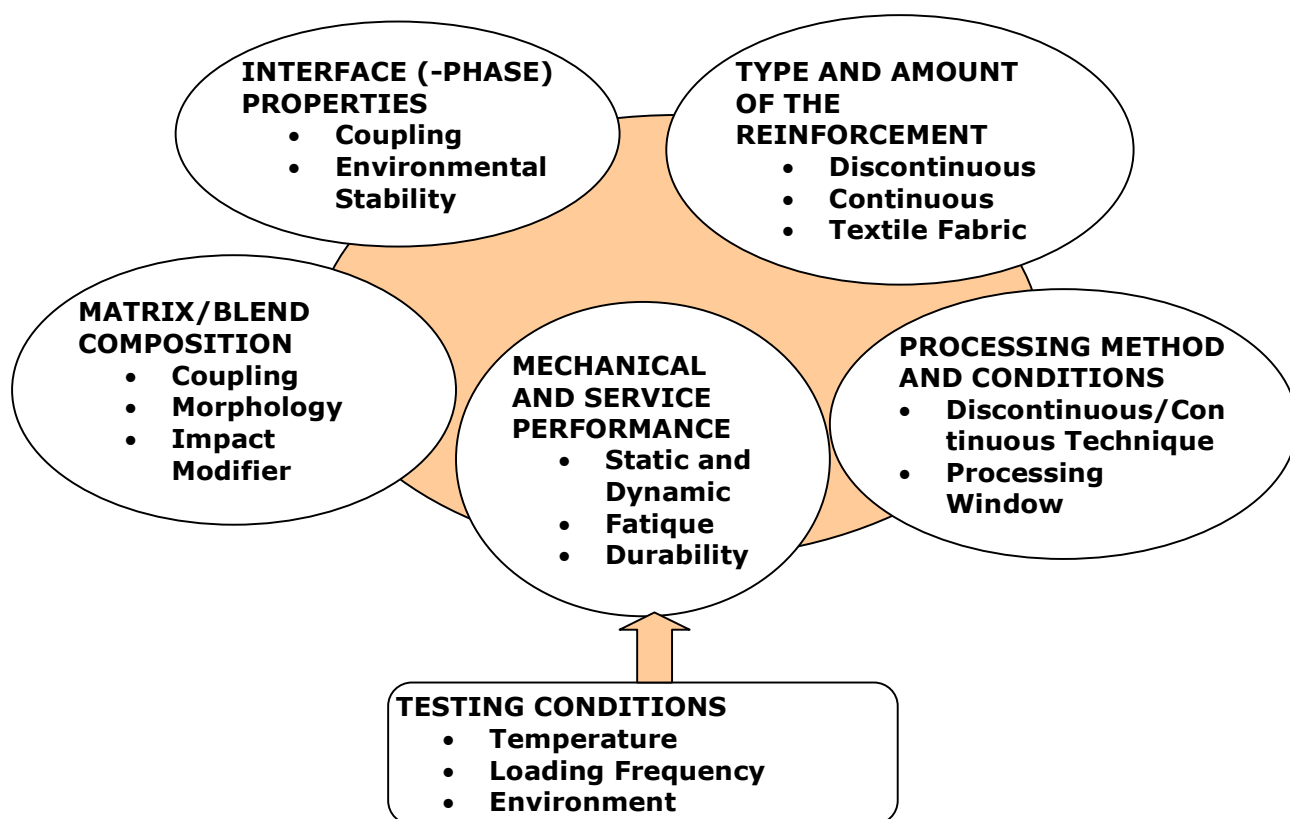


Figure 2.1 : Factors influencing the mechanical performance of reinforced polymer blends (Karger-Kocsis, 2000).

2.3 Compatibilisation of Polymer Blends and Composites

Compatibility is affected by the nature and extent of the wetting and absorption phenomena which is associated with adhesion. Compounds that are used in promoting adhesion in polymer blends are known as “coupling agents”, “compatibiliser”, “filler” and interfacial agents”. The common word being used in this field of study is compatibilisation. Compatibilisation is a process of modifying the interfacial properties of immiscible polymer blend, resulting in reduction of the interfacial tension coefficient, formation and stabilization of the desired morphology (Utracki, 2002). Therefore, the

compatibilisation is an essential process that converts a mixture of polymer into alloy that has the desired set of performance characteristics.

Blending of two different polymeric materials involves several steps that could produce blends with stable and reproducible properties. Since the material performances depend on morphology, so it must be optimized for the desired performance, i.e., during forming to be either stable or reproducibly modifiable.

The compatibilisation methods can be divided into two categories (Utracki, 2002):

- a) By addition of : (i) a small quantity of a third component which is miscible with both phases (co-solvent); (ii) a small quantity of copolymer which will miscible into both polymer phases; (iii) a large amount of a core-shell, multi purpose compatibiliser-cum-impact modifier.
- b) By reactive compatibilisation, which uses these strategies; (i) trans-reactions; (ii) reactive formation of graft, block or lightly crosslinked copolymer; (iii) formation of ionically bonded structures; and (iv) mechano-chemical blending that may lead to chain's breakage and recombination.

As have been mentioned by many researchers, that most of polymer pairs or blends are immiscible and therefore must be compatibilised by means of either one of the above method before they can be rendered "useful". According to Utracki (2002) the goals of compatibilisation process are as follows:

- a) To adjust the interfacial tension, thus engender the desired dispersion
- b) To ensure that the morphology generated during the alloying stage will yield optimum structure during the forming stage

- c) To enhance adhesion between the phases in the solid state, facilitating the stress transfer hence improving performance

2.4 Overview of polymer rheology

The science of deformation and flow is called rheology, and the flow properties of polymer are called rheological properties. The word rheology is derived from the Greek word, “rheos” meaning flow. Rheology is used to measure, describe, explain and apply the phenomena of plastics deformation and flow occurring in bodies on being deformed (Kirschke, 1976; Han, 1976). Another definition of rheology that can be found in most rheology textbooks is the science of flow and deformation of matter (Gupta, 2000; Carreau *et al.*, 1997; Barnes *et al.*, 1989; Cogswell, 1981). Definition by Morrison (2001) stated the rheology is the study of the flow of materials that behave in an interesting or unusual manner.

All the definitions do not specify whether the material is a solid or fluid because it can be applied to both materials. Like fluids, solids also undergo deformation and flow such as that occur in metal forming and stretching of rubber. Sometimes the flow of solids is very slow and unnoticeable for example creeping flow of polymer solids and soil movement. However, mostly the term of rheology is most commonly applied to the study of fluids or fluid-like materials such as paint, oil well drilling mud, blood, polymer solutions and molten polymers in which flows are more pronounced. Accordingly, the two key words in the definition of rheology are deformation or flow and force (Dealy and Wissbrun, 1990). Rheology is concerned with the description of the deformation of the material under the influence of stresses (Shenoy, 1999). In order to learn anything about the rheological properties of material, one must either measure the deformation

resulting from a given force or measure the force required to produce a given deformation.

Polymeric materials like any other materials are in need of forming process in order to make them useable. Regardless of the materials, any forming process involves deformation and flow, which transform them into shapes that are desired or required. Examples of forming processes for polymeric materials are injection moulding, extrusion, compression moulding and blow moulding. Generally, the polymeric materials are subjected to deformation induced by parameters such as pressure and temperature and are forced to flow in confined geometries such as barrels, runners, dies and moulds which directly or indirectly contribute to the final shapes. The flow that occurs inside these geometries can strongly influence the physical nature of the product. Therefore, it is important to understand the flow characteristics or patterns in which polymeric material flows, i.e. polymer rheology. A better understanding of polymer rheology is an essential step to the successful processing of polymeric materials.

Success in achieving good properties in a polymer system depends on understanding the behaviour of the polymer during processing and preparation (Borgaonkar, 1998). Most of polymer processing, including reshaping or forming are done in the molten phase. Therefore, amorphous polymer exhibits softening temperature range in which all the random chain entanglements slowly unwind, and flow of the polymer chains past each other occur, depending on the direction of the shear force.

In the 1970s, there has been a steadily growing interest, among both academic and industrial communities, in applying the fundamental concepts of rheology to polymer operations (Dealy and Wissbrun, 1990). The true interplay between rheology and polymer processing seems to have just started, and there are a number of challenging and difficult questions to be answered in many polymer operations of industrial importance.

The mechanical properties of multi-component polymer materials are first determined by the properties of the constituent polymers. However, to a high degree, they are influenced by the blend morphology, which in turn it depends on the thermodynamic interactions between the two polymers; the rheological behaviour of the constituents and the processing conditions (Xu *et al.*, 1999). Rheological studies can give access to information pertaining to the structure, morphology and processing of the materials (Utraki, 1993). Rheology is a key in polymer research, being an important link in the so-called 'chain of knowledge' reaching from the production of polymers to their end-use properties (Markus, 2001). So, the understanding of polymer rheology is the key to effective design material plus process selection, to efficient fabrication, and satisfactory service, yet few engineers make adequate use of what is known and understood in polymer rheology (Lenk, 1978).

2.5 Significance of rheological properties studies

A very common reason for the study of rheological properties is for the purpose of quality control where the raw materials must be consistent from batch to batch as such as flow behaviour is an indirect measure of product consistency and quality. Therefore, rheological properties are very important in quality control line during production or to process control in predicting and controlling a host of raw material and product properties, end-use performance and material behaviour.

Another reason for study of flow behaviour is that a direct assessment of processibility can be obtained. Knowing its rheological behaviour of polymer is useful when designing the process and usage of the polymeric materials for automotive application. It has also been suggested that rheology testing is the most sensitive method

for material characterization because flow behaviour is closely associated to properties such as molecular weight and molecular distribution.

Having a rheological knowledge is important in providing understanding of a forming process, which is considered as the heart of product fabrication. In polymer processing, an understanding of polymer rheology is the key to effective design, material and process selection, efficient fabrication and satisfactory service performance (Lenk, 1978). Usually, rheological data is used in determining whether or not a type of polymer can be extruded, moulded and shaped into a practical and useable product. In commercial processing, molten polymer is forced to flow through orifice or die as well as into cavities that may have various shapes. If the viscosity of the molten polymer is not suitable with processing conditions, defects may occur during a pre and post-processing.

Other than polymer processing, one of the main fields in polymer studies concentrates on the end properties and applications of polymer products where properties such as mechanical and physical properties are very important. Of course, these properties are influenced by rheological behaviour. Deformation and flow result in molecular orientation, which has dramatic effects on physical and subsequently mechanical properties of moulded parts, profile extrudates and films. The kind and degree of molecular orientation are largely determined by rheological behaviour of the polymer and the nature of the flow in the fabrication process (Gupta, 2000).

The extent of understanding rheology relies on the individual's needs and desires. Brydson (1981) has concluded that rheological study can lead to many benefits, as follows:

- a) It is possible to understand processing faults and defects which are of rheological origin and hence make logical suggestions for adjusting the processing conditions for either minimizing or completely removing the fault.

- b) It is possible to make a more intelligent selection of the best polymer or polymer compound to use under a given set of circumstances.
- c) It can lead to quantitative and to some extent quantitative, relationship between such factors as output, power consumption, machine dimensions, material properties and operational variables such as temperature and pressure.
- d) There are some, limited, use in providing information on molecular structure.

2.6 Application of rheology to polymer processing

Polymer processing operations resemble those of classical mechanical or chemical unit operations, which involve momentum, energy and mass transport of polymeric materials. Some representative polymer operations of industrial importance are extrusion, injection moulding, blow moulding and thermoforming (McKelvey, 1962; Pearson and Richardson, 1983; Tadmor and Gogos, 1979). However, because of the special characteristics (i.e. viscoelasticity) those polymeric materials possess, polymer processing operations are usually more complex than mechanical or chemical engineering unit operations. A good understanding of polymer operations requires knowledge of several branches of science and engineering, such as polymer chemistry, mechanics of non-Newtonian viscoelastic fluids and macromolecular behaviour under deformation, which is often accompanied by heat and mass transfer and/or chemical reactions.

The study of polymer operations demands the knowledge of the relationship between processing variables, mechanical properties and molecular parameters with the flow or rheological properties as shown in Figure 2.2.

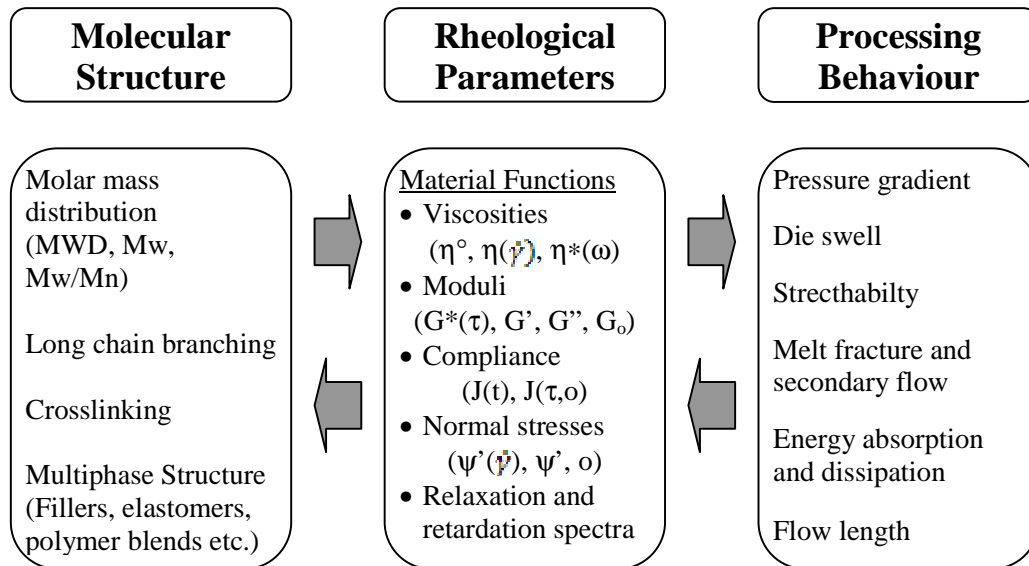


Figure 2.2. Rheological parameters acting as a link between molecular structure and final properties a polymer (Markus Gahleitner, 2001)

Figure 2.2 further shows that there are a number of areas where a better understanding of rheology can assist polymer processing operations. One such area is the characterisation of polymeric materials in terms of their viscoelastic properties either by using existing rheometers or developing new rheometers (Cogswell, 1981; Barnes *et al.*, 1989). Better understanding of the rheological properties would help in determining the molecular weight and molecular weight distribution of a polymer in order to provide optimum processing condition or achieve desired properties in the final product..

Rheology also help in determining optimal design of processing equipment, such as extrusion die, extrusion screws, various moulds for injection moulding and mixing

devices (Tadmor and Gogos, 1979; Micheali, 1992). A proper design of processing equipment requires information of flow properties of the material under consideration. For instance, in an extrusion operation, geometrical factors such as die entrance angle, the screw length-to-diameter ratio and the reservoir-to-capillary diameter ratio may significantly affect processing conditions and subsequently the mechanical and/or physical properties of the final product.

Besides experimental or practical assistance, rheology also helps to polymer processing in carrying out theoretical analysis of the flow mechanics of rheologically complex polymeric materials in various kinds of processing equipment. Theoretical analysis requires a rheological model, which describes reasonably well the flow behaviour of the material under consideration. Hence, given a flow field of a particular material, the development of an acceptable rheological model is very important to the success of the theoretical study of flow problems. Such a theoretical study should be useful for designing better processing equipment and determining optimal processing conditions (Han, 1976). Therefore, understanding the relationships between the rheological properties and processing conditions is essential to develop criteria for evaluating the processability of the plastics and optimizing the process (Bargaonkar, 1998).

Besides of the explanation above, in a composite technology, polymer scientists are interested because of the need to develop and process new composite materials with desired physical and mechanical properties. Therefore, the rheological behaviour of composite materials is not only governs the performance of end-products but also controls the fluid and heat transfer characteristics during polymer processing (Hsieh, 1982).

2.7 Rheometers

2.7.1 Introduction

Rheology includes almost every aspect of the study of deformation of materials under the influence of imposed stress; and rheometric techniques help to define the flow properties of materials from a practical view. Commercial interest in synthetic polymers has been the greatest impetus to the science of rheology. The rheology of a material dictates whether or not the polymer can be processed, shaped, and formed into desired product in an efficient and economical manner, at the same time maintains dimensional stability and high quality.

Rheometers are instrument designed to measure the rheological properties of materials. Most rheometers are built on the principle of shear deformation; the quantity measured by rheometers either force, pressure drop or torque that is directly related to the shear stress. The simplest type of shear deformation is “simple shear”, which is the deformation generated when a material is placed between two parallel flat plates and one of the two plates is then translated, while the gap between the plates is kept constant. If the gap is y and the linear displacement of the moving plate is Δx , then the deformation generated is the “shear strain”, γ , given by (see Figure 2.3):

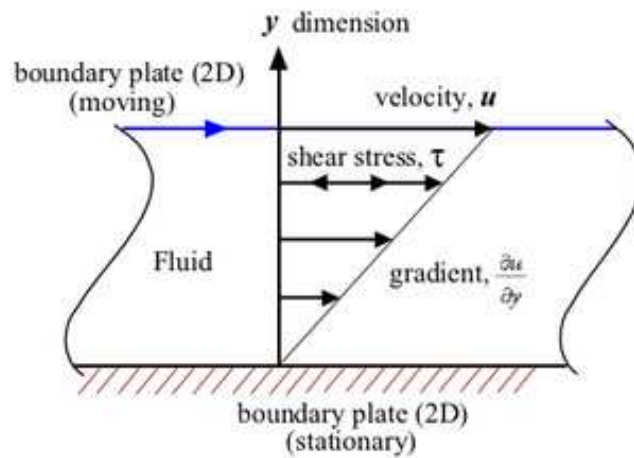


Figure 2.3: Shear flow results when plates move past one another

$$\gamma = \frac{\Delta x}{y} \quad (2.1)$$

If the plate moves at a constant velocity, u , then the “shear rate”, $\dot{\gamma}$ is

$$\dot{\gamma} = \frac{u}{y} \quad (2.2)$$

The quantity measured is the shear stress, τ , defined, as the force required to move the plate, divided by the area of the plate wetted by the material being deformed.

$$\tau = \frac{F}{A} \quad (2.3)$$

Such an arrangement can be used to measure rheological properties by displacing the moving plate in some prescribed way and measuring the resulting shear stress, τ . The

rheological behaviour can then be described by giving the relationship between the stress and the shear strain or the shear rate.

Materials consisting of a single liquid phase and containing only low molecular weight, mutually soluble components, are usual Newtonian fluids under normal conditions. For a Newtonian fluid, the shear stress, τ , is proportional to the shear rate, $\dot{\gamma}$. This can be expressed quantitatively by the following equation:

$$\tau = \eta \dot{\gamma} \quad (2.4)$$

where η is the viscosity of the fluid. For a Newtonian fluid the viscosity depends on composition and temperature but not on the shear rate. Many materials processed commercially are multiphase fluids, which include fermentation broths, mineral slurries, paints and foodstuffs. Another important category of materials is polymeric liquids, either polymer solutions or molten resins. All these materials can be non-Newtonian. The simplest manifestation of non-Newtonian behaviour is that the viscosity varies with the shear rate in steady simple shear, thus the relationship between them can be written as follows,

$$\frac{\tau}{\dot{\gamma}} = \eta(\dot{\gamma}) \quad (2.5)$$

where η is the viscosity. The most common type of non-Newtonian behaviour is that the viscosity decreases as the shear rate increases, and such a material is said to be “shear thinning” or pseudoplastics. Some concentrated suspensions can exhibit the opposite type of behaviour with η increasing with $\dot{\gamma}$, known as “shear thickening” or dilatant fluid. A simple empirical equation, the “power law” viscosity model for describing the dependence of viscosity on shear rate over a certain range of shear rates is shown below:

$$\eta = K\dot{\gamma}^{n-1} \quad (2.6)$$

where n and k are the power law index and consistency index, respectively. When $n = 1$, Newtonian behaviour is indicated, while $n < 1$ implies shear thinning behaviour, and $n > 1$ implies shear thickening behaviour.

Polymeric liquids exhibit a combination of elastic and viscous flow and called as “viscoelastic”. Consequently, their rheological properties are also time dependent. The viscoelastic properties of polymeric fluids, in particular the storage and loss moduli defined below, can be very useful for measuring of the extent of dispersion of particular filler. Polymer viscoelasticity is usually described in terms of response of fluid to a sinusoidal shearing, where the shear strain is given by

$$\gamma(t) = \gamma_0 \sin(\omega t + \delta) \quad (2.7)$$

where ω is the frequency of the oscillatory strain, δ is the phase angle or mechanical loss angle and γ_0 is the strain amplitude. If the strain amplitude is sufficiently small, the shear stress is also sinusoidal and is given by

$$\tau(t) = \tau_0 \sin(\omega t + \delta) \quad (2.8)$$

where τ_0 is the stress amplitude. τ_0 at a given frequency is proportional to γ_0 , if the strain is sufficiently small. This type of behaviour is called linear viscoelasticity. The linear viscoelasticity could be described using trigonometric identity as follows:

$$\tau(t) = \gamma_0 [G' \sin(\omega t) + G'' \cos(\omega t)] \quad (2.9)$$

where $G'(\omega)$ is the storage modulus and $G''(\omega)$ is the loss modulus, which are functions of frequency. Both are linear viscoelastic material functions.

Another term of importance is the ratio of loss to storage modulus defined as

$$\text{Loss tangent: } \frac{G''(\omega)}{G'} = \tan \delta \quad (2.10)$$

It is also possible to define a dynamic complex viscosity in terms of G' and G'' as follows:

$$\text{Dynamic viscosity : } \eta'(\omega) = \frac{G''(\omega)}{\omega} \quad (2.11)$$

$$\text{Imaginary part of the complex viscosity : } \eta''(\omega) = \frac{G'(\omega)}{\omega} \quad (2.12)$$

$$\text{Complex viscosity function : } \eta^*(i\omega) = \eta'(\omega) - i\eta''(\omega) \quad (2.13)$$

In the same manner as above, a complex modulus can be defined as below :

$$\text{Complex viscosity function : } G^*(i\omega) = G'(\omega) + iG''(\omega) \quad (2.14)$$

The storage modulus $G'(\omega)$ and imaginary part of the complex viscosity $\eta''(\omega)$, are to be considered as the elastic contributions to the complex functions. They are both measures of energy storage. Similarly, the loss modulus $G''(\omega)$ and the dynamic viscosity $\eta'(\omega)$ are the viscous contributions or measures of energy dissipation.

2.7.2 Measuring the Rheological Parameters

2.7.2.1 Capillary Rheometer

Capillary rheometers are the most popular of all rheometers, because of their simplicity in design and use. The basic principle of a viscosity measurement is the measurement of the pressure drop of a given flow rate. Alternatively, one can fix the pressure drop and measure the flow rate. They are broadly categorized as constant speed rheometers and constant pressure rheometers.

For fully developed flow in a tube, i.e. far from the entrance, both the pressure gradient and the velocity profile do not change with distance, z , along the tube. By carrying out a force balance on a length, Δz , of tube, it can be shown that the shear stress at the wall, τ_w , is related to the pressure P_d , P_L , at the upstream and downstream ends, of this length, and to the radius, R , of the tube.

$$\tau_w = \frac{(P_d - P_L)R}{2\Delta z} \quad (2.15)$$

This schematic of a rheometer is shown in Figure 2.4.

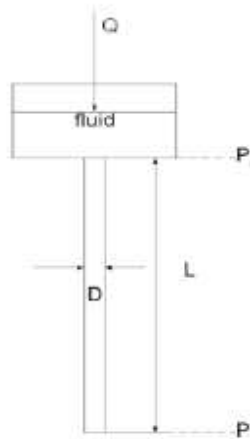


Figure 2.4 : Sketch of Capillary Rheometer Geometry

However, the common practice is to measure only the driving pressure P_d , in the reservoir feeding the tube rather than measure pressure at the two points in the fully developed flow region. If the pressure at the exit of the tube, P_t i.e. at $z = L$, is atmospheric, and this is assumed to be small compared to P_d , an apparent wall shear stress, τ_a , can be calculated

$$\tau_a = \frac{P_d R}{2L} \quad (2.16)$$

For a Newtonian fluid, the velocity profile is parabolic, and the shear rate at the wall is expressed as

$$\dot{\gamma}_w = \frac{4Q}{\pi R^3} \quad (2.17)$$

Thus, if Q is flow rate and fixed and P_d is measured, the viscosity can be calculated from Hagen-Poiseuille equation

$$\eta = \frac{\tau_w}{\dot{\gamma}_w} = \frac{\pi R^4 p_d}{8LQ} \quad (2.18)$$

If the fluid is non-Newtonian, i.e. if the viscosity depends on the shear rate, there is a technique to determine the true wall shear rate in such a case, but it requires the differentiation of pressure data for a number of flow rates. In this case it is convenient to define an apparent wall shear rate as follows:

$$\dot{\gamma}_a = \frac{4Q}{\pi R^3} \quad (2.19)$$

For the power law n , fluid, the true wall shear rate is given by:

$$\dot{\gamma}_w = \frac{3n+1}{4n} \dot{\gamma}_a \quad (2.20)$$

The value of n can be significantly different from 1 for many materials, so the difference between $\dot{\gamma}_a$ and $\dot{\gamma}_w$ can be large. Most capillary viscometers give as an output signal an “apparent viscosity” calculated as follows:

$$\eta_a = \frac{\tau_a}{\dot{\gamma}_a} = \frac{\pi R^4 p_d}{8LQ} \quad (2.21)$$

2.7.2.2 Rotational Rheometer

This flow geometry is illustrated in Figure 2.5. The shear rate varies linearly with radius, r , and is given by

$$\dot{\gamma} = \frac{\Omega r}{h} \quad (2.22)$$

where h is the gap between the disks, and Ω is the rotational velocity. For a Newtonian fluid, the viscosity is related to the torque as follows:

$$\eta = \frac{2Mh}{\pi\Omega R^4} \quad (2.23)$$

where R is the radius of the disk and M is the measured torque.

The cone-and plate rheometer is of special interest because the shear rate is approximately constant between the fixtures and is given by

$$\dot{\gamma} = \frac{\Omega}{\theta} \quad (2.24)$$

Where θ is the cone angle, usually less than 5° , and Ω is the angular velocity. For the ideal geometry shown in Figure 2.6, the apex of the cone just touches the plate without transmitting torque to it.

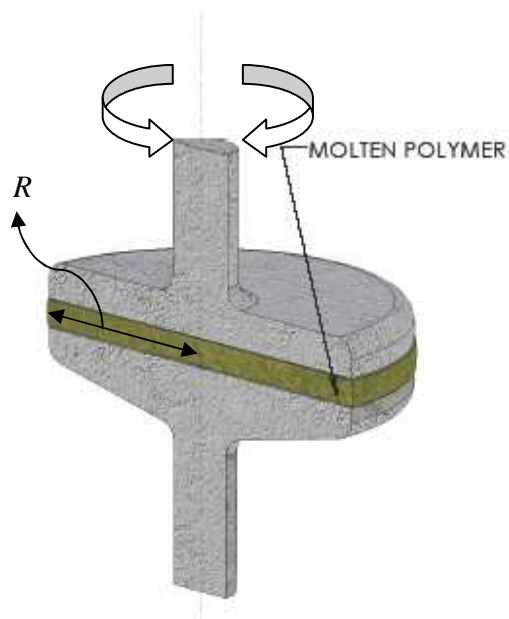


Figure 2.5 : Sketch of parallel disk rheometer geometry

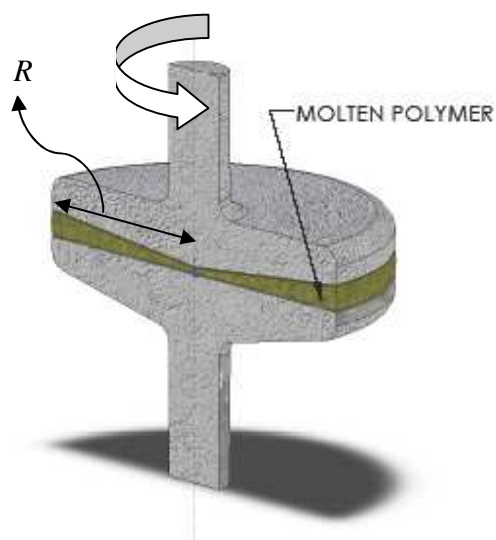


Figure 2.6 : Sketch of Cone and Plate Geometry.

The shear stress is therefore approximately uniform and is given by

$$\tau = \frac{3M}{2\pi R^3} \quad (2.25)$$

where M is the torque to turn the cone and R is the radius of the plate. Thus, the viscosity is

$$\eta = \frac{3M\theta}{2\pi\Omega R^3} \quad (2.26)$$

Because of the uniformity of the shear rate, it is valid for non-Newtonian fluids.

2.8 Dynamic Mechanical Analysis (DMA)

Dynamic mechanical analysis (DMA) is becoming more commonly seen in the analytical laboratory as a tool rather than a research curiosity. This technique is still treated with reluctance and unease, probably due to its importation from the field of rheology. DMA does not require a lot of specialised training to use for material characterisation. It supplies information about major transitions as well as secondary and tertiary transitions not readily identifiable by other methods. It also allows characterisation of bulk properties directly affecting material performance.

DMA can be described as applying an oscillating force to a sample and analyzing the material's response to that force. Therefore, the tendency to flow (called viscosity) from the phase lag and the stiffness (modulus) from the sample recovery can be calculated. These properties are often described as the ability to lose energy as heat

(damping) and the ability to recover from deformation (elasticity). One way to describe is the relaxation of the polymer chains (Matsuoka, 1992). Another way would be to discuss the changes in the free volume of the polymer that occur (Brostow, 1986). Both descriptions allow one to visualize and describe the changes in the sample.

The applied force is called stress. When subjected to a stress, a material will exhibit a deformation or strain. The stress–strain curves are common to researchers who are working with materials. These data have traditionally been obtained from mechanical tensile testing at a fixed temperature. The slope of the line gives the relationship of stress to strain and is a measure of the material's stiffness, the modulus. The modulus is dependent on the temperature and the applied stress. The modulus indicates the suitability of the material in applications. If the polymer is heated, it passes through its glass transition and changes from glassy to rubbery; the modulus will often drop significantly. This drop in stiffness can lead to serious problems if it occurs at a temperature different from expected.

The modulus measured in DMA is, however, not exactly the same as the Young's modulus of the classic stress–strain curve. Young's modulus is the slope of a stress–strain curve in the initial linear region. In DMA, a complex modulus (E^*), an elastic modulus (E'), and an imaginary (loss) modulus (E'') (McCrum *et al.*, 1991) are calculated from the material response to the sine wave as seen in Figure 2.8. DMA measures the amplitudes of the stress and strain as well as the phase angle (δ) between them. This is used to resolve the modulus into an in-phase component - the storage modulus, E' - and an out-of-phase component - the loss modulus, E'' and a useful quantity is the damping factor or loss tangent ($\tan \delta$) which is the ratio E''/E' and is the amount of mechanical energy dissipated as heat during the loading/unloading cycle. The relationship between these quantities and the dynamic (or complex) modulus (E^*) are represented by the diagram as shown in Figure 2.9:

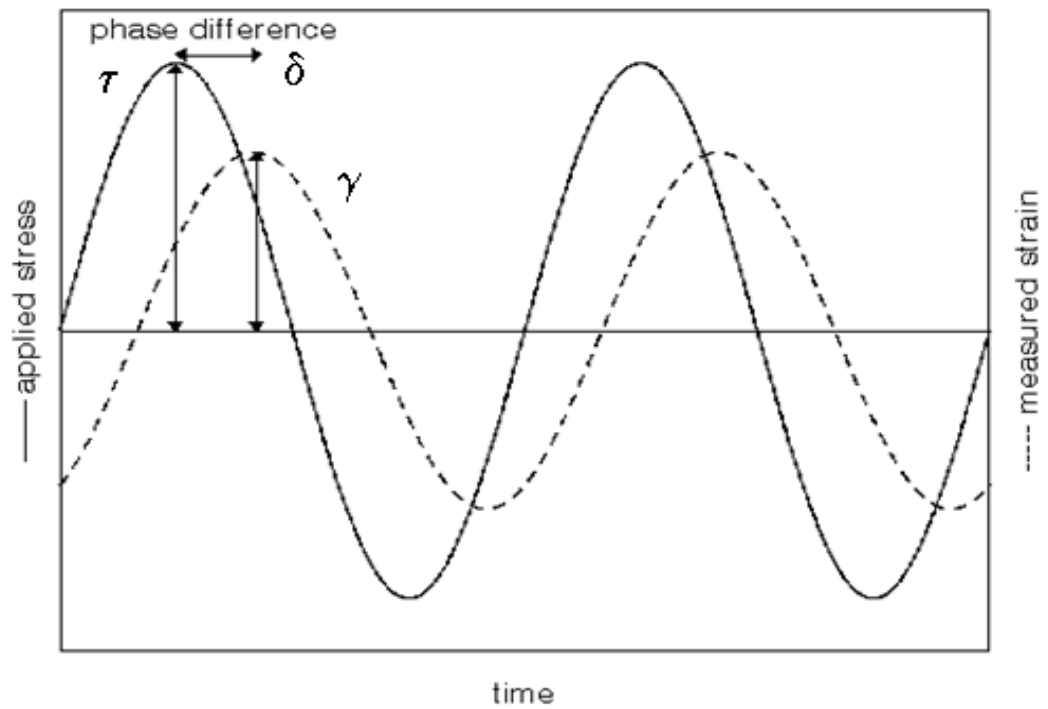


Figure 2.7 : Plot of dynamic stress-strain

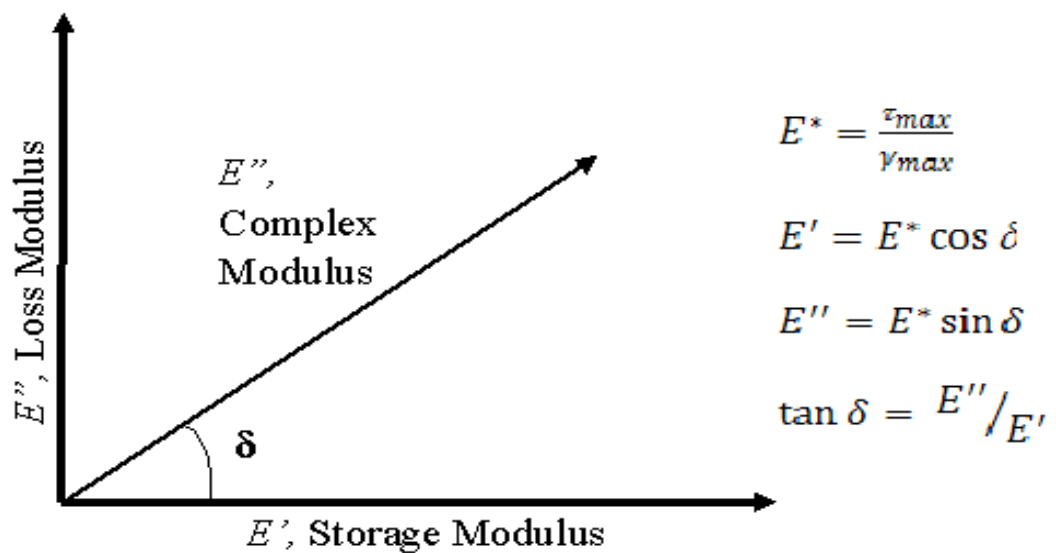


Figure 2.8 : Dynamic mechanical analysis relationship

DMA always used to study the miscibility and compatibility of the polymer blends and composites due to highly sensitivity to temperature (Gnatowski and Koszkuł, 2006; Hong *et al.*, 2007; Aoki *et al.*, 1999; Kader and Bhowmick, 2003). Therefore, DMA is often used in detecting T_g in blends than DSC (Stoeling *et al.*, 1970). The important parameter for this T_g analysis is $\tan \delta$. $\tan \delta$ used to detects changes in molecular motion or relaxation process. Araujo *et al.*, (2004) analysed the immiscibility of PA6/ABS blends produced by methyl methacrylate grafted maleic anhydride (MMA-MAH) using DMA. They confirmed that, PA6/ABS blend was immiscible for all the range of constituent composition. This was due to the presence of MMA-MAH did not affect significantly the T_g of the SAN phase in ABS phase. Beside of $\tan \delta$, the storage and loss moduli also can be used to investigate the phase behaviour of the blends.

2.9 Polyamide 6 (PA6) polymer

PAs contain the -CONH- amide group as a recurring part of the chain. The most popular PAs are PA6,6 and PA6 which are made by polymerisation of caprolactam. Other semicrystalline PAs include PA4,6, PA6,9, PA6,10, PA 6,12, PA11 and PA12 (Patel, 1998) as shown in Figure 2.10.

The amide group in PA creates hydrogen bonding, and hence the polymers are very strong with high melting points. After melting, the viscosity is low: thus PAs are easier to process. Sometimes PA6 and PA6,6 are copolymerized, which leads to a more amorphous polymer, yielding a tough, flexible and reasonably transparent polymer. Typical properties of PAs are high strength and stiffness. PAs have excellent resistance to fatigue and repeated impacts. PAs show low coefficient of friction on contact with other materials. They have a good abrasion resistance, and have excellent resistance to hydrocarbon fuels, lubricants and other non-polar organic solvents. PAs biologically

inert but absorb moisture due to their high polar nature. Moisture acts as a plasticiser, reducing PA strength. It is also make PA a poor electrical insulator; but generally, well compounded PAs are resistant to ordinary power frequency and voltage.

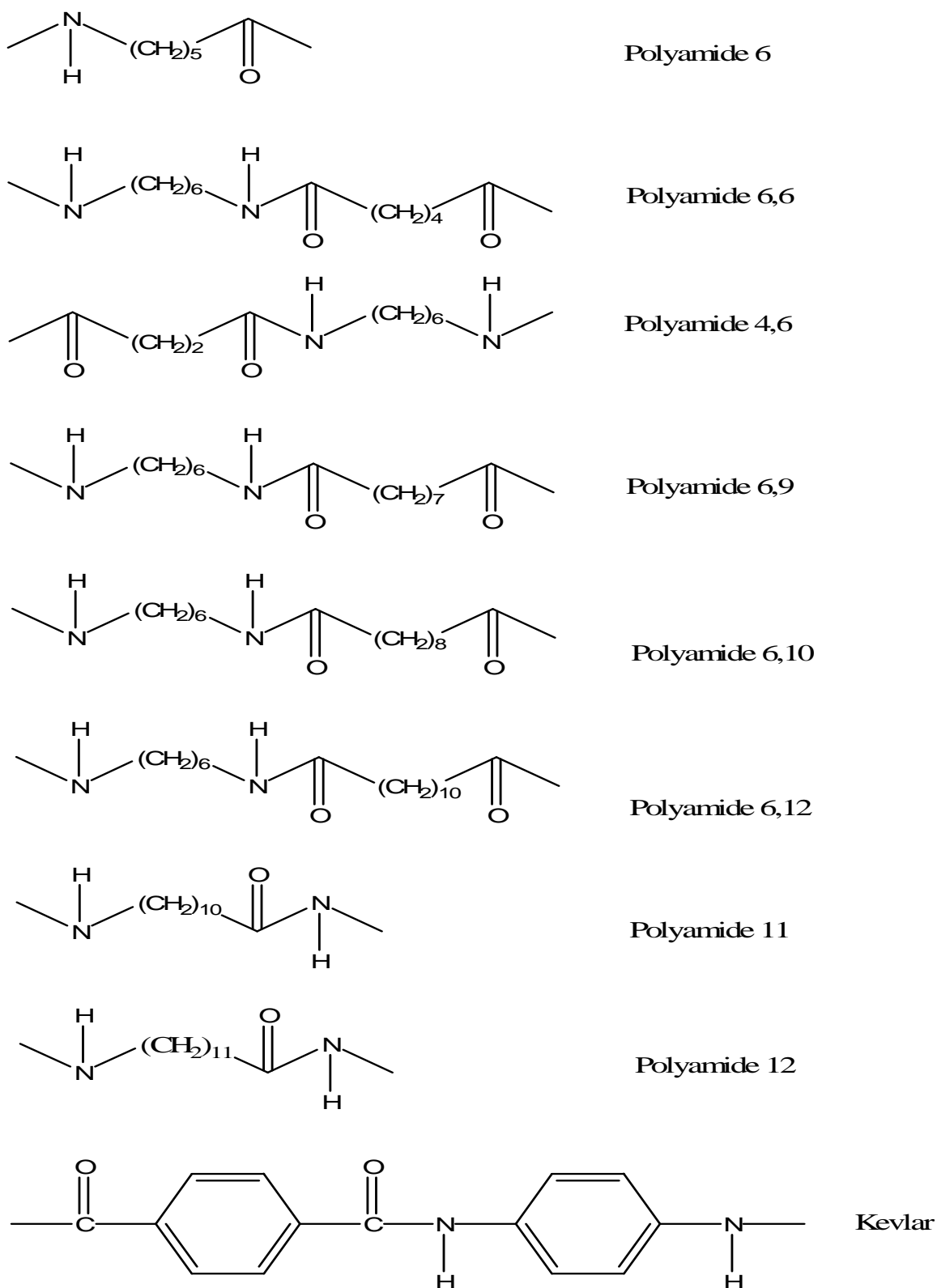


Figure 2.9 : Typical molecular structure of polyamide series

Major uses of PAs are in automotive parts where they are used as electrical connectors and light-duty gears. Glass reinforced resins are used for engine fans, radiator heaters, brake-fluid reservoir, valve covers and hydraulic hoses. They are also used as hammer handles, gears and sprockets, bushing and cams. Electrical applications include wiring devices, plugs, connectors, power-tool housing, washers and small appliances. They are also used in ski boards, roller skater, bicycle wheels and fishing lines. Biaxially oriented PA film is extremely tough and is used for meat and cheese packaging, cook-in-bags and vacuum-fill pouches. Blow moulded containers are also popular.

2.10 Acrylonitrile Butadiene Styrene (ABS) polymer

ABS is one of the most versatile families in thermoplastics, processing unique balance of properties. The ABS is made up of three monomers – acrylonitrile, butadiene and styrene, the molecular reaction is shown in Figure 2.11. Various grades of ABS with optimum properties can be tailor-made by varying the ratio of the three monomers varying the polymer structure and molecular weight. The most important properties varied include impact resistance, hardness, elastic modulus, gloss and melt viscosity.

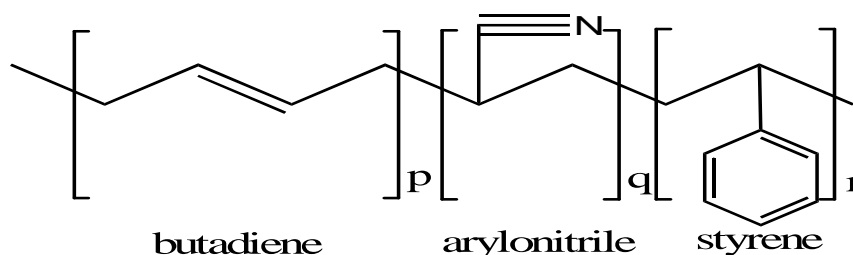


Figure 2.10 : Molecular structure of acrylonitrile-butadiene-styrene (ABS)

The first commercial ABS plastics, cycolac® was introduced in 1954 by Borg Warner Chemicals. The initial work was started in 1948. When styrene acrylonitrile (SAN) copolymer was blended with Buna N rubber, which is a copolymer of butadiene and acrylonitrile, the resultant material had much better impact strength than SAN plastics. The impact strength at low temperatures for the blend was still poor. Then, Borg Warner tried the use of polybutadiene (PB) rubber, which remains rubbery at lower temperatures than Buna N. Initial ABS plastics commercialised were physical blends, which soon gave way to much improved latex-grafted ABS polymers. Styrene and acrylonitrile are polymerised in the presence of PB in a reactor, causing formation of SAN grafted to rubber particles. The existence of PB as a separate phase, and its domain size are critical to the impact strength of ABS plastics. As a result, ABS consists of three elements that contribute with different properties; butadiene contributes impact strength, toughness and low temperature property retention; whilst acrylonitrile contributes to the heat resistance, chemical resistance and surface hardness of the system and the styrene component improves the processibility, rigidity and strength (Brydson, 1999).

Several different approaches are commercialised to produce ABS. In most cases, unsaturated PB rubber is first made by emulsion or solution polymerisation. In second stage, SAN polymer matrix is formed; and during that reaction, some SAN is grafted onto the unsaturation in the rubber. The reaction stage can occur by emulsion polymerization or by mechanical blending of highly-grafted, emulsion-made, high-rubber-content ABS with SAN.

The general properties of ABS vary, depending upon the additives, monomer ratios and molecular weight. Usual additives are UV stabilizers and internal lubricants. ABS electrical insulation properties are usually good. The chemical resistance of ABS is generally good, as it resists weak acids, strong and weak bases; but resistance to polar solvents like ethers, ketones and halogenated hydrocarbons is poor. Usually, the mechanical properties are high, with tensile strength from 3000 to 9000 psi and yield strain 2 – 5% (Brydson, 1999). Flame retardancy in ABS is usually imparted by halogenated additives or by alloying it with PVC and CPE. Heat resistance grades of ABS are made by partly replacing styrene with alpha-methyl styrene and also by adding maleic anhydride or alloying it with polycarbonates. Transparent grades are made by adding acrylics as a fourth comonomer. ABS can be formed by almost all the thermoplastic forming methods, but injection moulding, extrusion and rotational moulding are the most popular methods. ABS can be hot stamped, painted, vacuum metallised, printed and electroplated to give a variety of finishes.

2.11 Role of Compatibiliser

As discussed in the first chapter, immiscible blends often exhibit poor mechanical properties and have unstable phase morphology during processing. Adding a proper compatibiliser is an effective way to solve the problem associated with incompatible polymer mixtures (Qi *et al.*, 2003). Functionalised polymers have been widely used as reactive compatibilisers of polymer blends in various applications. In general, functionalised polymers can be obtained by graft polymerization of functional monomers with some commercially available polymers such as polybutadiene, styrene-butadiene block copolymers and ABS terpolymer.

Polymer alloys or blends may have up to six polymeric ingredients. If the number of components, m_i , is increased, it means the number of interfaces, N , between them becomes large, $N = m_i(m_i-1)/2$ (Utracki, 2002). Thus, compatibilisation of multicomponent polymer blends may pose serious problems – improperly designed interface may cause premature fracture. Therefore, two strategies may be adopted. The first addition of at least one ingredient has functional groups that react with several polymeric components; for example, a multicomponent copolymer that plays the dual role of compatibiliser and impact modifier, or a low molecular weight additive that at different stages of reactive blending binds to different components. The second, but more frequently applied strategy is the sequential reactive processing, where the blend(s) that is/are to form the dispersed phase(s) are compatibilised first, before combining them into the final composition. One of the common compatibiliser is maleic anhydride (MAH) reacted with rubber or rubbery like materials. MA groups can react with amine end group and form a graft copolymer at rubber-matrix interface, which reduces interfacial tension slow down particle coalescence forming during mixing (Carone *et al.*, 2000)

The driving force for blending ABS with PA6 is that ABS is lower price compared to PA6 and has good processibility, low water absorption and high impact strength. On the other hand, PA6 has excellent oil resistance, high water absorption and high toughness. By combining PA6 with ABS, the drawbacks of both components can be eliminated, and the resulting blend has outstanding performance. However, PA6 and ABS are poor compatibility. By incorporating of various compatibilisers can improve the compatibility. According to the above fact, the use of compatibiliser in GF reinforced PA6/ABS is also essential in order to eliminate the drawbacks and improve the poor compatibility. It is because glass fibre (GF) has high tensile strength and high chemical resistance, however, its unidirectional reinforcement makes to uneven shrinkage and warpage (Karger-Kocsis, 1999). Obviously, the type of GF sizing (PA – or– ABS compatible) determines the properties of PA6/ABS blends. The GF sizing and concentration must be matched to the matrix forming polymer in order to achieve optimum performance (Ozkoc, 2005; Thomason, 1999).

Few types of compatibiliser have been used in the previous studies of PA6/ABS blends such as poly(methyl methacrylate-co-maleic anhydride) (Araujo *et al.*, 2003), polybutadiene-grafted-maleic anhydride (Lai *et al.*, 2005), imidized acrylic polymer (Kudva *et al.*, 2000), glycidyl methacrylate-methyl methacrylate copolymers (Araujo *et al.*, 2005), maleic anhydride grafted polyethylene-octene elastomer (Chiu and Hsiao, 2004), styrene-acrylonitrile-maleic anhydride (Kudva *et al.*, 1999), polystyrene copolymerised with 25 wt. % maleic anhydride (Liu *et al.*, 2002), styrene-maleic anhydride (Misra *et al.*, 1993) and poly(*N*-phenyl-maleimide-styrene-maleic anhydride) (Lee *et al.*, 1997). Some of these compatibilisers were not fully miscible with the blends, due to the unsimilarity in molecular structure to ABS. Consequently, the final properties of the blends could not be achieved to the desired level. In addition, it was found very little literature reported on the use of ABS-grafted-maleic anhydride as a compatibiliser in PA6/ABS blends.

2.12 Glass fibre (GF) Reinforcement

A glass fibre was first produced in the 1920's, become popular after substituting the asbestos in the 1950's, when some of the deleterious health effects from asbestos were first becoming apparent. The diameter of the glass fibre based on single filaments is ranging from 3 to 19 micrometers. Single filaments are produced by mechanically drawing molten glass streams. The filaments are usually gathered into bundles called strands or rovings. The strands may be used in continuous form for filament winding; chopped into short lengths for incorporation into moulding compounds or use in spray-up processes; or formed into fabrics and mats of various types for use in hand coatings with a material known as a coupling agent, which serves to promote adhesion of the glass to the specific resin being used.

At present there are five major types of glass used to make fibres. The latest designation is taken from a characteristic property (Bader, 2001):

- i. A-glass is a high-alkali glass containing 25% soda and lime, which offers very good resistance to chemicals, but lower electrical properties.
- ii. C-glass is chemical glass, a special mixture with extremely high chemical resistance.
- iii. E-glass is electrical grade with low alkali content. It manifests better electrical insulation and strongly resists attack by water. More than 50% of the glass fibres used for reinforcement is E-glass.
- iv. S-glass is a high-strength glass with a 33% higher tensile strength than E-glass.
- v. D-glass has a low dielectric constant with superior electrical properties. However, its mechanical properties are not so good as E-or S-glass. It is available in limited quantities.

Glass fibres coated with nickel, by the electron beam deposition process, are used in moulding compounds and as reinforcements for electrically conductive parts. The major disadvantage of glass fibre is its unidirectional reinforcement leads to uneven shrinkage and warpage.

2.13 Glass Fibre Reinforced Polymer Composite

Polymer composites are prepared by mixing polymers with organic or inorganic materials such as reinforcing fibres (glass, carbon, aramid etc.) and particulate solids (talc, carbon black, calcium carbonate, mica etc.). Such composites exhibit physical properties synergistically derived from both the organic and inorganic components, for

example, they show superior mechanical properties and higher heat deflection temperature compared to the pristine polymers while maintaining processibility (Manson, 1976). Fibre reinforced polymer (FRP) composites were first developed in the 1940's mainly for military applications. Polymer composites since then have replaced metals and have found applications in diverse areas like construction, electronics and consumer products.

However, the improvement in properties is typically achieved at the expense of optical clarity and surface gloss, and often results in increased part weight. This is because high loading level of greater than 10-wt % of conventional reinforcing agents and fillers must be added in order to achieve significant improvement in the properties. Nowadays, the traditional composites being replaced with a new class of more effective composites using nano-fillers, and becoming an active field of industrial and academic research.

Short glass fibre (SGF) reinforced thermoplastics are attracting much interests because of their ease of manufacturing, good mechanical properties and economical. The traditional and most widely used methods of production of such materials are extrusion compounding and injection moulding. The performance and properties of these structural materials depend on not only the properties of individual components but also on the strength of interphase formed between them (Hamada *et al.*, 2000; Park *et al.*, 2000). Generally, SGF became widely used fillers to modify the modulus, strength, stiffness, and chemical properties of the virgin thermoplastics.

The fibre reinforced polymer composites are classified into the continuous fibre and discontinuous fibre composites. Fibre orientation, fibre length and fibre matrix adhesion play different important roles in the performance of both continuous and discontinuous fibre composites. The continuous fibre in a composite offers a strength and modulus properties in the fibre direction, while polymer dominates the properties of the composites in transverse direction to fibres.

Polymer composites are manufactured in two stages: the first stage include impregnation of the fibres by polymer, while the second stage includes consolidation using melt blending process [Nair *et al*, 1997; Ozkoc *et al*, 2004; Seema and Kutty, 2006]. Uniform distribution of the polymer and the fibres are achieved by the application of heat and pressure during the consolidation stage. Therefore, understanding of the polymer structure-property relationship and fibre-polymer interactions are important facts in order to achieve the desired properties of the fibre reinforced composite. In addition of the above facts, processing history of the composite structure can controls the final properties of the composite.

2.14 Uncompatibilised PA6/ABS blends

There are a lot of literatures describing toughed PA6 blends with various type of ABS. As already known, that PA6s are particularly exhibit good strength and resistance to hydrogen. PA6 is also brittle as compared to ABS. Therefore, in order to retain desirable properties from each blend constituents; melt blending is the answer. In another word is reactive blending or reactive compatibilisation. However, very limited publications discussed on uncompatibilised PA6/ABS blends due to unfavourable final properties.

Borg-Warner Chemicals introduced a new engineering material called Elemid®, which was an ABS/PA alloy. ABS/PA has a synergistic improvement in impact strength, modulus and excellent toughness at room temperature, and the blend was claimed to be superior to polycarbonate, acetals, PBT, PC/ABS, PBT/PC and PPO/PS. PA/ABS blends have lower equilibrium moisture content compared to PA6. PA/ABS blends are also resistant to aggressive agents like gasoline, antifreeze, diotyl phthalate, engine oil, brake fluid, grease and cleaner/degreaser.

Howe and Wolkowicz (1987) have studied the structures and physical properties of PA6/ABS near the midpoint compositions. They found that the physical properties of the blends were dependent on the fundamental properties of ABS and PA6 components. A sufficient interaction between the phases made the ductility of ABS phase penetrated into PA6 phase and reduced the notch sensitivity of the PA6 and lead to synergistic enhancement of the Izod impact strength of the blend.

The uncompatibilised PA6/ABS blends study was carried out by Bhaddwaj *et al.*, (1990). They have proved that melt flow index and density data indicated better physical and flow characteristics in blends compared to neat PA6. They also investigated the thermal properties of the blends and observed that blend ratios such as 50/50, 40/60, 25/75 and 15/85 of PA6/ABS were more compatible in comparison with other compositions.

Lavengood and Silver (1987) investigated the effects of PA6/ABS composition on properties using compatibilised alloys PA6 and ABS. They found that very high Izod impact strength achieved over a broad range of composition, tensile and flexural strength changed monotonically with composition. In order to improve the properties, Lavengood and Harris (1998) cooperated with Monsanto Chemical Company introduced a based blends of ABS and PA6 with a trade name Triax. ABS itself contributes melt strength and reduces the mould shrinkage, the blends tougher than polymer component. This first generation of uncompatibilised blends produced materials with high Izod impact values, but Triaxial stressed in thicker sections precipitated failures in field applications.

Again, tensile and impact properties of uncompatibilised PA6/ABS blends have been studied over the entire range of compositions by Mamat *et al.*, (1997) and related to the morphological investigation. The excellent mechanical performance has been observed when the composition was around 70% and this composition was found to have phase inversion resulting continuous morphology. As a conclusion, without a compatibiliser, PA6/ABS blends could achieve better properties especially impact properties with a proper combination, however, exhibited poor tensile properties.

2.15 Compatibilised PA6/ABS blends

Several approaches to the reactive compatibilisation of PA/ABS blends have been reported in the literatures (Majumdar *et al.*, 1994). Aoki and Watanabe (1992) studied the morphological, thermal and rheological properties of compatibilised PA6/ABS blends. Initial blends were simple mechanical blends and as a result, some rheological properties were anomalous at low concentration of each component. The PA6/ABS blends showed very high Izod impact strengths over a broad composition range. In fact, the most important characteristics of commercial PA6/ABS blends are synergistic improvement in impact strength. In their study, maleic anhydride modified ABS was used to improve the compatibility. Rheological investigation showed that below 30 wt. % ABS the PA6 is continuous phase; and above 70 wt. % ABS the ABS became a continuous phase. Therefore, the final properties of the blends will always dependent on ratio of its constituent.

Another PA6/ABS blend systems were investigated by Misra *et al.*, (1993) on the mechanical and morphological properties, and, styrene-maleic anhydride (SMA) copolymer was used as compatibiliser. They found that, the strength, modulus, and impact properties improved upon the addition of SMA. Further morphological studies using small angle light scattering, polarizing microscopy and scanning electron microscopy, showed that SMA surely acts as a compatibiliser for the blend system. Similar results have been done by Kim and Lee (1993); they have blended PA6 with ABS using two different strategies; grafting SMA with ABS before blending with PA6 and grafting SMA with PA6 before ABS being melt blended. Lee *et al.*, (1997) studied the effect of reactive compatibiliser [poly(*N*-phenylmaleimide–styrene–maleic anhydride)] on the morphological changes of blends of PA6/ABS blends as a function of viscosity ratio of the components and concentration of compatibiliser and the feed rate. The blending process has been done by using an intermeshing co-rotating twin screw extruder.

Kudva *et al.*, (2000) have studied on the mechanical, morphological and rheological properties of compatibilised PA6/ABS blends. Two types of compatibiliser were used; imidized acrylic (IA) and styrene/acrylonitrile/maleic anhydride (SANMA). They examined the mechanical properties, morphology and rheology of the blends as a function of processing history. They found that IA was miscible with SAN phase in ABS polymer, but SANMA was not fully miscible with SAN phase in ABS. However, both of compatibiliser improved the toughness of the blends as super-tough materials at room temperature using broad range of compatibiliser contents. Furthermore, when the parameter of processability and processing history were considered, the blends based on SANMA terpolymer had more desirable properties than those blended with IA. Previously, studied on glycidyl methacrylate/methyl methacrylate (GMA-MMA) copolymers as a compatibiliser showed that the compatibiliser failed to improve the mechanical, morphological and rheological properties of PA6/ABS blends (Kudva, 1998). They also found, GMA-MMA caused of poor ABS dispersion due to disfunctionality of the PA6 end groups with respect to the epoxide group of GMA, which leads to crosslinking-type reactions.

Kudva *et al.*, (2000) also studied the morphological, rheological and mechanical behaviours of the blends of PA6 blended with four type of ABS over a range of compositions using IA as a compatibilising agent at a fixed percentage about 5 wt. %. They found that ABS which is low melt viscosity has a monodisperse population of butadiene rubber particles generated blends with superior low toughness compared to those with broad particle size distributions and higher viscosity. However, using very small (0.5 wt %) amount of IA on the fixed ratio of PA6 to ABS blends resulted generating super tough materials.

Araujo *et al.*, (2003) studied the compatibilisation of PA6 with ABS using poly(methyl methacrylate-co-maleic anhydride) [MMA-MA] as a compatibiliser. This MMA-MA has PMMA segments that appear to be miscible with the SAN phase of ABS and the anhydride groups can react with amine end groups of the PA6 to form graft copolymers at the interface between PA6 and ABS rich phase. Tensile and impact were

enhanced by ABS domains were finely dispersed in PA6 matrix and led to the lowest ductile-brittle transition temperatures and highest impact properties. They reported that the MMA-MA became an alternative compatibiliser. They also conducted another study using different compatibiliser, poly(methyl methacrylate-co-glycidyl methacrylate) (MMA-GMA). They found, the incorporation of the MMA-GMA copolymer did not promote effective toughening of PA6/ABS. They believed due to the crosslinking-type reactions of this copolymer with both the acid and the amine groups of PA6 and ABS hindered the domains dispersion of ABS in PA6. That was not the case if the addition of MMA-MA copolymer to PA6/ABS blends, that significantly improved the impact properties and mechanical properties due to better interaction between two phases (Araujo *et al.*, 2003).

A study by Monsanto (Lacasse and Favis, 1999) on morphological and mechanical of PA6/ABS blends. Their study on the composition examined the impact strength performance of ABS/PA6 for an optimized interface fully saturated with compatibiliser. The maximum impact strength is obtained at a composition of 50 wt. % ABS for a system prepared using 10 wt. % of modifier (based on the dispersed phase). The scanning electron microscope demonstrates the presence of a co-continuous morphology at this concentration. This impact strength is fifteen times greater than polyamide-6 and four times greater than ABS, demonstrating exceptional synergistic effects.

Jang and Kim (2000) have studied on thermal, mechanical and water absorption properties of the blends of PA6 and ABS with and without MA as a compatibiliser. They found that the incorporation of MA in the PA6/ABS systems enhanced considerably the mechanical properties such as tensile, impact, flexural strength and hardness. A synergistic effect in the tensile and flexural properties was found when the weight fraction of ABS was about 20%. However, there was no significant effect on thermal properties such as melting and degradation temperature, and on water absorption properties. They found only the tensile and flexural were improved by the addition of MA into PA6/ABS blends.

Seung and Kim (2000) investigated the thermal, mechanical and water absorption properties of PA6 and ABS copolymer with and without MA as the compatibiliser, MA. They found that tensile and impact properties, hardness, heat deflection resistance and dimensional stability were enhanced by the incorporation of MA. Again, synergistic effects were observed for tensile elongation and flexural properties. However, the melting temperature and thermal stability were not significantly affected by the incorporation of MA.

Giusti *et al.*, (2003) reported the morphology and mechanical properties of PA6/ABS blends compatibilised with functionalised acrylic copolymer. They explained that the incorporation of ABS is somewhat similar to independently dispersing rubber and rigid phases in the PA6 matrix; the rubber phase improved low temperature toughness to the blend, while the rigid phase provided stiffness. In their work the poly (methyl methacrylate-co-maleic anhydride), MMA-MA, was used to compatibilise the PA6/ABS system. The binary blend (70/30) was brittle at all temperatures. Ternary blend with 5 wt. % of MMA-MA became super tough with impact strength values of above 800 Jm^{-1} and the ductile brittle transition temperature was 8°C . The tensile properties such as tensile yielding and modulus did not change significantly with compatibiliser addition. However the elongation at break improves from 24% for more than 100% with the addition of 5% of MMA-MA in blend. Previously, Ohishi and Nishi (2001) did similar study on morphological and mechanical properties of PA6/ABS, which focus on investigation of Izod impact strength, and SAN random copolymer (SAN) and polyarylate (PAr) block copolymer were applied as a reactive compatibiliser. Chiu and Hsiao (2004) have studied the effect of incorporation POE-g-MA as impact modifier on impact strength of PA6/ABS blends and their results showed that ABS particles dispersed uniformly in the PA6 phase and improved the interfacial bonding of the blends resulting a drastically improvement of impact strength.

Sun *et al.*, (2005), used epoxy-functionalised ABS as compatibiliser and modifier for PA6/ABS blends. This study showed the morphological observation that crosslinking reactions existed in the blends and resulted in the formation of grafted copolymer at the

interface, which promoted the dispersion of the minor phase and inhibited agglomeration. In other words, the tensile and impact properties of the blends were improved. A different compatibiliser and different type of PA6 were used in this similar method study (Lai *et al.*, (2005)). They blended polybutadiene-g-maleic anhydride (PB-g-MAH) into nano-PA6/ABS blends and found that the impact strength slightly increased as compared to PA6/ABS blends. These discrepancies were attributed by the degree of reaction sites amine end group at nano-PA6 and PA6 and the rigidity of clay in deteriorating toughness, which is nano-PA6, had higher reaction sites. Wang *et al.*, (2003) studied the PA6/ABS blends by using dynamic vulcanization of PA6/SAN/NBR blends. This was the new method of compatibilisation of PA6/ABS blends and resulting to the improvement of the toughness of the blends.

Fengmei Cheng *et al.*, (2006) studied two different type of compatibilisers – maleic anhydride-grafted polypropylene (MAP) and solid epoxy resin (bisphenol type-A) as compatibiliser for PA6/ABS blends. The results showed that the addition of epoxy and MAP into PA6/ABS blends has enhanced the compatibility of PA6 and ABS blends, and this led to the improvement of mechanical properties of the blends and reduced the size of the ABS particles in the PA6 continuous phase.

The rheological study of PA/ABS is very important in order to understand the relationship between properties of the material before and after processing. It also helps the researchers to understand the right application of the material. However, most of the rheological study particularly focused on the relationship between the reactions that take place during blending process and the viscosity instead of on the relationship between processing and flowability. All of the rheological studied reported found that the viscosity of the blends tend to increase with increasing of compatibiliser. Currently, there are very few reports on rheological properties of PA/ABS. Jafari *et al.*, (2002) investigated the rheological properties of the blends where the composition of PA6 was about 50 wt. %. The blend exhibited co-continuous structure and the viscosity and the elasticity was increased to be due to ABS has much higher viscosity than virgin PA6.

The also found that the increase of viscosity was caused by rubber particles in ABS phase.

2.16 Ternary Blends of PA6/ABS

The discussion of ternary blending of PA/ABS blends with reinforcement started two decades ago. Tjong and Jiang (2004) studied the structure-property relationship of ternary PA6/ABS/liquid crystalline polymer (LCP) blends compatibilised with anhydride-grafted polypropylene (MAP). They found that the incorporation of MAP and epoxy resin compatibiliser into PA/ABS/LCP blend improved its tensile strength, stiffness and impact toughness considerably.

Sawhney *et al.*, (1996) studied the effects of thermotropic liquid crystalline polymer (LCP) as a third component as well as reinforcement filler to commercial compatibilised PA6/ABS blends (Triax 1180). They studied the effect of LCP on mechanical and morphological properties of Triax 1180. It was found that the incorporation of LCP enhanced the mechanical properties of the blends and 15 – 20 wt. % was the appropriate level of LCP for self reinforcing blends. They also found that processing conditions play a vital role in determining the mechanical properties and morphology of the polyblends.

Lai *et al.*, (2003) investigated the impact behaviours of nanoclay filled PA6 (Nano-PA6) blended with ABS and mixed with metallocene polyethylene grafted maleic anhydride (POE-g-MA) as compatibiliser. They found that impact strength increased slightly for compatibilised nano-PA6/ABS blend system, and increased remarkably for the conventional PA6/ABS blends. These discrepancies could be attributed by a different degree of available reaction sites from amine group on Nano-PA6 and PA6.

Meincke *et al.*, (2004) studied the ternary blends of PA6/ABS with carbon nanotubes as reinforcement, which were prepared using co-rotating twin screw extruder. The transmission electron microscopy (TEM) showed that the carbon nanotubes were well dispersed homogeneously in the PA6 matrix and carbon nanotubes were selectively located in the PA6. Consequently, the carbon nanotubes blends showed superior mechanical properties in the tensile tests and in Izod notched impact tests as compared to without nanotubes.

2.17 Glass Fibre Reinforced Polymer Composite

2.17.1 Introduction

Glass fibre reinforced polyamides are widely used in many applications, such as stressed functional automotive parts (fuel injection rails, steering column switches) and safety parts in sports and leisure (snowboard bindings). These materials are known for their stiffness, toughness and resistance to dynamic fatigue.

Fibre reinforced thermoplastics compounds may be processed by conventional methods, such as injection moulding, and offer improvement in mechanical properties over unreinforced ones. These composites compete with metals in many engineering applications because of their ease of fabrication, light weight and economy. However, there are problems concerning material defects such as voids or cracks that may be present or initiated in one of three regions: the matrix, the fibre or the fibre/matrix interface (Akay *et al.*, 1995). Therefore, the thermoplastic composites containing short fibres have become the subject of much attention. The present of thermoplastics in the

composite reduce the void and prevent the crack and finally improve the mechanical properties. These properties are resulted from a combination of the fibre and the matrix properties and the ability to transfer stresses across the fibre/matrix interface. It is also depend on the injection conditions such as screw and barrel parameters, mould temperature and design (Takrej *et al.*, 1996; Guerrica-Echevarria *et al.*, 2001; Ota *et al.*, 2005; Gu'Lu' *et al.*, 2006).

According to the studies led by Thomason (1999) and Shao-Yun Fu *et al.*, (1996), other variables such as fibre ratio, diameter, length, orientation and the interfacial strength are also prime importance to the final properties of the thermoplastic composites. Therefore, the final properties could be influenced by many factors during a composites preparation, processing and finally the applications.

2.17.2 Glass Fibre Reinforced Polyamide Composites

There are several studies of glass fibre reinforced polyamide composite that will be discussed. Shao-Yun Fu *et al.*, (2006) studied the effects of incorporating short glass fibre reinforced on various PA6,6/PP ratio and rubber toughened PA6,6/PP blends. The glass fibre content was fixed at 40 wt. %. The polymer blends containing various PA6,6/PP ratios, plus a mixture of 10 wt. % styrene–ethylene–butylene–styrene (SEBS) and 10 wt. % maleic anhydride (MAH) grafted SEBS (SEBS-g-MAH). Two types (123D and 146B) of E-glass fibres were used to examine the influences of PA6,6/PP ratio on the mean fibre length and critical fibre length and in turn on the mechanical properties. The PA6,6/PP ratio was found to have significant effects on both the mean fibre length and the critical fibre length in the final samples, and then on the mechanical properties. It was shown that the composite strength increased while the elastic modulus decreased with increasing PA6,6/PP ratio. The elongation at break was higher for the

glass fibre-reinforced SEBS/SEBS-g-MAH toughened PA6,6/ABS blends than for glass fibre-reinforced toughened PA6,6/PP composites. However, the notched Charpy impact energy of the reinforced blends at 75/25 of PA6,6/PP ratio was exhibited to be higher than the reinforced rubber-toughened PA6,6/PP composites. It was concluded that control of the PA6,6/PP ratio would be effective way to produce composites with optimal combination of superior overall mechanical properties.

Benderly *et al.*, (1998) studied on dynamic rheological behaviour of PP/PA6/GF blends. The results indicated that the addition of PA6 to PP increased the principal relaxation time of the binary blends and addition of GF to the blends gave further increase in the principal relaxation time. Malchev *et al.*, (2005) studied an immiscible PE/PA6 thermoplastic and added to a conventional short fibre reinforced and investigate the effect on the mechanical properties. The results showed unexpectedly higher values of the tensile modulus of the ternary composites (PE/PA6/GF) as compared to without glass fibre. However, the upper limit of the 'applicability' of the material was determined by the melting point of the minor component. A simple model was derived to describe the mechanical properties of the composite (three phase system) because DMA model developed for the two systems failed to describe the mechanical data for the whole range of measured temperature. The simple model showed a good agreement with the experimental data.

2.17.3 Glass Fibre Reinforced PA6/ABS composites

Study on mechanical and morphological properties of SGF reinforcement PA6 and ABS blends was started by Kannan and Misra (1994). They investigated 70:30 blend of PA6/ABS as a matrix and styrene-grafted-maleic anhydride (SMA) as a compatibiliser, and the composition was kept to about 5 % by weight. The mechanical

properties results showed an improvement with the addition of GF to the blends matrices and increased with increasing GF content. However, the SMA has no significant effect on the mechanical of PA6/ABS composite and only for compatibilising purpose for PA6 and ABS phase. The SMA increased the viscosity of the blends and results a greater damage to the fibres in the composite. They concluded that the fibre matrix adhesion appears to be better in the absence of SMA.

Nair *et al.*, (1997) studied the fracture resistance of fibre reinforced PA6,6/ABS composites. They discovered that GF promoted shear yielding and as a result, enhanced both the fracture initiation as well as fracture propagation resistance of PA6,6/ABS composites. They also found that the role played by GF in the composites to be critically related to fibre/matrix interfacial strength.

The introduction of rubber phase into PA6, resulting a reduction of the strength and stiffness. GF became a right reinforcement filler to be introduced in order to restore the mechanical properties of PA6/ABS blends. Therefore, Cho and Paul (2001) studied GF reinforced PA6 composites toughened with ABS and ethylene-propylene-rubber-grafted-maleic anhydride (EPR-g-MA) as a compatibiliser. They investigated the mechanical properties and morphology of the composites. The mechanical properties showed that the balance of the impact strength and stiffness for both types of systems can be significantly improved by incorporation of GF.

The mechanical performance of GF reinforced polymer composites depend not only on the properties of individual components but also on the interfacial interactions established between the reinforcing agent and the matrix material (Frenzel *et al.*, 2000; Laura *et al.*, 2002; Bikiaris *et al.*, 2001). Therefore Seema and Kutty (2005) studied the effect of an epoxy-base bonding agent on the mechanical properties of short PA6 fibre reinforced ABS composites. They found that epoxy resin became a good interfacial-bonding agent resulting in increasing the modulus and tensile strength with increasing of the composition of the resin.

GF reinforced PA6/ABS composites can be considered as a new composite material therefore, the processing properties are very important. Ozkoc *et al.*, (2005) studied the effects of SGF concentration and extrusion conditions, such as the screw speed and barrel temperature profile, on the mechanical properties of the composites. Increasing the SGF concentration in the ABS matrix from 10 wt. % to 30 wt. % has resulted in improving tensile strength, tensile and flexural moduli, but drastically lowered the strain-at-break and the impact strength.

However, very limited numbers of researchers have carried out the study on processibility and flowability of the GF reinforced PA6/ABS composites. Thus, the study on the rheological properties is considered to be important. Understanding the rheological properties can help the polymer technologist to predict the processing and end use performance of the PA6/ABS composites.

CHAPTER 3

METHODOLOGY

3.1. Introduction

The preparation steps as shown in Figure 2.1, involved drying of all the raw materials followed by mechanically mixed to form polymer blends and composites: uncompatibilised PA6/ABS, compatibilised PA6/ABS and SGF reinforced PA6/ABS composites. The blends were injection moulded to form standard test specimens. Tensile, flexural, impact and dynamic mechanical analyser (DMA) were carried out to study the mechanical properties of all the materials either in static and dynamic conditions. Differential scanning calorimetry (DSC) was conducted to investigate the thermal properties. The most crucial or significant part of this work is the rheological study. The rheological properties were investigated using melt flow index, capillary and oscillatory rheometer.

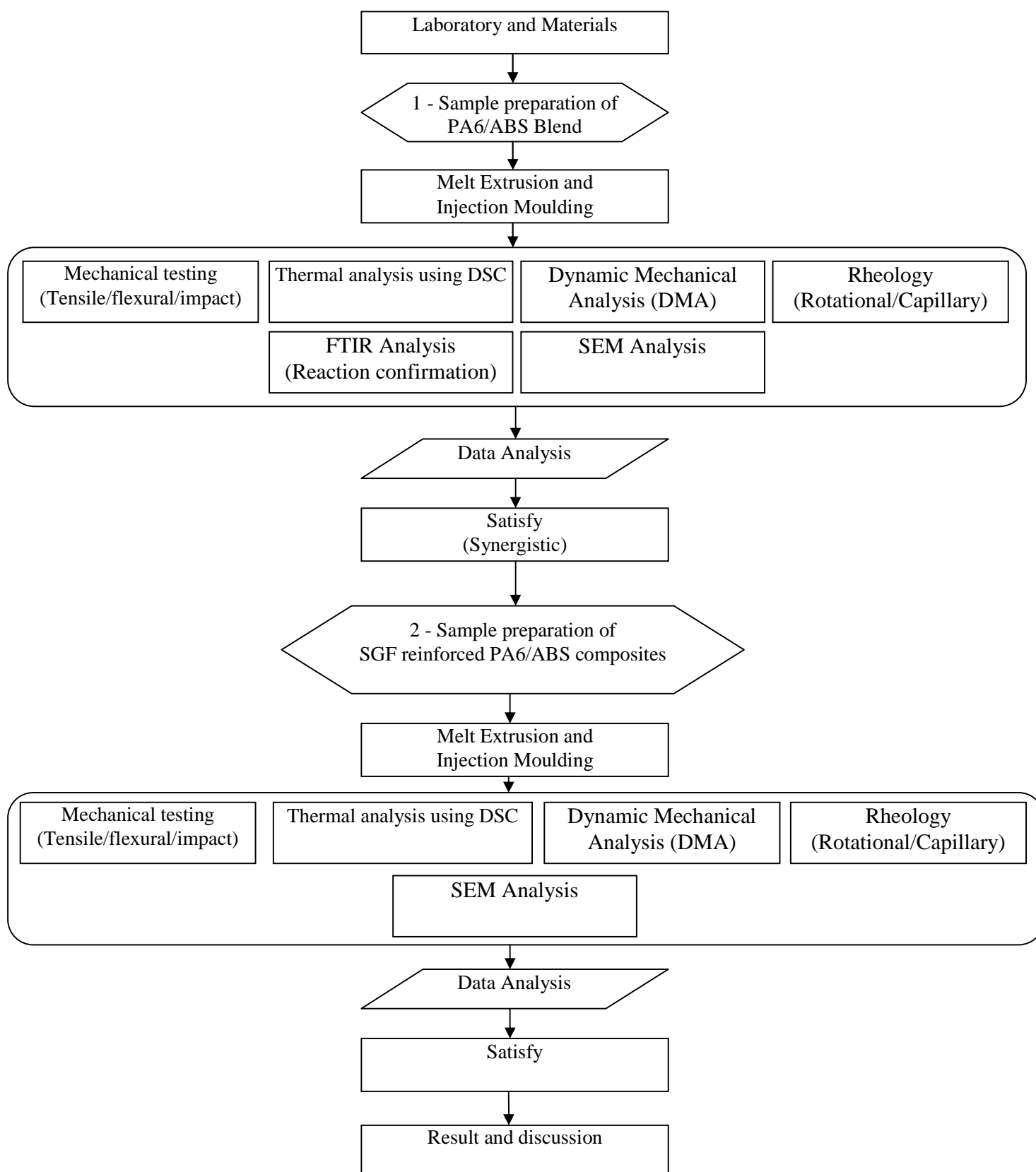


Figure 3.1: Research Flow chart

3.2. Raw Materials

3.2.1 PA6 and ABS

Both super high impact ABS (100-X01) and PA6 (Amilan CM1017) were supplied by Toray Plastics (Malaysia) Sdn. Bhd. They were originally in the pellet form. Their materials properties are listed in Table 3.1 and Table 3.2 respectively.

Table 3.1: Material Properties of Super High Impact ABS (100-X01) (Toray Industries, 2006)

Typical Resin Properties	Unit	Value	Test Method
Specific Gravity	-	1.04	ASTM D792
Water absorption at 23°C after 24 hours	%	0.3	ASTM D570
Melt Flow Rate at 220°C (10kg)	g/10min	14	ISO 1113
Tensile Strength at Yield	MPa	42	ASTM D638
Tensile Elongation at Break	%	>50	ASTM D638
Flexural Yield Strength	MPa	64	ASTM D790
Flexural Modulus	MPa	1960	ASTM D790
Notched Izod Impact Strength (23°C)	J/m	274	ASTM D256
Rockwell Hardness	R scale	108	ASTM D785
HDT at 18.56 kg/cm ²	°C	91	ASTM D648
Thermal Conductivity	W/K.m	0.15	ASTM C177

Table 3.2: Material Properties of PA6 (Amilan CM1017) (Toray Industries, 2006)

Typical Resin Properties	Unit	Value	Test Method
Melt Flow Index at 230°C (2.16kg)	g/10 min	35	ISO1113
Specific Gravity	-	1.13	ASTM D792
Water absorption at 23°C after 24 hours	%	1.8	ASTM D570
Tensile Strength at Yield	MPa	85	ASTM D638
Elongation at Yield	%	7	ASTM D638
Elongation at Break	%	150	ASTM D638
Flexural Strength	MPa	120	ASTM D790
Flexural Modulus	MPa	3000	ASTM D790
Notched Izod Impact Strength	J/m	50	ASTM D256
Rockwell Hardness	R-scale	119	ASTM D785
Compressive strength	MPa	85	D695
Temperature Melting Point	°C	225	DSC Method

3.2.2 Compatibiliser

In this study, the compatibiliser was obtained from Polyram, Ram-O Industries Limited with a brand name Bondyram® 6000. This compatibiliser is a maleic anhydride grafted ABS (ABS-g-MAH) recommended as coupling agent for styrene compound and composites with glass or other minerals. The melt index and density of compatibiliser are 8g/10min (at 220°C and 2.16kg load) and 1.05 g/cm³ respectively.

3.2.3 Short Glass Fibre (SGF) Reinforcement

Glass fibres were obtained from Taiwan Glass Industries Corporation, named as chopped strand TG183 with a filament diameter of 10 μ m and an average length of, 3.2mm. These fibres were provided by manufacturer with a propriety surface condition deemed to PA6. This SGF is an E-type glass fibre.

3.3 Samples Preparation

3.3.1 Blends Formulation

The basis of formulation was based on the percentage weight ratio between PA6 and ABS, PA6/ABS blends with ABS-g-MAH and compatibilised PA6/ABS with short glass fibres. The weight ratios of blends are shown in Table 3.3 (a) - (c).

Table 3.3 (a): Blends formulation for polyamide 6 and ABS blending process without compatibiliser.

Designation	PA6 (%)	ABS (%)
50PA650ABS	50	50
60PA640ABS	60	40
70PA630ABS	70	30

Table 3.3 (b): Blends formulation for polyamide 6 and ABS blending process with MA-g-ABS as compatibiliser.

No.	PA6 (%)	ABS (%)	ABS-g-MAH (%)
1	49.5	49.5	1
2	59.4	39.6	1
3	69.3	29.7	1
4	49	49	2
5	58.8	39.2	2
6	68.6	29.4	2
7	48	48	3
8	57.6	38.4	3
9	67.2	28.8	3
10	47.5	47.5	5
11	57	38	5
12	66.5	28.5	5

Table 3.3 (c): Blends formulation for compatibilised PA6/ABS blends and SGF blending process

No	Compatibilised PA6/ABS (%)	Short Glass fibre (%)
1	100	0
2	90	10
3	80	20
4	70	30

3.3.2 Preparation of Blends

The PA6, ABS and MA-g-ABS resins were obtained in the form of pellets. To remove moisture, PA6 was dried in a hopper dryer at 80 °C for 24 hours whereas ABS

and ABS-g-MAH were dried for 6 hours at 85 °C in vacuum desiccators for not longer 24 hours before blending. This is an important step before processing. All the materials were premixed in sealed container and shaken manually for 5 minutes.

3.3.3 Melt Extrusion Blending

PA6 and ABS blends were prepared according to Table 3.3 (a), (b) and (c). All the raw materials were blended using Brabender Plasticorder 2000, counter-rotating twin screw extruder with L/D = 36 at a speed of 80 rpm and the temperature profile was 220/230/240/250°C for the barrel zone temperatures. Then, the extruded strands were air-dried and palletised.

3.3.4 Injection Moulding

After the blends were compounded, the blends were injection moulded using an injection-moulding machine, JSW Model NIOOB II. The moulding machine was first preheated and each blend with the stated blend formulations were injection moulded into the mould. The barrel temperature ranged from 220-265 °C. The temperatures of the four zones of the injection moulding were: feed zone 220 °C; compression zone 230 °C; metering zone 240 °C and die zone 250 °C. All the pellets were dehumidified in a hopper dryer (82°C for 24 hours) and stored in desiccators for 24 hrs before testing for the relevant test.

3.4 Mechanical Testing and Analysis Procedures

In this research, only three compositions of PA6 were chosen and blended with ABS that was 50, 60 and 70 wt. %. This is because according to, Aoki and Watanabe (1992) and Lacasse and Favis (1998), the maximum mechanical strength of PA6/ABS blends could be obtained as compared to its constituent polymer at the PA6 composition about 50 to 70 wt. %. Lacasse and Favis (1999) have reported that 3 wt. % of compatibiliser concentration in blends was enough to achieve a uniform diameter of dispersed phase and potentially to have high impact properties (Kudva *et al.*, 2000). Therefore, the composition of compatibiliser was chosen in a range of 1 – 5 wt. %.

3.4.1 Tensile Test

Tensile testing was carried out according to ASTM D638-Type I at room condition on an Instron Universal Tester. The specimen was pulled at crosshead speed of 50mm/min. The instrument software calculated the properties such as tensile strength, Young modulus and elongation at break from the stress-strain curves. In this research, five tests were carried out for each blend sample and average reported.

3.4.2 Flexural Test

Determination of flexural modulus is important to overcome certain practical problem in measuring tensile strength of thermoplastics in brittle region. Flexural testing determines the strength of the material when a force is applied perpendicular to the longitudinal axis sample. In this section, flexural test was carried out using an Instron Machine according to ASTM D790-97 (Test Method 1, Procedure A).

Since the modulus was determined between small initial deflections, a low force load cell (100N) was used to ensure good accuracy. Flexural tests were carried out using a simple supported beam. The distance between the spans is 100 mm and a cross-head speed of 3 mm/min was used. The test was carried out at room temperature. In this research, five samples were tested for each composition and average values were recorded. Flexural toughness was calculated from the area under the stress-strain curve. The calculation for flexural modulus and strength is as follows:

$$\text{Flexural modulus} = \frac{L^3 \Delta W}{4bd^3 \Delta S} \quad (3.1)$$

$$\text{Flexural strength} = \frac{3wL}{2bd^2} \quad (3.2)$$

where W is the ultimate failure load (N), L is the span between the centre of support (m), b is the mean width of the specimens (m), d is the mean thickness of the specimens of the sample (m), w is the increment in load (N) and S is the increment in deflection.

3.4.3 Izod Impact Test

The Izod impact test was conducted according to the ASTM D256-93 standard test method to determine the pendulum impact resistance of notched specimens for plastic. The test method covered the determination of the resistance of plastic to breakage by flexural shock as indicated by the energy extracted from standard pendulum type hammers. Izod tests were done at room temperature with the conditions as follows: Hammer energy = 7.5J, Velocity = 3.0 m/s and Angle = 150°. The notch was milled with a 45° angle and 2.5 mm depth with an Automatic Notcher Machine. In all cases, five specimens of each were tested and average values were reported.

3.4.4 Dynamic Mechanical Analysis

The dynamic mechanical properties were measured using Perkin–Elmer Dynamic Mechanical Analyzer (DMA 7e, in flexural mode. The device applied a continuous sinusoidal oscillatory deformation on the sample and measured the force required to produce specific oscillation amplitude. The moduli were derived from the value of this force and its phase difference with respect to the deformation. These are the elastic (storage) modulus, E' , and viscous (loss) modulus, E'' , terms of the complex dynamic tensile modulus of a viscoelastic material and dynamic mechanical $\tan \delta$. All these data were taken as analysis data.

The temperature was raised at a constant rate of 5°C/min, from 25°C (room temperature) to 220°C (just above the melting point of the PA6 phase, T_m^{PA6}). The

frequency of the applied oscillations was 1 Hz and the deformation amplitude was set to 5 μm ($\sim 0.05\%$ strain). Data were collected every one degree Celsius.

3.5 Differential Scanning Calorimetry (DSC)

There are three set of samples with the set of range composition were prepared for DSC analysis besides that of the virgin PA6 and ABS: uncompatibilised PA6/ABS blends, compatibilised PA6/ABS and short glass fibre reinforced PA6/ABS composites. These samples were investigated under nitrogen using DSC7 device (Perkin Elmer). Heating and cooling rates approximately 10 mg samples are 10 K min^{-1} from 25°C to 300°C . The curves were analyzed as follows: The glass transition temperature (T_g) was taken as the average of the intersection points of the extrapolated lines before and after transition, respectively, with tangent at the point of return at the rising curve. Melting (T_m) and crystallisation (T_c) temperatures were taken as the temperatures at the peak heights. The heat was calculated from the areas under the curves as integrals between the onset points of the corresponding peaks. The heats are related to the masses of the components in the material according to their composition.

For the nonisothermal experiments, the enthalpy of fusion, ΔH_f was determined through Pyris software by analyzing the melting endothermic. The percent crystallinity will be calculated from the following equation:

$$\% \text{ Crystallinity} = \frac{\Delta H_f}{\phi_{\text{polymer}} \Delta H_f^0} \times 100 \quad (3.3)$$

where ΔH_f^0 is the enthalpy of 100% crystalline polyamide 6 and ϕ_{polymer} is the mass fraction of the polymer. Equation (3.4) represents a normalisation of the enthalpy such

that the changes in percentage of crystallinity are based on the amount of polymer present in PA6/ABS blends and composite. The onset is the beginning of the melting endothermic, and the width represents the difference in temperature between the end and onset of the endothermic. All the enthalpy of fusion and glass transition were obtained at a second heating of DSC curves. All the important data for analysis and calculation i.e. melting temperature, glass transition temperature, heat of fusion were taken at second heating run. First heating run was carried for elimination of history of memory in the samples and its raw data was used to compare with the data of second heating run. All testing were carried three times, to confirm the reproducibility of the results.

3.6 Rheological Testing and analysis

3.6.1 Capillary Rheometer

Rheological analysis of the various blends was performed using a Rosand Dual Capillary Rheometer at Technical Service Laboratory, Polyethylene (M) Sdn. Bhd. The picture of the machine is shown in Figure 3.2. The Rosand software is capable of measuring rheological data at up to sixteen different shear rates during one test. One barrel housed a 'zero' length die and the other is fitted with a long 16mm die of diameter 1mm, the calculated rheological data results are Bagley corrected. Rheological data were recorded for all the blends over a wide shear rate range of 10 to 3000 sec^{-1} to replicate both extrusion and injection moulding conditions.



Figure 3.2 : Picture of Rosand Capillary Rheometer, Technical Service Laboratory, Polyethylene (M) Sdn. Bhd. Kertih, Terengganu.

3.6.2 Rotational Rheometer

Small-amplitude oscillatory shear measurements were performed on a Rheostress TC501 in parallel-plate geometry at Technical Service Laboratory, Polyethylene (M) Sdn. Bhd. The picture of the machine is shown in Figure 3.3. The resin pellets were melting pressed. The round samples with 25 mm diameter and 1.5 thickness were prepared using compression moulding at 270°C for 6 min under 5×10^3 Pa. The picture of compression moulding for the sample preparation is shown in Figure 3.4. The samples were further pressed under 10×10^3 Pa for another 5 min and cooled using a cold press. The measurements were then run using time sweep method under 0.01 rad/s over one hour to check the thermal stability the blends and pure polyamide. After that, the dynamic rheological testing perform under frequency sweeps ranging from 0.05 to 100 rad/s, using strain and stress values determined to lie within the linear viscoelastic region. The frequency sweep measurements were carried out under nitrogen atmosphere at three different temperatures: 230, 245 and 260°C. All the frequency sweeps testing were repeated at least three times to confirm the reproducibility.



Figure 3.3: Picture of Rheostress TC501 at Technical Service Laboratory, Polyethylene (M) Sdn. Bhd. Kertih, Terengganu



Figure 3.4: Picture of compression moulding machine, for preparation of dynamic rheological specimens

3.7 Fourier Transform Infra-Red (FTIR)

Fourier Transform analysis were performed on a Perkin Elmer Spectrum1 for virgin PA6, ABS-g-MAH and compatibilised PA6/ABS blends to confirm the occurrence of grafting reaction between amine end group of PA6 and maleic anhydride. The ratio between the sample and potassium bromide (KBr) was at about 1: 1000 prior to compacting into this pallet using 8 tones force hydraulic press at 5 minutes. Infrared spectrums were obtained in transmission and were set to operate in the range of $360 - 3600 \text{ cm}^{-1}$.

3.8 Scanning Electron Microscope (SEM)

Scanning electron microscope (SEM) at Ibnu Sina, Faculty of Science of UTM was employed to study and record the morphology of fracture surface of the blends. The fractured surface was obtained by breaking the specimens under nitrogen liquid. The fractured surfaces were then sputtered with titanium in vacuum and surface characteristics were studied. These micrographs were analysed using image analysis software.

CHAPTER 4

RESULTS AND DISCUSSIONS

4.1 Mechanical Properties

4.1.1 Tensile Properties of PA6/ABS Blends

In this study, three compositions of PA6 were chosen to be blended with ABS that is 50, 60 and 70 wt. %. This is because according to, Aoki and Watanabe (1992) and Lacasse and Favis (1998), the maximum mechanical strength of PA6/ABS blends could be obtained as compared to its constituent polymer at the PA6 composition about 50 to 70 wt. %. Wang and Li (2001) reported that pure PA6 possess a tensile strength to about 70MPa and the elongation at break over 160% while Howe and Wolkowicz, (1987) reported that the uncompatibilised PA6/ABS in any ratio have poor values. The compatibilisation, however, can be improved by introducing ABS-g-MAH, because of the similarity of chain structure; ABS-g-MAH is miscible with ABS in all proportions. Maleic anhydride (MAH) reacted with free terminal amine end group of PA6, which made ABS-g-MAH a good compatibiliser between PA6 and ABS. The possible chemical reaction is shown in Figure 4.1.

It can be seen from Figures 4.2 and 4.3 respectively that the tensile modulus and strength increased with the amount of ABS-g-MAH. This is believed could be due to the compatibiliser enhanced the interfacial adhesion between PA6 phases as a continuous phase and ABS as a dispersed phase caused by grafting reaction. The low tensile properties were found with the absent of compatibiliser but achieved a maximum level when the amount of compatibiliser was about 1 wt. %. These low tensile properties of the uncompatibilised blends can be related essentially to the larger size of ABS domains with a poor adhesion to the continuous phase. These domains will act as gross material defects, causing premature rupture of the specimen soon after the beginning of yield. The maximum level at 1 wt. % of compatibiliser could be due to enough amount of maleic anhydride reacted with amine end group of PA6 as compared to 3 and 5 wt. %. This analysis is in agreement with the FTIR finding and will be discussed in FTIR Section 4.5. Also, at 1 wt. % composition of ABS-g-MAH, the degree of crystallisation is the highest among the blends (see Figure 4.14). This indicates the mechanical properties especially strength depends on the degree of crystallinity of the blends

However, when the amount of ABS-g-MAH was about 3 wt. %, the tensile modulus and strength decreased with the increasing amount of compatibiliser and seemly achieved a constant value beyond this point. This phenomenon could be due to the dilution of the hydrogen bonds among PA6 by the segments of ABS, and because of the repulsion between the polar segments of PA6 and acrylonitrile segments in ABS. After this point (3 wt. % of compatibiliser) the dilution and repulsion took place and at the same time, grafting was formed during blending to balance each other. Thus, it was found that the tensile modulus and strength considerably achieved a constant value.

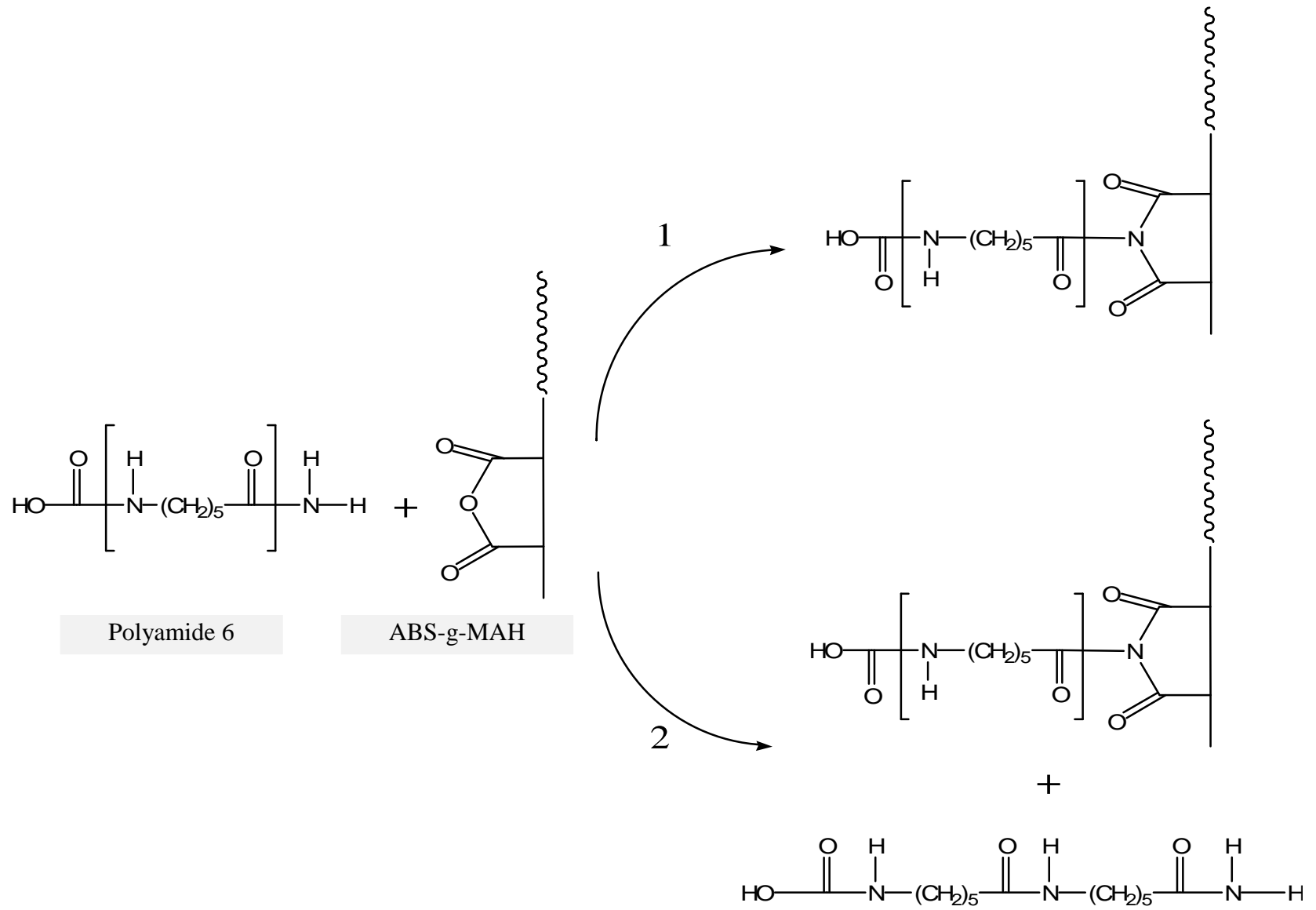


Figure 4.1 : Possible chemical reactions between PA6 and maleic anhydride

Figure 4.4 shows the elongation at break of PA6/ABS blends as a function of the amount of compatibiliser introduced into the blends system. For the uncompatibilised PA6/ABS blends as expected had a lower value of elongation at break. When compatibiliser ABS-g-MAH was introduced, the PA6/ABS system showed an increasing in elongation. The elongation at break for all blends began to achieve the constant value beyond 3 wt. % of ABS-g-MAH composition. It seems that the incorporation of ABS-g-MAH did not improve much on the toughness of the blends. Even if, it was expected that ABS-g-MAH which contains butadiene rubber particle enhanced the ductility of the blends.

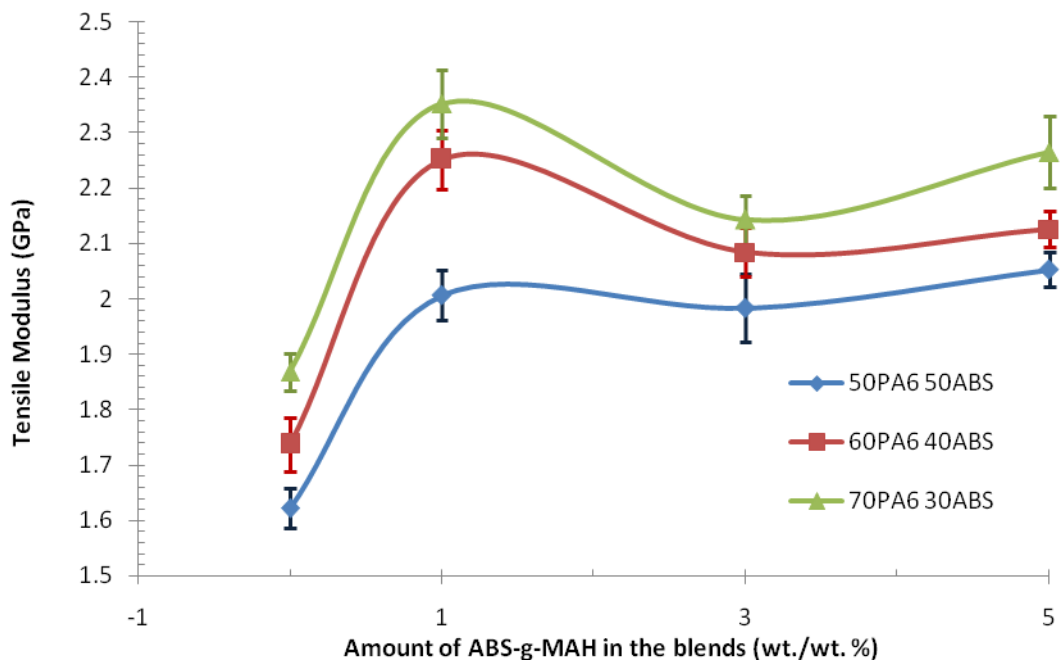


Figure 4.2 : Effect of compatibiliser composition on tensile modulus of PA6/ABS blends

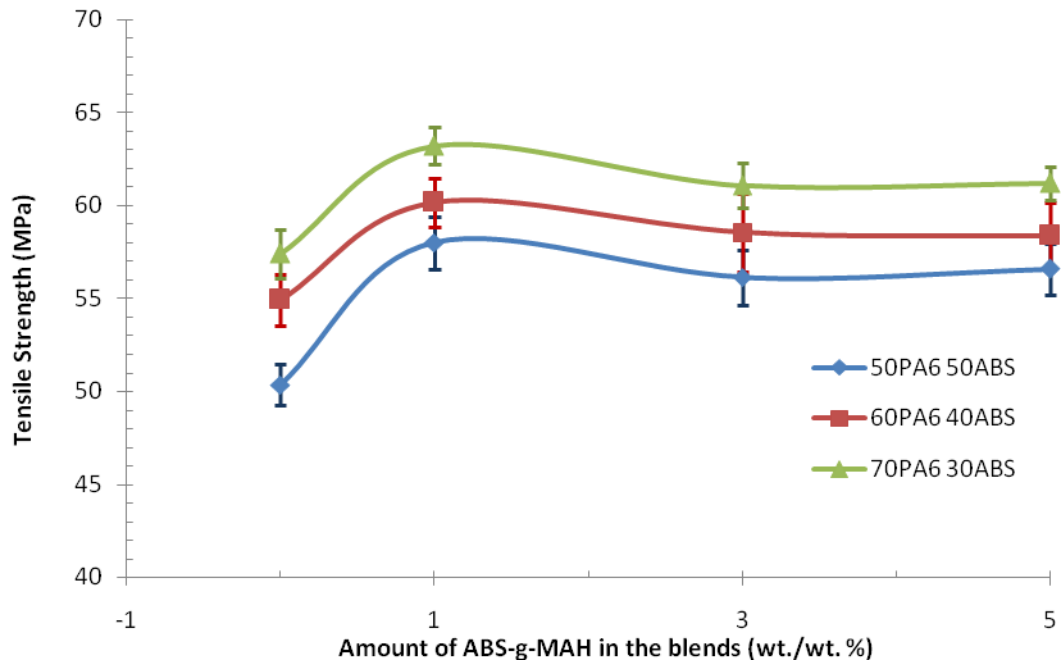


Figure 4.3 Effect of compatibiliser composition on tensile strength of PA6/ABS blends

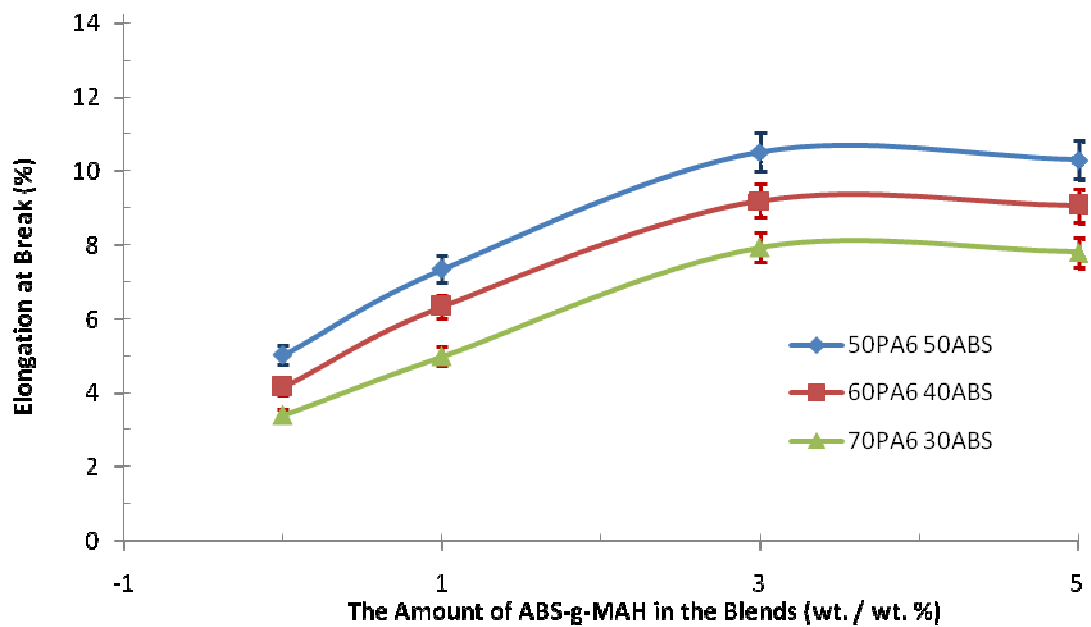


Figure 4.4 : Effect of compatibiliser composition on elongation at break of PA6/ABS blends.

4.1.2 Flexural Properties of PA6/ABS Blends

The flexural properties of PA6/ABS blends are plotted against the amount of ABS-g-MAH as a compatibiliser in Figure 4.5 and 4.6, respectively. The compatibilised blends showed a higher flexural modulus values than the uncompatibilised blend over an entire range of compatibiliser contents, except at 70 wt. % PA6. This is believed to be due to sufficient amount of anhydride function in ABS-g-MAH to react with amine end group in PA6 to form a bridge between PA6 phases and ABS phases. From this result, it can be assumed that the present of ABS-g-MAH could reduce the interfacial tension thus, increased the adhesion between PA6 and ABS phases. However, the un-linear effect of compatibiliser compositions is believed to be due to the uneven reactions was occurred in the blends between amine end group of PA6 and maleic anhydride (Kudva *et al.* 2000). At 5 wt. % of ABS-g-MAH compositions, there was a slightly reduction in flexural modulus and strength. This reduction is not in agreement with the tensile modulus and strength results, which was discussed earlier in section 4.1.1. During the incorporation of ABS-g-MAH into PA6/ABS blends, ABS component in compatibiliser tends to agglomerate within ABS phases, and resulted partially maleic anhydride reacted with PA6. This effect consequently reduced the properties as compared to 3 wt. % of compatibiliser. This also could be due to repulsion of polar segments of PA6 and acrylonitrile segments in ABS. Consequently, more phase separation occurred as compared to lower concentration of ABS-g-MAH.

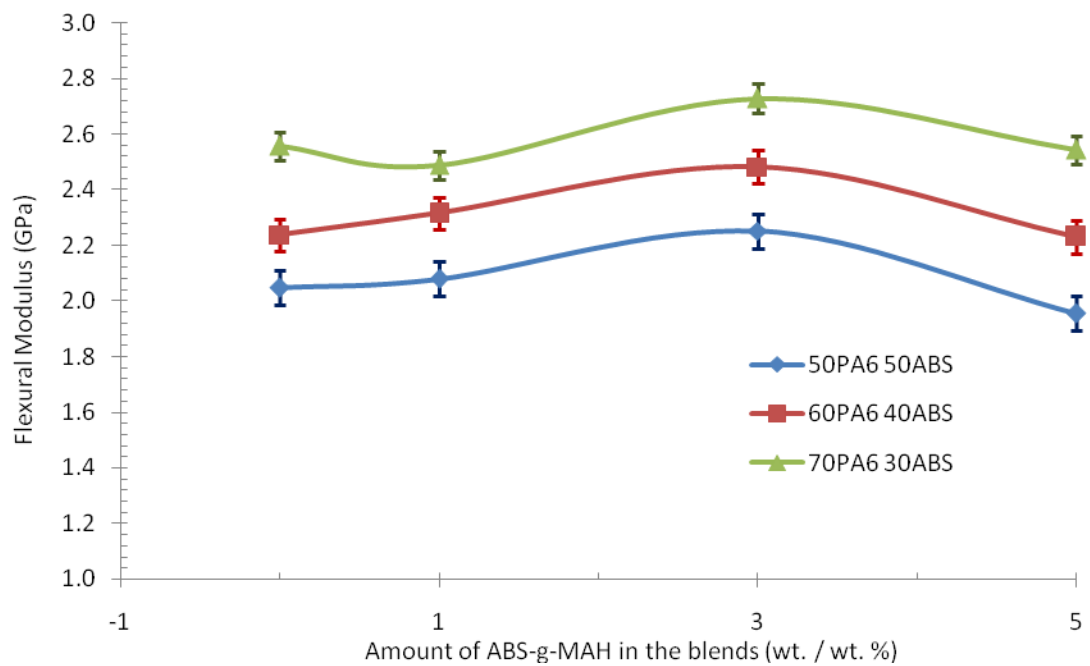


Figure 4.5 : Effect of compatibiliser composition on flexural modulus of PA6/ABS blends.

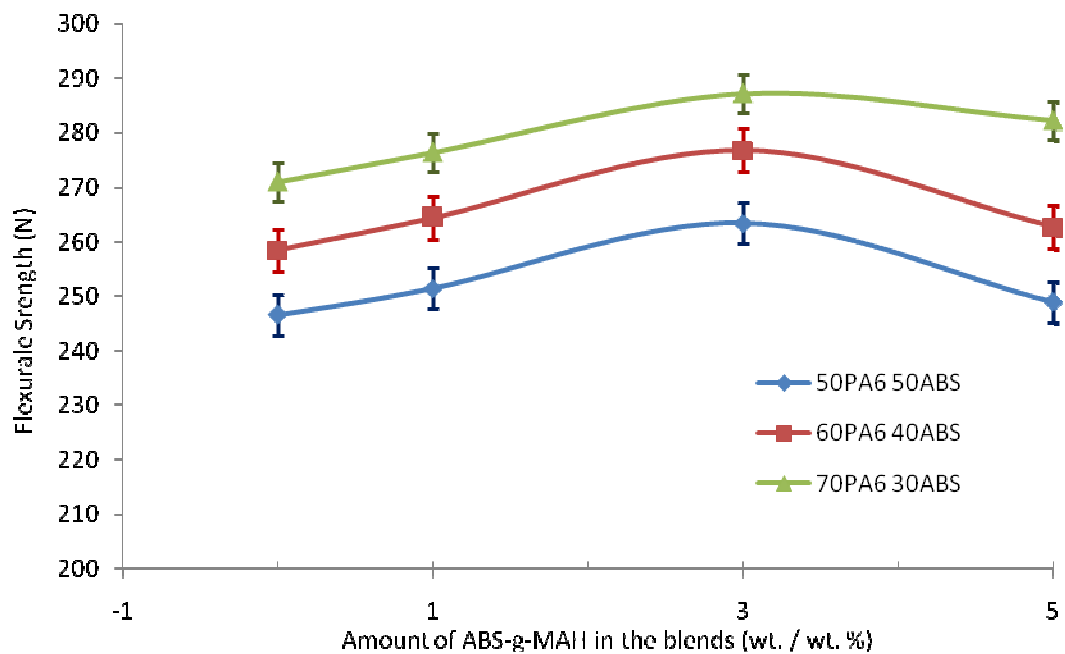


Figure 4.6 : Effect of compatibiliser composition on flexural strength of PA6/ABS blends

4.1.3 Impact Properties of Polymer Blends

The notched Izod impact strength of virgin PA6 and ABS were measured at about 4.4 and 24.9 kJ/m², respectively. The lower notched impact strength of PA6 is owing to the poor mobility of the segments resulted from high crystallinity as compared to virgin ABS. The Izod impact strengths for the uncompatibilised blends were lower than those of the virgin PA6 at any composition of ABS. When the ABS was increased to a certain amount, the blends exhibited higher level of Izod impact strength as the virgin PA6. Figure 4.6 shows the impact energy absorption properties of PA6/ABS blends as a function of the blends composition and the amount of ABS-g-MAH copolymer added. For the uncompatibilised PA6/ABS materials, as expected, there was a continuous increase in toughness with ABS content since the amount of rubber in the system was also increased. In the absence of ABS-g-MAH compatibiliser, addition of ABS led to minor toughening, whereas with compatibilisation, there was a significant toughening.

The introductions of ABS increased the proportion of the amorphous part and increased the mobility of the segments, also higher than the uncompatibilised blends. Also with an adequate amount of ABS-g-MAH, the Izod impact strength of PA6/ABS blends were slowly improved at all PA6 blends compositions. This indicates a direct enhancement of interaction between amine group on PA6 and anhydride group in compatibiliser. In other words, ABS-g-MAH again increased the adhesion at interfaces of different domains, and reduced the repulsion among the segments of PA6 and ABS. Therefore, as shown in Figure 4.2, 4.3 and 4.4, the tensile properties of PA6/ABS blends were significantly improved by introducing ABS-g-MAH.

As shown in Figure 4.7, ABS-g-MAH itself constitutes a good impact modifier for PA6 and the toughening effect is obvious due to the presence of ABS in compatibiliser itself. However, when the amount of ABS-g-MAH was further increased to 3 wt. %, the impact property was slightly increased and the blending system underwent a brittle-ductile transition. In addition of that, when the amount of

ABS-g-MAH is about 1 wt. %, the notched impact strength dramatically increased at the amount of compatibiliser was about 3%. This is because the incorporation of enough ABS-g-MAH made the blends became tougher than the uncompatibilised blends. ABS-g-MAH acted like a 'bridge' between PA6 and ABS phase and made the links stronger as well as enhanced the quality of the component interfaces (Misra *et. al.*, 1993). Then, it can be concluded that, the incorporation of ABS-g-MAH increased the compatibility between the PA6 and ABS, which is reflected in the increased of impact strength.

Form the figure, it can be obtained that 3 wt. % of ABS-g-MAH content was selected as a composition for PA6/ABS blends compatibilisation. This is the because, further increase in ABS-g-MAH content was allowed an accessible amount in PA6/ABS blends thus reduction in flexural properties as discussed in Section 4.1.2 and slightly increased in impact strength. Considering to the fact that the flexural strength represents a stiffness of material and impact strength as a material toughness, hence 3 wt. % was chosen as content of ABS-g-MAH was blended with addition of short glass fibre to form PA6/ABS composites. Besides that, the ratio of 60/40 for PA6 and ABS component was selected to be due to the same reason. It can be observed the impact and flexural strength of the PA6/ABS blends at the ratio was about 60/40 were consistent as compared to 70/30 and 50/50. This is can be explained that 70/30 PA6/ABS blends is the highest flexural strength at all range compatibiliser as compared to 60/40 and 50/50. Whereas, 50/50 PA6/ABS blends is the highest impact strength as compared to 60/40 and 70/30 PA6/ABS blends.

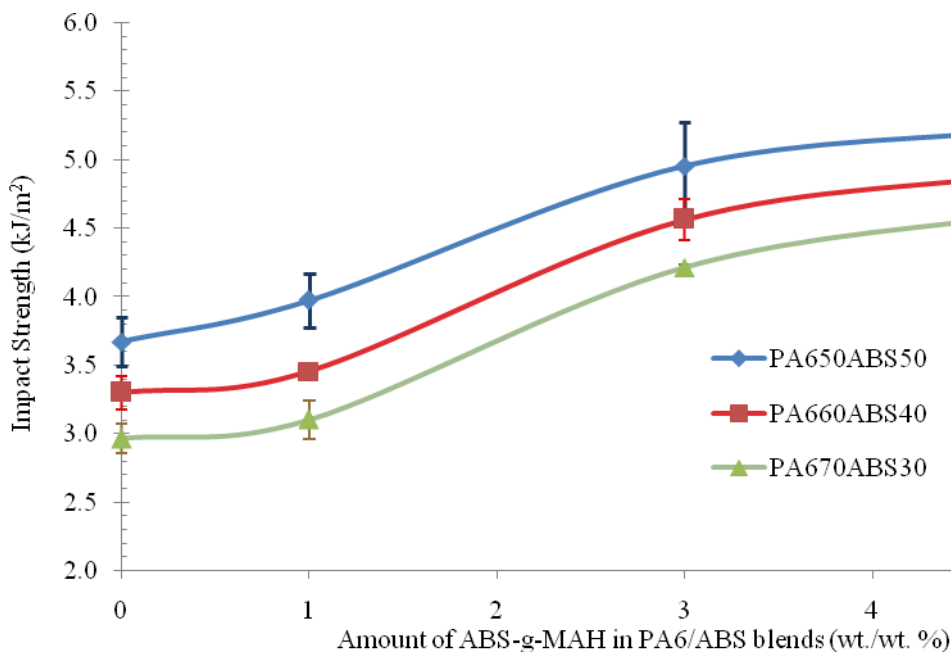


Figure 4.7 : Effect of compatibiliser composition on impact strength of PA6/ABS blends

4.1.4 Tensile Properties PA6/ABS Composites

Figures 4.8, 4.9 and 4.10 show the effect of glass fibre composition up to 30 wt. % on tensile modulus, strength and elongation at break of 60/40 PA6/ABS composites with the compatibiliser content was about 3 wt. %. Figure 4.8 shows that tensile modulus increased exponentially with increasing amount of glass fibre. This suggests that the present of glass fibres acted as reinforcement on the 60/40 PA6/ABS blends. The trend indicates that the SGF phase melt-blended with PA6/ABS blends improved the modulus and increased the stiffness of the material. However, the composites appeared to more breakable or brittle compared to the one without SGF. This phenomenon is supported by the trend of elongation at break of PA6/ABS composites.

In addition to the tensile modulus, the tensile strength also was calculated for SGF reinforced PA6/ABS composites. It is shown in Figure 4.8 that the SGF reinforced PA6/ABS composites revealed an almost linear increased in tensile

strength with SGF content. It can be concluded that, SGF improved the tensile properties of PA6/ABS composite with exponentially increased in modulus, linearly increased in tensile strength and reduced in elongation at break.

Further increase in SGF content decreased the elongation at break, as shown in Figure 4.10. However, above 10 wt. % of SGF content, the elongations at break of PA6/ABS composites are considering achieve almost a constant at value. It can be seen that the incorporation of SGF reduced the compatibility between PA6 and ABS, which is reflected in the slightly decreased in elongation of these blends. These observations which refer to the tensile properties can be rationalised in that the SGF acted as a reinforcing agent in the PA6/ABS composites, and the pure SGF is known to be quite susceptible to break at room temperature. The tensile properties of SGF were not measured due to difficulties and inconsistencies that would arise due to the relatively, extremely brittle nature of the pure glass. Several researchers (Cho and Paul, 2000; Kannan and Misra, 1994; Ozkoc *et al.*, 2005) have studied the trend of increasing tensile modulus and decreasing elongation at break with the increasing amount of SGF in the composites. Studied by Young and Baird (2000) on tensile strength, modulus and elongation of phosphate glass in poly (ether ether ketone) (PEEK) and poly(ether imide) (PEI) also showed a similar behaviour. These results explained that SGF enhanced the stiffness of the composites but reduced the performance of the toughness.

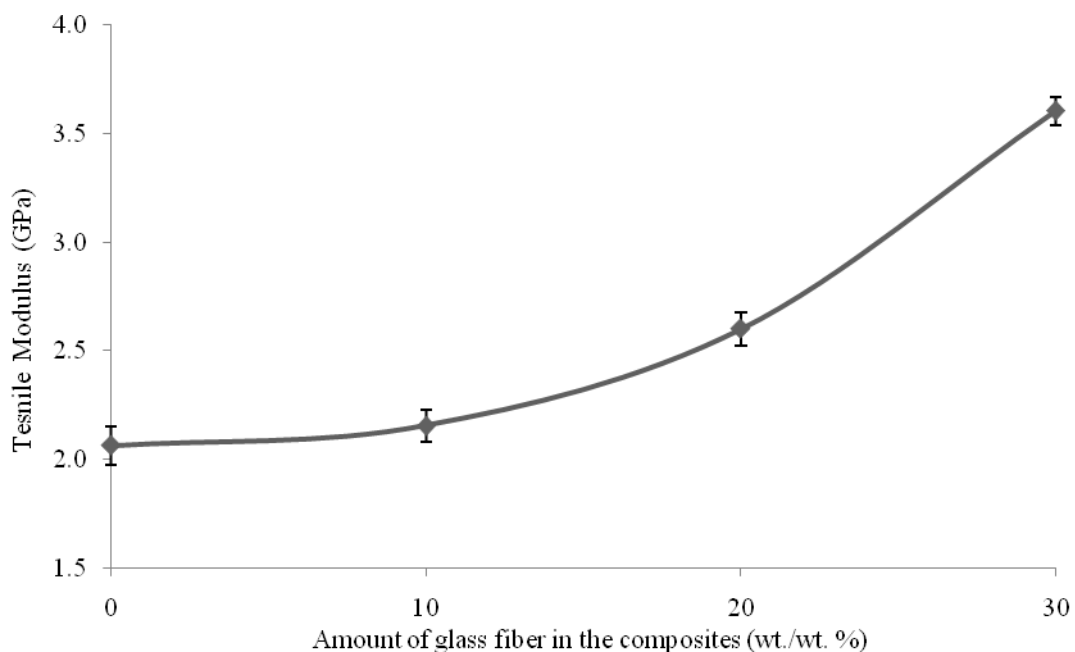


Figure 4.8 : Effect of glass fibre composition on tensile modulus of 60/40 PA6/ABS composites

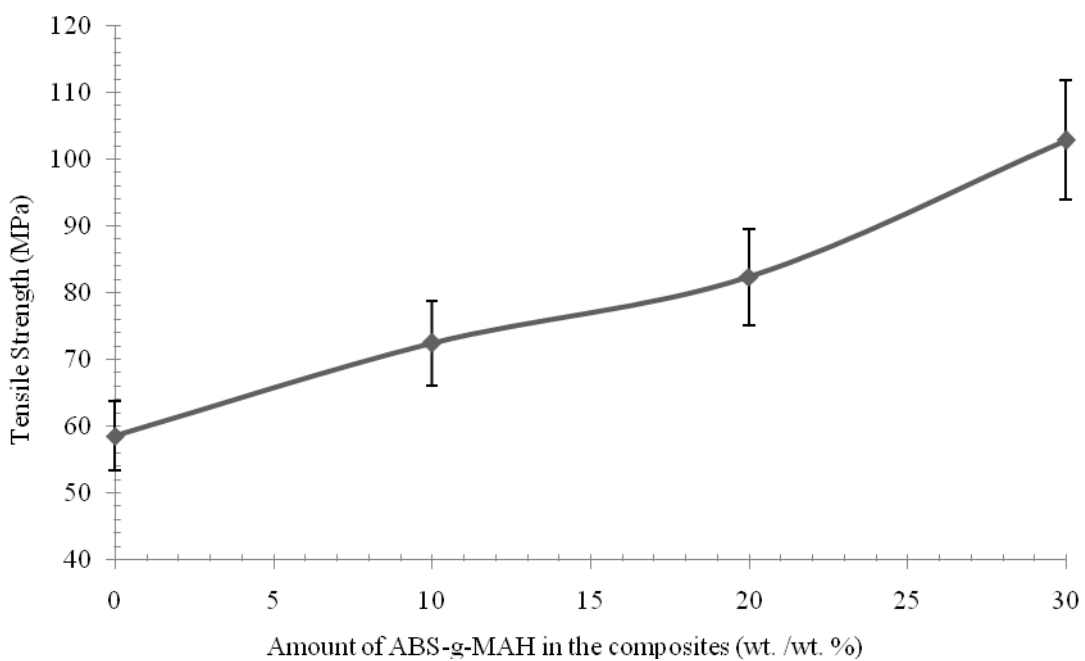


Figure 4.9 : Effect of glass fibre composition on tensile strength of 60/40 PA6/ABS composites

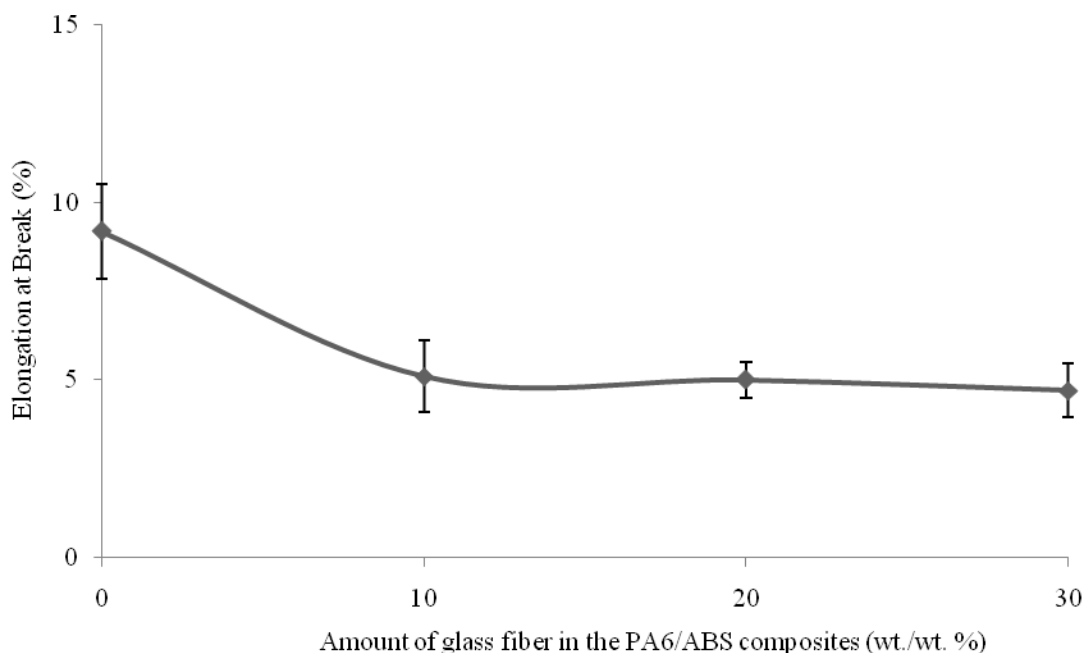


Figure 4.10 : Effect of glass fibre composition on elongation at break of 60/40 PA6/ABS composites

4.1.5 Flexural Properties PA6/ABS Composites

The flexural modulus and strength values are plotted as a function of SGF content shown in Figures 4.11 and 4.12, respectively. For blends of PA6 and ABS, it was found that by increasing the percentage of SGF, the flexural modulus and strength increased. The incorporation of SGF in these polymer blends showed better strength values. As the SGF content was increased from 0 to 30 wt. %, the corresponding strength properties were also improved significantly. The trend is similar to the result of tensile properties as explained in section 4.1.4.

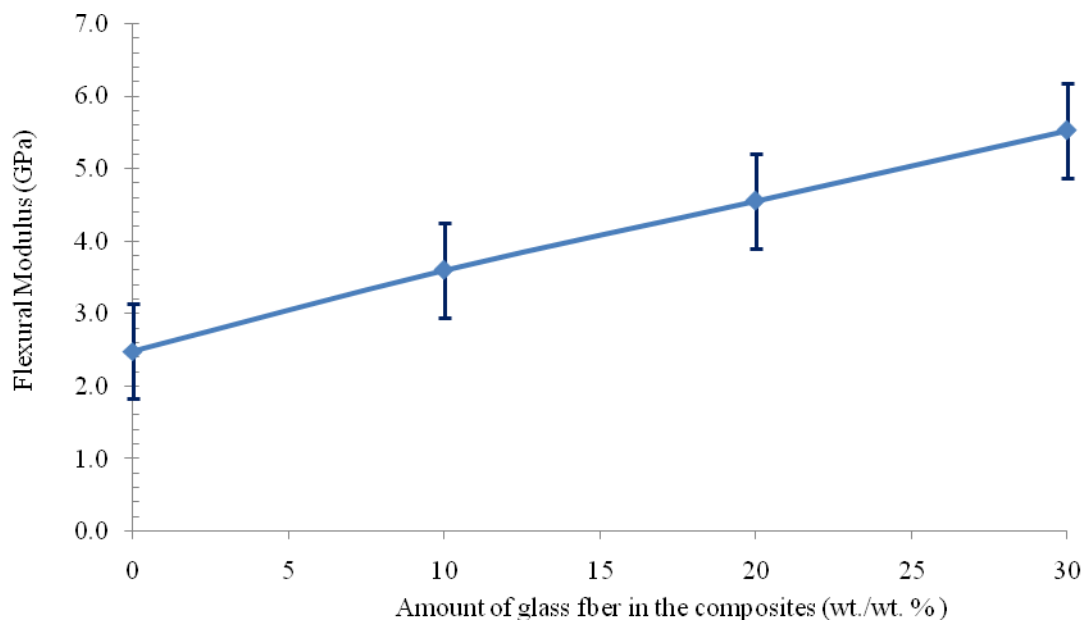


Figure 4.11 : Effect of glass fibre composition on flexural modulus of PA6/ABS composites.

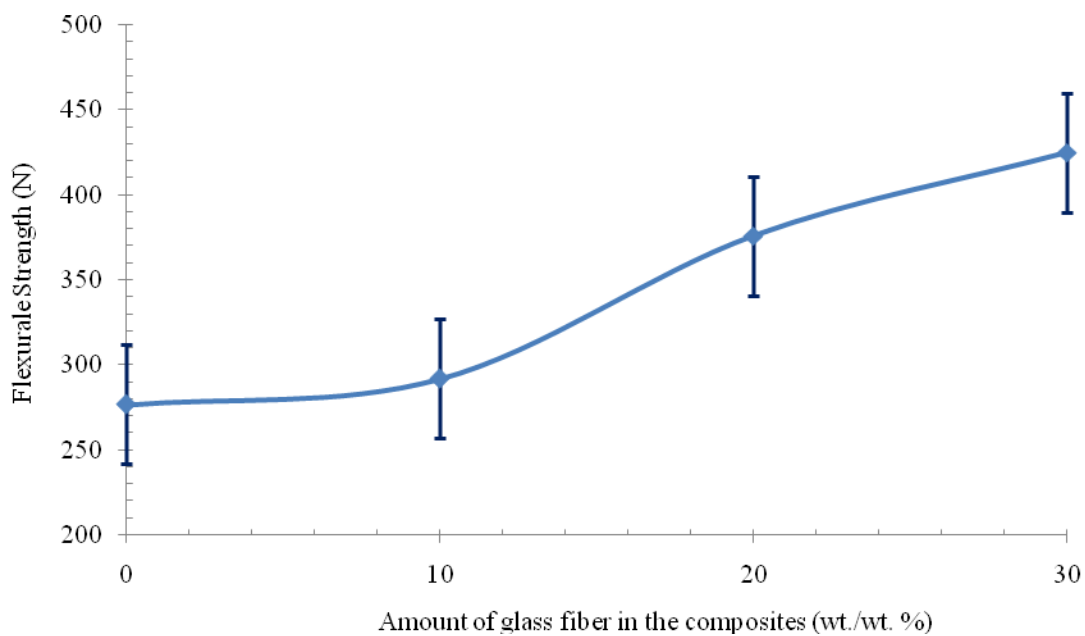


Figure 4.12 : Effect of glass fibre composition on flexural stress of PA6/ABS composites

4.1.6 Impact Properties of PA6/ABS Composites

Figure 4.13 shows the notched Izod impact energy of composites (60/40 PA6/ABS compatibilised with 3 wt. % ABS-g-MAH) versus the composition of SGF. The unreinforced PA6/ABS materials, as expected, the toughness was higher than the reinforced PA6/ABS composites due to the amount of rubber in the system is higher. It was found that, when the SGF was introduced into the system, the blends showed a continuous linearly reduction in impact properties. Generally, it can be explained that, the toughness was increased by incorporation of ABS due to ABS has a strong a ductility properties. At the addition of SGF substantially decreased the toughness and increased the stiffness all the materials. It is well known that the SGF stiffer than the ABS and PA6. These results are not in agreement with the impact study by Cho and Paul (2000). They studied glass-fibre reinforced PA6 toughened with ABS and EPR-g-MA as compatibiliser and found that, with increasing of amount of SGF and compatibiliser, the impact strength of the their composites increased to be due to the ABS phase became more efficiently dispersed and the PA6 phase became more continuous in character.

It is clear that when the amount of SGF was increased to about 10 wt. %, the impact strength decreased drastically. The drastically reduction at 10 wt. % could be due to matrix embrittlement (Kanan and Misra, 1994). They studied 70/30 PA6/ABS as a matrix and compatibiliser was kept at the percentage of 5 wt. % styrene-grafted maleic anhydride. Beyond this point, the small increment in impact strength with further addition about 20 wt. % SGF to be due to the fact that the fibres are shorter length and shorter fibres are effective energy absorbers by pull-out and debonding. Kanan and Misra (1994) commented again a trend that further addition of glass fibre leads to improvement of impact strength. However, the trend was not observed in this study which was, generally, the incorporation SGF reduced the impact properties of the composites.

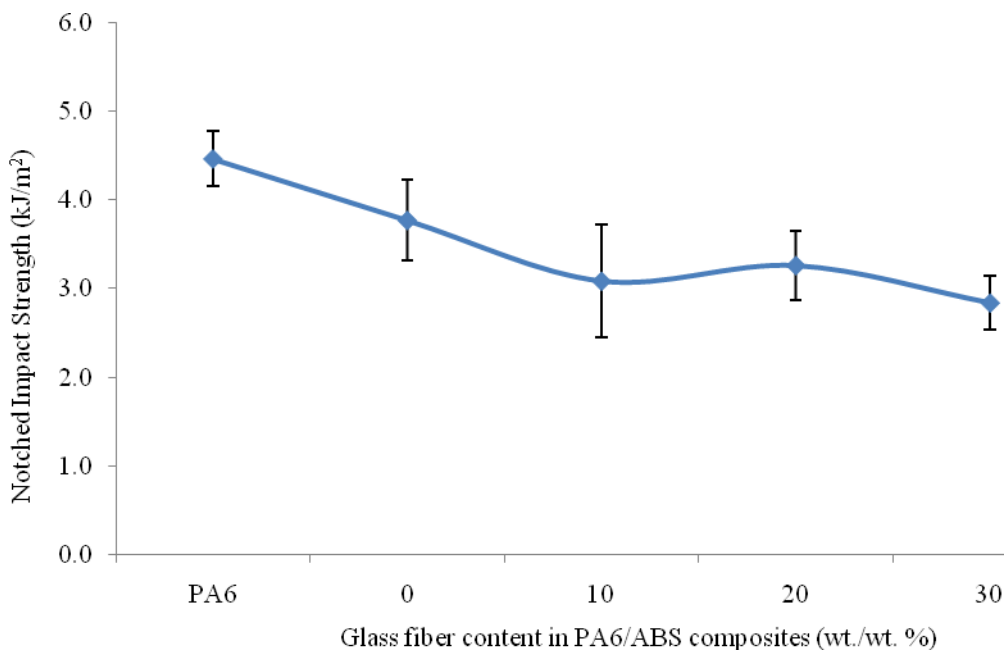


Figure 4.13 : Effect of glass fibre composition on notched Izod impact strength of 60/40 PA6/ABS composites

4.2 Thermal Properties

4.2.1 Thermal Properties of PA6/ABS Blends

Semicrystalline PA6 have its melting and crystallisation behaviour changed by the presence of a second component in PA6 blends (Araujo *et al.*, 2005, Araujo *et al.*, 2004). Any significant change in PA6 melting and crystallisation behaviour in the blend can lead to changes in properties of moulded parts. Those changes can become more significant when in situ reactive compatibilisation is used for the blending. PA6 molecular grafting, due to reactive compatibilisation, may modify its kinetics of crystallisation, which certainly would lead to different crystal dimensions and different degree of crystallinity as compared to virgin PA6.

DSC was used to evaluate the melting and crystallisation behaviour of the PA6 component in the blends. Melting temperature at second heating run, T_{m2} , heat of fusion at second heating run, ΔH_{m2} and degree of crystallisation, X_c were determined from second heating thermograms and T_c and ΔH_c were measured from cooling thermograms. As can be seen from Tables 4.1, 4.2 and 4.3, the addition of ABS to the pure PA6 slightly changed the melting behaviour of the components at first heating run. Compatibilised blends exhibited a lower melting temperature with respect to uncompatibilised blends at first heating but the melting temperature almost constant value at the second heating run. This indicates that compatibility of the system was improved with the addition of compatibiliser according to T_m depression criteria (Hage *et al.*, 1999). At second heating run, two melting peaks were observed in the DSC thermograms for all blends system with all composition of compatibiliser as shown in Figures 4.14, 4.15 and 4.16, respectively. This is could be, at the first melting peak, less perfect PA6 crystals which has been formed in the cooling step, then forms more perfect crystals upon crystallisations, then finally melts at the second melting peak (Tol *et al.*, 2005).

For all the blends system, the small peak observed before the melting is the reorganisation of the less perfect PA6 crystals. These crystals are the monoclinic γ -crystals of the PA6 (Ozkoc *et al.*, 2006; Tol *et al.*, 2005). The formation of this structure at the presence of compatibiliser might results in an increased extend of reaction of MAH with amine end group of PA6; thus the formation of α -crystals is hindered because of this grafting reaction. This phenomenon is also observed from X_c and T_c , which are lower when compared to the uncompatibilised blend systems. The chemical reaction leads to an increase in the viscosity of the media and reduce the crystallisation rate and crystal growth.

Figure 4.17 illustrated the degree of crystallinity PA6/ABS blends as a function of ABS-g-MAH concentration, at various PA6 compositions. The degree of PA6/ABS blends were calculated using the equation 3.3 and heat of melting for PA6 at 100% crystalline is about 191 J/g (Bandrup and Immergut, 1989). Generally, The X_c of all the blends were lower than virgin PA6 to about 35% crystallinity. The presence of ABS exhibits the crystallisation (Bhardwaj *et al.*, 1990). The

crystallinities of these blends were independent of the composition of blends, and decreased with the increase of ABS-g-MAH amount in the blends. The reduction of crystallinity may be due to the formation of graft copolymers by the reactions of amide end groups of PA6 with ABS-g-MAH (Gao *et al.*, 1999). This effect can also be observed from T_c values. Addition of the second phase together with a compatibiliser decreased the crystallisation temperature as a result of retardation effect of increasing viscosity due to the compatibilisation reactions.

Table 4.1 shows that the addition of ABS-g-MAH to the PA6/ABS blends has significantly changed the melting temperature for the first heating run. For the second heating run, the melting temperature of 50/50 PA6/ABS has not significantly effected by the addition of ABS-g-MAH. However, it is shown that the ABS-g-MAH interfere in the crystallisation of PA6/ABS blends. The heat of crystallisation for compatibilised 50/50 PA6/ABS blends has shown a reduction as compared to uncompatibilised PA6/ABS blends. Jannash *et al.*, (1999) have observed that the addition of reactive compatibiliser affected the crystallisation of the blends. Compatibilisation of PA6/ABS made by ABS-g-MAH has strongly changed the crystallisation parameters.

There were also depressions in the crystallisation temperature and the heat of crystallisation as a function of ABS-g-MAH concentration. ABS-g-MAH could strongly affect melting and crystallisation in PA6/ABS blends, where crystallisation properties increased when the amount of compatibiliser increased. However, the increasing of crystallisation has reached a maximum value when ABS-g-MAH concentration was about 1 wt. % and gradually decreased as ABS-g-MAH increased as shown in Figure 4.17. It is suggested that ABS-g-MAH fully reacted with amine end group of PA6 at 1 wt. %. These findings are in agreement with tensile modulus and strength as discussed at Section 4.1.1. Further increase in compatibiliser content has attributed the excess of the amount and affected the thermal properties thus reducing the crystallisation of the blends. This trend is similar for 60/40 and 70/30 PA6/ABS blends as shown in Tables 4.2 and 4.3, respectively.

Table 4.1 : DSC data for 50/50 PA6/ABS Blends

wt/wt % of ABS-g- MAH	T_m^1 (°C)	ΔH_m^1 (J/g)	T_c (°C)	ΔH_c (J/g)	$T_{g(PA6)}$ (°C)	$T_{g(ABS)}$ (°C)	T_m^2 (°C)	ΔH_m^2 (J/g)	X_c (%)
0	224.4	34.5	191.4	32.0	56.0	112.7	223.3	30.5	16
1	223.8	34.3	191.9	31.6	65.7	110.1	222.4	34.3	18
3	223.8	33.0	191.0	31.3	66.0	107.2	223.1	32.1	17
5	224.9	31.6	190.9	30.9	65.7	108.0	223.8	29.5	15

Table 4.2 : DSC data for 60/40 PA6/ABS Blends

wt/wt % of ABS-g- MAH	T_m^1 (°C)	ΔH_m^1 (J/g)	T_c (°C)	ΔH_c (J/g)	$T_{g(PA6)}$ (°C)	$T_{g(ABS)}$ (°C)	T_m^2 (°C)	ΔH_m^2 (J/g)	X_c (%)
0	224.8	39.3	192.7	38.8	51.7	109.4	223.4	38.1	20
1	224.1	38.6	194.1	40.8	60.9	106.1	223.4	44.0	23
3	223.2	36.7	191.7	39.8	61.3	104.5	223.1	41.7	22
5	224.3	35.4	191.8	38.3	61.6	102.2	223.6	36.1	19

Table 4.3 : DSC data for 70/30 PA6/ABS Blends

wt/wt % of ABS-g- MAH	T_m^1 (°C)	ΔH_m^1 (J/g)	T_c (°C)	ΔH_c (J/g)	$T_{g(PA6)}$ (°C)	$T_{g(ABS)}$ (°C)	T_m^2 (°C)	ΔH_m^2 (J/g)	X_c (%)
0	226.4	46.5	192.8	43.0	47.5	104.7	216.9	44.6	23
1	225.0	40.3	193.6	47.1	56.9	104.2	223.5	49.9	26
3	225.3	41.4	192.4	44.7	58.1	103.1	223.5	46.5	24
5	225.0	42.4	192.4	46.2	55.0	102.9	224.1	44.1	23

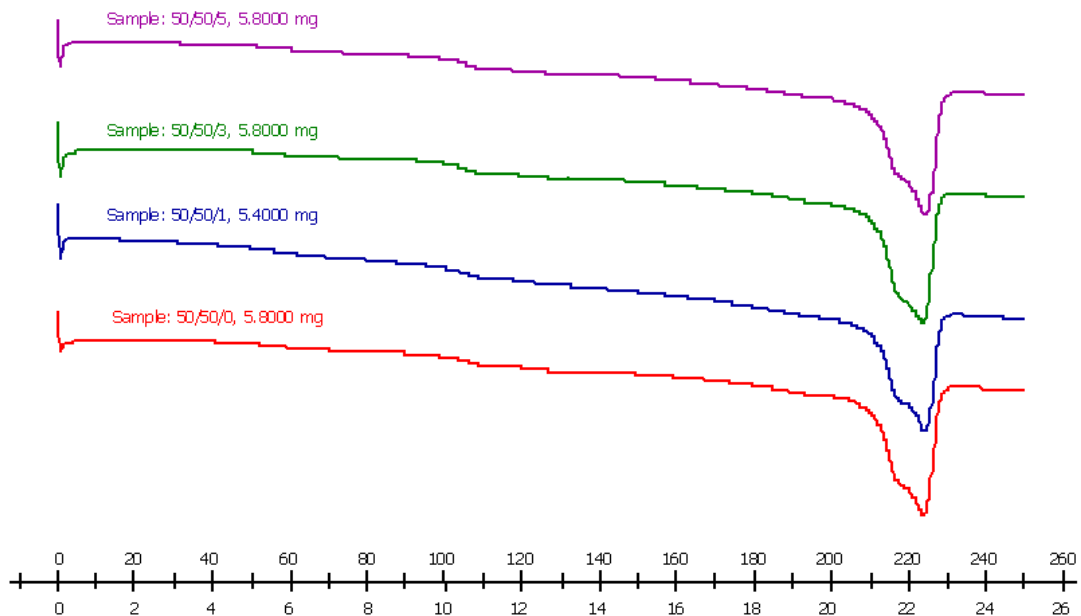


Figure 4.14 : DSC second heating run thermogram of 50/50 PA6/ABS blends at different composition of compatibiliser

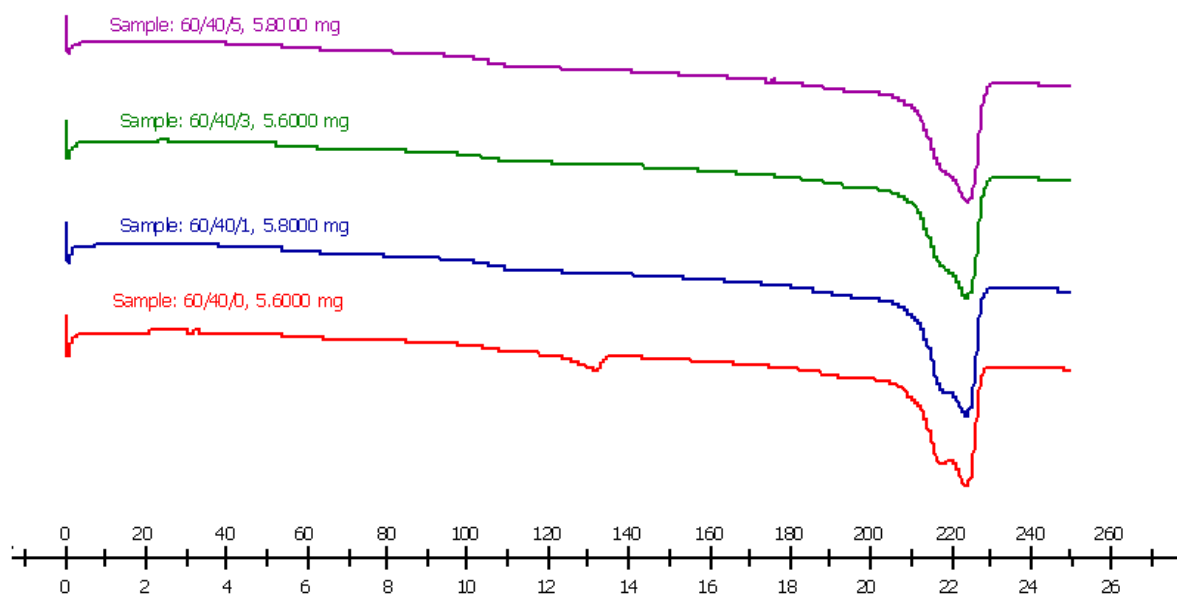


Figure 4.15 : DSC second heating run thermogram of 60/40 PA6/ABS blends at different composition of compatibiliser

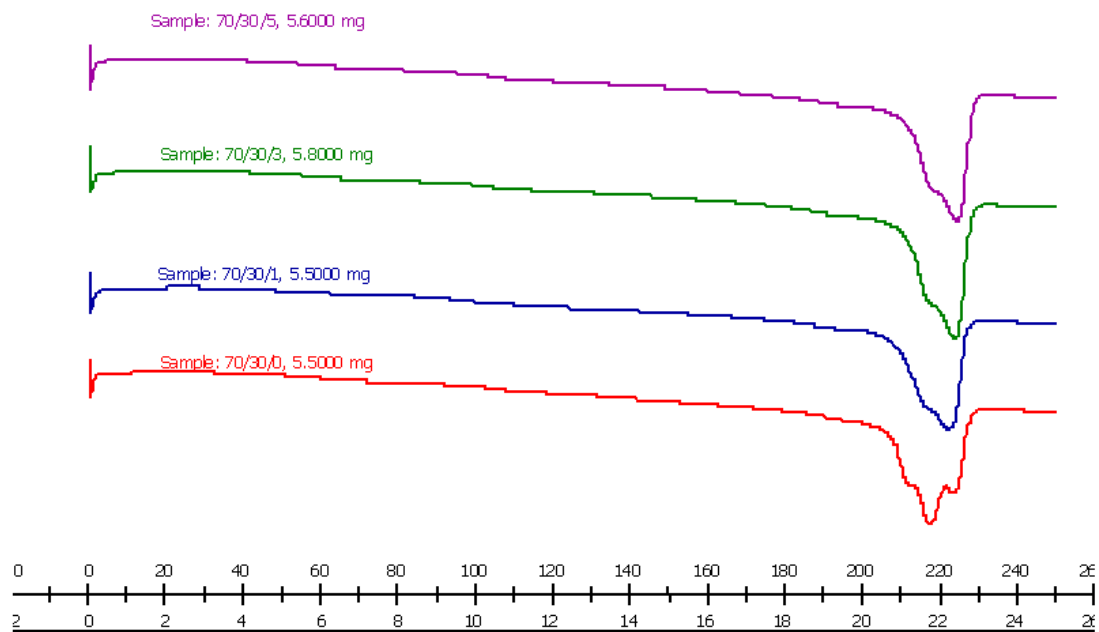


Figure 4.16 : DSC second heating run thermogram of 70/30 PA6/ABS blends at different composition of compatibiliser

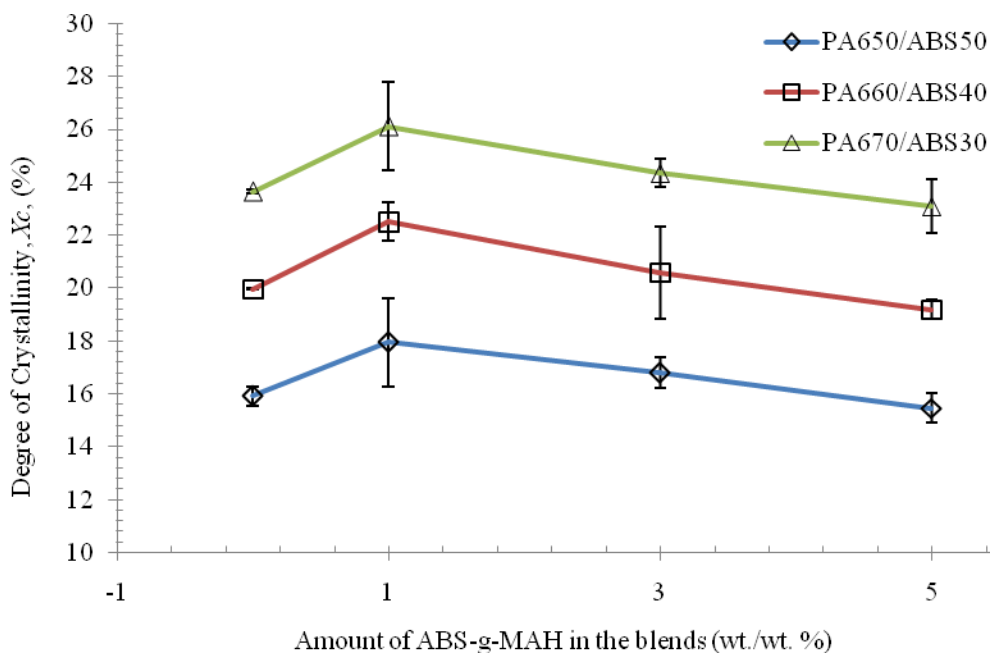


Figure 4.17 : Degree of crystallinity of PA6/ABS blends as a function of ABS-g-MAH concentration, for various PA6 compositions

4.2.2 Thermal Properties of 60/40 PA6/ABS Composites

The DSC thermal studies were scanned for 60/40 PA6/ABS composites with 3 wt. % compatibiliser and SGF concentration varied from 0 to 30 wt. %. Table 4.4 shows the numerical results of the temperature scanned and Figure 4.18 illustrates the degree of crystallisation for PA6/ABS composites. It is obvious from the data that SGF affected on thermal properties of the composites. The melting temperatures at first heating run appeared to change as observed with increasing the SGF content in the composites and considerably small change at second heating run. Teh (1983) suggested that no shift in melting temperature implies incompatibility between the components. Therefore, it seems that the incompatibility has not appeared in our composites system by increasing amount of SGF. This indicates the incorporation of SGF has maintained the compatibility of the system. This is believed that, the selected SGF has a good adhesion with PA6 resulted a little increased in melting temperature either in first or second heating run.

The heat of melting and the percent of crystallinity decreased significantly with the addition of SGF to the matrix. This phenomenon suggested that the presence of SGF inhibits crystalline formation in any particular composition. Jog and Nadkani (1986) reported that the crystallinity of semicrystalline polyphenylene sulphide (PPS) filled with glass fibre decreased due to the mobility of the PPS chain was inhibited with the presence of glass fibre. However, other researchers (Avalos *et al.*, 1998; Gupta *et al.*, 1982) found that by incorporation of GF increased the crytallinity of the polymer matrix. They commented that the increase in crystallinity was due to the polymer matrix which forms crystallinity along the surface of the fibre. As a conclusion, it is clear that the crystallinity decreased with increasing amount of compatibiliser. This indicates that, the SGF tends to agglomerate within their phase due to short in length that form multiphase in the composite system.

Table 4.4 : DSC data for 60/40 PA6/ABS Blends

wt/wt % of SGF	T_m^1 (°C)	ΔH_m^1 (J/g)	T_c (°C)	ΔH_c (J/g)	$T_{g(PA6)}$ (°C)	$T_{g(ABS)}$ (°C)	T_m^2 (°C)	ΔH_m^2 (J/g)	X_c (%)
0	223.2	36.7	191.7	39.8	61.3	104.5	223.1	41.7	22
10	225.1	24.1	191.9	31.8	61.5	107.0	223.6	31.8	17
20	224.3	26.2	191.4	31.6	62.1	107.2	224.4	29.0	15
30	225.4	26.8	193.2	25.7	62.6	108.2	224.9	25.6	13

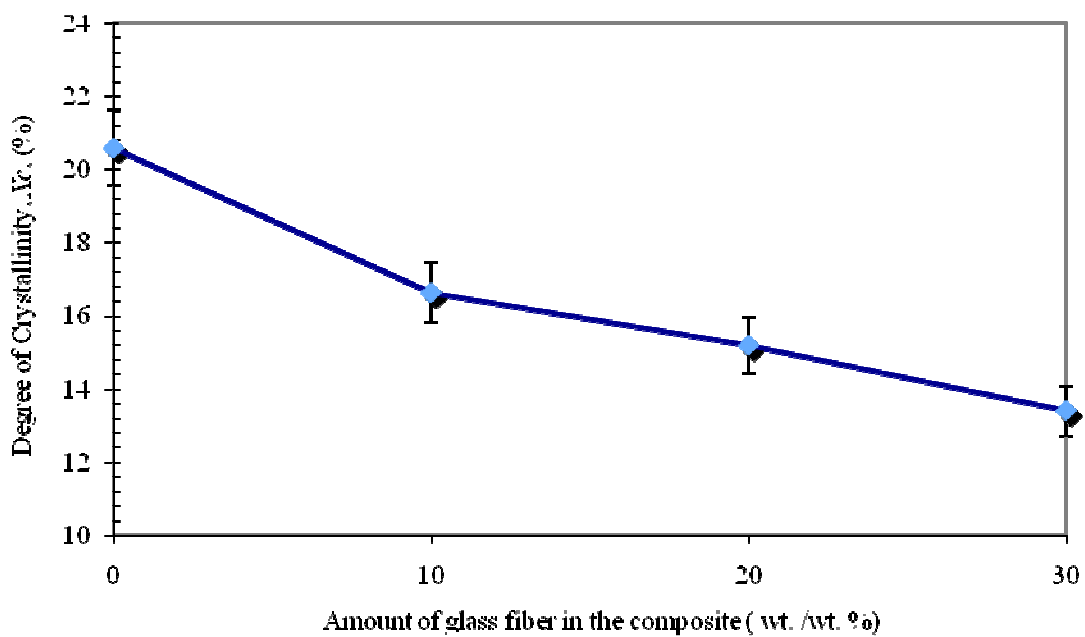


Figure 4.18 : Degree of crystallinity of 60/40 PA6/ABS composites as a function of different amount of short glass fibre

4.3 Dynamic Mechanical Analysis (DMA)

4.3.1 PA6/ABS Blends

The demand of PA6/ABS blends for external application in electronic and automotive application especially as high performance parts has been increasing from time to time because its good mechanical properties. On top of that, this material is mainly used in under vibration damping. Therefore, dynamic mechanical analysis (DMA) result can be utilised in mechanical damping application to reduce vibrations. DMA properties of polymer blends depend on various factors such as reaction of compatibiliser to form grafted and nature of dispersed-matrix interface region. DMA over a wide range of temperature is especially sensitive to all kinds of transitions and relaxation process of polymers and also to the morphology of the polymers blends. DMA method can also be used to investigate the miscibility or compatibility of polymer systems through some kind of specific interaction by various groups (Higgins and Walsh, 1984) such as reactive compatibilisation by forming grafting between the polymers phases. The specific information that can be obtained by this method includes the storage modulus, E' , the loss modulus, E'' and $\tan \delta$ as a function of temperature or frequency.

4.3.1.1 Storage Modulus of PA6/ABS Blends

Dynamic storage modulus (E') is the most important property to assess the load bearing capacity of the blends material. It is also represents the elastics components of the blends during the dynamic deformation. The variations of storage modulus of PA6/ABS blends ratio as a function of temperature are given in Figure 4.19, 4.20 and 4.21. There was a prominent increase in the modulus of the blend with the incorporation of compatibiliser over the entire region. As the temperature

increased, E' decreased and then there was a sharp decline in the E' value at the glass transition region. This behaviour can be attributed to the increase in a molecular mobility of the polymer chains above T_g . The drop in the modulus in the glass transition region was much less for higher PA6 amount than for the lower composition of PA6 in the blends. That is, the difference between the moduli of the glassy state and the rubbery state was smaller in higher amount of PA6 than with lower PA6. This is due to the considerable increase in the modulus both in the rubbery region and glassy region.

It is clear from Figure 4.19 that at lower temperature (transition region), the uncompatibilised 50/50 PA6/ABS had lower moduli compared to the compatibilised PA6/ABS. It seems that, with the addition of compatibiliser, the moduli of PA6/ABS were enhanced and 5 wt. % showed the highest value of storage modulus. This is evident that ABS-g-MAH has successfully acted as compatibiliser. However, the addition 3 wt. % of ABS-g-MAH did not improve much the storage modulus of the blends as compared to 1 wt. %. This is believed that, to be due to the enhancement could be fully occurred at 1 and 5 wt. % of compatibiliser. At 3 wt. % the amount of compatibiliser considered not all the compatibiliser reacted with amine end group of PA6 and affected the elastic component of the blends. This phenomenon is supported by the discussion of FTIR analysis in Section 4.4.4.8. In addition to that, the ABS domains in PA6 phase for 1 and 5 wt. % restricted the mobility of the chain. These results are in agreement with tensile modulus, which was discussed earlier in section 4.1.1. At higher temperature, the storage modulus for all the 50/50 PA6/ABS blends showed almost identical.

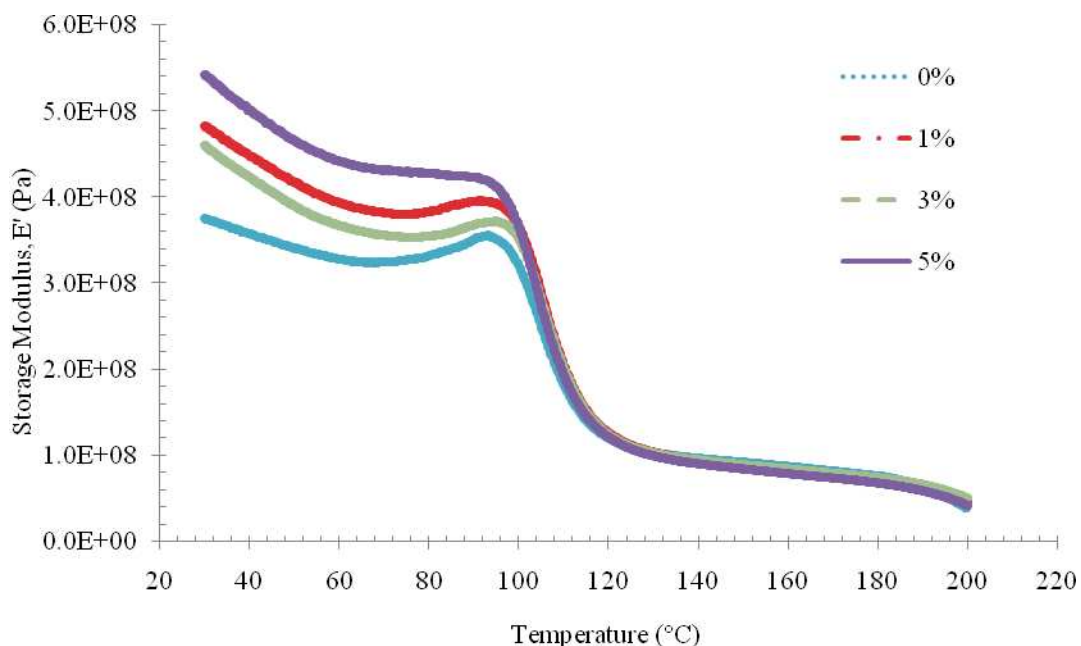


Figure 4.19 : Storage modulus vs. temperature plot for different composition of compatibiliser in 50/50 of PA6/ABS blends

Figure 4.20 shows the effect of compatibiliser contents on storage modulus of DMA for 60/40 PA6/ABS blends. The maximum E' value was exhibited by the blends having 1 wt. % of compatibiliser content at 680 MPa, and for the uncompatibilised was only 480 MPa at room temperature. It is clear that the storage modulus of the blends was enhanced by more than 40% upon the addition of 1 wt. % ABS-g-MAH at room temperature. On further increasing the compatibiliser content to 3 wt. %, E' value was found to decrease and slightly increased at 5 wt. %. This depicts showed an un-linearly improvement in strength by the addition of compatibiliser. These results are not in agreement with impact strength, in which is impact strength was linearly enhanced by the addition of compatibiliser. Thus, it needs other properties to explain this phenomenon. Then, the moduli of all the 60/40 PA6/ABS blends are considered identical at highest temperature (after the transition region). Generally, the DMA results are in agreement with the tensile results was discussed in section 4.1.1, where the highest elastic properties at 1 wt. % of compatibiliser.

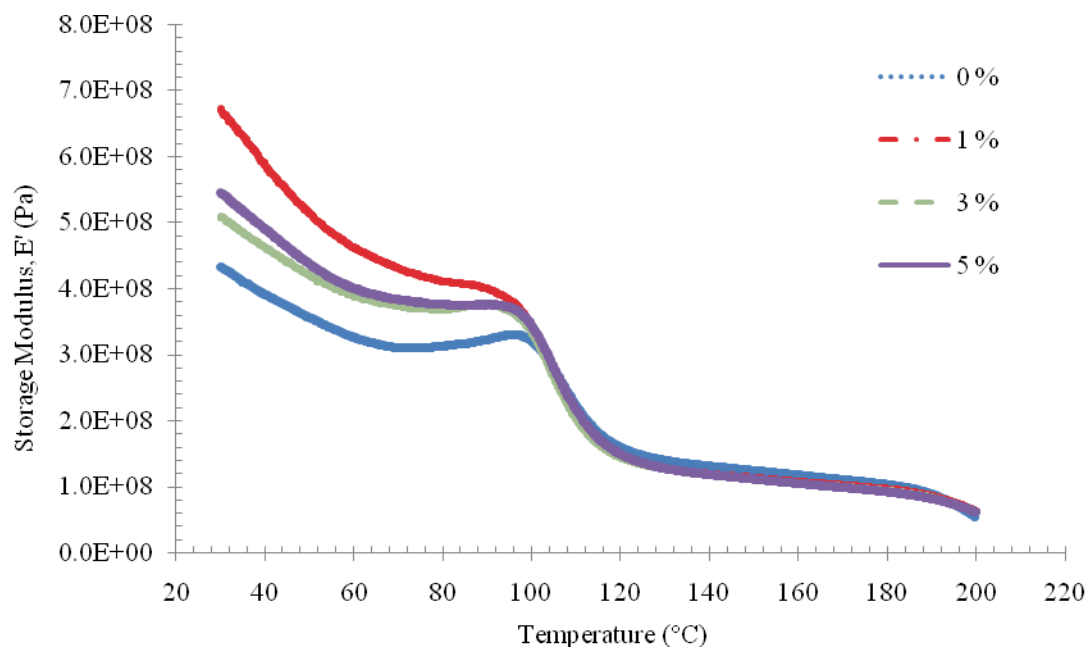


Figure 4.20 : Storage modulus vs. temperature plot at different composition of compatibiliser in 60/40 PA6/ABS blends

Figure 4.21 shows the effect of temperature on the storage modulus of 70/30 PA6/ABS blends at different composition of compatibiliser. The incorporation of compatibiliser proved the improvement of moduli as well as elastic component of the blends at below transition region. However, when the temperature was higher than T_g of SAN rich phase (transition region), again, the addition of compatibiliser did not affect the DMA properties of the blends as was found in 50/50 and 60/40 blend compositions.

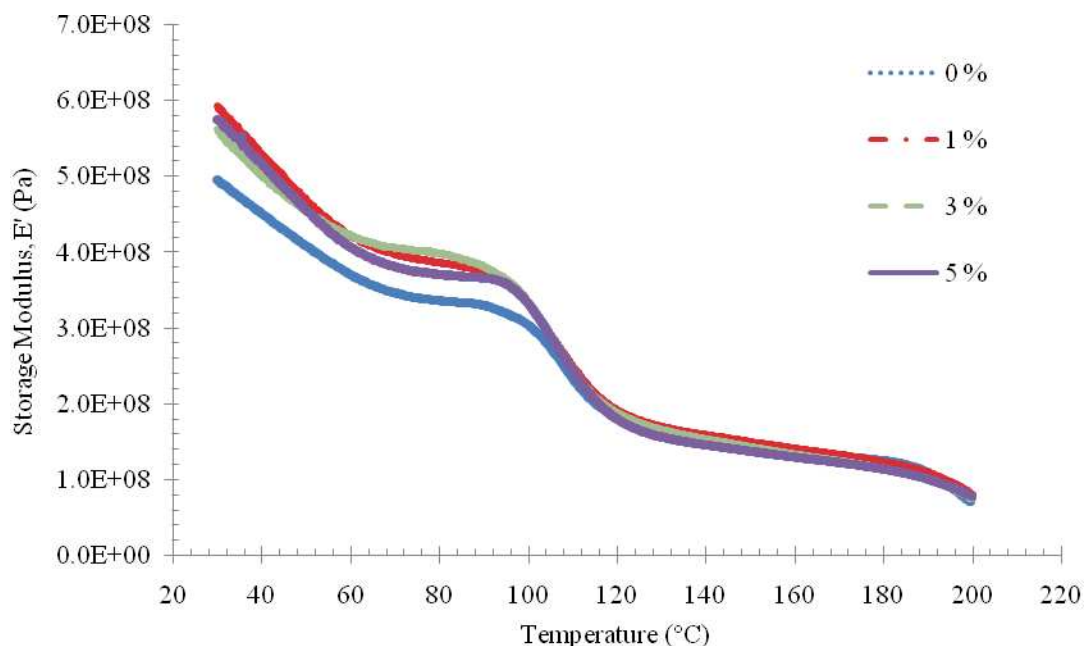


Figure 4.21 : Storage modulus vs. temperature plots at different composition of compatibiliser in 70/30 PA6/ABS blends

4.3.1.2 Loss Modulus of PA6/ABS Blends

Loss modulus (E'') is a measure of the energy dissipated as heat per cycle under deformation, or it is the viscous response of the material. Figures 4.22, 4.23 and 4.24 show the variation in trend of loss modulus at different blends systems with temperature. Generally, from the figures it is clear that, the incorporation of ABS-g-MAH caused broadening of the loss modulus peak. The peak broadening can be attributed to the inhibition of relaxation process within the blends. This may be due to the increase in the number of chain segments as well as less free volume upon compatibilisation. There is a shift in the glass transition temperature T_g towards the lower temperatures on increasing the compatibiliser content (see Table 4.5). This could be primarily attributed to the segmental immobilisation of the matrix chain at the interface due to the formation of graft copolymers by the reactions of amide end groups of PA6 with ABS-g-MAH. Also, the loss moduli of the blends were increased with increasing the compatibiliser content. These results are in agreement as expected that the enhancement taken place upon the incorporation of compatibiliser.

The blends also showed an increasing trend in loss modulus upon the decreasing of PA6 contents. It is clearly shown that higher ABS content is more flexible than higher PA6 content in the blends. This phenomenon is in agreement with impact result as discussed earlier in Section 4.1.3. The loss modulus value in the transition region was much high for compatibilised blends when compared to the uncompatibilised one. The higher modulus at this transition region was due to the increase in internal friction that enhanced the dissipation of energy.

Figure 4.22 shows the effect of temperature on the E'' of 50/50 PA6/ABS blends with various amount of compatibiliser. It is clearly shown that E'' increased by increasing amount of compatibiliser. From the figure, 5 wt. % of compatibiliser in the blends caused highest E'' . This is because higher energy was dissipated when more amount of compatibiliser was introduced into the system. This is believed to be due to the presence of ABS-g-MAH reduced the stress relaxation of the blends, and energy was dissipated in the form of heat. However, at 1 and 3 wt. % amount of compatibiliser, the moduli are considered identical, before and after transition. At this concentration, the compatibiliser considerably has not affected the energy dissipation during a dynamic deformation.

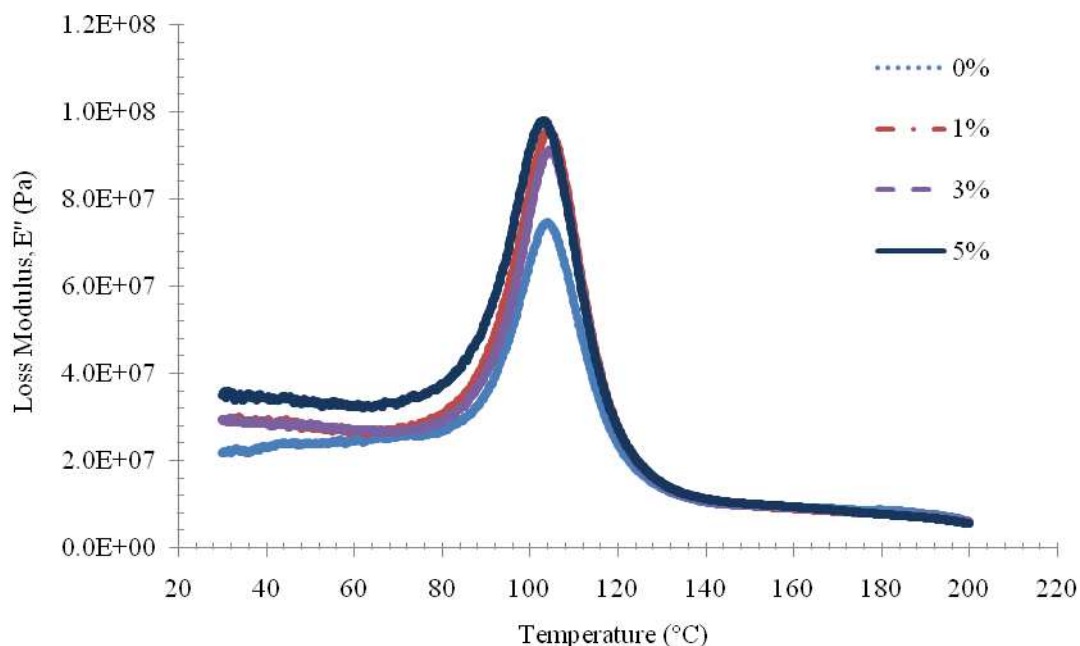


Figure 4.22 : Loss modulus vs. temperature plot for different compositions of compatibiliser in 50/50 of PA6/ABS blends

Figure 4.23 shows the loss modulus values of 60/40 PA6/ABS blends containing various amount of ABS-g-MAH as a function of temperature. It was found that the loss modulus of the polymer blends at the peak points was higher with the introduction of compatibiliser. It is clearly shown that 1 wt. % is the highest peak, followed by 5 and 3 wt. %, respectively. These trends are agreement with the tensile strength and modulus results as previously discussed. It is very difficult to claim a single and precise comment on dynamic mechanical properties because it is depend on dispersing state of dispersed phase, interface interaction and reaction between compatibiliser and polymer phase. Therefore, all the phenomena were supported by the results of thermal study was discussed in Section 4.2.1.

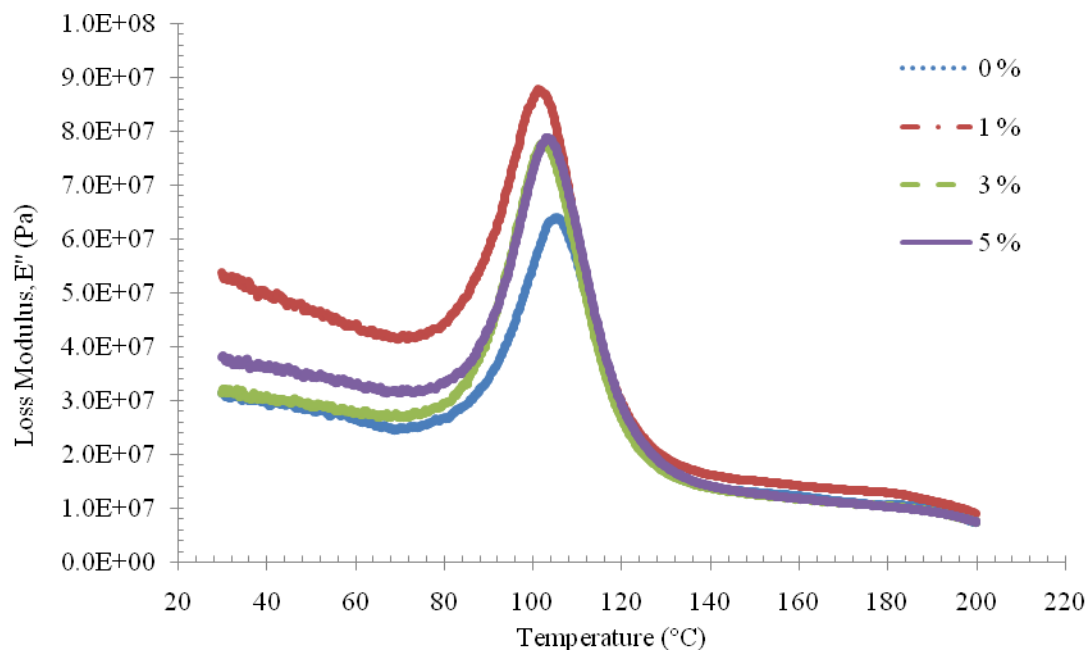


Figure 4.23 : Loss modulus vs. temperature plot at different composition of compatibiliser in 60/40 PA6/ABS blends

Figure 4.24 shows the influence of temperature on the loss modulus of 70/30 PA6/ABS blends with various amount compatibiliser up to 5 wt. %. At lower the transition region, it was found that 3 wt. % of compatibiliser is the highest loss moduli as compared to the uncompatibilised blends. These results are in agreement with power law index analysis will be discussed in Section 4.4.3.3. In general, the introduction of compatibiliser slightly enhanced the loss modulus of the blends.

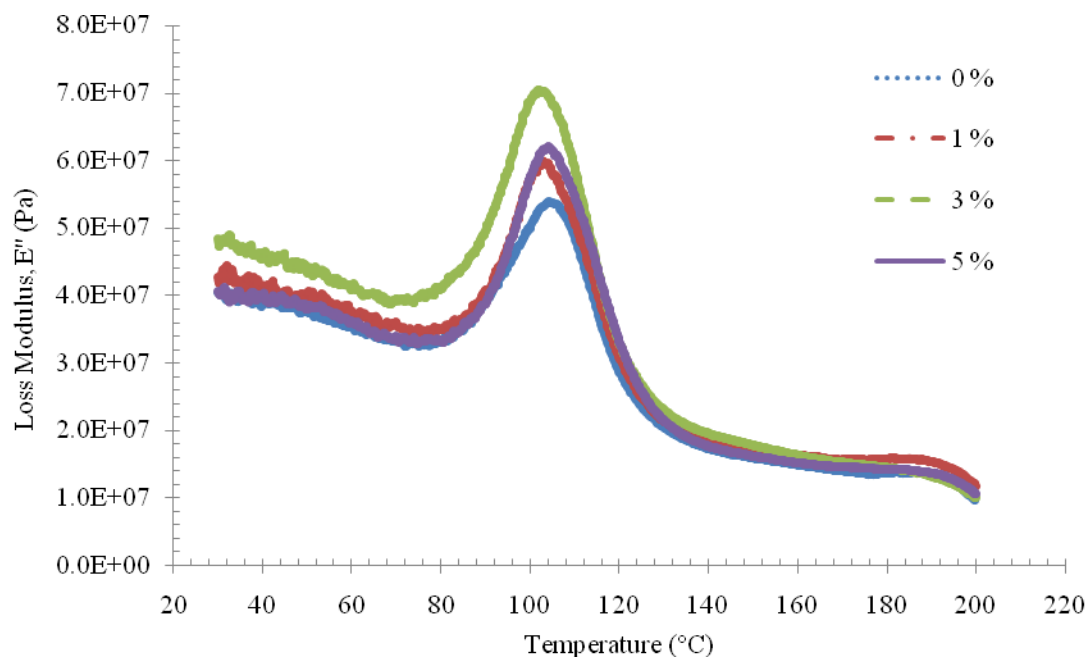


Figure 4.24 : Loss modulus vs. temperature plot for different composition of compatibiliser in 70/30 of PA6/ABS blends

4.3.1.3 Tangent delta ($\tan \delta$) of PA6/ABS Blends

The loss tangent delta (δ) is the ratio of the loss modulus to the storage modulus, dimensionless term that expresses the out-of-phase time relationship between a shock impact or vibration and the transmission of the force to the material support during application. It is also known as $\tan \delta$, the loss damping coefficient, or the loss factor. Generally, the higher the tangent of delta the better the material performance is in shock and vibration. A peak in $\tan \delta$ typically represents an energy absorbing transition, where the area under the curve represents the amount of energy absorbed. The $\tan \delta$ curves can be used to associate to the amount of compatibiliser in the polymer blends, which is influenced by the incorporation of compatibiliser. The variation of $\tan \delta$ curves with variation of temperature for different amount of compatibiliser in the blend systems is shown in Figure 4.25, 4.26 and 4.27. The maximum of $\tan \delta$ for all blends ratio is shown in Table 4.5.

The $\tan \delta$ of the 50/50 PA6/ABS blends is shown in Figure 4.25 and found to increase as the compatibiliser was increased. It was observed that at lower temperature, only a small increase in $\tan \delta$ as compared at higher temperature. In the lower temperature or at the glassy state, most of the molecular chain segments were still in the frozen-in, and at high temperature or at rubbery state almost all the molecule of the blends are free to move. The difference between the compatibilised and uncompatibilised blends was more pronounced at transition region ($\tan \delta$ peak). The value of maximum $\tan \delta$ at the peak of 50/50 PA6/ABS blends is shown in Table 4.5. It is clearly shown that, with the introduction of compatibiliser reduced the size of ABS domains in PA6 matrix and resulted increasing in scale of dispersion (see SEM micrograph), and improved the molecular motion of the molecular chain of PA6/ABS blends. This explanation is associated with the partial loosening of the PA6/ABS blends structure thus that the ABS domains, which are a smaller segment in the blends, could move well than in the uncompatibilised blends (Gnatowski and Koszkuł, 2006).

Figure 4.26 shows clearly the different effects of compatibiliser concentration in 60/40 PA6/ABS blends as compared to 50/50 PA6/ABS blends. Increasing the compatibiliser concentration in PA6/ABS blends resulted in increasing the $\tan \delta$ value. From the figure, it can be observed that 1 wt. % of ABS-g-MAH has highest value of $\tan \delta$ for all ranges of frequency, followed by 5 wt. % and 3 wt. %, respectively. This result is in agreement with the tensile modulus and strength as discussed in mechanical 4.1.1.

Figure 4.27 shows the variation of $\tan \delta$ of 70/30 PA6/ABS blends with a different concentration of ABS-g-MAH. As discussed in 60/40 and 50/30 PA6/ABS blends, $\tan \delta$ was improved through the incorporation of ABS-g-MAH. Again, this is mainly because compatibiliser improved the dispersion of ABS as a result the ABS domains free to move within PA6 phase. In this series of blends, the highest $\tan \delta$ was obtained at 3 wt. % followed by 5 wt. % and 1 wt. % of compatibiliser.

From temperature point of view, it was observed that as temperature increased, damping passed through a maximum in transition region and then

decreased in the rubbery region. The peak maximum temperature of $\tan \delta$ or transition region corresponds to the T_g of ABS and called T_g at styrene-acrylonitrile rich phase (SAN rich phase). Below T_g , damping is low because, in that region, chain segments are in the frozen state. Hence, the deformations are primarily elastic and the molecular slips resulting in the viscous flow are low. Also, at the rubbery region (above the transition region), the molecular segments are quite free to move and hence the damping is low and thus there is no resistance to flow. In the transition region, damping is high due to the initiation of micro motion of the molecular chain segments and their stress relaxation, even though not all the segments will take part in such relaxation together. In fact, a frozen-in segment in the glassy state can store more energy for a given deformation than a rubbery segment, which can move freely. At the transition region, every time stressed frozen-in segment becomes free to move, its excess energy is dissipated. Micro motion is concerned with the cooperative diffusion motion of the molecular chain segments. The region where most of the chain segments take part in this cooperative motion under a given deformation, maximum damping will occur in that region. The position and height of $\tan \delta$ peak are indicative of the structure and properties of the PA6/ABS blends.

Higher composition of PA6 had a very less damping in the transition region compared to the lower one because PA6 carries a greater extent of stress and allow only a small part of it to strain the interface. The $\tan \delta$ peak height and peak width at half height are summarised in Table 4.5. It can be observed that the high of $\tan \delta$ peak was decreased with the increasing amount of PA6 and compatibiliser in the blends. This may be due to the restriction of movement of PA6 molecules and by the formation of graft copolymers. The lowering of peak height also indicates good interfacial adhesion. The width of $\tan \delta$ peak also becomes broader than the without compatibiliser. At lower compatibiliser concentrations, the interfacial will become inefficient leading to continuous rich regions and therefore, not enough compatibiliser to restrain the continuous and highly localised strains. If there is sufficient amount of compatibiliser, and thus the formation of graft copolymers will prevent crack propagation. Effective stress transfers between the continuous and dispersed phase takes place at higher concentration of PA6, as shown by the lowest peak height. However, further increase in the compatibiliser content led to

compatibiliser-compatibiliser interaction and achieved high degree of agglomeration. This explains that the $\tan \delta$ for 5 wt. % was always lower than 3 wt. % and 1 wt. % compatibiliser, except for 50/50 PA6/ABS blends series.

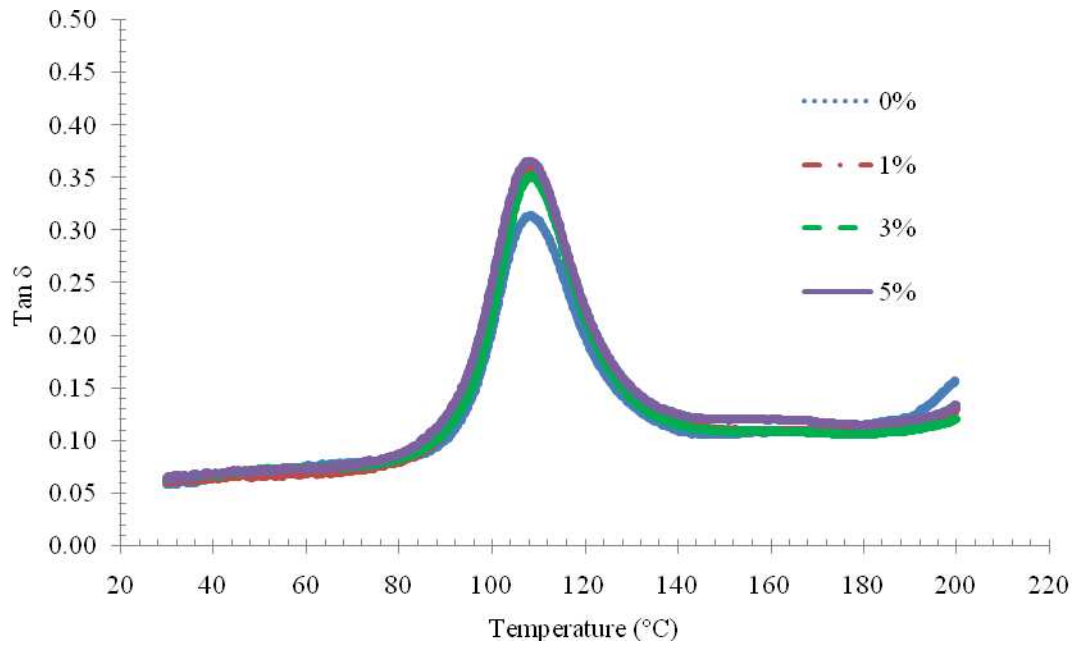


Figure 4.25 : $\tan \delta$ vs. temperature plots at different composition of compatibiliser in 50/50 PA6/ABS blends

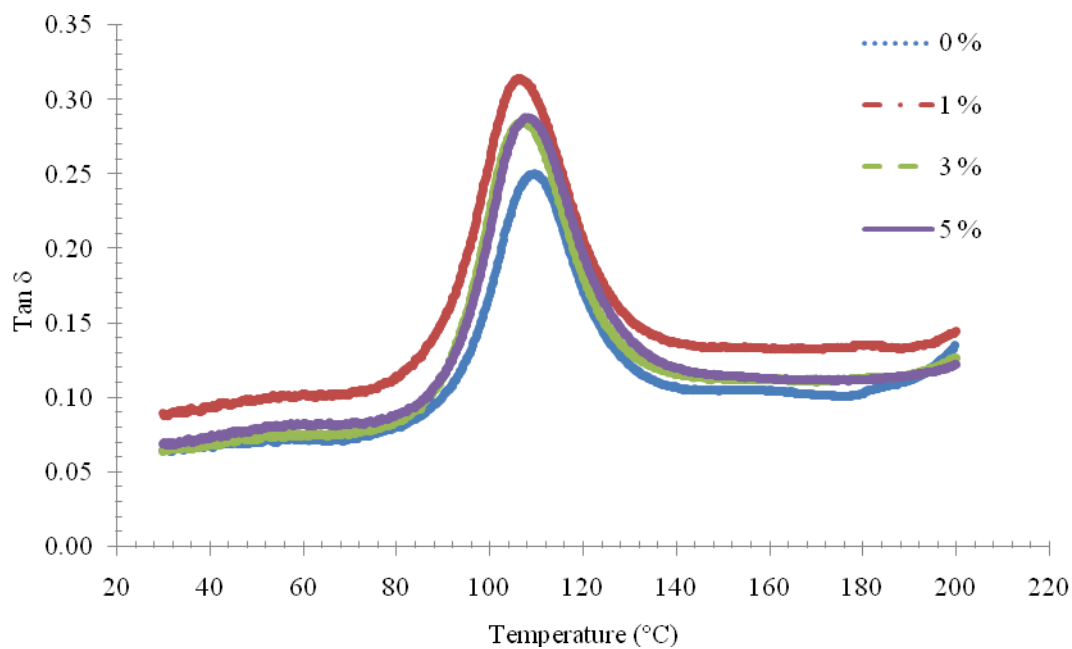


Figure 4.26 : Tan δ vs. temperature plot for different composition of compatibiliser in 60/40 of PA6/ABS blends

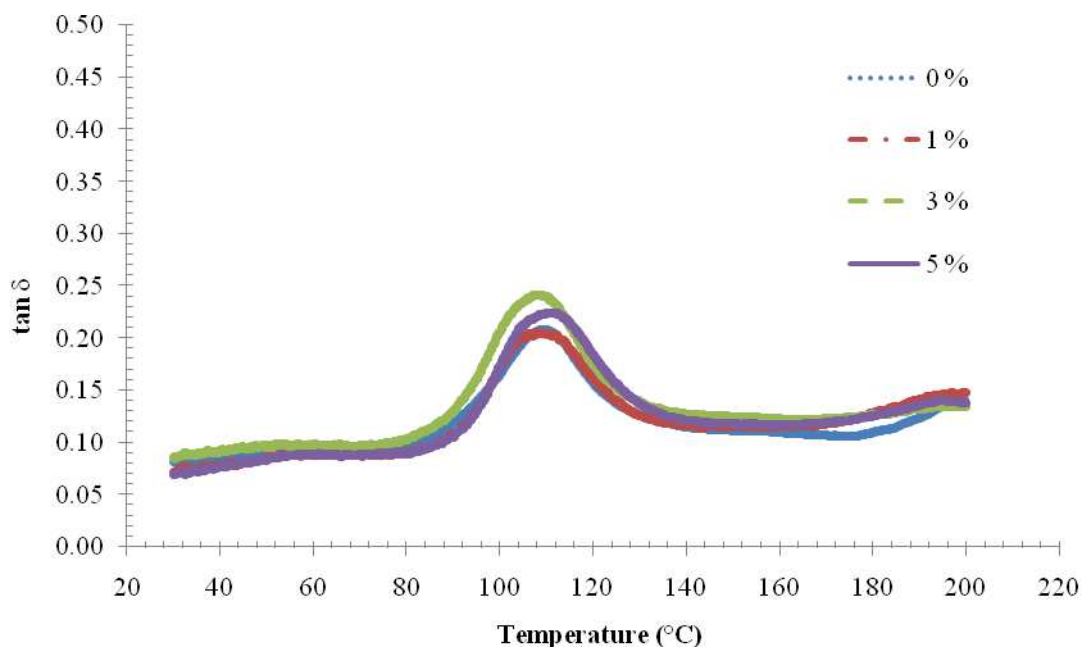


Figure 4.27 : Tan δ vs. temperature plots at different composition of compatibiliser in 70/30 PA6/ABS blends

Table 4.5 : The T_g , compositional dependence of maximum $\tan \delta$ and peak width at half height for PA6/ABS blends with various ABS-g-MAH contents. The maximum $\tan \delta$ was collected by measuring the height of peaks in $\tan \delta$ curve versus temperature.

PA6/ABS (50/50)			
Composition of ABS-g-MAH (wt. %)	T_g (°C)	$\text{Tan}_{\max} \delta$	Peak width at half height
0	109.6	0.313	20
1	108.2	0.358	19
3	108.3	0.352	20
5	108.7	0.367	21
PA6/ABS (60/40)			
Composition of ABS-g-MAH (wt. %)	T_g (°C)	$\text{Tan}_{\max} \delta$	Peak width at half height
0	109.3	0.251	20
1	106.4	0.315	22
3	106.7	0.286	21
5	108.3	0.289	22
PA6/ABS (70/30)			
Composition of ABS-g-MAH (wt. %)	T_g (°C)	$\text{Tan}_{\max} \delta$	Peak width at half height
0	109.5	0.209	23
1	109.5	0.216	24
3	110.3	0.242	23
5	110.8	0.225	24

4.3.2 PA6/ABS Composites

4.3.2.1 Storage and Loss Modulus of 60/40 PA6/ABS Composites

The results of storage and loss modulus at different ratio short glass fibre (SGF) reinforced 60/40 PA6/ABS composites are shown in Figures 4.28 and 4.30, respectively. It can be seen that the storage modulus and loss modulus increased by

increasing amount of SGF volume fraction. It was found earlier that the tensile and flexural properties of the composites increased almost exponentially with SGF content. Unlikely, the flexural properties increased linearly with increasing of SGF content. This is evident from the fact that the SGF appeared to have higher storage modulus, E' than the compatibilised PA6/ABS blends. Also, the incorporation of SGF into PA6/ABS matrix caused the T_g peaks for SAN rich phase in ABS to grow in size. The loss modulus data represents the viscous damping behaviour as well as phase behaviour. Again, an increase in E' and E'' modulus were observed as the SGF concentration was increased. E'' modulus can also be used to discuss the dissipation energy behaviour and interfacial bonding of the composites. According the loss modulus results as shown in Figure 4.29, the highest of SGF concentration has the highest loss modulus than the lower SGF concentration and indicates a poor interfacial bonding between SGF and the PA6/ABS matrix. Composites with poor interfacial bonding tends to dissipate more energy that with good interfaces bonding (Tan *et al.* 1990). Therefore, at high fibre content, when strain is applied to the composite, the strain is taken mainly by the fibre in such a way that the interface, which is assumed to be the more dissipative component of the composite, is strained to a lesser degree (Ibarra L. *et al.* 1995).

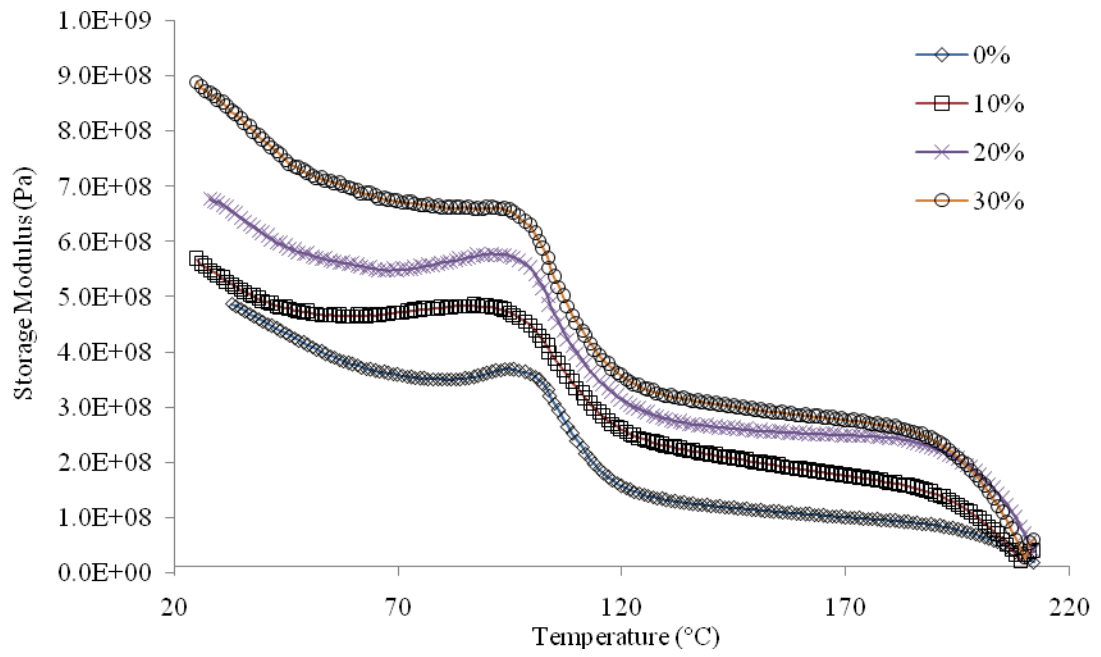


Figure 4.28 : Effect of SGF loading with temperature on the storage modulus values of 60/40 PA6/ABS composites

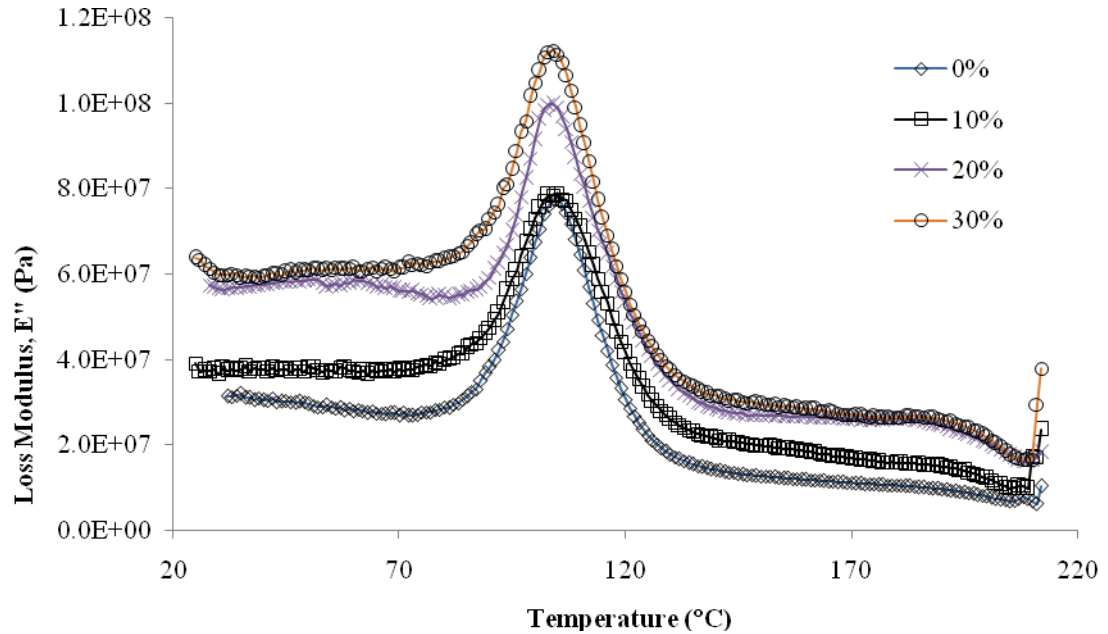


Figure 4.29 : Effect of SGF loading with temperature on the loss modulus values of 60/40 PA6/ABS composites

4.3.2.2 Tangent delta ($\tan \delta$) of 60/40 PA6/ABS Composites

Tan δ is a damping term that can be related to the impact resistance of a material. The effect of tan δ on fibre mass fraction as a function of temperature is delineated in Figure 4.30. It is observed that the tan δ peak of the unfilled sample was higher than the filled sample. At 10 wt. % glass fibre, the value of tan δ decreased and beyond 20 wt. % it considerably achieved a constant value. It is associated with the glass transition temperature for SAN rich phase.

In addition the above facts, there was no change in area under the curve. Area under the curve attributes to the amount of energy absorbed by the polymer which undergoes a transition (Chopra, 2002) during application with changing of temperature. The incorporation of SGF had less effect to the energy absorbed by PA6/ABS composites. The introduction of SGF lowered the tan δ peak, as expected. It is believed to be due to the inefficiently packing of the fibres in the composites,

leading to the matrix rich region, and consequently less energy to separate the phase at the interfacial region. During a closer packing of the fibres, the neighbouring fibres would prevent a crack propagation and separation. It is clear from the figure that the unreinforced PA6/ABS composite had the highest $\tan \delta$ and $\tan \delta$ decreased with increasing concentration of SGF. Hong *et al.* (2007) reported that the decrease of the height of the $\tan \delta$ peak of filled polymer system suggested that the molecular chain motion was restricted by the reinforcement fillers in the matrix phases. This indicates that further increase in SGF concentration would lead to a high extent of agglomeration and fibre-fibre interaction, and the randomly oriented formation of SGF in the matrix thus prevented the phases in the PA6/ABS composites to slip. Another reason is an effective transfer took places between fibre and the matrix at the above 10 wt. % SGF concentration and better interfacial interaction was achieved at this fibre loading.

Generally, as fibre concentration in the composites increased, the T_g value will also increased. The positive shifts in T_g value shows effectiveness of the fibre as a reinforcing agent. Moreover, the introduction of SGF increased the value of T_g , and reduced the magnitude of the $\tan \delta$. The shifting of T_g to a higher value showed the association with the decreased mobility of the polymer chains. The elevation of T_g is taken as a measure of the interfacial interaction (Idicula *et al.*, 2005). Therefore, the shifting of T_g to higher value indicates at 20 wt. % SGF has better interfacial interaction between SGF and PA6/ABS matrix as compared to 10 and 30 wt. % concentration.

Table 4.6 shows a trend that the width of half height of $\tan \delta$ peak became broader with increasing the SGF content and the maximum width was obtained with fibre loading at about 20 wt. %. This is believed due to the molecular relaxation took place in the SGF, which was not present in the PA6/ABS matrix. Dong and Gauvin (1993) reported that the molecular motions at the interface contribute to the damping of the material apart from those of the constituents. Therefore, the above phenomenon occurred due to the decrease in stress transfer from fibre to matrix because of the fibre agglomeration and increase in fibre to fibre interaction (Idicula *et al.*, 2005).

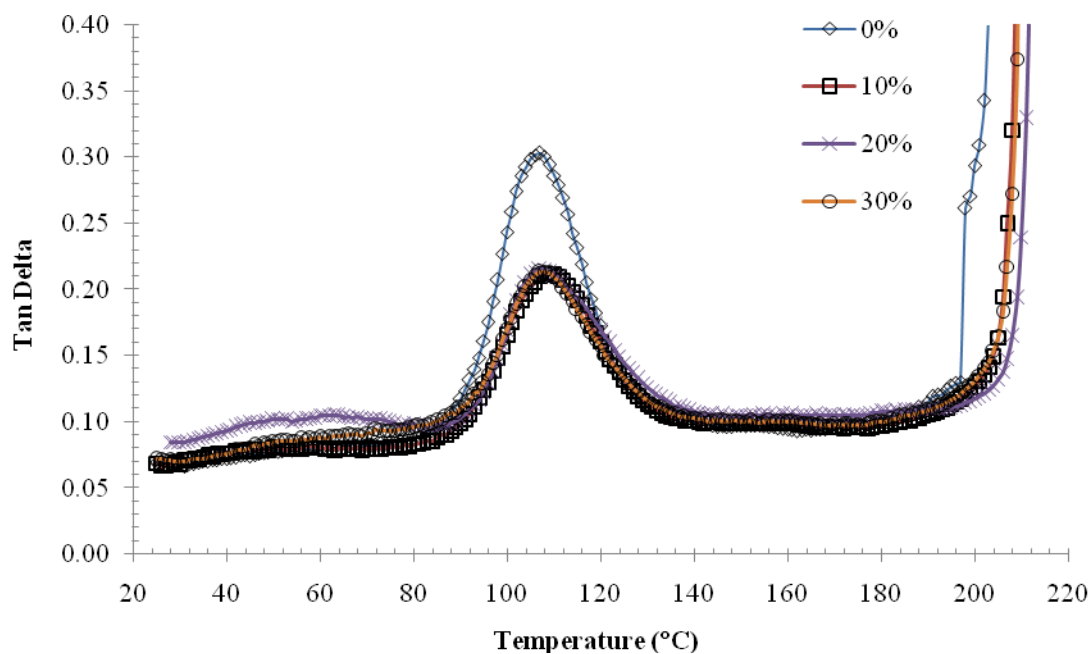


Figure 4.30 : Effect of SGF loading with temperature on the $\tan \delta$ values of the 60/40 PA6/ABS composites

Table 4.6 : Area under the curve at $\tan \delta$ maximum, $\tan \delta$ maximum, T_g for SAN rich phase and peak width of 60/40 PA6/ABS composites at different fibre loading.

60/40 PA6/ABS Composites				
Composition of SGF in composites (wt. / wt. %)	Area under the curve	T_g (SAN rich phase) ($^{\circ}\text{C}$)	$\tan_{\max} \delta$	Peak width at half height
0	12.41	106.2	0.28	21.23
10	9.83	110.3	0.21	41.53
20	8.65	110.6	0.22	48.38
30	8.21	109.5	0.21	47.07

4.4 Rheological Properties

4.4.1 Rheological Properties of Virgin PA6 and ABS

Small amplitude oscillatory rheological tests were performed on the virgin component samples of the PA6 and ABS. The complex viscosity, η^* dependence of frequency, ω is shown in Figure 4.28. PA6 showed a typical behaviour, exhibiting an initial Newtonian plateau at low frequencies followed by a shear thinning or pseudoplastic regime at moderate frequencies as compared to ABS. It is also meant that, the virgin PA6 has a long Newtonian plateau within the range of frequencies studied. The viscosity of PA6 was not significantly affected with increasing the frequencies. However ABS showed a different trend which is frequency dependence, pseudoplastic behaviour started at low frequencies to moderate frequencies.

Figure 4.29 reveals the viscoelastic properties (G'' and G') with various frequencies of each component, PA6 and ABS at 230°C. It is important to note that the loss modulus, G'' , was larger than the storage modulus, G' , throughout the frequencies studied for the PA6 and ABS, implying that the rheological response of these polymeric materials were dominated by viscosity. The storage modulus of PA6 was more frequencies dependent than the loss modulus, showing larger deviation at lower frequencies. ABS had a roughly smaller deviation of viscous and elastic character and achieved equally at frequency around 90 rad/s. This can be seen at larger frequencies where ABS became more elastic dominant than viscous character. ABS also changed its characters from liquid-like ($G'' > G'$) to solid-like ($G' > G''$) material with increasing of frequencies. However, PA6 showed liquid like material for the whole range of frequencies studied. Basically, in the range of frequencies lying to the left of the intersection point at G'' higher than G' , the polymer demonstrates the flow behaviour (viscous), while in the frequencies range to the right of this point at G' higher than G'' , the polymer behave a rubbery like material (elastic). This indicates that, above intersection point, the elasticity of the

ABS is primarily determined by the density of entanglement network of the styrene-acrylonitrile copolymer (Dreval *et al.*, 2006).

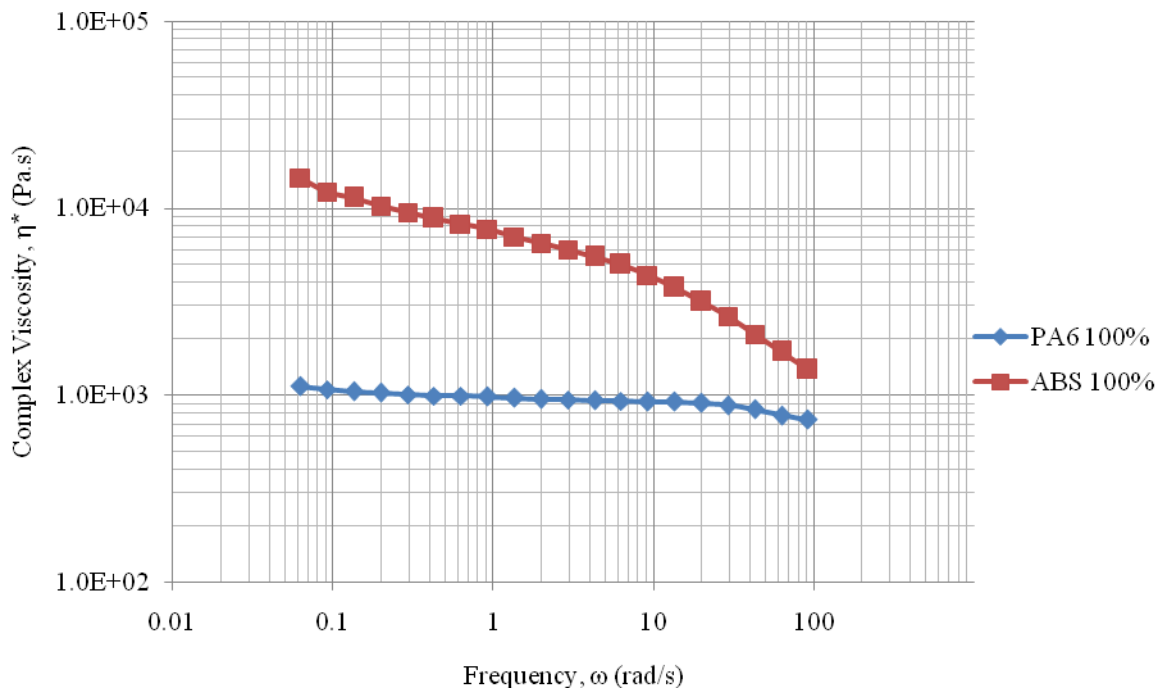


Figure 4.31 : Complex viscosities of blend components (PA6 and ABS) measured at 230 °C

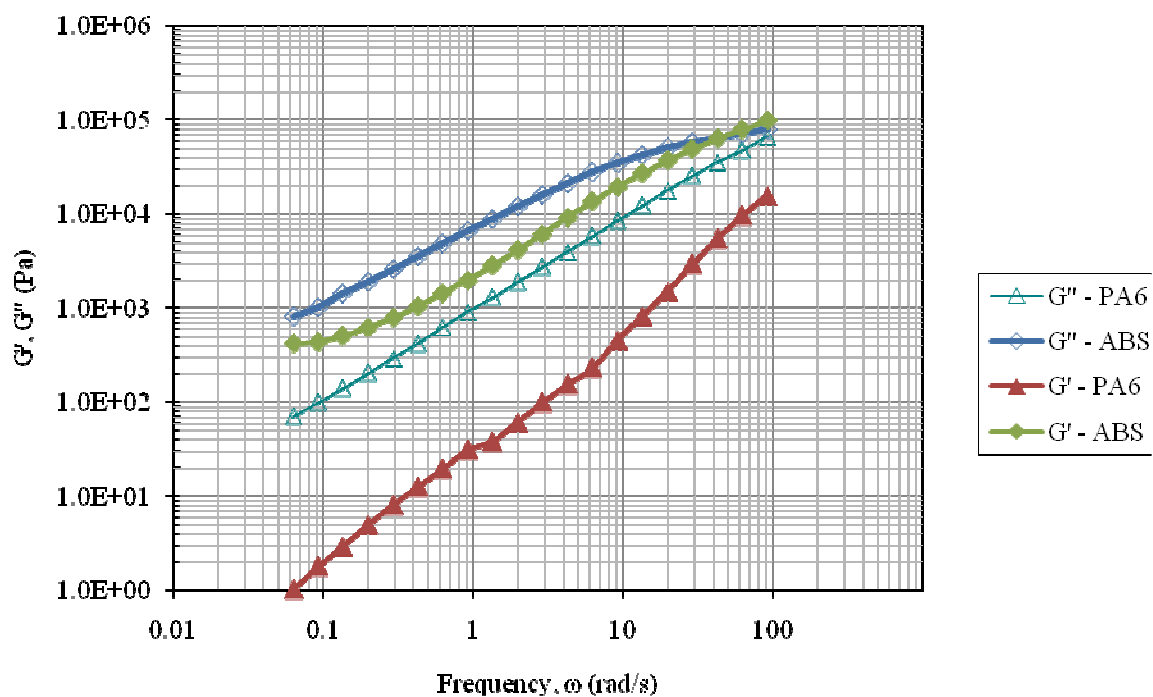


Figure 4.32 : Dynamic moduli of blend components (PA6 and ABS) measured at 230 °C

4.4.2 Dynamic Rheological Properties of PA6/ABS Blends

4.4.2.1 Complex Viscosity Analysis

The complex viscosity is an important parameter to characterise the rheological properties of polymer blends. The real part of the complex viscosity is an energy-dissipation term similar to the imaginary part of the complex modulus. The complex viscosity dependence on frequency at different blend ratios of PA6/ABS blends are

shown in Figure 4.33, 4.34 and 4.35, respectively. Generally, the highest of ABS-g-MAH composition in the mixture was found to be much more viscous and elastic than the lower and without ABS-g-MAH as compatibiliser. Therefore, the data indicates that the viscosities of PA6/ABS blends were hardly affected by adding small amounts of ABS-g-MAH compatibiliser. When adding ABS-g-MAH as compatibiliser to PA6/ABS blends, the rheological properties of the blends changed significantly. During blending of PA6 with ABS and ABS-g-MAH the melt viscosity of PA6/ABS blends strongly increased as a result of graft formation reaction between the PA6 amine-end groups and the ABS-g-MAH anhydride groups.

The 50/50 PA6/ABS blends exhibited relatively strong frequency-rheology or big frequency-dependence compared to that of 60/40 and 70/30 PA6/ABS blends. In generally, all the polymer blends showed a typical behaviour, exhibiting a shear-thinning regime at all frequencies studied. It showed that at a fixed frequency, the complex viscosity increased with the amount of compatibiliser. This indicates that, compatibiliser reduced the interfacial tension and enhanced the interfacial adhesion between the domains phase and matrix phase. At 1 and 3 wt. % concentration of compatibiliser in 50/50 PA6/ABS blends, the complex viscosity showed almost equally value and similar trend. Specifically, the incorporation of 5% of ABS-g-MAH into 50/50 PA6/ABS blends revealed a sharp drop in viscosity beyond 30 s^{-1} of the shear rate. After this point, it could be that the rubber particles of ABS loose its entanglement and agglomeration to form uniform orientation and increased the flowability (Marrie-Pierre Bertin *et al.*, 1999) shown by reduction in complex viscosity. The rest of the blends, either 60/40 or 70/30 PA6/ABS had rather a linearly shear-thinning regime.

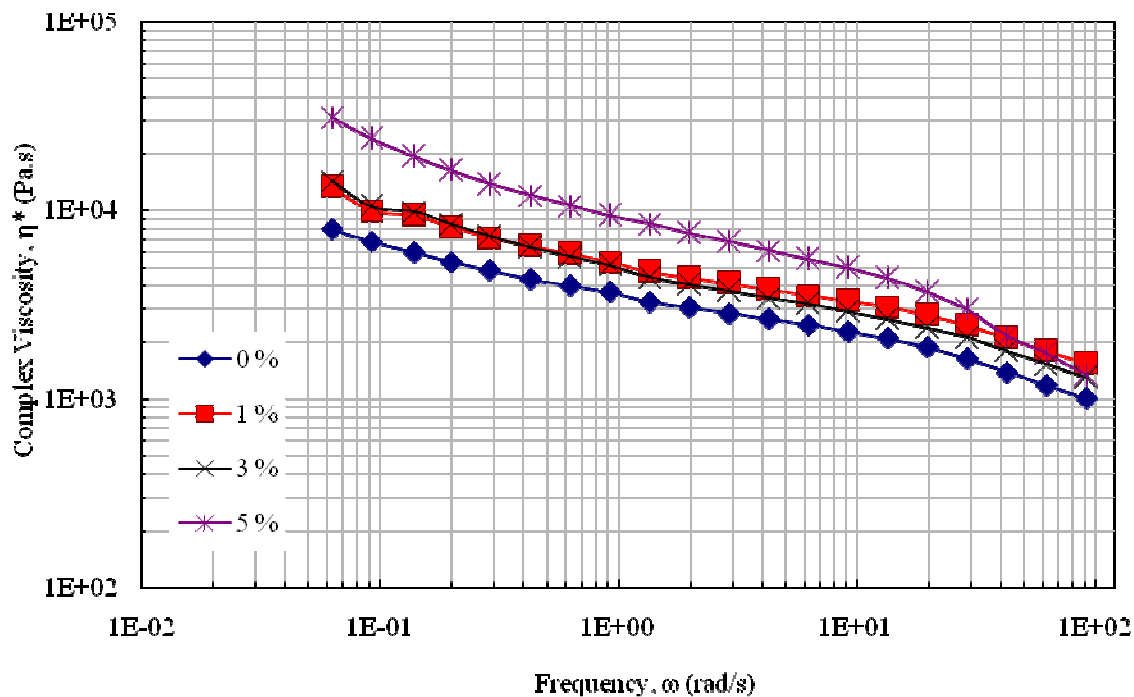


Figure 4.33 : Plot of complex viscosity versus frequency at different amount of compatibiliser for 50/50 PA6/ABS blends, at 230°C

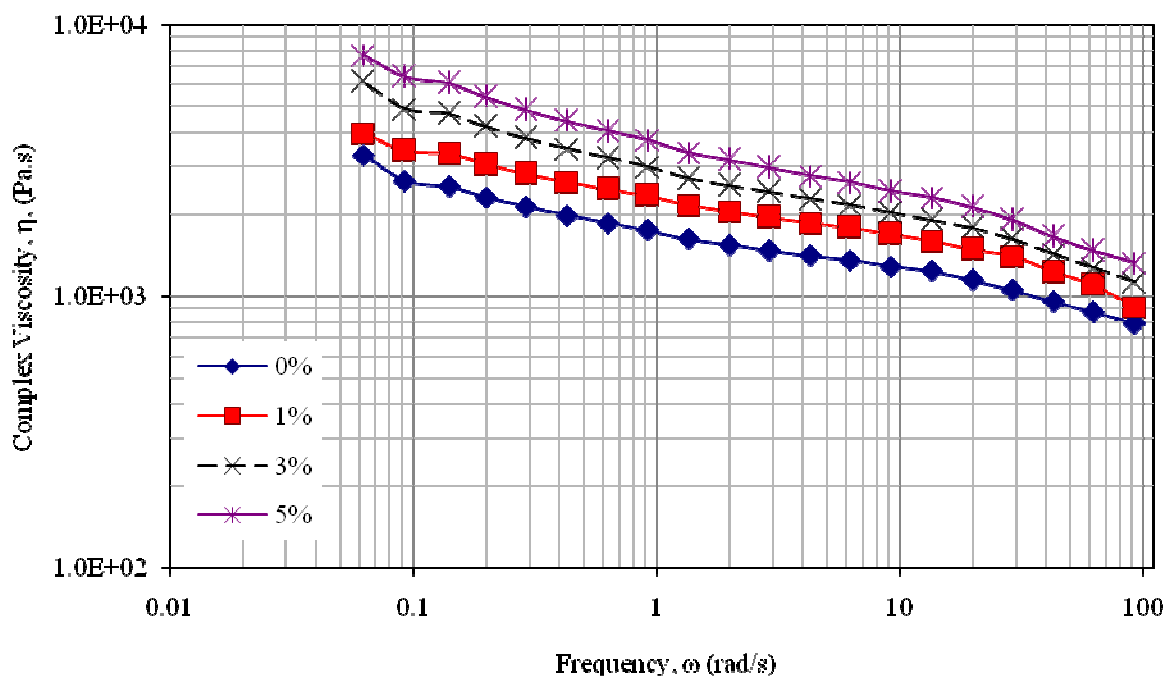


Figure 4.34 : Plot of complex viscosity versus frequency at different amount of compatibiliser for 60/40 PA6/ABS blends, at 230°C

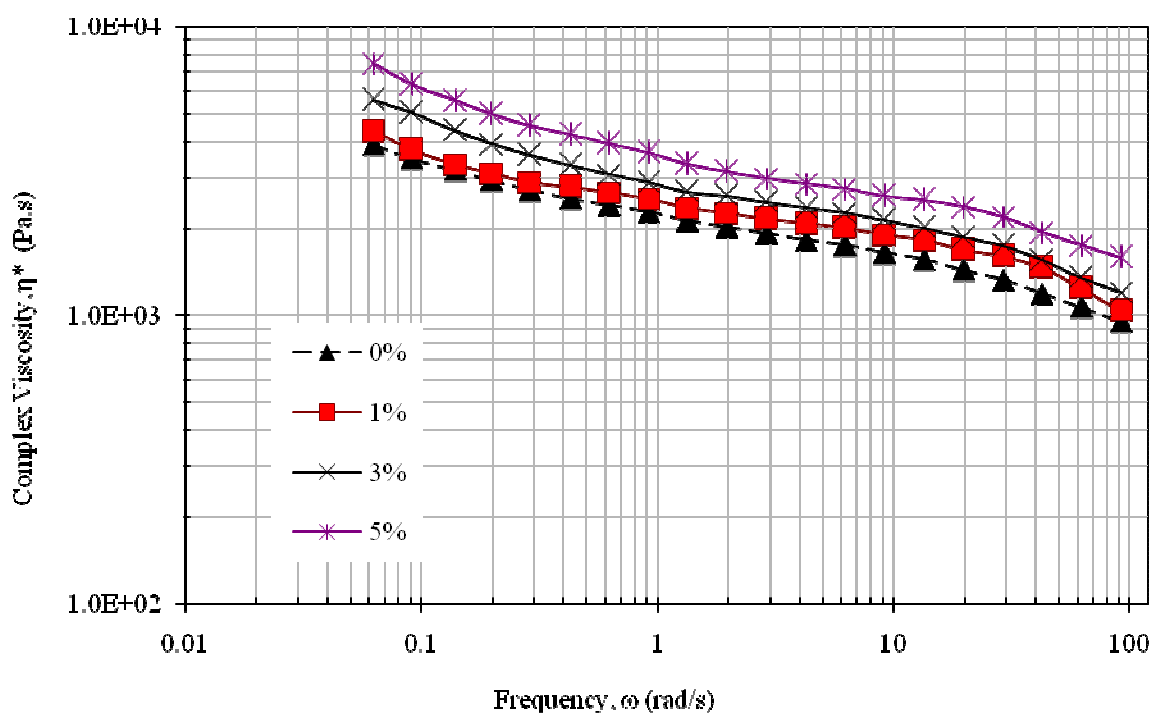


Figure 4.35 : Plot of complex viscosity versus frequency at different amount of compatibiliser for 70/30 PA6/ABS blends, at 230°C

4.4.2.2 Storage Modulus Analysis

Figures 4.36, 4.37 and 4.38 show the relationship between rheological storage modulus G' and frequencies ω for the PA6/ABS blends at 230°C containing different amounts of ABS-g-MAH. It can be seen that within the frequency range tested, the storage modulus decreased with increasing the frequency. The curves of G' versus ω almost followed a linear mixing rule which is at fixed frequency, the storage increased with increasing the amount of compatibiliser. It has been reported by Jafari *et al.* (2002) the virgin PA6 obeys the linear viscoelasticity model i.e. Newtonian behaviour at lower frequencies while the blends showed pseudoplastic behaviour at all frequencies tested. It was found that the storage modulus of the compatibilised blend had slightly different as compared to the uncompatibilised blends. The values of G' for the compatibilised blends within the whole frequencies region were higher than uncompatibilised, indicating the formation of new structure in these blends

except for 70/30 PA6/ABS blends. Similar results of PA6 blended with maleated triblock copolymer styrene-*b*-(ethylene-*co*-butylenes)-*b*-styrene (SEBS-*g*-MA), have been reported by Wang and Zheng (2005). It is believed that the interaction has occurred between amine end-groups of PA6 with the malic anhydride groups in ABS-*g*-MAH and form co-polymers at the interface of the blends.

The interaction can stabilise the interface by reducing the coalescence and interfacial tension, resulting in enhancement of the interfacial adhesion and viscosity. This is the reason why the compatibilised blends of PA6/ABS/ABS-*g*-MAH exhibited higher G' than the uncompatibilised of PA6/ABS blends. On the other hand, it should be emphasised that with the increasing amount of ABS-*g*-MAH, the storage modulus of the blends at low frequency region seems to gradually deviated from the uncompatibilised PA6/ABS blends, which is responsible for the existence of heterogeneous structure. This phenomenon could be attributed to the results of increasing the relaxation time due to the enhancement of macromolecular chains in PA6/ABS/ABS-*g*-MAH blends.

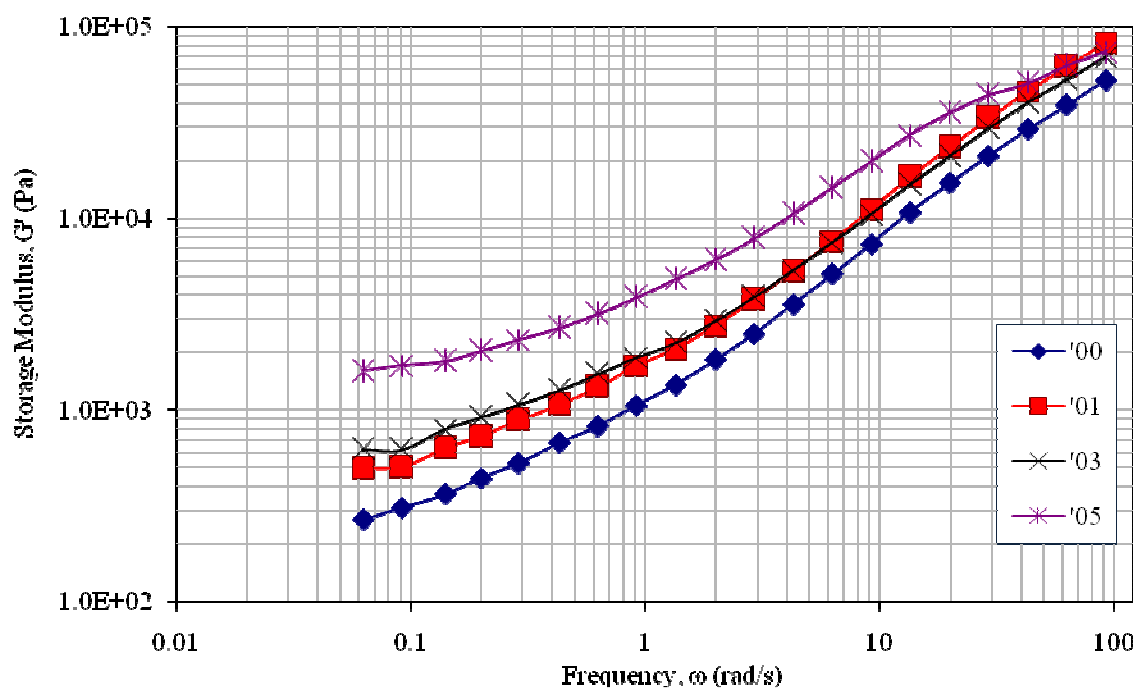


Figure 4.36 : Plot of storage modulus versus frequency at different amount of compatibiliser for 50/50 PA6/ABS blends, at 230°C

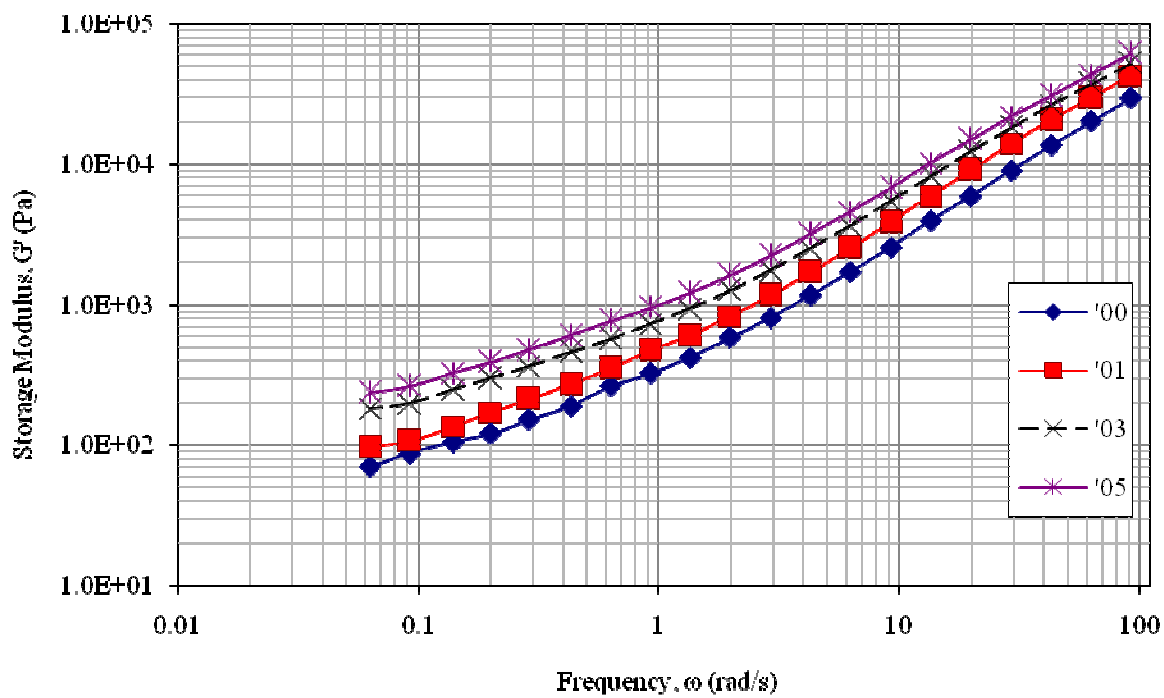


Figure 4.37 : Plot of storage modulus versus frequency at different amount of compatibiliser for 60/40 PA6/ABS blends, at 230°C

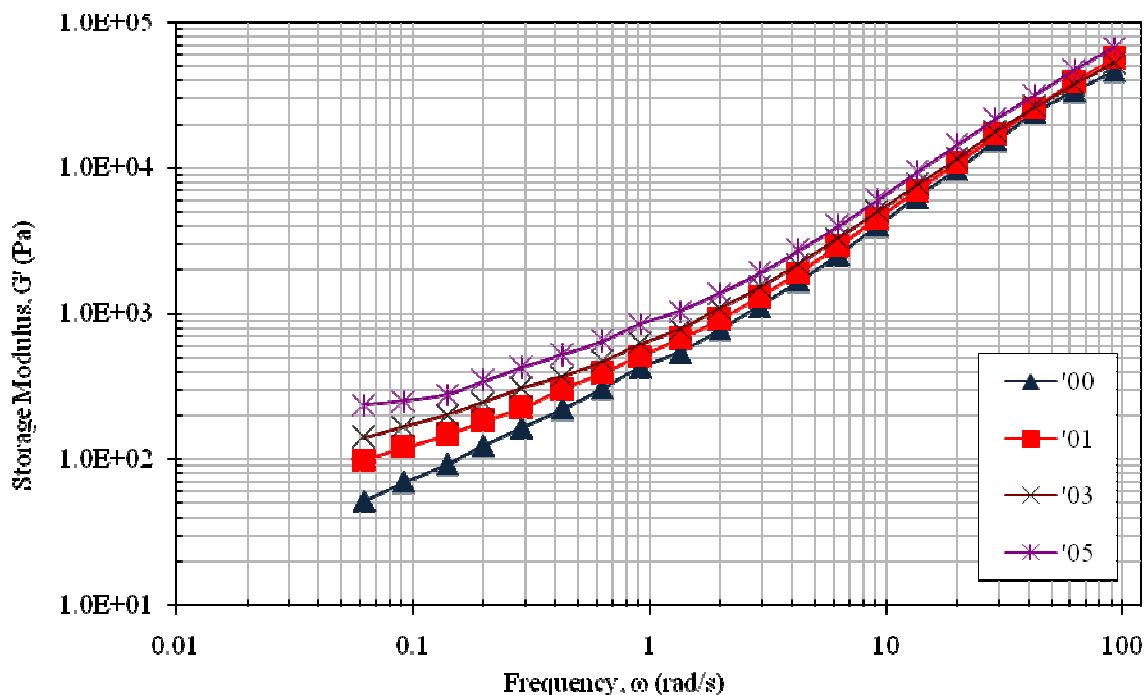


Figure 4.38 : Plot of storage modulus versus frequency at different amount of compatibiliser for 70/30 PA6/ABS blends, at 230°C

4.4.2.3 Loss Modulus Analysis

Figures 4.39, 4.40 and 4.41 present the response of loss modulus G'' against frequencies at different amount of compatibiliser for 50/50 PA6/ABS, 60/40 PA6/ABS and 70/30 PA6/ABS blends, respectively. The temperature was setup at 230°C. As far as G'' is concern, it can be seen that higher content of compatibiliser (5 wt. %) in the blends had a higher loss modulus, indicating higher energy dissipation compared to the lower compatibiliser content. These loss modulus responses of PA6/ABS blends appeared to be systematic deviation from the behaviour either without compatibiliser to higher compatibiliser content. In other words, the loss modulus behaviour followed the 'rule of mixtures', which should show a predictable increasing trend with increasing compatibiliser content. Khan *et al.* (2005) reported that the addition of compatibiliser into PC/ABS blends changed slightly the ratio of the plastic phase components (polystyrene, acrylonitrile-styrene) to the rubbery phase component (polybutadiene, butadiene-styrene, butadiene-

acrylonitrile) altering the interaction between these phases. This indicates the viscous component of the blends could be changed, since; the compatibiliser has a similar ABS basic component. Previous study by Yuji Aoki (1986), Marie-Pierre Bertin *et al.* (1995), Lee *et al.* (2002) and Dreval *et al.* (2006) indicated that the viscoelastic behaviour as well as loss modulus of ABS depends strongly on the rubber phase or more precisely on the degree of grafting of the rubber particles. As results, the change of rubber phase ratio due to incorporation of compatibiliser increased the loss modulus responses of PA6/ABS blends.

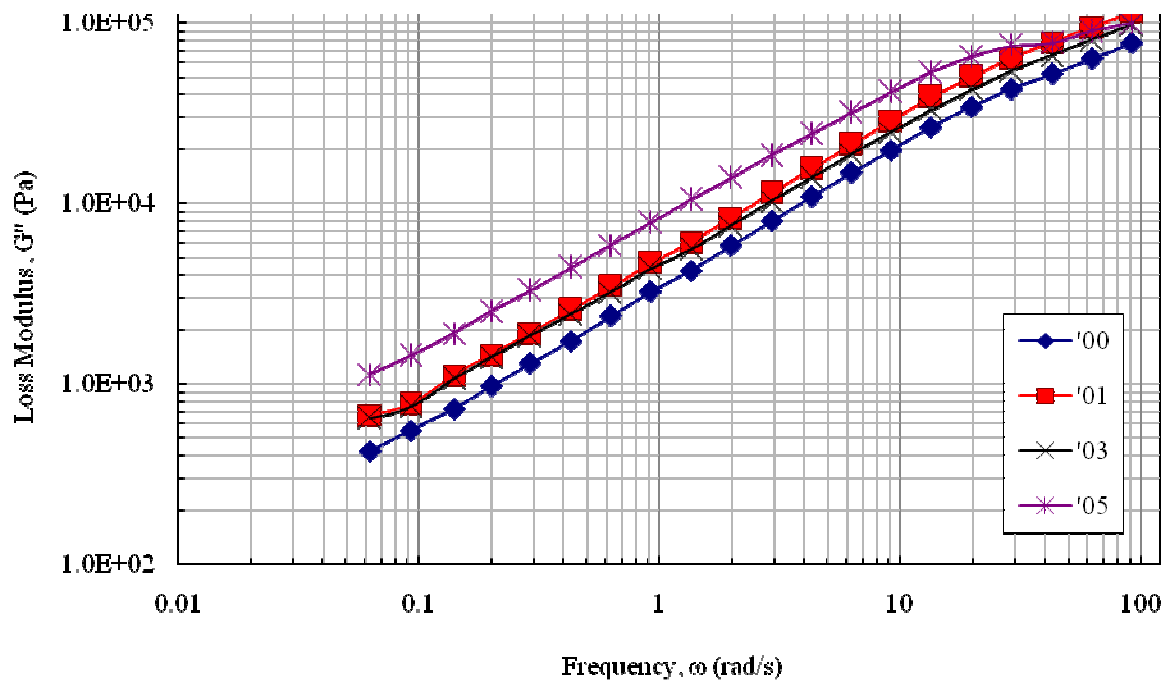


Figure 4.39 : Plot of loss modulus versus frequency at different amount of compatibiliser for 50/50 PA6/ABS blends, at 230°C

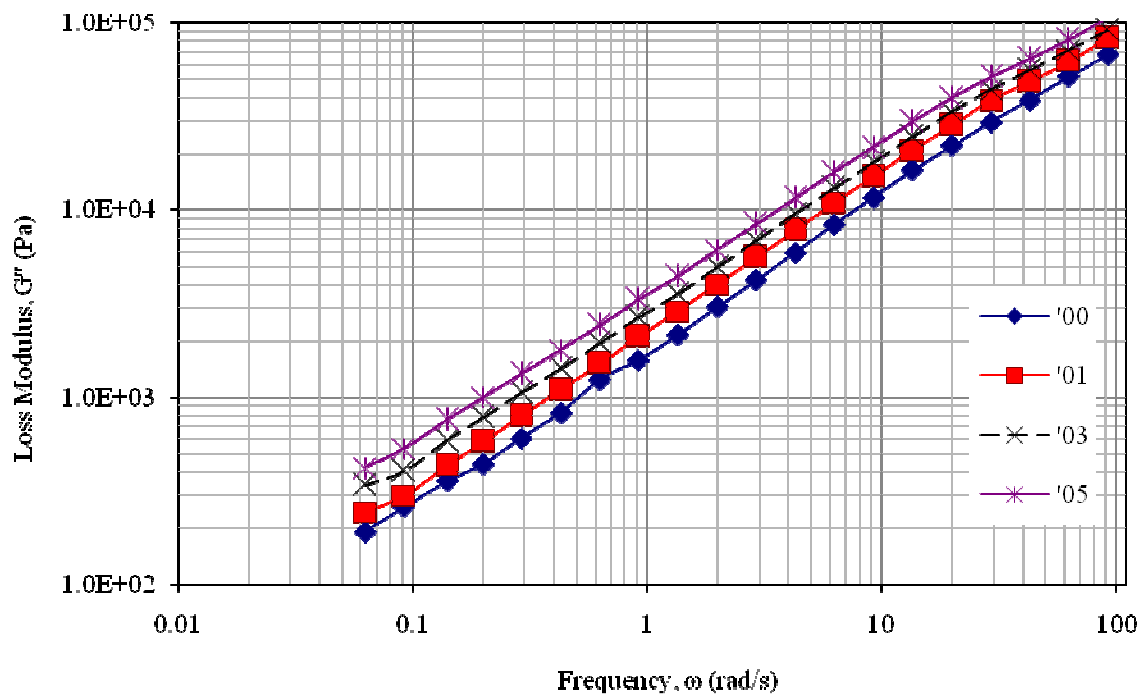


Figure 4.40 : Plot of loss modulus versus frequency at different amount of compatibiliser for 60/40 PA6/ABS blends, at 230°C

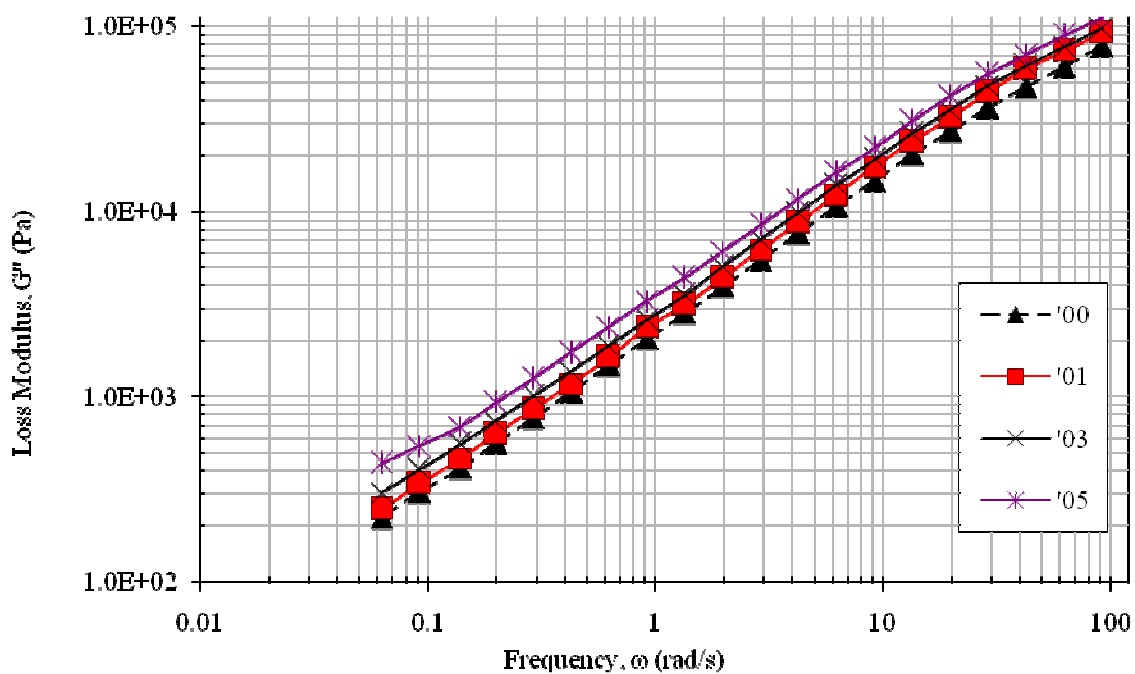


Figure 4.41 : Plot of loss modulus versus frequency at different amount of compatibiliser for 70/30 PA6/ABS blends, at 230°C

4.4.2.4 Tan δ Analysis

The curve of $\tan \delta$ as a function of the frequency has been used as a method of understanding the interaction of PA6 phase and ABS phase with the presence of ABS-g-MAH as a compatibiliser. Figure 4.42, 4.43 and 4.44 show the magnitude of $\tan \delta$ as a function of frequencies at different composition of ABS-g-MAH in PA6/ABS blends. It has been reported that, the melt strength is related to $\tan \delta$, and suggesting that higher elasticity can lead to higher melt strength (De-Mario and Dong, 1997). It is also can be related to the enhancement of interfacial interaction by incorporation of compatibiliser, resulted to the enhancement of melt strength. Therefore, the incorporation of compatibiliser can lead to higher melt strength, higher elasticity, lower viscous and lower $\tan \delta$. From the figures, it can be seen that the blend without compatibiliser showed the highest $\tan \delta$. The introduction of ABS-g-MAH into PA6/ABS reduced the $\tan \delta$ value, increased the melt strength and elasticity. It can be concluded that ABS-g-MAH has successfully compatibilised the blend of PA6 and ABS. This trend was found similar for the 60 wt. % and 70 wt. % amount of PA6 in the blends.

According to this study, it is very difficult to find any crossover of G' and G'' curves at which G' is equal to G'' and a $\tan \delta$, defined as G''/G' , is equal to one at the crossover. Because of the intensive increment in $\tan \delta$ values of most obtained PA6/ABS blends, the value of $\tan \delta$ should always be more than one. Therefore, the crossover of G' and G'' curves could not be found, except for 3 and 5 wt. % compatibiliser in 50/50 PA6/ABS blends. Every real material has viscoelastic behaviour, therefore G' and G'' are finite (Nachbaur *et al.*, 2001). Thus, the material can exhibit solid like behaviour, with G' more than G'' , or liquid like behaviour, with G'' more than G' . As a result, the sample exhibits solid-like behaviour when $\tan \delta$ more than one (1) and the sample exhibits liquid-like behaviour at $\tan \delta$ more than one (1). According to figures almost all samples showed $\tan \delta$ more than one except for 3 and 5 wt. % amount of compatibiliser in 50/50 PA6/ABS blends, and this means that solid-like behaviour was found in these compositions. This is also

indicates that, the minimum concentration of ABS-g-MAH with solid like behaviour of PA6/ABS blends is 3 wt. %. The rest of the samples showed a liquid-like behaviour and can be categorised as material which is easy to be processed at this processing temperature. The rest of the samples behave liquid-like material because they have more amount of PA6 in the systems, since PA6 has good processibility at this setting temperature as compared to ABS.

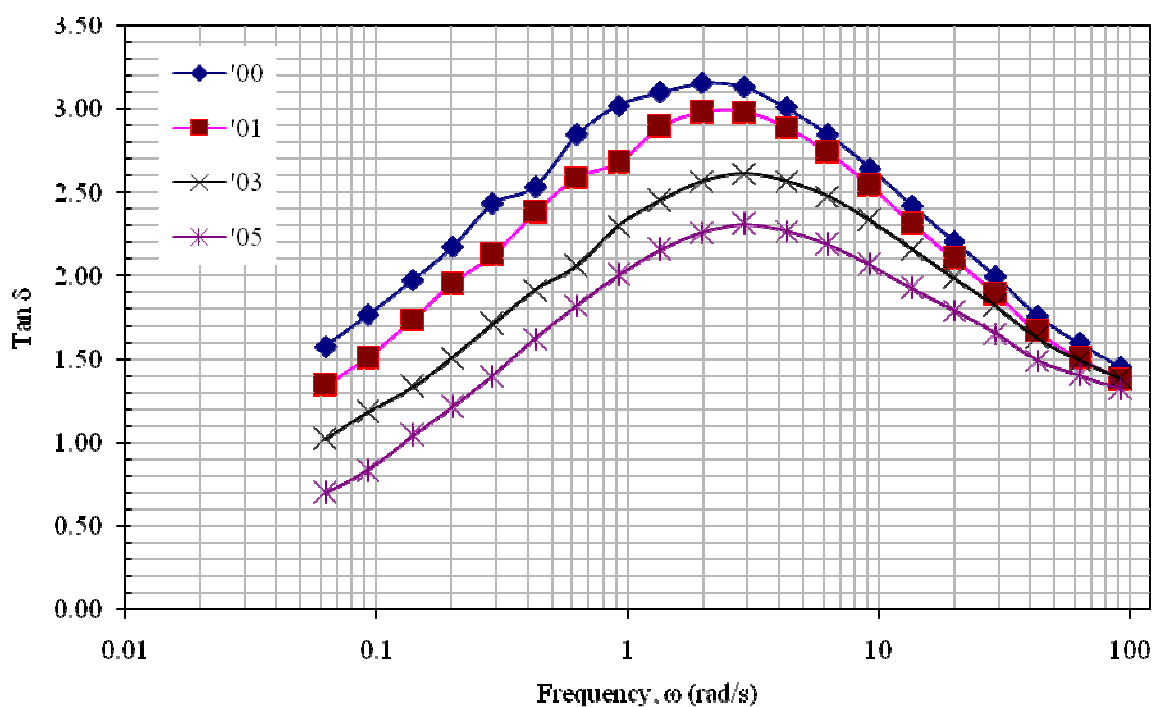


Figure 4.42 : Plot of $\tan \delta$ versus frequency at different amount of compatibiliser for 50/50 PA6/ABS blends, at 230°C

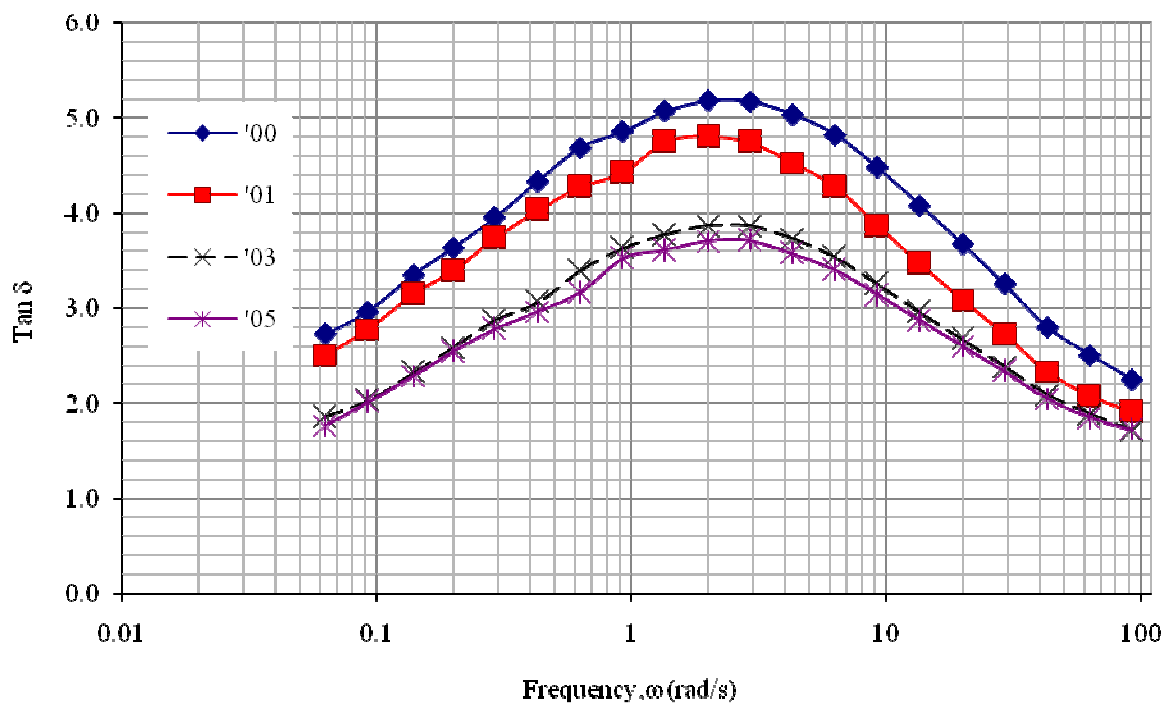


Figure 4.43 : Plot of $\tan \delta$ versus frequency at different amount of compatibiliser for 60/40 PA6/ABS blends, at 230°C

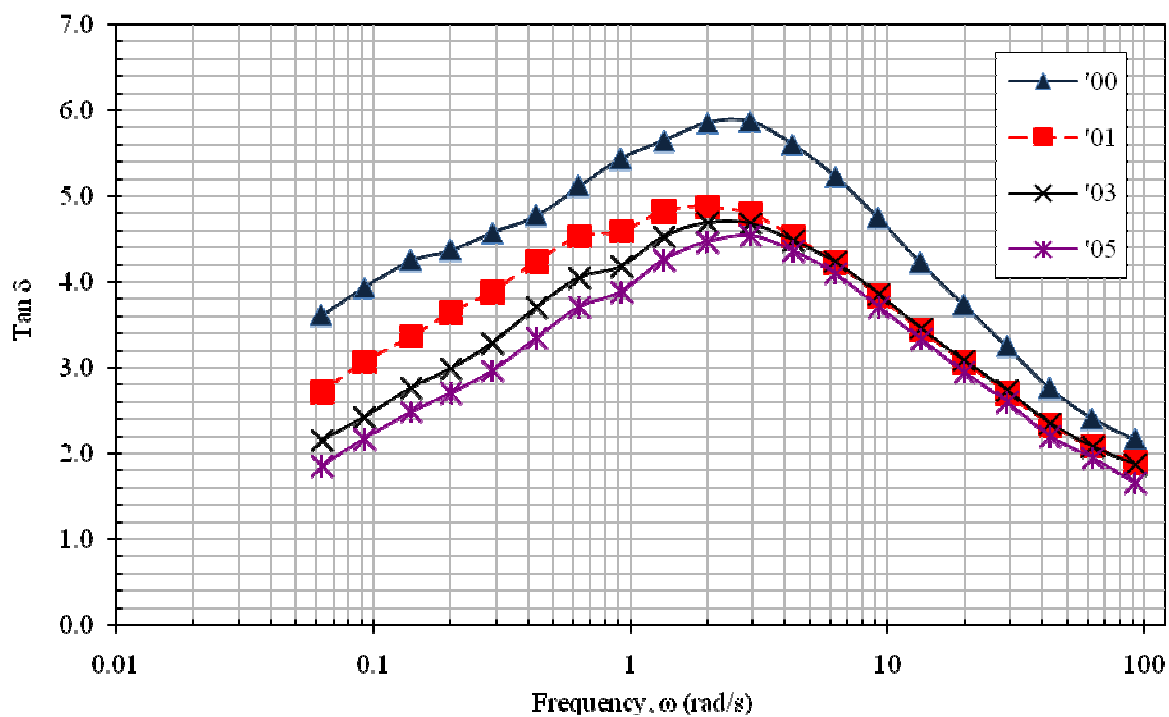


Figure 4.44 : Plot of $\tan \delta$ versus frequency at different amount of compatibiliser for 70/30 PA6/ABS blends, at 230°C

4.4.2.5 The Cole-cole plot analysis

Figures 4.45, 4.46 and 4.47 present a comparison of the curves of G' versus G'' at different compositions of PA6/ABS blends. This mode of presentation, called Cole-cole plots of modulus, is used to explain the rheological behaviour of the blends because it was found to be independent of the temperature and molecular weight for monodisperse materials and very sensitive to the molecular weight distribution and to short-chain and long branches. This type of explanations was previously used by Han and Chuang (1985) and Han and Yang (1987) to investigate the miscibility and compatibility of polymer blends. Hussein *et al.* (2006) have reported that the plot of G' versus G'' qualitatively can be used to study the effect blend miscibility or compatibility and molecular architecture for polymeric systems. In addition, the increase of G' could be attributed to the entanglements and grafting reaction in the compatibilised blend. According to Krache *et al.*, (2004), the change in the microstructure of the blends and the compatibility of the polymers will be predicted from variation of G' versus G'' of the polymer blends.

Figure 4.45 illustrates the relationship between G' and G'' for 50/50 PA6/ABS blends. It can be observed that, the incorporation of compatibiliser reduced the slope of the curve G' versus G'' . In other words, the addition of compatibiliser increased the elasticity due to grafting reaction of amine-end group and maleic anhydride function in ABS-g-MAH. It is more prominent at low frequency. Krache *et al.* (2004) reported that the elasticity of the compatibilised blends was increased due to yield stress effects and the development co-continuous structure. This indicates that the ABS-g-MAH improved the compatibility of PA6/ABS blends. The maximum value of compatibiliser referring to this analysis was about 1 wt. %. This analysis is in excellent agreement with the tensile modulus and strength was reported in Section 4.1.1. This trends are similar with the trend of 70/30 PA6/ABS blends are shown in Figure 4.46.

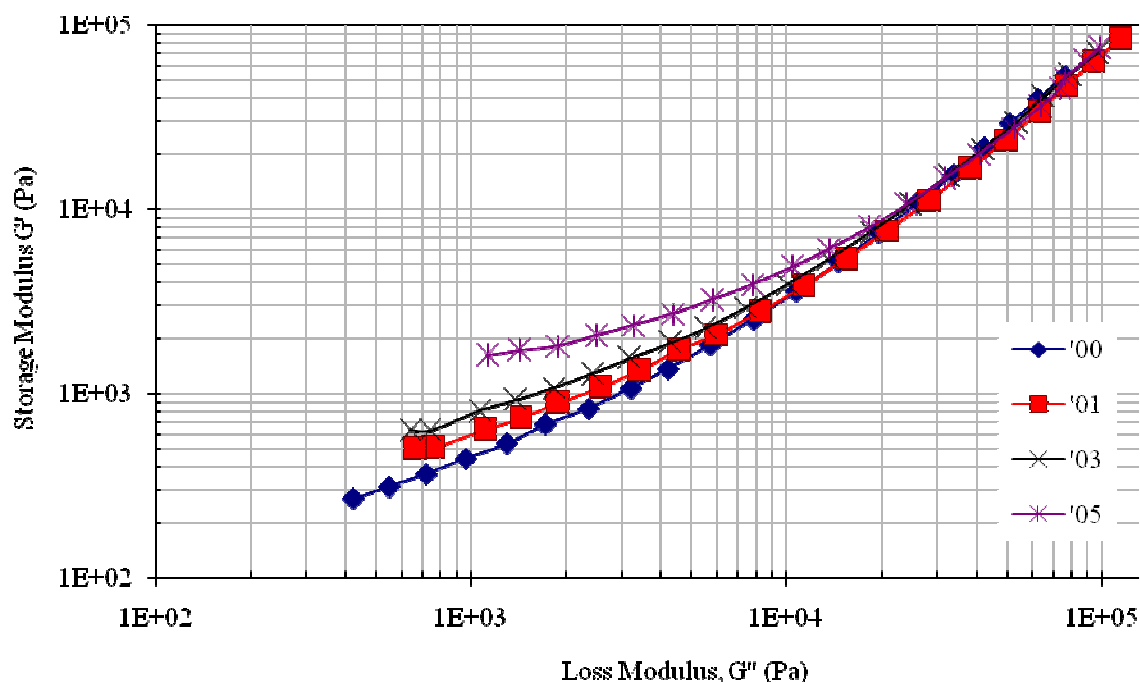


Figure 4.45 : Plot of log G' versus log G'' for 50/50 PA6/ABS blends at different amount of compatibiliser, at 230°C

However, there was a slightly different trend for 60/40 PA6/ABS blends as compared to 50/50 and 70/30 PA6/ABS blends. From Figure 4.46, the slopes of the graph without ABS-g-MAH and 1 wt. % were almost similar; although for 3 and 5 wt. % they were different. At low frequency, the structure of 3 and 5 wt. % compatibilised blends changed with respect to that of without and low amount of ABS-g-MAH in the blends. This indicates that 3 wt. % is the maximum amount of compatibiliser to achieve a good interaction between PA6 and ABS phases. It is believed that grafting reaction between compatibiliser and matrix has occurred to form a bridge and thus restrict the mobility of the constituent polymer chains. However, according to our flexural properties results obtained previously, by adding compatibiliser beyond 3 wt. % not improve the properties because the compatibiliser has acted as fillers. However, the rheological properties were improved and more prominent at lower frequency. Beyond 3 wt. %, the excess of compatibiliser in the system capable to store more energy elastically and to dissipate more mechanical energy when compared to the uncompatibilised blends (Shenoy, 1999).

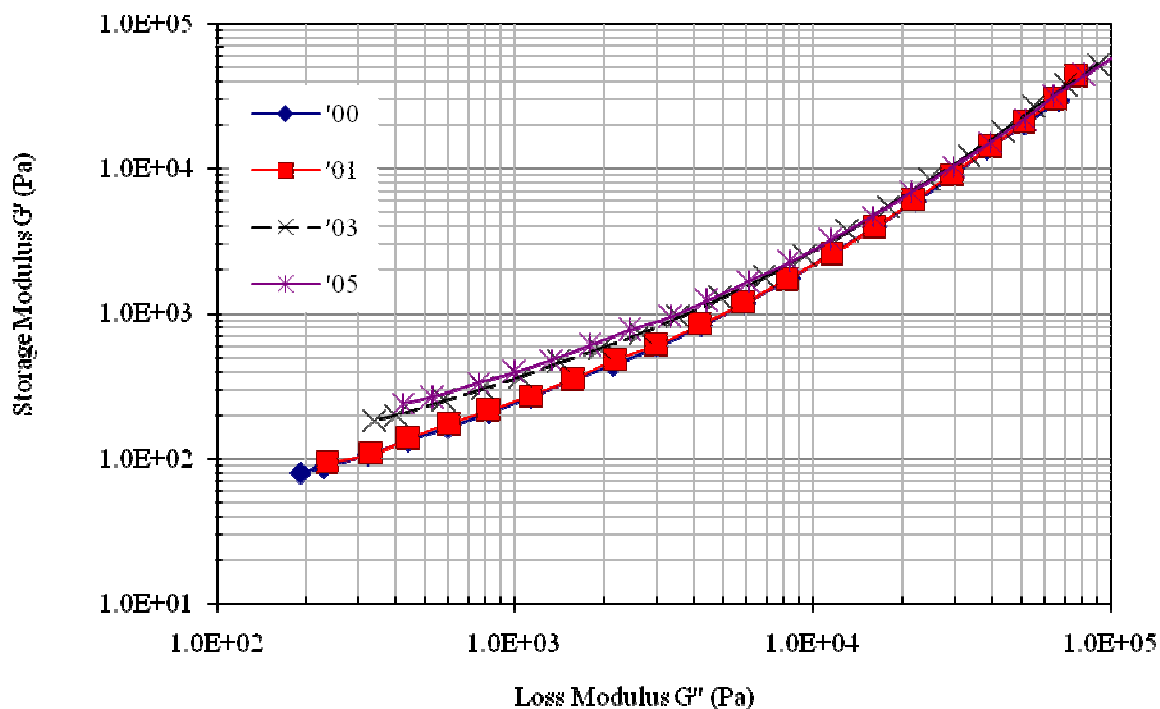


Figure 4.46 : Plot of $\log G'$ versus $\log G''$ for 60/40 PA6/ABS blends at different amount of compatibiliser, at 230°C

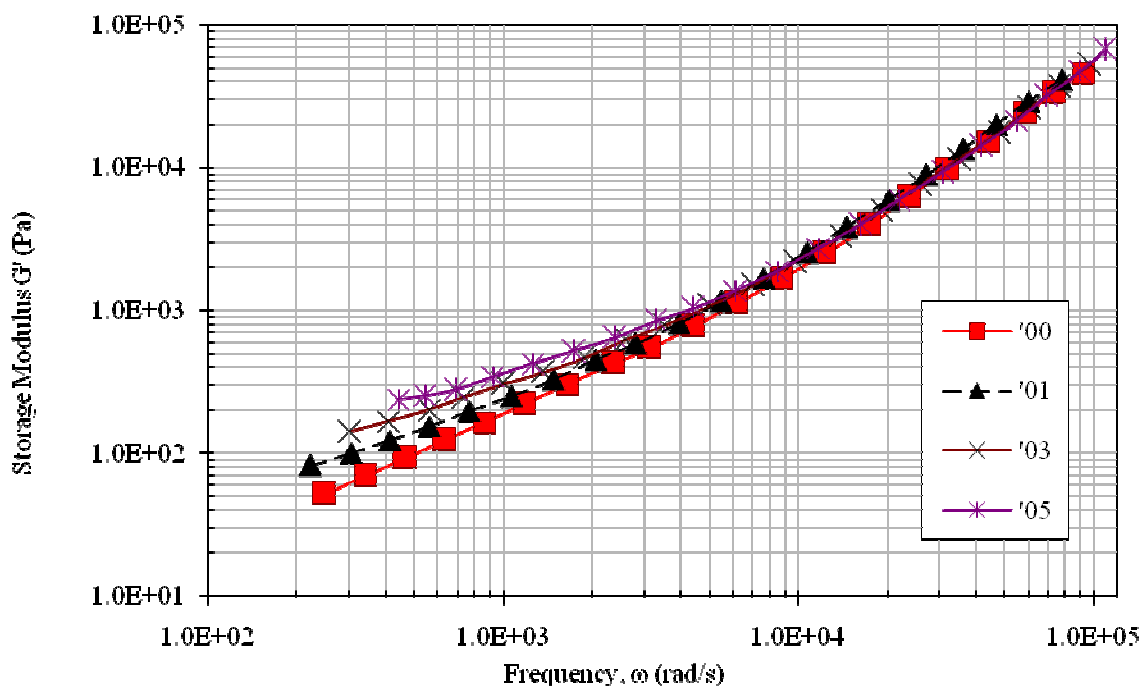


Figure 4.47 : Plot of $\log G'$ versus $\log G''$ for 70/30 PA6/ABS blends at different amount of compatibiliser, at 230°C

4.4.2.6 Activation Energy of Flow

Controlling the processing temperature is an important means to regulate the flowability of polymer melts. In general, melt viscosity of polymer has inversely proportional with temperature. Therefore, the increasing of temperature will improve the flow behaviour of the molten polymers. It is due to the fact that when the temperature increases, the melt free volume increases, causing an enhancement of chain segments motion and a reduction of interactions between chain segments (Li and Lu, 2008). This will result in the reduction of melt viscosity.

In this study, the dynamic rheological behaviour of the PA6/ABS blends and composites has undergone variations of temperature used (230°C, 245°C and 260°C) quantitatively. Generally, the viscosity always changed with changing the temperature. Therefore, in order to understand the rheological behaviour of PA6/ABS blends, the dependence of viscosity of the blends on temperature followed the well known William-Landel-Ferry (WLF) equation (Ferry, 1970).

$$\log a_T = -C_1(T - T_0)/(C_2 - (T - T_0)) \quad (4.1)$$

where C_1 and C_2 are constants, T_0 is a reference temperature and a_T is a temperature shift factor. The value of C_1 and C_2 are 17.4 and 51.6, respectively.

The data of PA6/ABS blends were plotted in a form of $\log \tau$ versus $\log \omega$ curves at different temperature and a_T was determined by the horizontally shift necessary to obtain superposition on the corresponding $\log \tau$ versus $\log \omega$ curve of reference temperature T_0 . All the blends under study were found to be thermorheologically simple over the entire range of frequencies and temperatures studies. The temperature dependence of the temperature shift factor, a_T was stated using the Arrhenius equation (Sepehr *et al.*, 2005):-

$$\ln a_T = \ln A + \frac{E_a}{R(T - T_0)} \quad (4.2)$$

Where A is pre-exponential factor, E_a is the activation energy and $R = 8.31432 \text{ J/g.mol.K}$ is the universal gas constant.

The activation energy of the blends were calculated from the slope obtained by linear regression $\ln a_T$ versus inverse of temperature, $1/T$, as shown in Figure 4.48, 4.49 and 4.50, respectively.

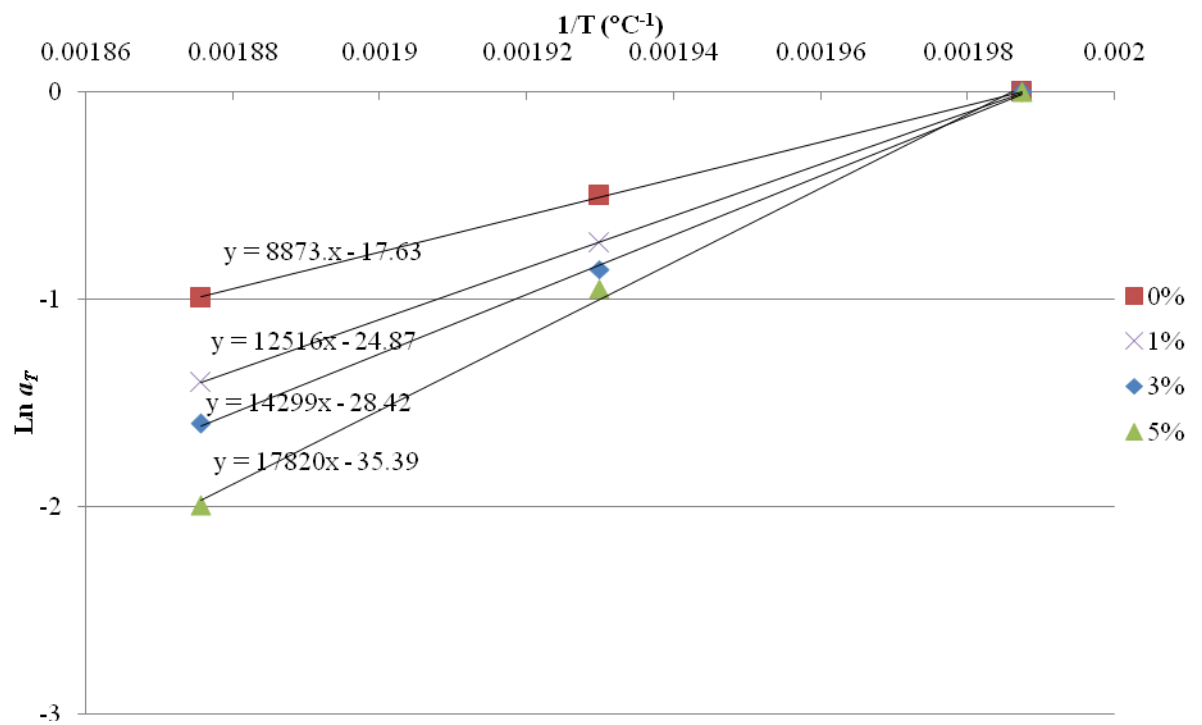


Figure 4.48 : Effect of temperature on shift factor, a_T of 50/50 PA6/ABS blends at different compatibiliser concentration

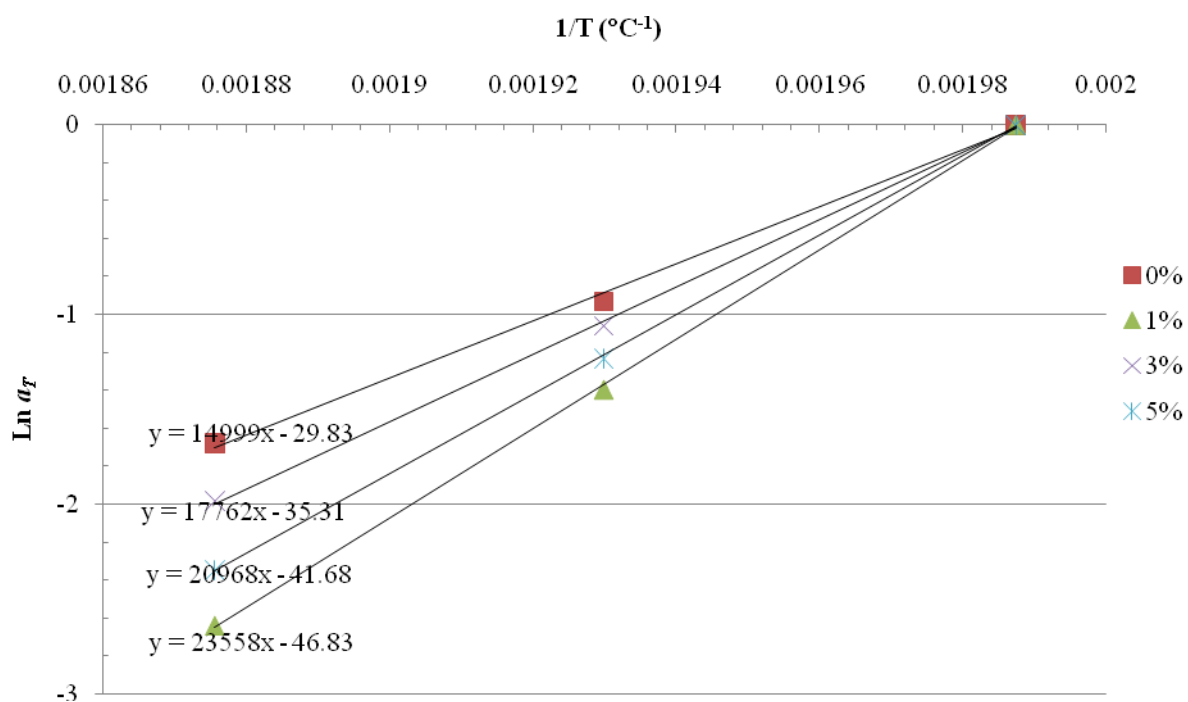


Figure 4.49 : Effect of temperature on shift factor, a_T of 60/40 PA6/ABS blends at different compatibiliser concentration

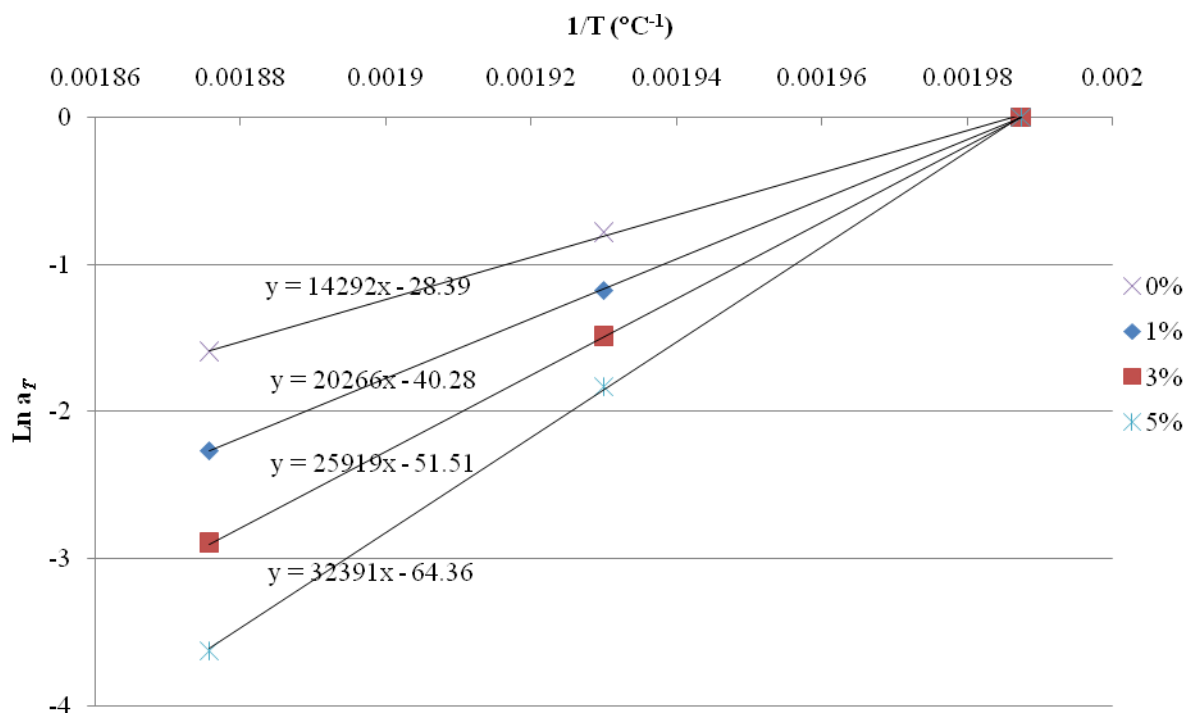


Figure 4.50 : Effect of temperature on shift factor, a_T of 70/30 PA6/ABS blends at different compatibiliser concentration

The activation energy of flow, E_a is the energy that needs to be consumed for breaking up the interactions among the chain segments when the melts flow. It reflects the dependence of melt viscosity on temperature. The higher the E_a the more pronounced the dependence is. In addition, the activation energy decreases with increasing temperature because the number of entanglement coupling points are reduced and hence results in a decrease of interaction between chain segments. The interaction between chain segments will be influenced by the addition of compatibiliser.

Figure 4.51 shows that the effect of amount compatibiliser on activation energy of viscous flow at different PA6 concentration. At 50/50 and 60/40 PA6/ABS blends, adding 1 wt. % of compatibiliser decreased the activation energy of flow. This is likely because at this compatibiliser level the amount was fairly enough to reduce interfacial tension and enhance the interfacial adhesion between PA6 and ABS phases. This result is confirmed with the tensile modulus and strength results obtained previously. It could also be explained by the addition of compatibiliser has

generally lead to decrease in the E_a of polymer blends and therefore this addition made the polymer blends more temperature sensitive (Gribben F. *et al.*, 2005). However, the activation energy increased with the addition of more than 3 wt. % ABS-g-MAH. When increasing amount of compatibiliser, ABS-g-MAH became excess able material in the blends, it meant that the functional group also excess able and may result in overwhelming interfacial interaction due to repulsion of polar group in ABS phase to the PA6 phase. The figure also shows that the higher amount of PA6 in the blends showed the higher activation energy. It could be explained that, the lower is the flow activation energy means that the material behaves more elastic or in other words, increasingly solid-like (Davendra *et al.*, 2006). In short, the compatibilised interaction and activation energy of flow could be correlated because more energy is needed to break the interactions and allow the material to flow. Enough amount of compatibiliser could provide stronger interaction than lower or without compatibiliser. This result is in agreement with the tensile strength and modulus results were discussed earlier. This pattern is similar to the power law and consistency index results that will be discussed in Section 4.4.3.3.

At 70/30 PA6/ABS blends the addition of 3 wt. % of compatibiliser showed the lowest of activation energy of flow as compared to the previous composition where 1 wt. % was the maximum amount of compatibiliser. This indicates that the maximum compatibiliser content was 3 wt. %, and enough amount to initiate interaction between the amine end-group of PA6 and maleic anhydride. This could be due to because, more amount of compatibiliser reacted with 70 wt. % of PA6 than 60 and 50 wt. %.

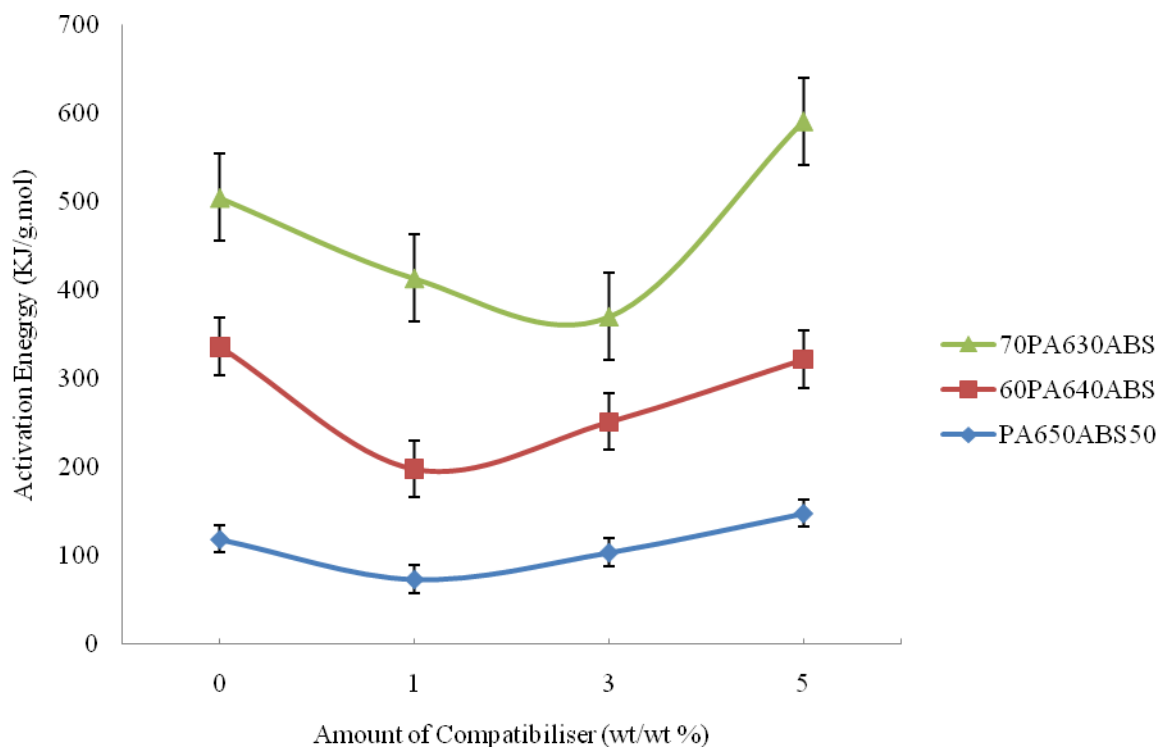


Figure 4.51 : Plot of activation energy of flow versus amount of compatibiliser at different concentration of PA6.

4.4.3 Capillary Rheological Properties of PA6/ABS Blends

4.4.3.1 Shear Stress Analysis

The rheological properties of blends reveal some information on the compatibilisation effect. To probe it, the rheological properties of the PA6/ABS blends were investigated using capillary rheometer. Figures 4.52, 4.53 and 4.54 show the plot of actual shear stress versus actual shear rate for 50/50, 60/40 and 70/30 PA6/ABS blends with different amount of ABS-g-MAH, respectively. The temperature was setup at 230°C. It can be seen that the curves apparently deviate from linear relationship of shear stress with shear rate inclining to the axis of shear rate, which means that the blends are pseudoplastics fluids (Han, 1976). This observation is similar to most polymeric melts (Han, 1982). All the blends showed a

pseudoplastics behaviour. It seems that, the addition of compatibiliser did not change the shear stress of all the PA6/ABS blends at low shear rate. It could be due to small amount of compatibiliser attributed less to the change of shear stress. However the effect of compatibiliser on the shear stress was more obvious at higher shear rate, specifically for 60/40 and 70/30 PA6/ABS blends. This indicates that at higher concentration of PA6 more grafting reaction has occurred in polymer melts during testing, thus to higher amount of amine-end group of PA6 as compared to 50/50 PA6/ABS blends. These reasons could attribute to the increase of shear stress at higher shear rate.

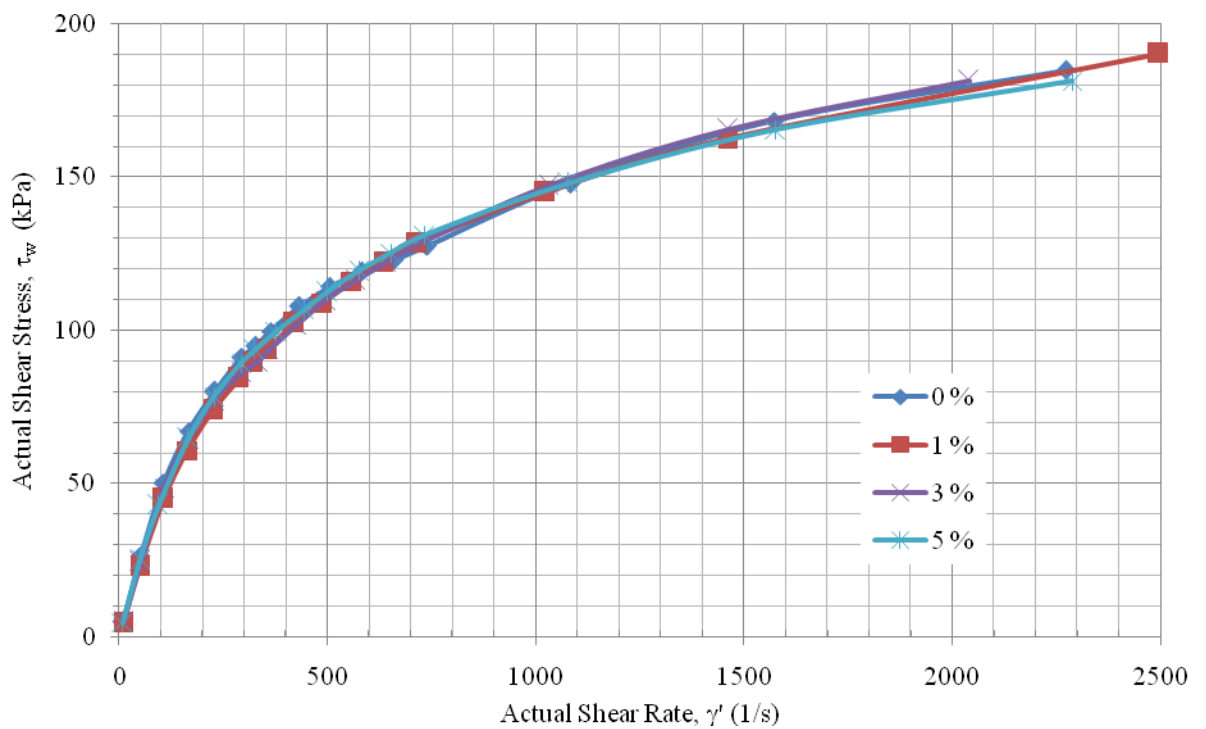


Figure 4.52 : Plots of shear stress as a function of shear rate for 50/50 PA6/ABS blend at different compositions of ABS-g-MAH

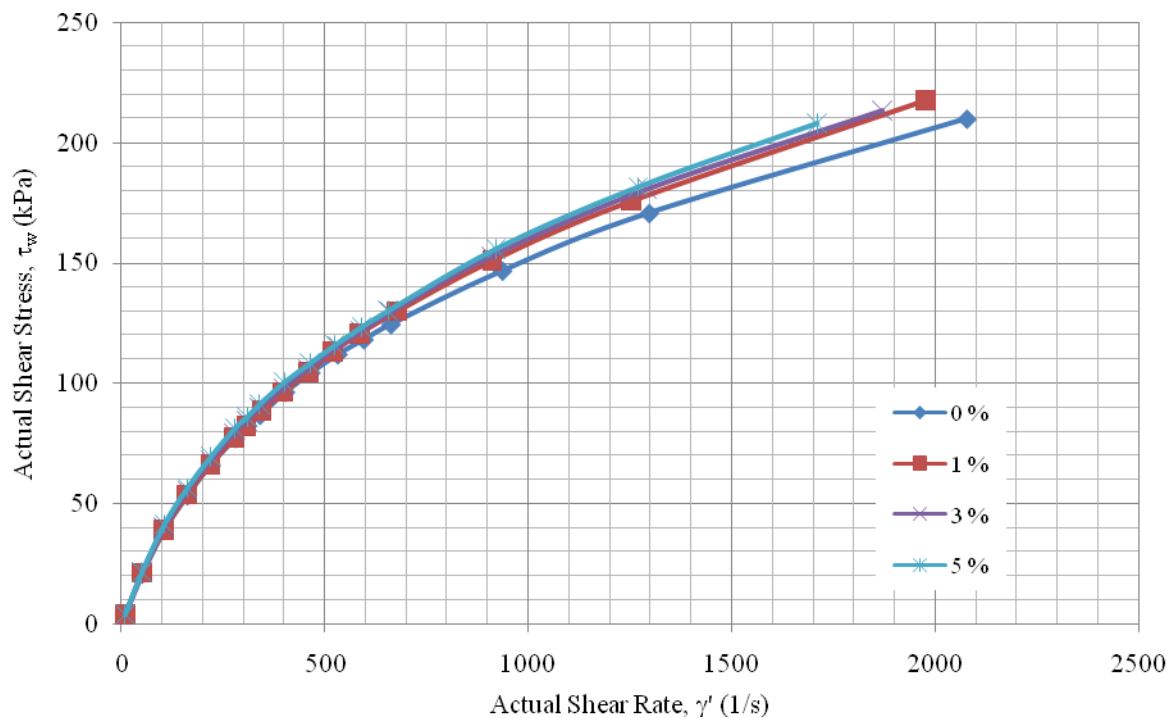


Figure 4.53 : Plots of shear stress as a function of shear rate for 60/40 PA6/ABS blend at different compositions of ABS-g-MAH

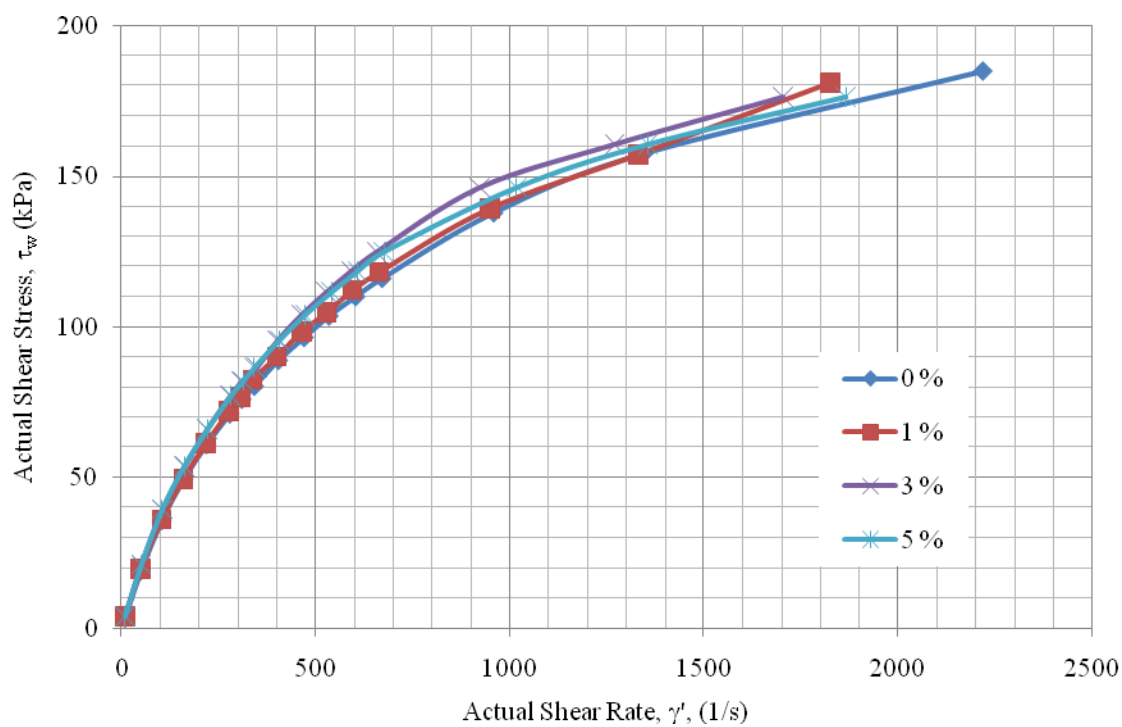


Figure 4.54 : Plots of shear stress as a function of shear rate for 70/30 PA6/ABS blend at different compositions of ABS-g-MAH

4.4.3.2 Shear Viscosity Analysis

Shear viscosity, η , is the viscosity coefficient when the applied stress is a shear stress. Shear viscosity is the ratio shear stress and shear rate. Therefore, in this study, shear viscosity of the samples were analysed and discussed in order to understand the compatibilisation effects on the blends composition. The effect of compatibilisation for 50/50, 60/40 and 70/30 PA6/ABS blends using ABS-g-MAH at 230°C and at various shear rates is seen in Figures 55, 56 and 57, respectively. Flow curves for the compatibilised blends were basically similar to uncompatibilised blends. It shows that the shear viscosity of all the blends decreased with increasing shear rate showing a typical property of pseudo-plastics non-Newtonian or shear-thinning plastics. The decrease in shear viscosity can be attributed to the alignment of chain segments of PA6/ABS blends in the direction of applied stress.

At lower shear rate, it closed to zero shear, it can be predicted all the blends showed a Newtonian molten flow. This means that the incorporation of compatibiliser significantly did not change much the non-Newtonian behaviour at lower shear rate. However, the dependence of the shear viscosity on shear rate is different as the amount of compatibiliser varies, especially for 50/50 PA6/ABS blends at low shear rate regime. The compatibiliser had a little effect on the shear viscosity. At a fixed shear rate, the viscosity increased with increasing the amount of compatibiliser. The increase in viscosity has been attributed to the increased of interaction between the PA6 and ABS as a result of decreased interfacial tension and increased entanglement. This finding is in a good agreement with the study by Joseph *et al.* (2007) on the effect of blend of polystyrene and polybutadiene by using two different types of compatibiliser.

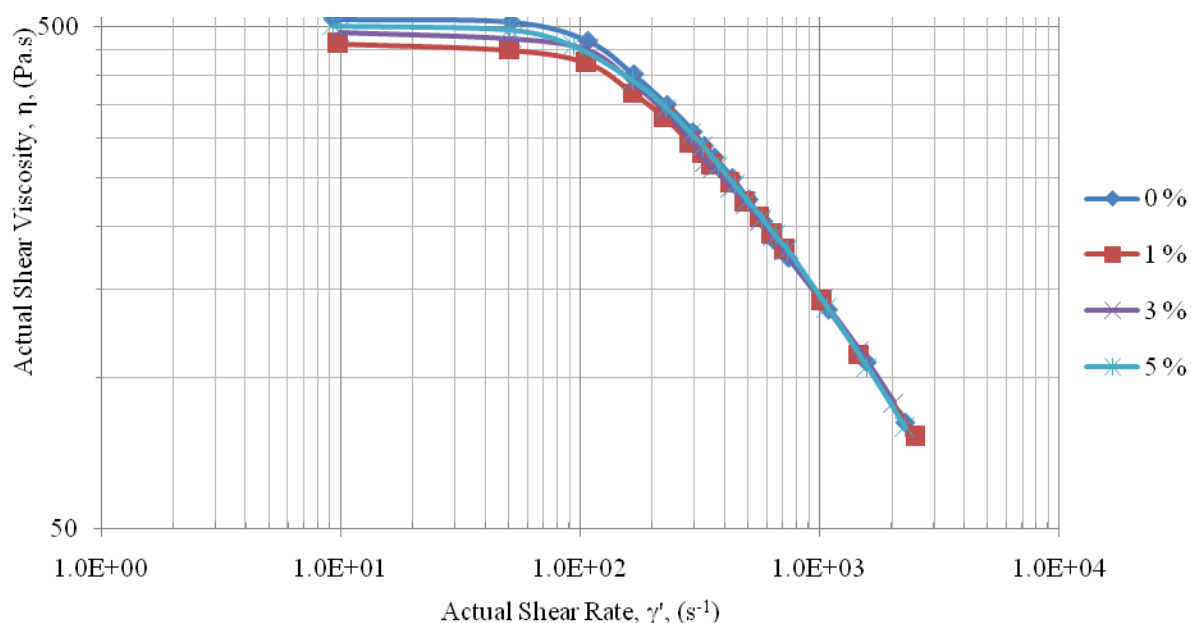


Figure 4.55 : Plots of shear viscosity as a function of shear rate for 50/50 PA6/ABS blend at different compositions of ABS-g-MAH

Figure 4.56 shows the plots of shear viscosity versus shear rate for 60/40 PA6/ABS blends. In the shear rate range explored, the blends exhibited pseudo plastics behaviour and it is predictable that all the blends could achieve Newtonian plateau at low shear rates (shear rate lower than $50 s^{-1}$). This means that, the addition of compatibiliser did not significantly affect the Newtonian behaviour at low shear rate as compared to uncompatibilised blends. In the shear thinning region, the addition of interfacial modifier (compatibiliser) made the blends more resistant to flow, suggesting the interactions brought by the interfacial modification. The restriction in chain mobility is appeared at all range of shear rate studied, where the gap between the flow curves of the blends became bigger and bigger with increasing of compatibiliser.

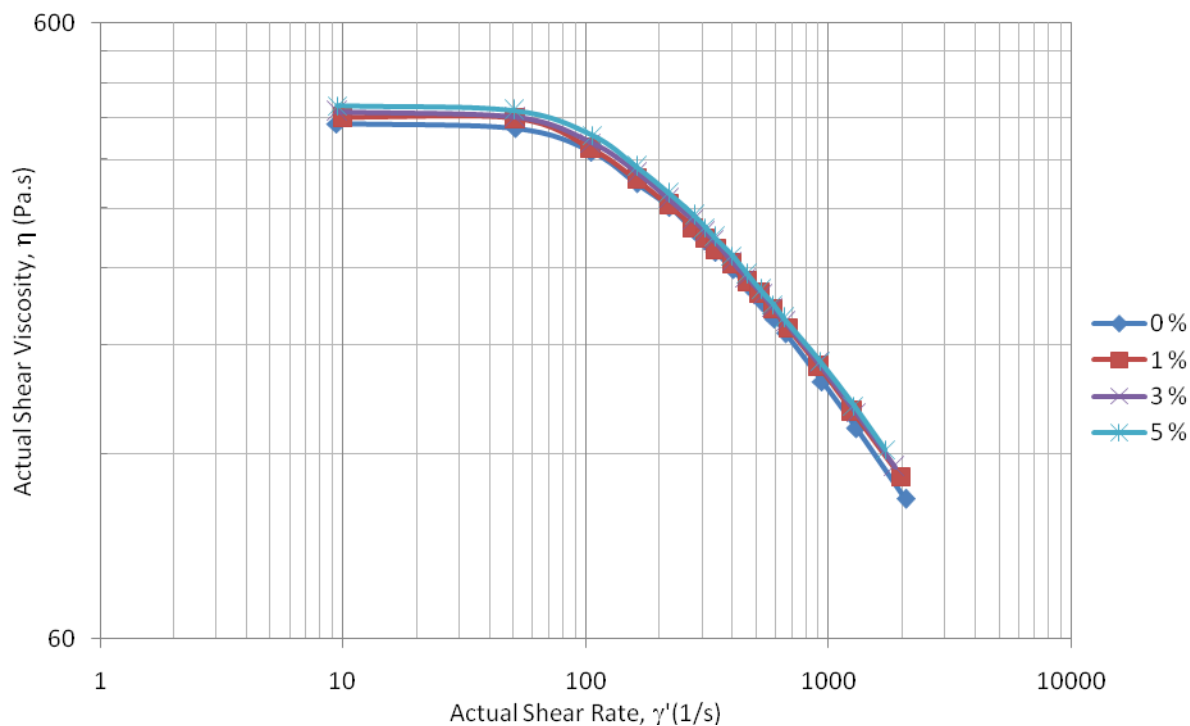


Figure 4.56 : Plots of shear viscosity as a function of shear rate for 60/40 PA6/ABS blend at different compositions of ABS-g-MAH

Figure 4.57 shows the dependence of shear viscosity for 70/30 PA6/ABS blend with variation of compatibiliser content up to 5 wt. %. From that figure, it can be observed that a considerably little changed in shear viscosity has occurred with increasing of compatibiliser at lower shear rate. With greater proportions of compatibiliser, the inhibition of polymer chain motion by the compatibiliser phase has increased, and the flow resistance increased correspondingly, leading to a slightly increased in shear viscosity.

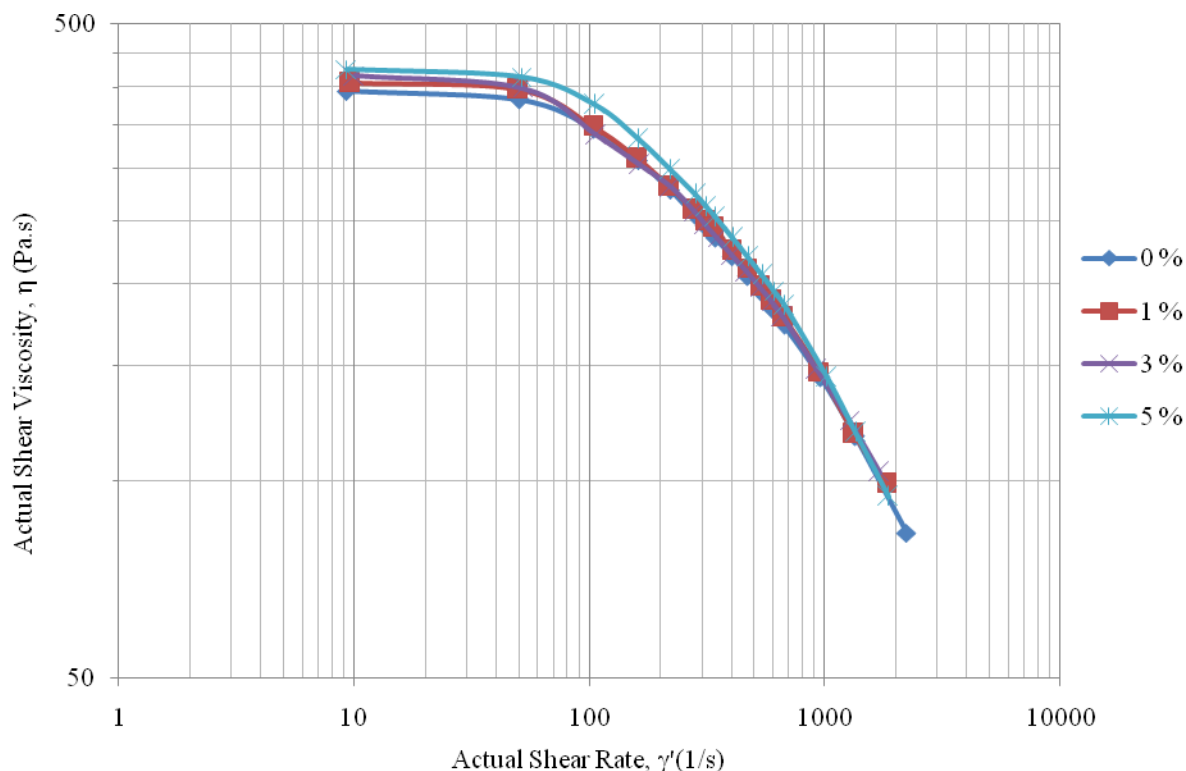


Figure 4.57 : Plots of shear viscosity as a function of shear rate for 70/30 PA6/ABS blend at different compositions of ABS-g-MAH

4.4.3.3 Power Law Index Analysis

The power law index can accurately represent the shear-thinning behaviour of viscosity with respect to shear rate (Oswald and Menges, 1996). In addition of that, the pseudo-plastics materials have n values less than unity and value of n indicates a low shear thinning nature. Generally, the flow curve is an important method of characterising the processing properties of polymer melts under technology conditions. It is usually represented by the relationship curves between shear stress τ_w , shear viscosity η_w and shear rate $\dot{\gamma}_w$ and during die extrusion of polymer extrusion. Previously, the curves of shear stress τ_w , versus shear rate $\dot{\gamma}_w$, for PA6/ABS samples at various concentration of ABS-g-MAH was shown in Figures 4.52, 4.53 and 4.54. It can be seen that shear stress increased non-linearly with increasing shear rate when the test temperature was constant at 230°C. This indicates that the sample melt shear flow did not strictly obey the power law over a wide range

of extrusion rates. The effect of compatibiliser concentration on the flow behaviour index or power law index, n and consistency index, K of the 50/50, 60/40 and 70/30 PA6/ABS blends are shown in Figures 4.56, 4.57 and 4.58.

For 50/50 PA6/ABS blends, a drastically effect was noticed upon increasing the concentration of compatibiliser as shown in Figure 4.58. There was a reduction in power law index upon the addition of 1 wt. % of compatibiliser and increased when the compatibiliser was increased to 3 wt. %. This reduction of power law index at 1 wt % of compatibiliser could be due to a good interaction between ABS phase and the PA6 phase. This behaviour was confirmed by tensile modulus and strength result as discussed previously. The increase of power law index when the compatibiliser was about 3 wt. %, is believed to be due to an excess of compatibiliser that tends to form agglomeration within their phases and reduced the interfacial adhesion. This also can be related to the value of consistency index, where it attributes to the viscosity. Furthermore, the power law index has slightly decreased with increasing the compatibiliser concentration up to 5 wt. %. Though, the consistency index increased with added compatibiliser. The increase in compatibiliser could recover more entanglement and thus made the molecular orientation more difficult. This result is similar to the study of PA6/LDPE blends compatibilised by poly(ethylene-co-methacrylic acid) reported by Sinthavathavorn *et al.* (2009). From the figure, it can be observed that, 1.5 wt. % is the minimum of power law index and maximum consistency index, thus the amount has been suggested as the optimum concentration of compatibiliser for 50/50 PA6/ABS blends.

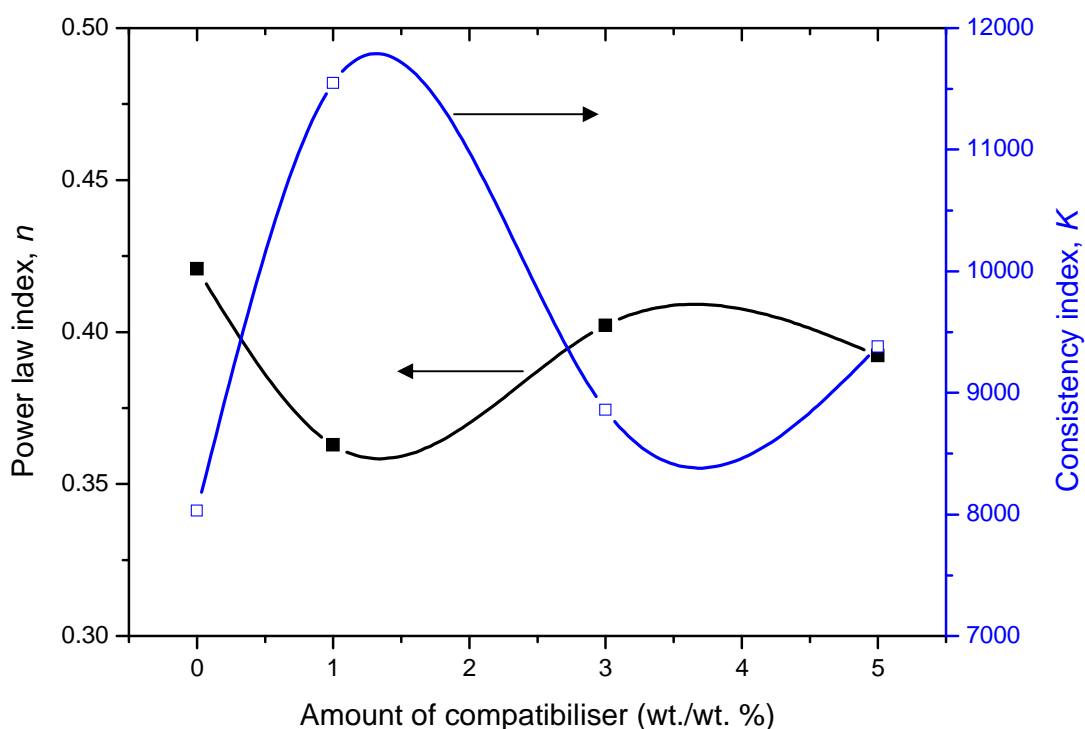


Figure 4.58 : Power law index, n and consistency index, K for 50/50 PA6/ABS blends with various amount of compatibiliser at 230 °C

For 60/40 PA6/ABS blends, similar effects were noticed with 50/50 PA6/ABS blends upon increasing the concentration of compatibiliser as shown in Figure 4.59. It is clear from the figure that n decreased with increasing 1 wt. % of compatibiliser. The reduction of n value could be caused by direct interaction of anhydride with amine end-group of PA6 and thus resulted in enhancement of interfacial adhesion. Increasing amount of compatibiliser higher than 5 wt. % caused an increasing trend of the n value. Therefore, the highest pseudoplastics in the flow of 60/40 PA6/ABS blends with compatibiliser was found at 1.5 wt. %. Furthermore, the pattern of consistency index was found to be opposite as compared to power law index.

The trend of power law index and consistency index for 70/30 PA6/ABS blends as shown in Figure 4.60 were found to be different as compared to the previous composition of PA6/ABS blends. It can be seen that 3 wt % was the optimum value of compatibiliser in which power law index was minimum and

consistency index was maximum. This could be attributed to the chemical interaction between different phases of the blend caused by compatibilisers, which consists of chemically reactive segments to their respective counterparts in the polymer pairs. It was affected the enhancement of interaction and improved interfacial adhesion and thus restricted a movement of molecular level in polymer melt flow.

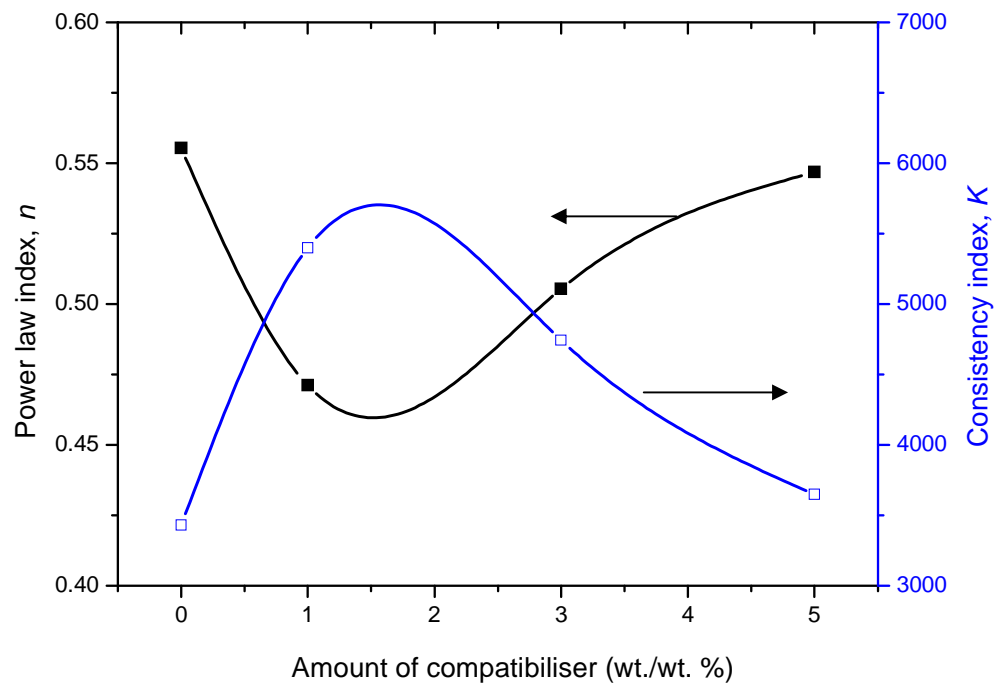


Figure 4.59 : Power law index, n and consistency index, K for 60/40 PA6/ABS Blends with various amount of compatibiliser at 230 °C

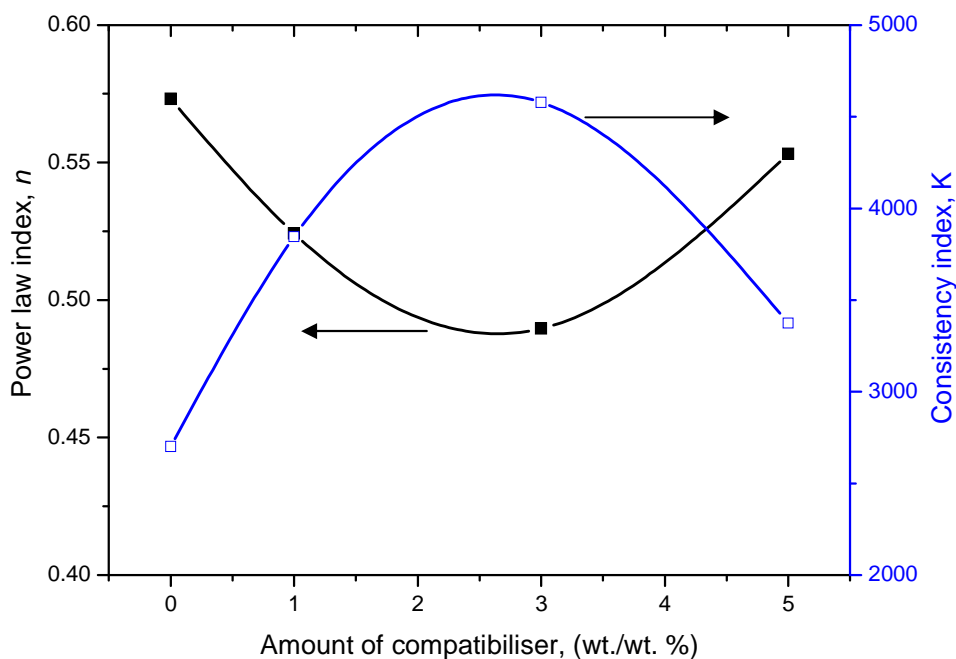


Figure 4.60 : Power law index, n and consistency index, K for 70/30 PA6/ABS Blends with various amount of compatibiliser at 230 °C

4.4.4 Dynamic Rheological Properties of 60/40 PA6/ABS Composites

4.4.4.1 Loss and Storage Modulus Analysis

The G' and G'' results for the polymer composites and polymer blends are shown in Figures 4.61 and 4.62, respectively. Again, rises in storage modulus with increasing SGF concentration was observed at all frequencies. Moreover, these polymer composites can be categorised as liquid-like material, because the G'' was greater than G' at all range of frequencies studied regardless the amount of SGF in the systems. This could be due to SGF acted as a 'lubricant' and caused the polymer phase of PA6 and ABS easily slipped at interphase and interface level.

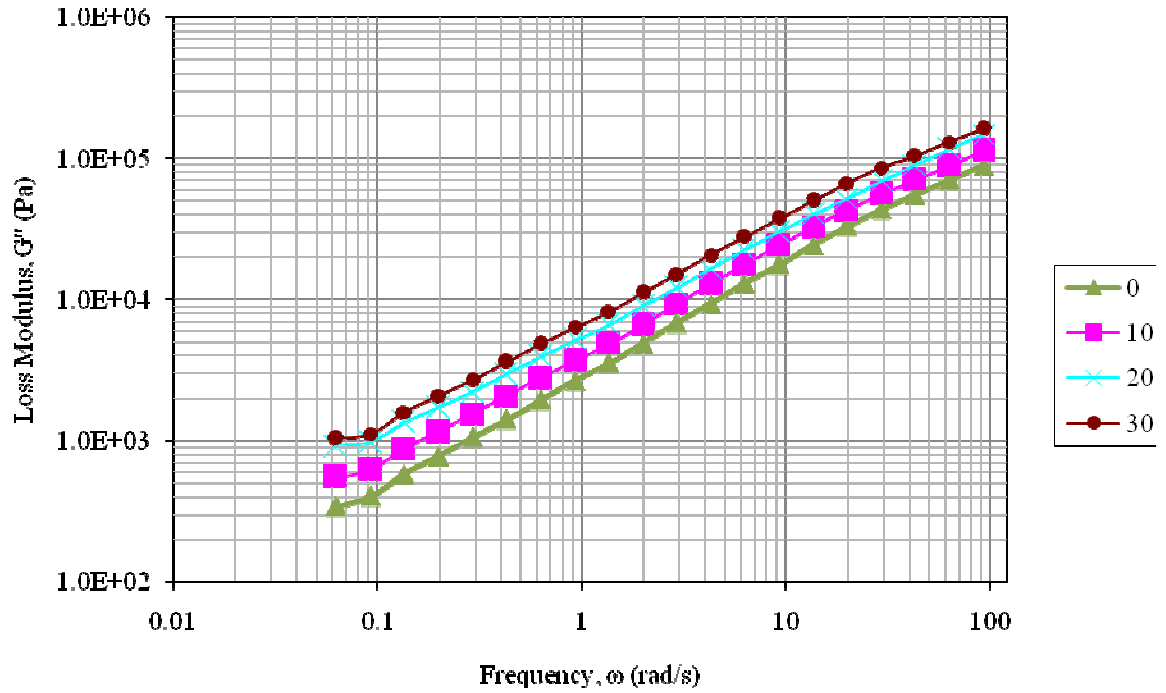


Figure 4.61 : Effects of loss modulus of 60/40 PA6/ABS composite versus frequency at different amount of SGF

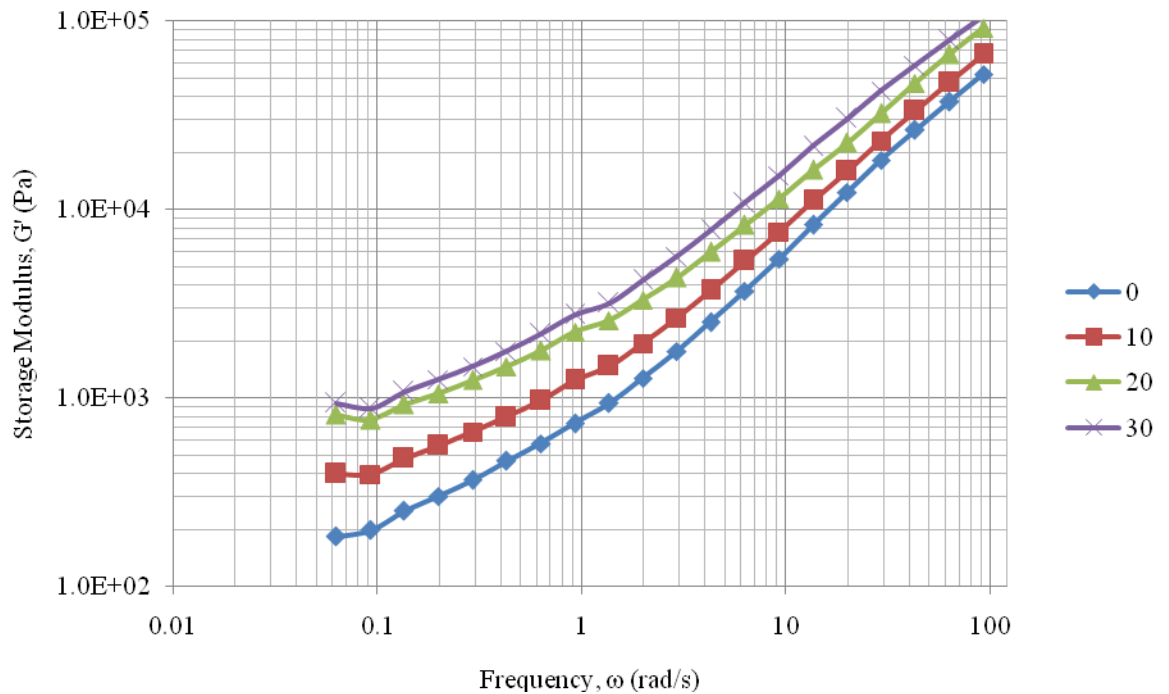


Figure 4.62 : Effects of storage modulus of 60/40 PA6/ABS composite versus frequency at different amount of SGF

4.4.4.2 Complex Viscosity Analysis

Figure 4.63 represents the relationship between complex viscosity and frequencies, ω for PA6/ABS composites containing different amount ranging from 0% to 30% of SGF at 230°C. It can be seen that the trend in complex viscosity growth associated with SGF loading. At all frequencies, the complex viscosity of polymer composites was larger than unfilled PA6/ABS blends. It can also be found, that the complex viscosity decreased with the increasing of frequencies. This observation is due to the deformation of the SGF at high frequencies and its associated contribution to an increase in fluidity of the matrix phase. When more SGF was added into the blends, the SGF droplets begin to grow and coalesce, causing an increase in the complex viscosity (Guschl and Otaigbe, 2003). Generally, all the blend systems showed a non-Newtonian behaviour at all frequencies. The increase in viscosity of the composites with increasing fibre concentration could be due to the interaction between fibre-fibre and fibre-matrix (Prasantha Kumar *et al.*, 2000; Dweiri and Azhari, 2004).

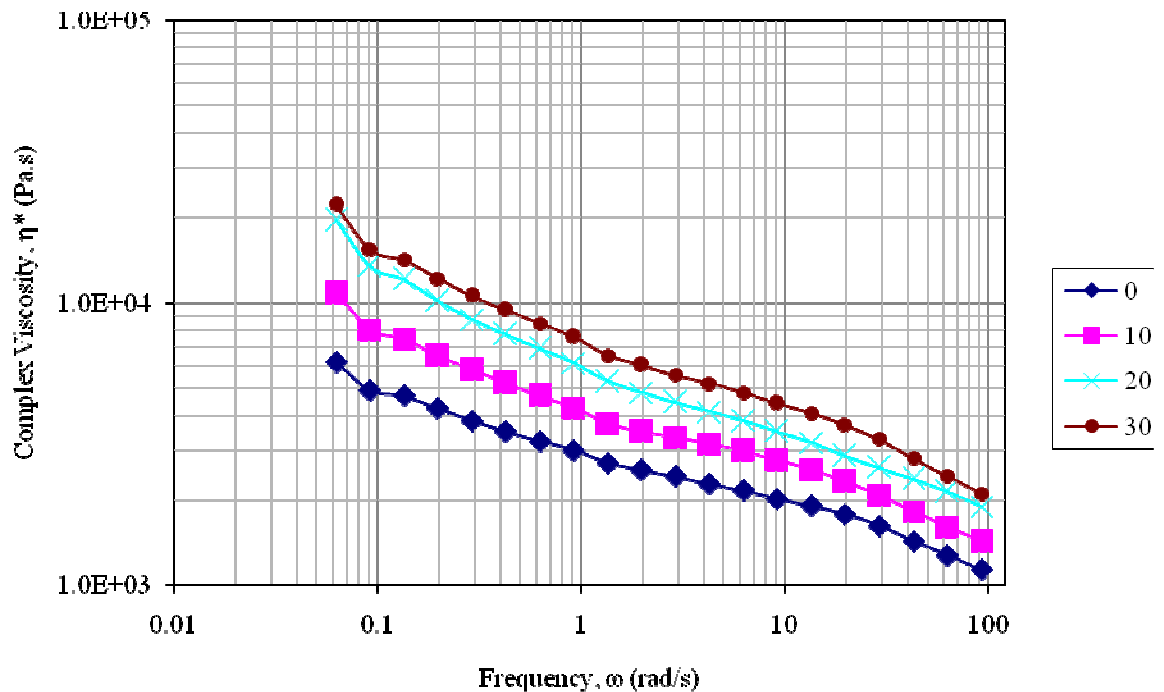


Figure 4.63 : Effects of complex modulus of 60/40 PA6/ABS composite versus frequency at different amount of SGF

4.4.4.3 Tan δ Analysis

In order to obtain information on how efficient the polymer composites lose energy to molecular rearrangements and internal friction, the relation between tan δ of PA6/ABS composites versus frequency were obtained and it is shown in Figure 4.64. The tan δ is very sensitive with structural change (Xiao *et al.*, 2006) and decreased with the incorporation of short glass fiber, which is due mainly to the existence of effective interfacial bonding between SGF and PA6/ABS matrix so that the energy dissipation in the composite was limited. Otherwise, if the interfacial adhesion is poor, applied energy will be dissipated in the form of heat due to the interaction between the fiber and matrix. Consequently, the peak of tan δ will be increase with decreasing the interfacial adhesion. Similar to other composite systems, the decreasing of tan δ to be due to incorporation of SGF, resulting an improvement in damping and showing that the polymer composites are more elastics (Lozano *et al.*, 2004). From the figure, it can be observed the tan δ decreased drastically when 10 wt. % of SGF was introduced into the composite. From the figure, it can be observed that 20 and 30 wt. % of SGF considerably have a similar effect on tan δ at all frequency studied. Therefore, the incorporation of SGF has improved the damping and elasticity of PA6/ABS composites.

Tan δ is very sensitive with structural change of the composites and viscoelastic behaviour can be determined using the analysis of tan δ peak. From the figure, a viscoelastic peak occurred at the frequency around 2 – 5 rad/s and depends on concentration of SGF in the PA6/ABS composites. It can be observed, the unfilled composite has a highest tan δ , indicates less elastics than the filled composites. The elastic behaviour became more prominent with the highest amount of SGF. In other word, the viscoelastics disappeared with increasing the SGF content. Tan δ peak also indicates a solid-liquid transition, which is the composite undergo a transition with increasing a frequency. At the transition point, tan δ is expected to be independent of frequency. When the frequency increased beyond this transition point, a dominating

elastics response (solid behaviour) of the composite became more obvious. At frequency is about 100 rad/s, all the composites considerably showed identical $\tan \delta$ value indicating the SGF has not affected the viscoelastic behaviour of the composites.

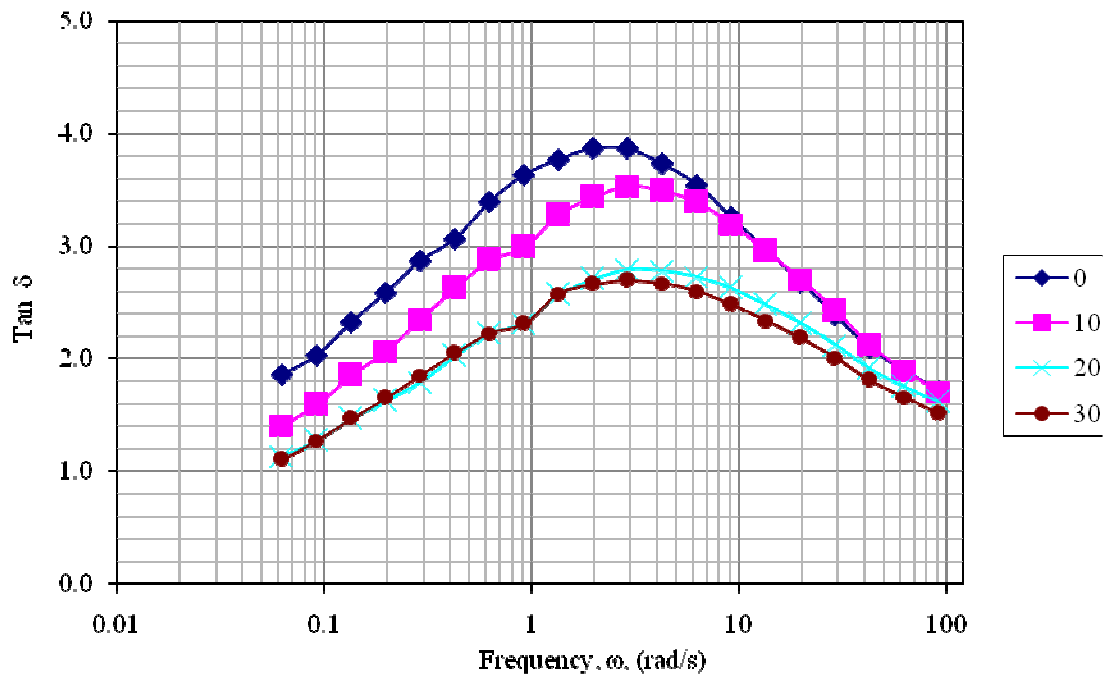


Figure 4.64 : Effects of short glass fibre on the composite $\tan \delta$ of the PA6/ABS blends

4.4.4.4 The Cole-cole plot Analysis

Figure 4.65 illustrates a plot of storage modulus, G' versus loss modulus, G'' for PA6/ABS composites with various amount of short glass fibre. From the figure, it can be seen that the cole-cole plot of PA6/ABS composites deviated from scaling G' versus G'' of the unreinforced polymer blends indicating that a long relaxation mechanism has occurred in these samples. This indicates that the composites behave in an anomalous way and a phase separation of PA6 and ABS has incurred. In other words, the addition of SGF into PA6/ABS composites has enhanced the interfacial adhesion, increased the elasticity and improved the properties of the composites.

However, the interaction between the SGF and PA6/ABS composites will be more obvious by discussing the power law index and consistency index in Section 4.4.4.7. At the concentration of SGF beyond 20 and 30 wt. %, it was found that the deviation trend considerably similar. This indicates that further incorporation of SGF has not improved much the elasticity, even though the complex viscosity of the both concentration was different.

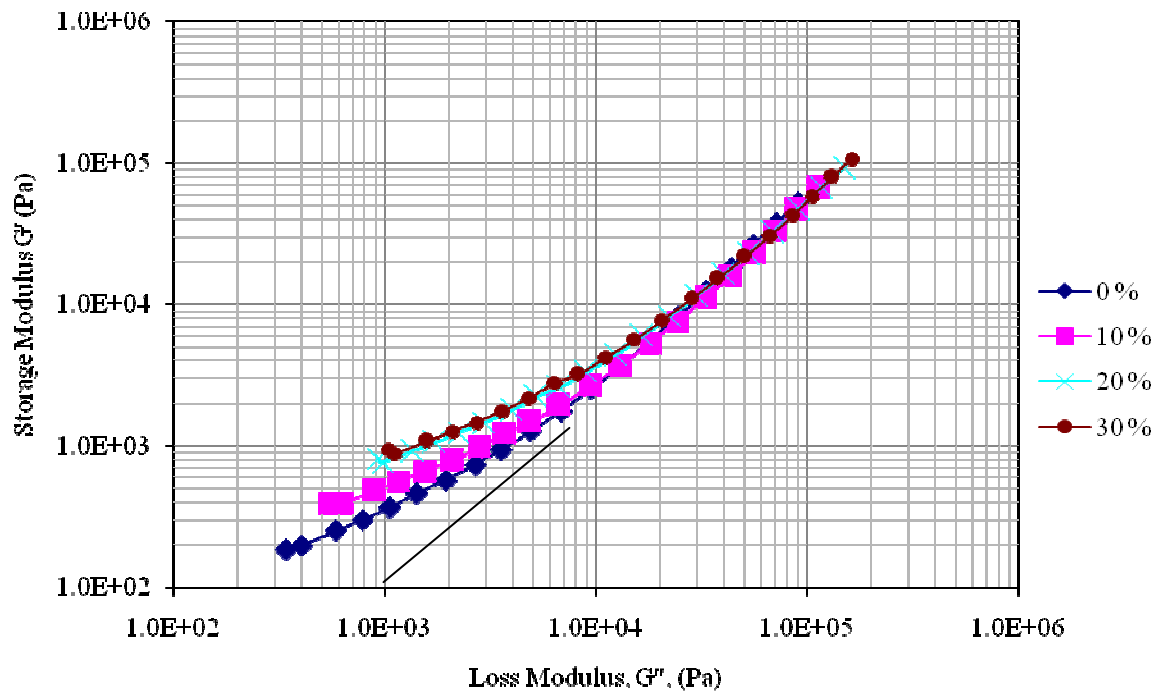


Figure 4.65 : Plot of storage modulus, G' versus loss modulus, G'' of 60/40 PA6/ABS composites at different amount of SGF, at 230°C

4.4.4.5 Activation Energy of Flow Analysis

The activation energy of polymer composites were calculated from Arrhenius equation plots of $\ln a_T$ versus reciprocal of temperature as shown in Figure 4.65. From the Figure 4.65, the activation energy of flow, that is an indication of temperature sensitivity of the melts, was reduced in the present of fibre. This explains that the higher temperature sensitivity of the polymer matrix was increased in the present of 10 wt. % fibres. This result is not in agreement with the study

carried out by Pransantha Kumar *et al.* (2000). They reported that the activation energy of fibre reinforced styrene-butadiene rubber composites increased with increasing of fibre concentration, and indicating that the melt viscosity of the composite is higher temperature sensitive than that of without fibre. However, from Figure 4.67, increasing of activation energy was clearly seen at the concentration of fibre beyond 10 wt. % though the value was till lower than the unfilled PA6/ABS composite. This is also indicates that the present of 10 wt. % concentration of SGF in the composite reduced the sensitivity of the composite, as a result, reduced the compatibility of the system. However, the sensitivity of the composites to temperature increased with further increase of SGF concentration beyond 10 wt. %, indicates the compatibility of the composite between SGF with PA6/ABS matrix was restored with further increase in SGF concentration.

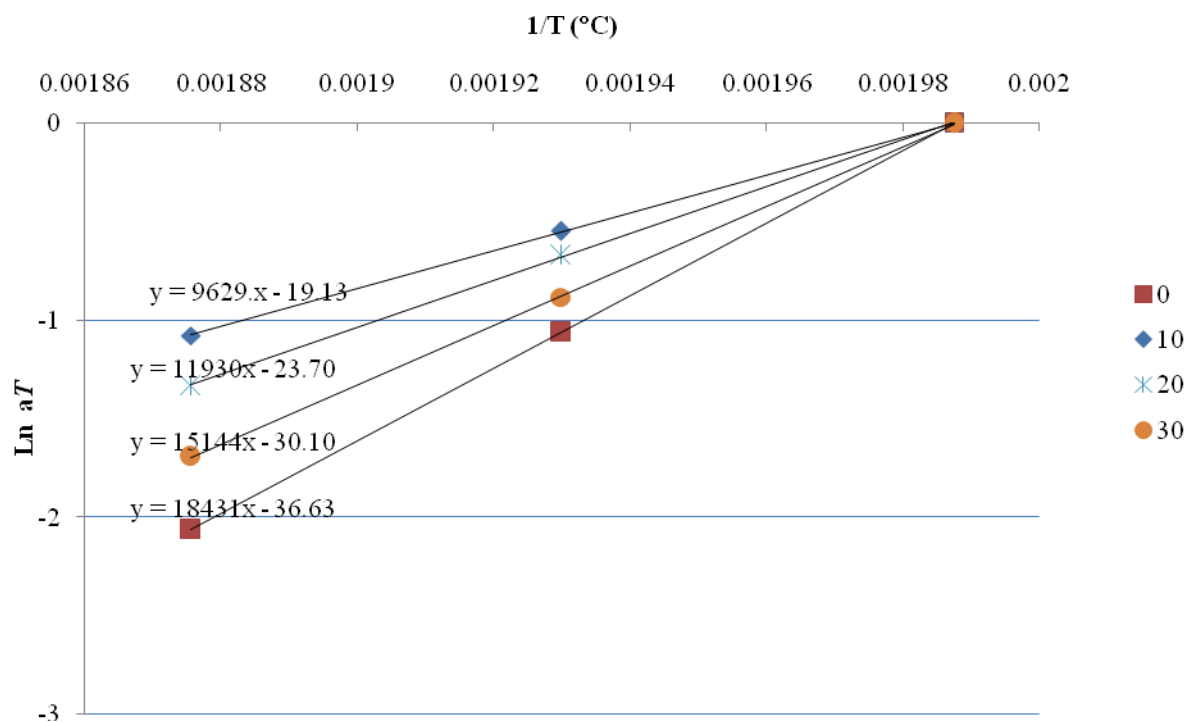


Figure 4.66 : Effect of temperature on shift factor, a_T for 60/40 PA6/ABS Composites

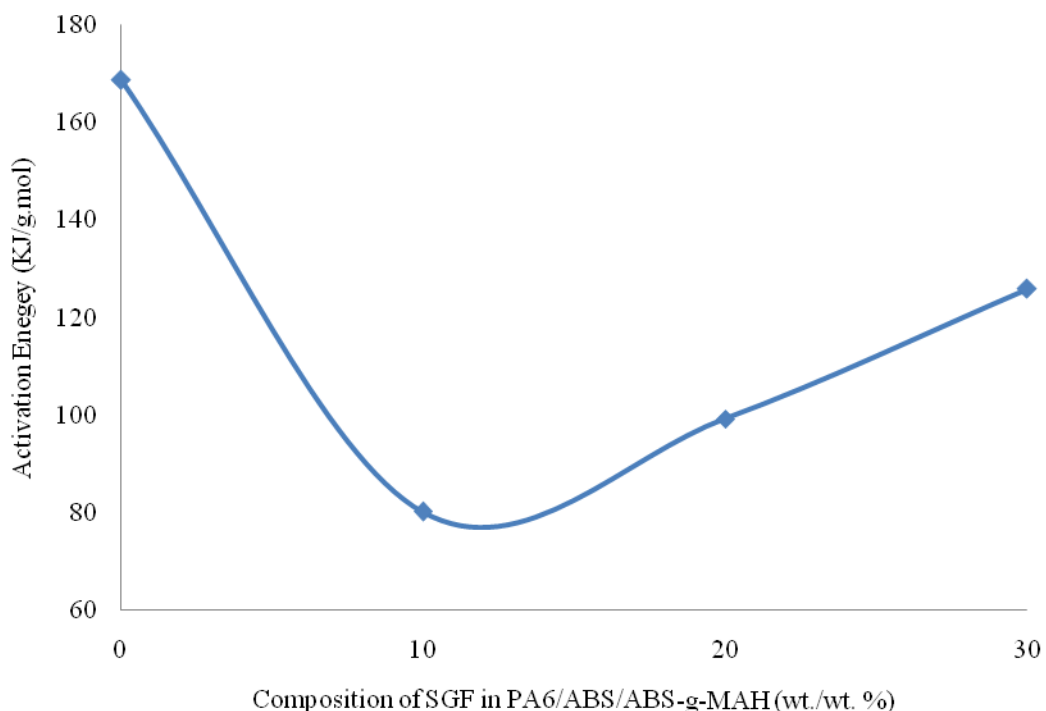


Figure 4.67 : Effect of activation energy for 60/40 PA6/ABS composites with different composition of SGF

4.4.5 Capillary Rheological Properties of 60/40 PA6/ABS Composites

4.4.5.1 Shear Stress Analysis

The graph of shear stress versus shear rate for 60/40 PA6/ABS composites covering at different SGF composition at 230 °C was plotted and shown in Figure 4.68. A typical result of pseudoplastics behaviour of PA6/ABS composite is shown in the figure. At lower shear rate, the incorporation of SGF followed the ‘rule of mixing’ where, the shear stress increased with increase of SGF concentration. However, at higher shear rate and the incorporation of SGF reduced the shear stress of the composites. This could be due to; SGF increased the volume fraction of the matrix and create more free space for matrix to flow and the SGF inclusions can

move in the matrix to produce the 'bearing effect', resulting in reduction of shear stress.

Generally, for the entire composites studied, it can be seen that the curves apparently deviated from linear relationship inclining to the axis of shear rate, showing a typical pseudoplastics fluids. When shear rate is fixed, shear stress increased with the increase of SGF concentration. With greater proportion of reinforcement, the inhibition of polymer chain motion by the SGF particles was increased, and flow resistance increased correspondingly, leading to the increase of shear stress.

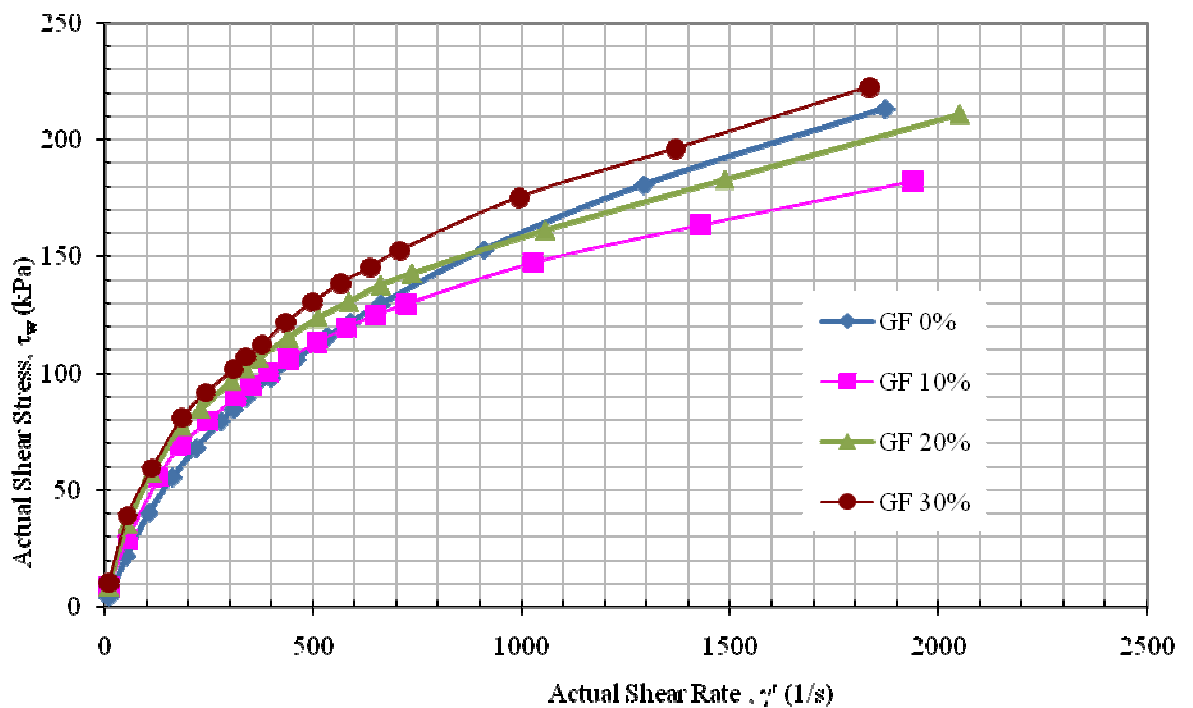


Figure 4.68 : Effects of short glass fibre on the composite shear stress of the PA6/ABS blends

4.4.5.2 Shear Viscosities Analysis

The shear viscosity curves obtained for the composites with varying content of SGF as a function of shear rate are shown in Figure 4.67. The curves show a

significant drop in viscosity with increasing of shear rate beyond 100s^{-1} indicating a pseudoplastic behaviour of the composite. It could be due to with increasing shear rate may arise from the molecular alignment during flow through the capillary. Rheological study of short PA6 fibre reinforced styrene-butadiene rubber by Seema and Kutty (2005) also found a similar observation in which PA6 fibre while restricted the free flow of the composite melt; also get aligned in the direction of flow.

It can also be seen from the figure that, at a fixed shear rate, the viscosity increased with SGF, where 30 wt. % produced the highest among the composites. These results followed the 'rule of mixing', where the highest SGF concentration produces the highest viscosity. The present of fibre restricted the molecular mobility under shear resulted a shift to higher viscosity. According to Prasantha Kumar *et al.* (2000) the increase in viscosity of the composites with increasing fibre concentration is due to the interaction between fibre–fibre and fibre–matrix. However, further increase in fibre concentration resulted in not much increase in shear viscosity at high shear rate as compared to low shear rate. Barnes *et al.* (1989) have commented that the shear viscosity value will increase at Newtonian plateau region by increasing the SGF content. This means that the effect of fibre on shear viscosity is prominent at lower shear rates. It can be seen that the different in shear viscosity between reinforced composites with unreinforced composites became bigger and bigger with increasing amount of SGF. This observation is in agreement with earlier study of short PA6 fibre reinforced styrene-butadiene rubber (Seema and Kutty, 2005; Kutty *et al.*, 1991) and concluded that high concentration of SGF resulting in fibre-fibre and fibre-matrix interactions.

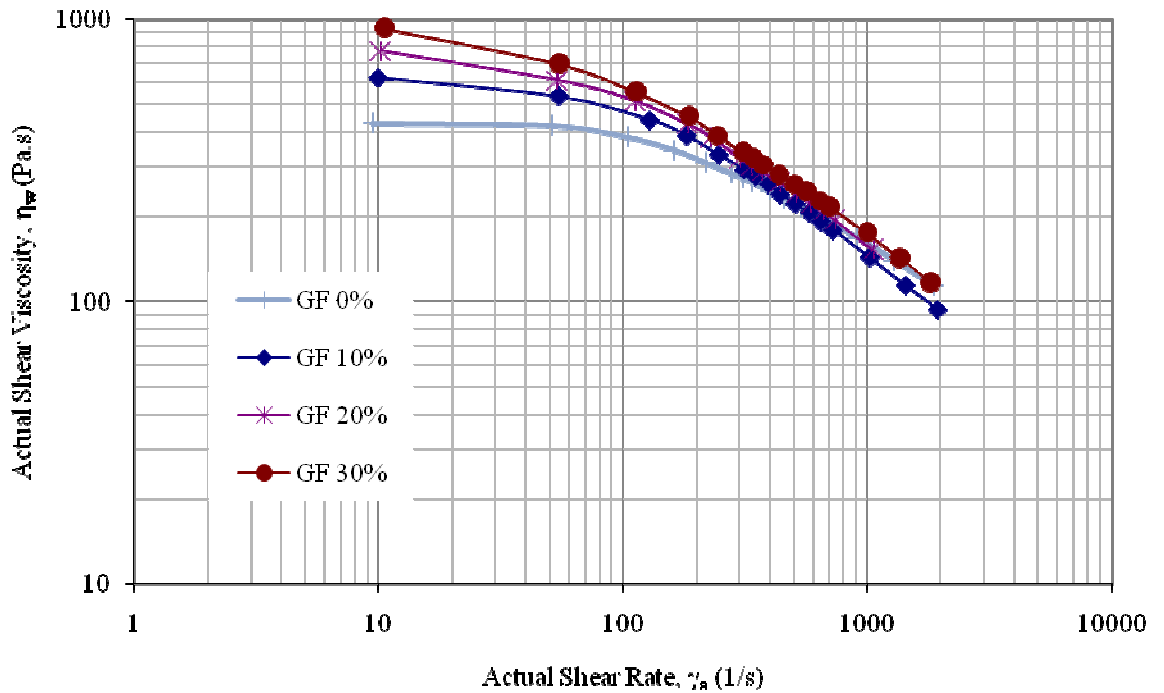


Figure 4.69 : Effects of short glass fibre on the composite shear viscosity of the PA6/ABS blends

4.4.5.3 Power Law Index Analysis

The values of flow behaviour index and consistency index as a function of fibre content at 230°C is given in Figure 4.70. Non-Newtonian pseudoplastic materials have n values less than unity. In the case of SGF reinforced PA6/ABS composites, the n values were found to be less than unity indicating that the pseudoplastic nature of the system. Without SGF, n value is high, indicates that compatibiliser works effectively to enhance the interfacial adhesion and resulted low pseudoplastics behaviour. As the fibre concentration was introduced to 20 wt. %, the values of n drastically decreased indicating more pseudoplastic nature for the composites. This increased in pseudoplasticity is due to the orientation of the fibres. However, the n value increased from 0.33 to 0.45 with further increasing of SGF concentration from 20 wt. % to 30 wt. % in PA6/ABS composites. This indicates the reduction of pseudo-plastics behaviour. It could be because, at higher concentration of SGF the entanglement has occurred and the free volume in the composite was

increased and provide more space for PA6 and ABS phase free to flow. Consequently, the viscosity of the composites increased with further increasing the SGF composition. From the figure, it can be concluded that, the optimum concentration of SGF is about 20 wt. % where the power law index was minimum and consistency index was maximum. At this point, it is believed that the composite has a good interaction between fibre and matrix as well as a good compatibility indicating higher pseudoplastic behaviour as compared to the rest of the composite studied.

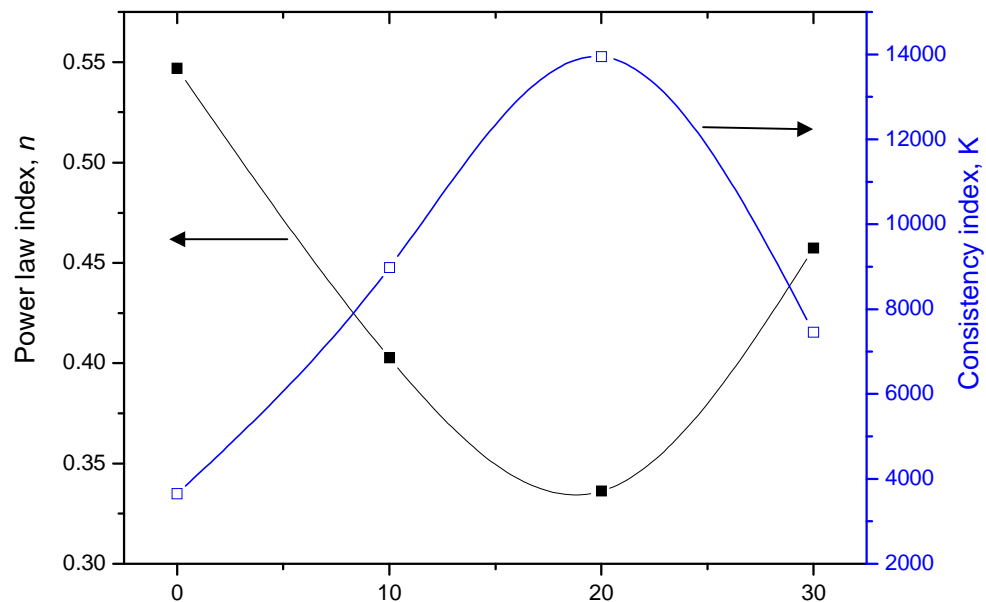


Figure 4.70 : Power law index, n and consistency index, K for 60/40 PA6/ABS composites with various amount of short glass fibre at 230 °C

4.5 Fourier Transform Infra-Red (FTIR) Analysis

The FTIR analysis of virgin PA6, virgin ABS-g-MAH and 3 wt. % compatibiliser in 60/40 PA6/ABS blends were carried out to identify the occurrence of the reaction between compatibiliser and PA6. As seen in Figure 4.68, the broad of the peak at 3306.43 cm^{-1} corresponded to the N-H (amine end group of PA6) stretch in PA6 and was not appeared at ABS-g-MAH, whereas the peak at 1071.81 cm^{-1} corresponds to the aromatic C-O (maleic anhydride) stretch in ABS-g-MAH appeared in the spectrum of virgin PA6, and both peaks will dependent on the reaction. However, at the spectrum of 60/40 PA6/ABS blend compatibilised by 3 wt. % of ABS-g-MAH, both peaks, N-H and C-O stretches were appeared at 3306.70 and 1076.47 cm^{-1} , respectively. It is clearly shown, that the size of the both peaks decreased significantly. This is in agreement with suggested possible reactions between PA6 and maleic anhydride that could be occurred during melt blending of PA6/ABS blends as summarised in the Figure 4.1. This suggests that the reaction occurred between amine end-group and maleic anhydride to form a 'bridge' between PA6 phase and ABS phase. This analysis in an agreement with the idea was reported by Kudva *et al.* (2000). The appearance of the C-O peak at compatibilised blends (3 wt. % ABS-g-MAH in PA6/ABS blend) spectrum has suggested that only a certain composition of maleic anhydride has been reacted with amine end group of PA6. This indicates that the remaining of maleic anhydride in PA6/ABS acted as fillers and affects the properties of either the blends or composites. This idea is supported by FTIR spectrum as shown in Figure 4.72, which is the C-O peak disappeared when the amount of compatibiliser was about 1 wt. %, indicates all the ABS-g-MAH fully reacted with amine end group of PA6.

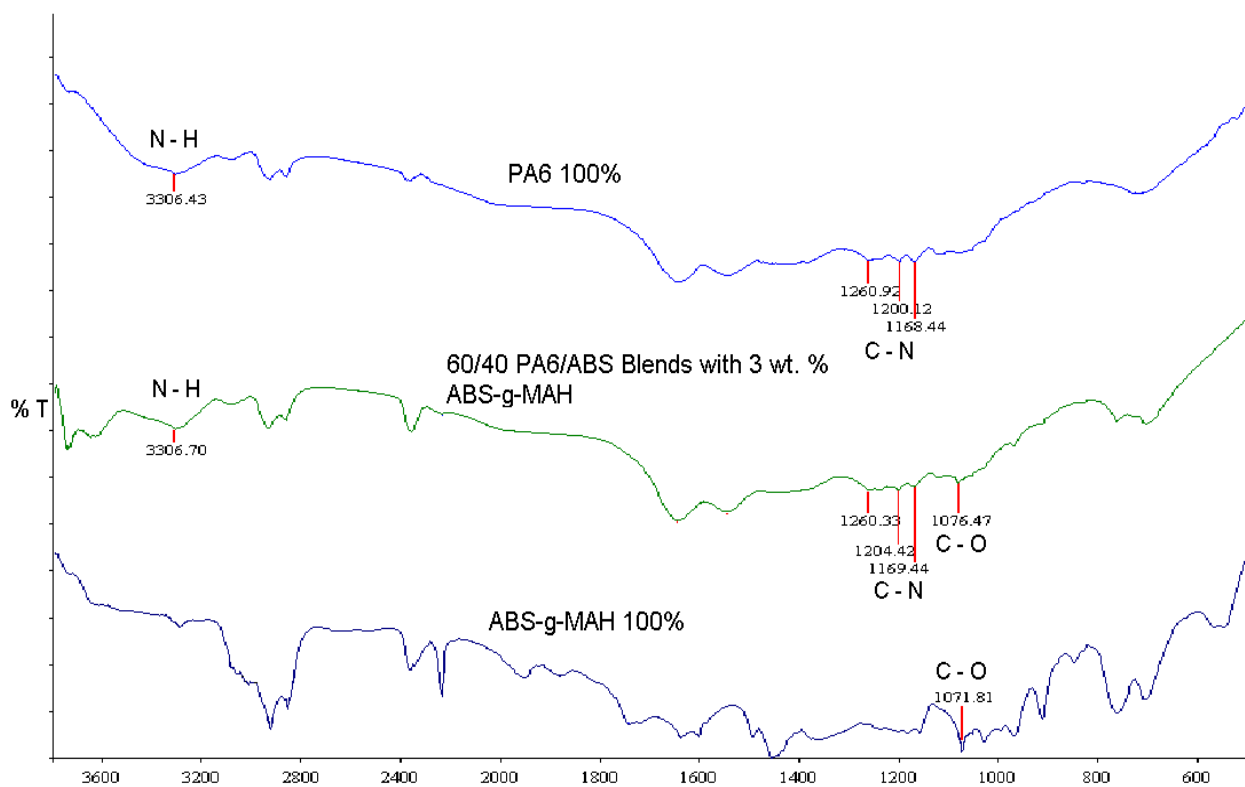


Figure 4.71 : FTIR spectra of (a) virgin of PA6, (b) 60/40 PA6/ABS blend compatibilised by 3 wt. % of ABS-g-MAH and (c) virgin of ABS-g-MAH

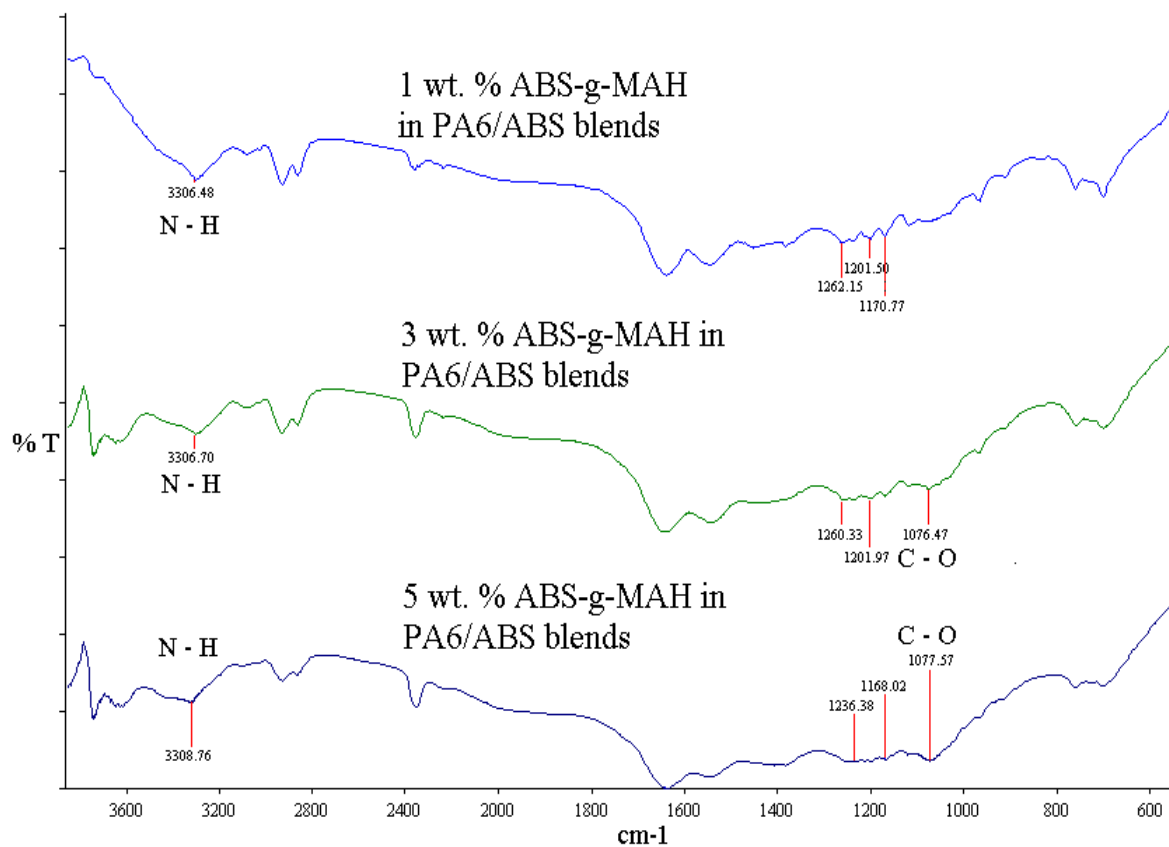


Figure 4.72 : FTIR spectra of (a) 1 wt. % (b) 3 wt. % and (c) 5 wt. % of ABS-g-MAH in PA6/ABS blends

4.6 SEM Micrograph Analysis

SEM micrograph is the most convenient approach to differentiate the morphologies between compatibilised and uncompatibilised blends. In general, the morphology can be improved by the addition of compatibiliser (Kudva *et al.*, 1998). The morphology of fractured samples of PA6/ABS blends by liquid nitrogen were investigated in the entire of composition and shown in Figures 4.73, 4.74 and 4.75. In the case of PA6/ABS blends there exists a clear distinction between the PA6 matrix and ABS phase. Micrographs show the dispersed phase was an ABS phase while the matrix was the PA6 phase. This phenomenon occurred to be due to PA6 had less viscosity than ABS during sample preparation (Kudva *et al.*, 2000a; Chang *et al.*, 1994; Liu *et al.*, 2001), and this fact was supported by rheological analysis as discussed in Section 4.4.1.

It is clear shown that in the absence of compatibiliser, interface adhesion was very poor where the gap between the dispersed phased and the matrix was bigger (see Figures 4.73 (a), 4.74 (a) and 4.75 (a)). It can be observed that the size of dispersed phase was appreciably affected by the addition of MAH. These analyses are in agreement with the previous studies (Lacasse and Davis, 1999; Kudva *et al.*, 1999; Ozkoc *et al.*, 2006). This indicates that ABS-g-MAH has decreased the interfacial tension between PA6/ABS phases and aided in finer dispersion of ABS in the PA6 matrix. This was resulted the enhancement of the interfacial adhesion thus the mechanical and other properties also improved. This phenomenon was clearly observed at the addition of compatibiliser at 1 wt. % into PA6/ABS blends. Generally, further increment of ABS-g-MAH reduced the particles size to be more uniform and fine spherical.

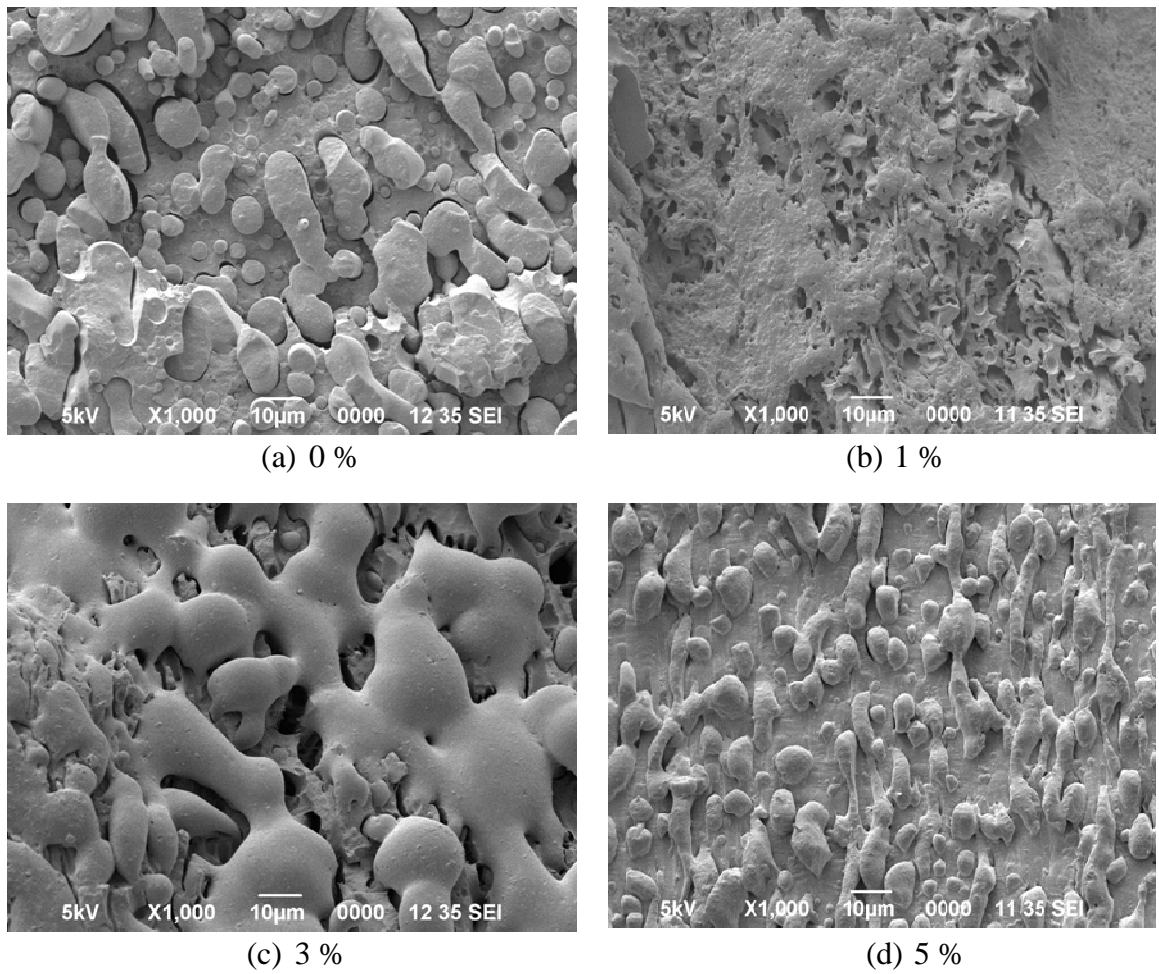


Figure 4.73 : SEM photographs of fractured of 50/50 PA6/ABS blends at various amount of ABS-g-MAH (a) 0 wt. %, (b) 1 wt. %, (c) 3 wt. % and (d) 5 wt. %

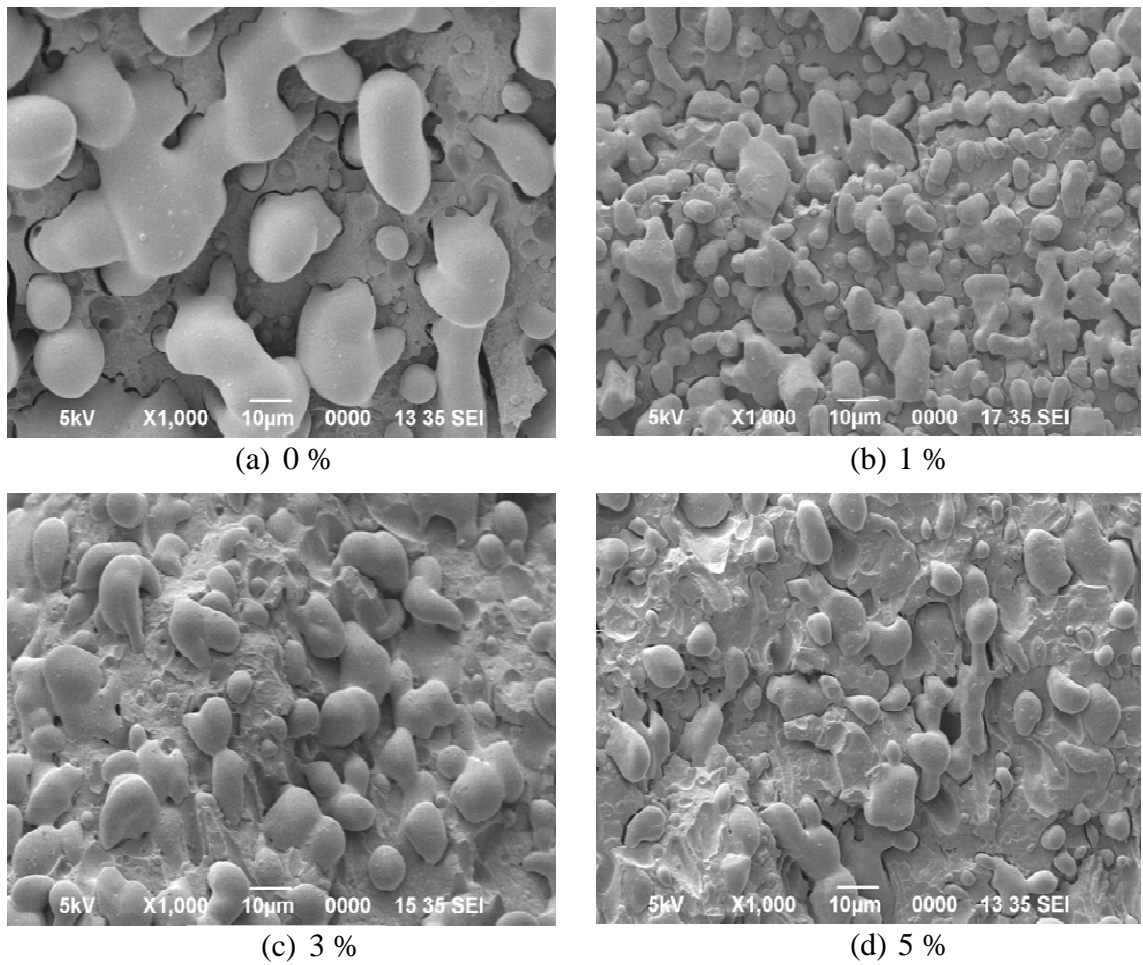


Figure 4.74 : SEM photographs of fractured of 60/40 PA6/ABS blends at various amount of ABS-g-MAH (a) 0 wt. %, (b) 1 wt. %, (c) 3 wt. % and (d) 5 wt. %

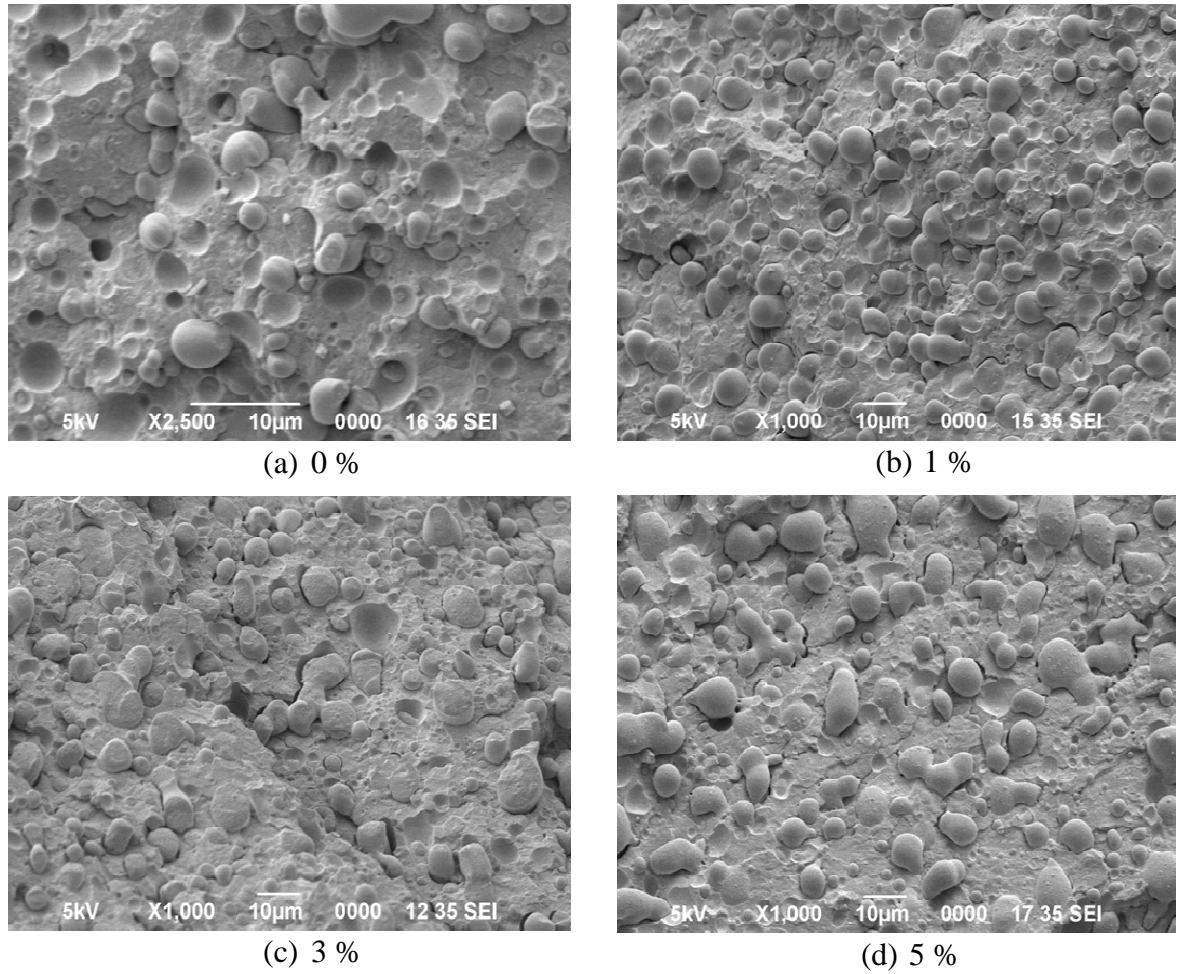


Figure 4.75 : SEM photographs of fractured of 70/30 PA6/ABS blends at various amount of ABS-g-MAH (a) 0 wt. %, (b) 1 wt. %, (c) 3 wt. % and (d) 5 wt. %

CHAPTER 5

CONCLUSION AND RECOMMENDATION

5.1. Conclusion

The mechanical of PA6/ABS blends and short glass fibre reinforced PA6/ABS composites were systematically investigated. Addition of ABS-g-MAH as compatibiliser in the PA6/ABS blends showed that the blends became compatible. It was found that the tensile modulus and strength of PA6/ABS blends increased with increasing in compatibiliser content. The present of ABS-g-MAH in the blends system enhanced the interfacial adhesion between PA6 and ABS phases. The maximum tensile modulus and strength were found at 1 wt. % of ABS-g-MAH concentration. This could be due to enough amount of ABS-g-MAH reacted with amine end group of PA6. Further increase in ABS-g-MAH content reduced the tensile modulus and strength and considerably achieved a constant value beyond concentration at about 3 wt. %.

The elongation at break of the PA6/ABS was improved by the addition of ABS-g-MAH at all composition studied. Flexural modulus and strength exhibited different trend as compared to tensile modulus and strength, achieved maximum value at ABS-g-MAH content was about 3 wt. %. Beyond this point, reduction in flexural modulus and strength occurred could be due to repulsion of polar segment of PA6 and acrylonitrile segment in ABS and excess able amount of ABS-g-MAH acted as filler. Impact strength showed a similar patent as compared to elongation at break. This indicates ABS-g-MAH enhanced the interfacial adhesion and improves the compatibility of the blends. However, the incorporation of short glass fibre to the 60/40 PA6/ABS blends with a 3 wt. % compatibiliser has not significantly improved the impact strength, but exponentially enhanced the tensile modulus and strength and linearly improved the flexural properties. Generally, the addition of SGF reduced the toughness even though the stiffness increased exponentially.

The thermal properties of PA6/ABS blends decreased with the increase of ABS-g-MAH concentration. The introduction of compatibiliser has also affected the degree of crystallisation the PA6/ABS blends. It was found that 1 wt. % was showed the highest degree of crystallisation of PA6/ABS blends and considered as the optimum ratio for compatibilisation of all PA6/ABS blends. The introduction of SGF into 60/40 PA6/ABS composites reduced the thermal properties especially degree of crystallisation. The glass transition temperature, T_g and the heat of melting decreased significantly with the addition of SGF to the matrix. This indicates that, the SGF tends to agglomerate within their phase due to short in length that form multiphase in the composite system.

From the results of the dynamic mechanical properties of 50/50, 60/40 and 70/30 PA6/ABS blends, generally, the DMA properties especially storage modulus were increased by the addition of compatibiliser at low temperature (before transition region) and showed no improvement at high temperature (after transition region).

Specifically, for 60/40 PA6/ABS blends, it was found that the maximum dynamic mechanical properties was achieved at the concentration of compatibiliser at about 1 wt. % as compared to 50/50 and 70/30 PA6/ABS blends at about 5 wt. % of compatibiliser. The increased in dynamic mechanical properties suggested that the PA6 and ABS chain motion were restricted by the formation of graft copolymer within the phases. The reaction has been confirmed by FTIR analysis. The introduction of short glass fibre in 60/40 PA6/ABS increased the storage and loss modulus of the composites. In other word, the present of SGF in PA6/ABS composites increased the elasticity of the system, but resulted poor interfacial bonding with further increase in SGF concentration. From DMA results, 20 wt. % of SGF concentration is considered as optimum composition of SGF for 60/40 PA6/ABS composites.

In this research, detailed rheological analysis of PA6/ABS blends and composites were performed on oscillatory and capillary rheometer. For the oscillatory rheometer, the effects of compatibiliser concentration, frequency, and temperature on rheological properties were studied. The 50/50 PA6/ABS blends exhibited relatively strong frequency-rheology or big frequency-dependence compared to that of 60/40 and 70/30 PA6/ABS blends. In general, all the polymer blends showed a typical behaviour, exhibiting a shear-thinning regime at all frequencies studied. It showed that at a fixed frequency, the complex viscosity increased with the amount of compatibiliser. This indicates that, compatibiliser reduced the interfacial tension and enhanced the interfacial adhesion between the domains phase and matrix phase. However, the viscoelastic behaviour in dynamic mechanical properties of PA6/ABS blends, strongly dependent on the rubber phase of ABS and compatibiliser and grafting reaction of compatibiliser with amine end group of PA6. The incorporation of SGF enhanced dynamic rheological properties of the composites. The complex viscosity, storage and loss modulus increased with increase in SGF concentration. From the dynamic rheological $\tan \delta$ point of view; it can be observed the $\tan \delta$ decreased drastically when 10 wt. % of SGF was introduced into the composite. Moreover, it can be observed that 20 and 30 wt. % of SGF considerably have a similar effect of $\tan \delta$ at all frequency

studied. Generally, the incorporation of SGF improved the damping and elasticity of PA6/ABS composites.

The activation energy of flow, E_a is the energy that needs to be consumed for breaking up the interactions among the chain segments when the melts flow. It reflects the dependence of melt viscosity on temperature. At 50/50 and 60/40 PA6/ABS blends, adding 1 wt. % of compatibiliser decreased the activation energy of flow. However, at 70/30 PA6/ABS blends the addition of 3 wt. % of compatibiliser showed the lowest of activation energy of flow as compared 60/40 and 50/50 PA6/ABS blends. The lower is the flow activation energy means that the material behaves more elastic and more energy is needed to break the interactions and allow the material to flow. At 10 wt. % concentration of SGF in the composite reduced the sensitivity of the composite, as a result, reduced the compatibility of the system. However, the sensitivity of the composites to temperature increased with further increasing of SGF indicates the compatibility of SGF with PA6/ABS matrix was restored.

From capillary rheological point of view, all the blends showed a pseudoplastics behaviour. At low shear rate, the addition of compatibiliser did not change the shear stress of all the PA6/ABS blends. It could be due to small amount of compatibiliser attributed less to the change of shear stress. However the effect of compatibiliser on the shear stress was more obvious at higher shear rate, specifically for 60/40 and 70/30 PA6/ABS blends. It shows that the shear viscosity of all the blends decreased with increasing shear rate showing a typical property of pseudo-plastics non-Newtonian or shear-thinning plastics. The decrease in shear viscosity can be attributed to the alignment of chain segments of PA6/ABS blends in the direction of applied stress. At lower shear rate, it closed to zero shear and can be predicted as Newtonian molten flow.

It was found that for 60/40 PA6/ABS composites, the curves of shear stress versus shear rate apparently deviated from linear relationship inclining to the axis of shear rate, showing typical pseudoplastics fluids. When shear rate was fixed, shear stress increased with increasing of SGF concentration. With greater proportion of reinforcement, the inhibition of polymer chain motion by the SGF particles was increased, and flow resistance increased correspondingly, leading to the increase of shear stress. The results show a significant drop in viscosity with increasing of shear rate beyond 100s^{-1} indicating a pseudoplastic behaviour of the composite. The power law index, n values were found to be less than unity indicating that the pseudoplastic nature of the composite system. Without SGF, n value was high, indicates that compatibiliser works effectively to enhance the interfacial adhesion and resulted in low pseudoplastics behaviour. As the fibre concentration was introduced to 20 wt. %, the values of n drastically decreased indicating more pseudoplastic nature for the composites and concluded that, the optimum concentration of SGF was about 20 wt. %.

In order to confirm the reaction between maleic anhydride of ABS-g-MAH amide end group for PA6, FTIR analysis was carried out. The FTIR analysis confirmed that the reaction took place during melt intercalation process. FTIR analysis suggested that only a certain composition of maleic anhydride has been reacted with amine end group of PA6. This indicates that the remaining of maleic anhydride in PA6/ABS acted as fillers and affects the properties of either the blends or composites.

5.2. Recommendation for Future Work

Based on the experience gained during this study, the following recommendations for future work can be made.

- i. Extend the investigation of the rheological behaviour of PA6/ABS blends and composites using spiral mould method. This method is close to the actual processing situation; where the flow behaviour of the blends and composite can be evaluated directly from the spiral mould data. Also, using the spiral mould data, we can easily predict the flow behaviour of the material using the injection moulding.
- ii. Extend the knowledge of dynamic mechanical analysis and rheology of the PA6/ABS blends to ternary blends and blends formulation containing different type of filler loading.
- iii. Improve understanding of the dynamic mechanical properties of PA6/ABS composite with the study below ambient temperature and different frequency in order to understand the behaviour of the composite during application in cold environment. Run the testing using a temperature sweep instead of frequency sweeps in order to evaluate the dynamic mechanical properties under different degree of vibration. This information can be used to understand more the behaviour of the composite in different conditions.

REFERENCES

- Acierno, S. and Puyvelde P.V. (2004). Rheological Bheviour of Polyamide 11 with Varying Initial Moisture Content. *Journal of Applied Polymer Science*. 97 : 666 - 670
- Ahn, Y.C. and Paul. D.R. (2006). Rubber Toughening of Nylon 6 Nanocomposites. *Polymer*. 47 (8) : 2830–2838.
- Akay, M., and O’regan. D.F. (1995). Fracture behaviour of glass fibre reinforced polyamide mouldings. *Polymer Testing*. 14 : 149–162.
- Amano, O. and Ainoya, K. (2000) Pressure dependent viscosity of polymer melts, Antec’00 Conference Proceeding, page 89
- Aoki, and Watanabe (1992). Morphological, thermal, and rheological properties of nylon/acrylonitrile-butadiene-styrene alloys. *Polymer Engineering and Science* 32(13): 878 – 885.
- Aoki, Y. (1986). Dynamic Viscoelastic Properties of ABS Polymers in the Molten State : Effect of Grafting Degree. *Macromolecules* 20 : 2208 – 2213
- Araujo, E. M., Hage E. Jr. and Carvalho A. J. F (2003). Morphological, Mechanical and Rheological properties of Nylon 6/Acrylonitrile-Butadiene-Styrene Blends Compatibilized with MMA/MA copolymers. *Journal of Material Science*. 38 (17): 3515 – 3520
- Araujo, E. M., Hage E. Jr. and Carvalho A.J.F. (2004). Thermal Properties of Nylon 6/ABS Polymer Blends: Compatibilizer Effect. *Journal of Material Science*. 39 : 1173 – 1178.
- Araujo, E. M., Hage Jr. E. and Carvalho A. J. F. (2003). Acrylonitrile–Butadiene–Styrene Toughened Nylon 6: The Influences of Compatibilizer on Morphology and Impact Properties. *Journal of Applied Polymer Science*. 87 : 842 – 847.

- Araujo, E.M., Hage E. Jr. and Carvalho A.J.F. (2005). Morphological, mechanical and Thermal Properties of Nylon 6/ABS using Glycidyl Methacrylate-Methyl Methacrylate Copolymers. *Journal of Material Science*. 40 : 4239 – 4246.
- Aroon, V. and Shenoy (1999). *Rheology of Filled Polymer System*. page 39. Kluwer London, Academic Publishers
- Bader, M. G. (2001). Polymer composites in 2000: structure, performance, cost and compromise. *Journal of Microscopy*. 201 (2) : 110–121.
- Bader, M. G. and Collins J. F. (1983). The effect of fibre-interface and processing variables on the mechanical properties of glass-fibre filled nylon 6. *Fiber Science and Technology*. 18 (3):217 – 231.
- Bandrup, J. and Immergut, E. H. (1989) *Polymer Handbook 2nd Ed.* John Wiley & Sons, New York
- Barnes, H. A., Hutton, J. F. and Walters, K, (1989) *Rheology Series Volume 3: An Introduction to Rheology*. New York, Elsevier.
- Barnes, H. A., Hutton, J.F., and Walters, K. (1989). *An Introduction to Rheology*. B.V Amsterdam, Elsevier Science Publishers.
- Bertin, M. P., Marin, G. and Montfort, J. P. (1995) Viscoelastic properties of acrylonitrile-butadiene-styrene (ABS) polymers in the Molten State. *Polymer Engineering and Science* 35(17): 1394
- Bhardwaj, L S., Vijai Kumar., Mathur A. B. and Anil, Das. (1990). Characterization of multiphase polymer system Nylon6/ABS blends. *Journal of Thermal Analysis*. 36 : 2339 – 2347
- Bikiaris, D., Matzinos, P., Prinos, J., Flaris V., Larena, A. and Panayiotou, C. (2001). Use of silanes and copolymers as adhesion promoters in glass fiber/polyethylene composites. *Journal of Applied Polymer Science*. 80: 2877 – 2888
- Biolzi, L., Castellani, L., and Pittacco I. (1994). On the mechanical response of short fibre reinforced polymer composites. *Journal Material Science*. 29(9): 2507 - 2512
- Borgaonkar, H. M. (1998). *Processing and Rheology in Thermoplastics and Themoplastics Composite*. PhD Thesis. Purdue University.
- Braun, B. B. and Rosen M. R. (2000). *Rheology Modifiers Handbook : Practical Use and Application*. page: 12, Norwich, New York: William Andrew Publishing

- Brostow, W. and Corneliussen R., Eds. (1986), *Failure of Plastics*, New York, Hanser Publications
- Brydson, J. A. (1999). *Plastics Materials. 7th Edition*. Oxford. Butterworth Heinemann.
- Carone. E. Jr., Kopcak U., Goncalves, M. C. and Nunes S. P. (2000) In-situ compatibilization of Polyamide 6/Natural Rubber Blends with Maleic Anhydride, *Polymer*, 41: 5929 – 5935
- Chang, H. –H.; Wu, J. –S and Chang, F. –C. (1994). Reactive compatibilisation of ABS/Nylon 6,6 blends: Effects of reactive group concentration and blending sequence. *Journal of Polymer Research*. 1(3), 235 - 245
- Chen, H. L and Porter R. S. (1993). Melting behavior of poly(ether ether ketone) in its blends with poly(ether imide). *Journal Polymer Science Part B: Polymer Physics*, 31(12):1845 - 1850
- Cheng, F., Li H., Jiang W. and Chen D. (2006). Properties of compatibilized Nylon6/ABS polymer blends. *Journal of Macromolecular Science Part B : Physics*. 45(4): 557 – 561
- Chiu, H. T. and Hsiao, Y. K. (2004) Studies on Impact-Modified Nylon 6/ABS Blends. *Polymer Engineering and Science*. 44(12): 2340 – 2345
- Cho, J. W. and Paul, D.R. (2001). Glass Fiber-Reinforced Polyamide Composites Toughened with ABS and EPR-g-MA. *Journal of Applied Polymer Science*. 80: 484 – 497.
- Chopra, D. (2002). *Thermodynamics and Rheological of Partially Miscible Polymer Blends*. PhD Thesis. The University of British Columbia.
- Clavera, I., Javierre, C. and Ponz, L. (2005) Method for generation of rheological model to characterize non-conventional injection moulding by means of spiral mold. *Journal of Materials Processing Technology*. 162 – 163: 477 – 483.
- Cogswell, F. N. (1981). *Polymer Melt rheology: A Guide for Industrial Practice*. London. George Godwin Limited.
- Crawford, R. J. (1990). *Plastics Engineering 2nd Edition*. Oxford: Pergamon Press.
- Davendra, R. and Hatzikiraikos S. G. (2006) Rheology of metallocene polyethylene-based nanocomposites : influence of graft modification. *Journal of Rheology* 50(4) : 415 – 434.
- Dealy, J. M. and Wissbrun, K. F. (1990). *Melt Rheology and Its Role in Plastics Processing*. New York: Van Nostrand Reinhold.

- De-Mario, V. and Dong, D. (1997) Proceeding of Society of Plastics Engineering Annual Technical Conference. 43 : 1512
- Dobkowski, Z. (1986). Application of melt flow index for rheological characterization of branched and linear polymer. *Rheologica Acta*. 25: 195 – 198.
- Doi, M. and Ohta, T. (1991). Dynamics and Rheology of Complex Interfaces . *Journal Chemical Physics*. 95: 1242 - 1248
- Dong, S. and Gauvin R. (1993). Application of dynamic mechanical analysis for the study of the interfacial region in carbon fiber/epoxy composite materials. *Polymer Composites*. 14(5): 414 – 420
- Dreval, V.E., Vasil'ev G. B., Borisenkova E. K. and Kulichikin V. G. (2006) Rheological and Mechanical properties of ABS prepared by bulk polymerization. *Polymer Science* 46(3): 338 – 345
- Dweiri, R. and Azhari, C. H. (2004). Thermal and Flow Property-Morphology Relationship of Sugarcane Bagase Fiber-Filled Polyamide 6 Blends. *Journal of Applied Polymer Science*. 92 : 3744 – 3754
- Fayt, R., Jérôme, R., and Teyssié, Ph. (1982). Molecular design of multicomponent polymer systems. III. Comparative behavior of pure and tapered block copolymers in emulsification of blends of low-density polyethylene and polystyrene. *Journal Polymer Science: Polymer Physics Edition*. 20(12): 2209 - 2217
- Ferry, J. D. (1970). *Viscoelastic Properties of Polymers*. 2nd edition. New York. Wiley and Son,
- Fox, C. W., Poslinski, A. J. and Kazmer, D. O. (2003). Correlation of Spiral Mold and Radial Flow Lengths for Injection Molded Thermoplastics Parts. ANTEC. SPE
- Frenzel, H., Bunzel, U., Hassler, R. and Pompe, G. (2000). Influence of different glass fiber sizings on selected mechanical properties of PET/glass composites. *Journal of Adhesion Science and Technology*. 14(5) : 651 – 660
- Fu, S. Y. and Lauke, B. (1998). Fracture resistance of unfilled and calcite-particle-filled ABS composites reinforced by short glass fibers (SGF) under impact load. *Composite Part A*, 29 (6): 631 - 645
- Fu, S.-Y., Lauke B. and San, A., (1996) Effect of fiber length and fiber orientation distributions on the tensile strength of short fiber reinforced polymers. *Composite Science Technology*. 56 : 1179–1190.

- Fu, S-Y., Lauke B., Li R. K. Y. and Mai Y-W. (2006) Effects of PA6,6/PP ratio on the mechanical properties of short glass fiber reinforced and rubber-toughened polyamide 6,6/polypropylene blends. *Composites: Part B*. 37 : 182 – 190.
- Fu, S. Y., Lauke, B., Mader, E., Yue, C.Y. and Hu, X. (2000). Tensile properties of short-glass-fiber- and short-carbon-fiber-reinforced polypropylene composites. *Composite Part A*. 31(10) : 1117 – 1125.
- Gao, G., Wang, J., Yin, J., Yu, X., Ma, R., Tang, X., Yin, Z. and Zhang, X. (1999). Rheological, Thermal and Morphological Properties of ABS-PA1010 Blends. *Journal of Applied Polymer Science*. 72 : 683 – 688.
- George, J., Joseph, R., Thomas, S. and Varughese, K. T. (1995). High density polyethylene/acrylonitrile butadiene rubber blends: Morphology, mechanical properties, and compatibilization. *Journal of Applied Polymer Science*. 57(4), 449 – 465.
- Giusti, L., Hage, Jr. E., Ito, E. N. and Ueki, M. M. (2003) Morphological and mechanical properties of PA6/ABS blends compatibilized with functionalized acrylic copolymer. *Acta Microscopica*, Volume 12, Supplement C, September 2003 XIX Congress of the Brazilian Society for Microscopy and Microanalysis.
- Gnatowski, A. and Koszkul, J. (2006) Investigation on PA/PP mixture properties by means of DMTA method. *Journal of Materials Processing Technology* 175: 212 – 217
- Gribben, F., McNally G. M., Murphy W. R. and Clarke A. H. (2005) The effect of compatibilisation of the rheology of polyamide blends. *Antec 2005* : 2395 – 2399
- Guo, A., Zdemir, A. O. and Zdemir, E. O. (2006) Experimental investigation of the effect of glass fibres on the mechanical properties of polypropylene (PP) and polyamide 6 (PA6) plastics. *Material Design*. 27 : 316 – 323.
- Guerrica-Echevarria, G., Eguiazabal, J. I. and Nazabal, J. (2001) Influence of the preparation method on the mechanical properties of a thermoplastic liquid crystalline copolyester. *Polymer Testing*. 20 : 403–408.
- Gupta, A. K., Gupta, V. B., Peters, R. H., Harland, R. G. and Berry, J. P. (1982). The effect of addition of high density polyethylene on the crystallization and mechanical properties of polypropylene and glass-fiber-reinforced polypropylene. *Journal of Applied Polymer Science*. 27(12) : 4669 - 4686

- Guschl, P. C. and Otaigbe, J. U. (2003) An Experimental Study of Morphology and Rheology of Ternary P-glass-PS-LDPE hybrids. *Polymer Engineering and Science* 43 (6) : 1180 – 1196
- Guschl, P. C., Kim, H. S. and Otaigbe, J. U. (2002). Effects of a Nd - Fe - B magnetic filler on the crystallization of poly(phenylene sulfide). *Journal of Applied Polymer Science*, 83(5) : 1091 - 1102
- Hage, E. Jr. Ferreira L. A. S., Manrich S. and Pessan L. A. (1999). Crystallization behavior of PBT/ABS polymer blends. *Journal of Applied Polymer Science*. 71(3) : 423 – 430
- Hamada, H., Fujihara, K. and Harada, A. (2000). The influence of Sizing Condition on Bending Properties of Continuous Glass Fiber Reinforced Polypropylene Composites. *Composites : Part A*, 31 : 979 – 900.
- Han C. D and Chuang H. K (1985). Criteria for rheological compatibility of polymer blends. *Journal of Applied Polymer Science*. 30(11), 4431 - 4454
- Han C. D and Yang H. H. (1987). Rheological Behavior of Compatible Polymer Blends. I. Blends of Poly(styrene-co-acrylonitrile) and Poly(ϵ -caprolactone). *Journal of Applied Polymer Science*. 33(4): 1199 - 1220
- Han C. D. (1976) *Rheology in Polymer Processing*. Academic Press. New York. Chapter 5
- Han C. D. (1982) *Multiphase Flowing in Polymer Processing*. Academic Press. New York.
- Henry S. and Hsieh. Y. (1982). Composite Rheology – I. Elastomer – Filler Interaction and Its Effect on Viscosity. *Journal of Material Science*. 17: 438 – 446
- Higgins J. S. and Walsh D. J. (1984) Interaction in polymer blends – relationship between thermodynamic and scattering measurements. *Polymer Engineering and Science*. 24 : 555 – 562
- Hong J. H., Sung Y. -T., Song K. H., Kim W. N., K B. I., Kim S. L. and Lee C. H. (2007). Morphology and dynamic mechanical properties of poly(acrylonitrile-butadiene-styrene)/polycarbonate/clay nanocomposites prepared by melt mixing. *Composite Interfaces*. 14(5): 519 - 532
- Howe, D. V. and Wolkowicz, M. D. (1987). Structure-property relationships in polyamide/acrylonitrile-butadiene-styrene (ABS) blends. *Polymer Engineering and Science*. 27(21) : 1582 – 1590.

- Huang, C. C and Chang, F.C (1997b). Reactive compatibilization of polymer blends of polybutylene Terephthalate (PBT)/polyamide-6,6(PA-6,6): 2. Morphological and mechanical properties. *Polymer*. 38 : 4287
- Hussein, I. A., Hameed, T. and Williams, M. C. (2006) Influence of molecular structure on the Rheology and Thermorheology of Metallocene Polyethylenes. *Journal of Applied Polymer Science*, 102 : 1717 – 1728
- Ibarra, L., Macias, M. and Palma, E. (1995). Viscoelastic properties of short carbon fiber thermoplastic (SBS) elastomer composite. *Journal of Applied Polymer Science*. 57 : 831
- Idicula, M., Malhorta, S. K., Joseph, K. and Thomas Sabu. (2005). Dynamic mechanical analysis of randomly oriented intimately mixed short banana/sisal hybrid fibre reinforced polyester composites. *Composites Science and Technology*. 65 : 1077 – 1087
- Jafari, S. H., Potchke, P., Stephan, M., Warth, H., and Alberts H., (2002) Multicomponent blends based on polyamide 6 and styrenic polymers: morphology and melt rheology. *Polymer* 43 : 6985 – 6992
- Jang, S. P and Kim, D. J. (2000). Thermal, mechanical and diffusional properties of Nylon6/ABS polymer blends : compatibilizer effect. *Polymer Engineering and Science*. 40(7) : 1635 – 1642
- Jannasch, P. and Wesslen, B. (1999). Poly(styrene-graft-ethylene oxide) as a compatibilizer in polystyrene/polyamide blends. *Journal of Applied Polymer Science*. 58 : 753 - 758
- Joseph, S., Menon, A. R. R. and Joseph, A. (2007) Melt rheology and extrudate morphology studies of polystyrene/polybutadiene blends in the presence and absence of compatibiliser. *Journal of Material Science*. 42 : 2054 – 2063
- Kamal, M. R. and Kernig, S. (1972a). The Injection Molding of Thermoplastics part I: Theoretical Model. *Polymer Engineering and Science*. 12(4) : 294 - 301.
- Kamal, M. R. and Kernig, S. (1972b). The Injection Molding of Thermoplastics part I: Eksperimental Test of Model. *Polymer Engineering and Science*. 12(4) : 302 - 308.
- Kannan, K and Misra. (1994) A Short glass fiber reinforced PA6 and ABS blends – mechanical properties and morphology. *International Polymer Processing*. 9(2) : 184 – 192.
- Karger-Kocsis, J. (1996) in Salamone, J., ed. *Polymeric Materials Encyclopedia*, Vol 2, CRC Press : Boca Raton, Florida. 1378.

- Karger-Kocsis, J. (2000) Reinforced Polymer Blends. in Paul D.R. and Bucknall C.B. (ed). *Polymer Blends Volume 2 : Performance*. A Wiley-Interscience Publications : New York
- Khan, M. M. K., Liang, R. F., Gupta, R. K. and Agarwal, S. (2005). Rheological and Mechanical Properties of ABS/PC blends. *Korea-Australia Rheology Journal*. 17(1) : 1 – 7
- Kim, B. K., and Lee, Y. M. (1993). Physical properties of BS/SMA/nylon -6 ternary blends: effect of blending sequence. *Polymer*. 34(10) : 2075 – 2080.
- Kim, J. K. and Song, J. H. (1997) Rheological properties and fiber orientations of short fiber orientation plastics. *Polymer Engineering and Science*, 41 : 1061 – 1085
- Kirschke. K. (1976). The Documentation Rheology. *Rheologica Acta*. 15 : 508 – 515.
- Krache, R., Benachour, D. and Potschke, P. (2004) Binary and ternary blends of polyethylene, polypropylene, and polyamide 6,6: the effect of compatibilization on the morphology and rheology. *Journal of Applied Polymer Science*. 94 : 1976 – 1985
- Krause, S. (1978). Polymer-polymer Compatibility. In Paul. D.R and Newman. S. ed. *Polymer Blends : Volume 1*. New York : Academic Press, Inc. 16 – 113.
- Kudva, R. A, Keskkula, H. and Paul, D. R (2000a), Properties of compatibilized nylon 6/ABS blends Part I. Effect of ABS type. *Polymer*. 41(1): 225 – 237.
- Kudva, R. A, Keskkula, H. and Paul, D. R (2000b). Properties of compatibilized nylon 6/ABS blends - Part II. Effects of compatibilizer type and processing history. *Polymer*. 41 (1) : 239 – 258.
- Kudva, R. A., Keskkula, H. and Paul, D. R. (1998). Compatibilization of nylon 6/ABS blends using glycidyl methacrylate/methyl methacrylate copolymers. *Polymer*. 39(12). 2447 – 2460.
- Kudva, R. A., Keskkula, H. and Paul, D.R (1999). Properties of Compatibilized Nylon 6/ABS Blends Part II : Effects of Compatibilizer Type and Processing History. *Polymer* . 41 : 239 – 258.
- Kumar, A. and Gupta, R. K. (1998), *Fundamentals of Polymers*. McGraw-Hill, New York.
- Kutty, S. K. N., De, P. P. and Nando, G. B. (1991) Rheology of short Kevlar fibre-reinforced thermoplastic polyurethane. *Plastic, Rubber Processing & Applications* **15(1)**: 23 – 29

- Lacasse, C and Favis, B. D. (1999). Interface/Morphology/Property Relationships in Polyamide-6/ABS Blends. *Advances in Polymer Technology*. 18(3) : 255 – 265.
- Lai, S. M., Liao, Y.C. and Chen, T. W. (2005) The Preparation and Properties of Compatibilized Nylon 6/ABS Blends Using Functionalized Polybutadiene Part I: Impact Properties. *Polymer Engineering and Science*. 45 : 1461 – 1470.
- Lai, S.M., Chen, W.C., Liao, Y.C., Chen, T.W., Shen, H. F. and Shiao, Y-K. (2003) Compatibilization of Polyamide 6 Nanocomposites/ABS Blends Using Functionalized Metallocene Polyolefin Elastomer. SPE Antec Proceeding. 2286 – 2291.
- Laura, D. M., Keskulla, H., Barlow, J. W. and Paul, D.R (2002). Effect of glass fiber surface chemistry on the mechanical properties of glass fiber reinforced, rubber-toughened nylon 6. *Polymer*. 43 (17) : 4673 – 4687.
- Lavengood, R. E and Silver, F.M (1987). “New polyamide/ABS alloys: structure property relationship part 1”. SPE Antec Proceeding, May 4 – 7 : 1369 – 1374.
- Lavengood, R. E. and Harris A. R. US Patent, No 4713415. 1987 (assigned to Monsanto)
- Lazano, K., Yang, S. and Zeng, Q. (2004). Rheological Analysis of Vapor-Grown Carbon Nanofiber-Reinforced Polyethylene Composites. *Journal of Applied Polymer Science*. 93 : 155 – 162
- Lee, C. W., Ryu, S. H. and Kim, H.S. (1997) Morphological Changes in Nylon 6/Acrylonitrile-Butadiene-Styrene Reactive Blend. *Journal of Applied Polymer Science*. 64 : 1595 – 1604.
- Lee, J. K., Virkler, T. K. and Scott, C. E. (2002) Effects of ABS Rubber particles on Rheology, Melt Failure and Thermoforming. *Polymer Engineering and Science* 42(7) : 1541 – 1557
- Lenk, R. S. (1978). *Polymer Rheology*. London: Applied Science Publishers Ltd. page vii
- Li, S. -C. and Lu, L. -N. (2008). Melt rheological properties of reactive compatibilized HDPE/PET blends. *Journal of Applied Polymer Science*. 108 : 3559 – 3564

- Liu, X., Boldizar, A., Rigdal, M. and Bertilsson, H. (2002). Recycling of Blends of Acrylonitrile-Butadiene-Styrene and Polyamide. *Journal of Applied Polymer Science*. 86 : 2535 – 2543
- Majumdar, B., Keskkula, H. and Paul, D. R. (1994) Morphology of Nylon-6 ABS Blends Compatibilized by a Styrene-Maleic Anhydride Copolymer. *Polymer* , 35(15) : 3164 – 3172.
- Majumdar, B., Keskkula, H. and Paul, DR (1994). Deformation Mechanisms in Nylon-6 ABS Blends. *Journal of Polymer Science Part B: Polymer Physics*, 32 (12): 2127 – 2133.
- Malcheva, G. M., David C. T., Pickena S. J. and Gotsisa, A. D., (2005). Mechanical properties of short fiber reinforced thermoplastic blends. *Polymer*. 46: 3895 – 3905.
- Mamat, A., Vu-khanh, T., Cigana, P. and Favis, B.D. (1997). Impact Fracture Behavior of Nylon-6/ABS Blends. *Journal of Polymer Science: Part B: Polymer Physics*, (35): 2583 – 2592.
- Manson, J. A. and Sperling, L. H. (1976) *Polymer Blends and composites*. New York, Plenum Press
- Markus, Gahleitner. (2001). Melt Rheology of Polyolefins, *Progress in Polymer Science*, 26: 895 – 944.
- Mascosko, C. (1994) *Rheology Principles, Measurements, and Applications*. New York, VCH
- Matsuoka, S. (1992) *Relaxation Phenomena in Polymers*, Hanser : New York
- McCrum, N., Williams, B. and G. Read (1991) *Anelastic and Dielectric Effects in Polymeric Solids*, New York, Dover
- McKelvey, J. M. (1962). *Polymer Processing*. New York: John Wiley & Sons.
- Meincke, O., Kaempfer D., Weickmann H., Friedrich C., Vathauer, M. and Warth, H. (2004). Mechanical properties and electrical conductivity of carbon-nanotube filled polyamide-6 and its blends with acrylonitrile/butadiene/styrene. *Polymer*. 45(3) : 739 – 748
- Misra, A., Sawhney G., and Ananda Kumar. R. (1993) Structure and Properties of Compatibilized Blends of Polyamide-6 and ABS. *Journal of Applied Polymer Science*. 50 : 1179 – 1186.
- Morrison. F. A. (2001). *Understanding Rheology*. London: Oxford University Press.

- Nachbaur, L., Mutin, J. C., Nonat, A. and Choplin, L. (2001) Dynamic mode rheology of cement and tricalcium silicate pastes from mixing to setting. *Cement and Concrete Research*. 31:183–192
- Nair, S. V., Subramaniam, A. and Goettler L.A (1997). Fracture Resistance of Polyblends and Polyblends Matrix Composites. Part II. Role of Rubber Phase in Nylon 6/ABS Alloys. *Journal of Material Science*. 32: 5347 – 5354.
- Nair, S. V., Subramaniam. A. and Goettler L. A (1997). Fracture Resistance of Polyblends and Polyblends Matrix Composites. Part I. Unreinforced and Fiber- Reinforced Nylon 6,6/ABS Polyblends. *Journal of Material Science*. 32: 5335 – 5346.
- Ohishi, H. and Nishi, T. (2002). Application of Styrene-Acrylonitrile Random Copolymer–Polyarylate Block Copolymer as Reactive Compatibilizer for Polyamide and Acrylonitrile-Butadiene-Styrene Blends. *Journal of Applied Polymer Science*. 83 : 2300 – 2313.
- Oswald, T. A. and Menges, G. (1996). Materials science of polymer for Engineers. Hanser Publications. New York.
- Ota, W. N., Amico, S. C., and Satyanarayana, K. G. (2005) Studies on the combined effect of injection temperature and fiber content on the properties of the polypropylene–glass fiber composites, *Composite Science Technology*. 65 : 873 – 881.
- Ozkoc, G. Bayram, G. and Bayramli, E. (2005) Short Glass Fiber Reinforced ABS and ABS/PA6 Composites: Processing and Characterization. *Polymer Composites*. 26(6) : 745 – 755.
- Ozkoc, G., Bayram, G. and Bayramli, E. (2004). Effects of Polyamide 6 Incorporation to the Short Glass Fiber Reinforced ABS Composites: an Interfacial Approach. *Polymer*. 45: 8957 – 8966
- Ozkoc, G., Bayram, G. and Bayramli, E. (2005). Short glass fiber reinforced ABS and ABS/PA6 composites: Processing and Characterization. *Polymer Composite*. 26 (6) : 745 – 755.
- Ozkoc, G., Bayram, G. and Bayramli, E. (2006). “Compatibilization of ABS/PA6 blends using olefin based polymers.” *Antec 2006 Proceeding of 64th SPE Annual Conference*. Charlotte North Carolina, May 7 – 11th : 650 – 654
- Park J. S., Jin, J. S. and Lee, R. J. (2000). Influence of Silane Coupling Agents on the Surface Energetics of Glass Fibers and Mechanical Interfacial Properties of Glass Fiber-Reinforced Composites, *Journal Adhesion Science and Technology*. 14 : 1677 – 1689.

- Patel, S. (1998). *Polymer Blends Containg ABS*, Master Thesis. University of Massachusetts Lowell,
- Pearson, J. R. A. and Richardson, S. M. (1983). *Computational Analysis of Polymer Processing*. London: Applied Science Publishers Ltd.
- Pellerin, C., Prud'homme, R. E. and Pezolet, M. (2000). Orientation and Relaxation Study of Miscible Polystyrene/Poly(vinyl methyl ether) Blends. *Macromolecules*, 33(19):7009 - 7015
- Perry, R. H. and Green, D. (1984). *Perry's Chemical Engineer's Handbook*, Sixth Edition, p 2 - 116
- Prasanth Kumar, R., Manikandan Nair, K. C., Sabu Thomas., Schit S. C. and Ramamurthy K. (2000) Morphology and melt rheological behaviour of short-sisal-fibre-reinforced SBR composites. *Composites Science and Technology*. 60 (9): 1737-1751
- Qi, R., Qian, J., Chen, Z., Jin, X., and Zhou, C. (2004). Modification of Acrylonitrile-Butadiene-Styrene terpolymer by graft copolymerization with maleic anhydride in the melt. II Properties and phase bheaviour. *Journal of Applied Polymer Science*. 91 : 2834 – 2839.
- Rao, N. S. (1991). *Design Formulas for Plastics Engineers*, Hanser, Munich.
- Rao, N. S. and O'Brien K. T (1998). *Design Data for Plastics Engineers*, Hanser, Munich.
- Rudin, A. (1982) in *The Elements of Polymer Science and Engineering*. Academic Press Inc : New York. pp. 428 – 464.
- Sawhney, G., Gupta S. K. and Misra A. (1996). Structure and Properties of Polyblends of a Thermotropic Liquid Crystalline Polymer with an Alloy of Polyamide-6 and ABS. *Journal of Applied Polymer Science*. 62 :1395 – 1405.
- Seema, A. and Kutty, S. K. N. (2005) Rheology of short Nylon-6 Fiber Reinforced Styrene-Butadiene Rubber. *International Journal of Polymeric Materials*. 54: 933 – 948
- Seema, A. and Kutty, S. K. N. (2006), Effect of an Epoxy-Based Bonding Agent on the Cure Characteristics and Mechanical Properties of Short-Nylon-Fiber-Reinforced Acrylonitrile-Butadiene Rubber Composites. *Journal of Applied Polymer Science*, 99: 532 – 539.
- Sepehr, M., Utracki, L. A., Zheng, X. and Wilkie, C. A. (2005) Polystyrenes with micro-intercalated organoclay. Part II. Rheology and mechanical performance. *Polymer*. 46 : 11569 – 11581

- Shenoy, A. V. (1999). *Rheology of Filled Polymer Systems*. Dordrecht, Netherlands. : Kluwer Academic Publishers.
- Shenoy, A.V. and Saini D.R. (1984). Rheological model for unified curves for simplified design calculations in polymer processing. *Rheological Acta*, 23 : 368 – 377
- Shenoy, A.V. and Saini D.R. (1986). Melt Flow Index : More than just a quality control rheological parameter. Part 1. *Advances in Polymer Technology*. 6(1): 1 – 58.
- Sheung, P. J. and Kim, D. (2000), Thermal, Mechanical and diffusional Properties of Nylon 6/ABS Polymer blends : Compatibilizer effect. *Polymer Engineering and Science*. 40(7). 1635-1642.
- Shi-Ai, Xu, Lei Zhu., Jing-Wei, Xie. and Ming Jiang. (1999). Melt rheology of compatibilized polystyrene/low density polyethylene blends. *Polymer International*. 48(11): 1113 – 1120.
- Shonaike, G. O., Hamada, H., Maekawa, Z., Yamaguchi S. and Toi, K. (1995). Studies of blends of poly(phenylene sulfide) and a liquid crystalline polymer : time-temperature superposition. *Journal of Macromolecular Science Physics*. 34(3): 177 - 197.
- Sinthavatharon, W., Nithitanakul, M., Grady, B. P., and Magaparan, R. (2009). Melt Rheology and Die Swell of PA6/LDPE blends by Using Ionomer as a Compatibiliser. *Polymer Bulletin*. 63 (1) : 23 - 35
- Sridharan, S. and Zureick, A. -H. and Muzzy J. D. (1998). Annual Technology Conference, Society of Plastic Engineer. 56th : 2255.
- Stein, R. S. (1992) in Andrews G.D. and Subramanian P.M. (eds.). *Emerging Technologies in Plastics Recycling*. American Chemical Society : Washington DC. pp. 39-48.
- Sun, S.L., Tan, Z.Y., Xu X. F., Zhou, C., Ao, Y. H. and Zhang H. X. (2005) Toughening of Nylon 6 with epoxy-functionalized Acrylonitrile-butadiene-styrene copolymer. *Journal of Polymer Science Part B: Polymer Physics*. 43 : 2170 – 2180.
- Tadmor, Z. and Gogos, C. G. (1979). *Principles of Polymer Processing*. New York: John Wiley & Sons.
- Tai, H. J., Chiu W. Y., Chen, L. W. and Chu L. H. (1991). Study on the crystallization kinetics of PP/ GF composites. *Journal of Applied Polymer Science*. 42(12) : 3111 – 3122.

- Tan, J. K., Kitano, T. and Hatakeyama, T. (1990). Crystallization of carbon fibre reinforced polypropylene. *Journal Material Science*. 25(7): 3380–3384
- Tancrez, J. P., Pabiot, J. and Rietsch, F. (1996) Damage and fracture mechanisms in thermoplastic-matrix composites in relation to processing and structural parameters, *Composite Science Technology*. 56 : 725–731.
- Tang, C. Y. and Liang, J. Z. (2003). A study of the melt flow behaviour of ABS/CaCO₃ composites. *Journal of Materials Processing Technology*. 138 : 408 - 410
- Teh, J. W. (1983) Structure and Properties of Polyethylene-Polypropylene Blend. *Journal of Applied Polymer Science*. 28(2) : 605 - 618
- Thomason J. L. (1999). The Influence of Fibre Properties of The Performance of Glass Fibre Reinforced Polyamide 6,6. *Composites Science and Technology*. 59 : 2315 – 2328.
- Thorne, J. L. (1979) *Plastics Process Engineering*. Marcel Dekker Inc : New York
- Tjong, S. C. and Jiang, W. (2004). Performance characteristics of compatibilized ternary Nylon 6/ABS/LCP in-situ composites. *Journal of Material Science*, 39(8): 2737 – 2746.
- Tjong, S. C. and Xu, S. A. (2001). Ternary Polymer Composite: PA6,6/maleated SEBS/Glass beads. *Journal of Applied Polymer Science*. 81: 3231 – 3237.
- Tjong, S. C., Xu, S. A, Li, R. K. Y. and Mai, Y. W. (2002). Short glass fiber-reinforced Polyamide 6,6 composites toughened with maleated SEBS. *Composites Science Technology*. 62(15) : 2017-2027.
- Tol R. T., Mathot, V. B. H., Reynaers, H., Goderis, B. and Groeninckx, G. (2005). Confined crystallization phenomena in immiscible polymer blends with dispersed micro-and nanometer sized PA6 droplets part 4: polymorphous structure and (meta)-stability of PA6 crystals formed in different temperature regions. *Polymer*. 46(9) : 2966 - 2977
- Toray Industries. (2006). Basic Physical Properties. *Toray Plastics*. Retrieved May 15, 2009, from <http://www.toray.co.jp/english/plastics/products/nylon/cm1017.html>
- Toray Industries. (2006). Basic Physical Properties. *Toray Plastics*. Retrieved May 15, 2009, from <http://www.toray.co.jp/english/plastics/products/abs/100.html>
- Triacca, V. J., Ziaee, S., Barlow, J. W., Keskkula, H. and Paul, D. R. (1991). Reactive compatibilization of blends of nylon 6 and ABS materials. *Polymer*. 32(8) : 1401 – 1413.

- Utracki, L. A. (1983). Melt flow of polymer blends. *Polymer Engineering Science*. 23(11) : 602 – 609.
- Utracki, L. A. (1990) *Polymer Alloys and Blends: Thermodynamics and Rheology*. Carl Hanser Verlag. New York.
- Utracki, L. A. (2002). Compatibilization of Polymer Blends. *The Canadian Journal of Chemical Engineering*. 80 : 1008 – 1016.
- Utracki, L. A., Walsh, D. J. and Weiss, R. A. (1989) in *Multiphase Polymers: Blends and Ionomers.*, L.A. Utracki and R.A. Weiss (eds.), American Chemical Society, Washington DC, pp. 1-35.
- Vlachopoulos, J. and Wagner, J. R (eds.) (2001). *The SPE guide on extrusion technology and troubleshooting*. Society of Plastics Engineers, Brookfield.
- Wahit, M. U., Hassan, A., Mohd Ishak, Z. A., Rahmat, A. R. and Othman, N. (2006) The Effect of Rubber Type and Rubber Functionality on the Morphological and Mechanical Properties of Rubber-toughened Polyamide 6/Polypropylene nanocomposites. *Polymer Journal*. 38(8): 767 – 780.
- Walsh, D. J., Higgins, J. S. and Zhikuan, C. (1982) The compatibility of Poly(methyl methacrylate) and chlorinated polyethylene. *Polymer* 23 : 336 – 339
- Wang, W. and Zheng, Q. (2005). The dynamic rheological behaviour and morphology of nylon/elastomer blends. *Journal of Material Science*. 40 : 5545 – 5547
- Wang, Z., Zhang, X., Zhang, Y., Zhang, Y. and Zhou, W. (2003). Effect of dynamic vulcanization on properties and morphology of Nylon/SAN/NBR blends: A new compatilization method of nylon 6/ABS blends. *Journal of Applied Polymer Science*. 87 : 2057 – 2062.
- Xiao, K. Q., Zhang, L. C. and Zarudi, I. (2006) Mechanical and rheolical properties of carbon nanotube-reinforced poleytehylene composites. *Composites Science and technology*, 67 : 177 - 182
- Young, R. T. and Baird D. G. (2000). Processing and properties of injection molded thermoplastic composites reinforced with melt processable glasses. *Polymer Composites* : 21 (5) : 645 – 659